Doctoral theses at NTNU, 2022:18

Haoran Li

Economic optimization for heat-prosumer-based district heating systems in unidirectional heating markets

Doctoral thesis

NTNU
Norwegian University of Science and Technology
Thesis for the Degree of
Philosophiae Doctor
Faculty of Engineering
Department of Energy and Process Engineering

NTNU
Norwegian University of
Science and Technology

Haoran Li

Economic optimization for heat-prosumer-based district heating systems in unidirectional heating markets

Thesis for the Degree of Philosophiae Doctor

Trondheim, January 2022

Norwegian University of Science and Technology
Faculty of Engineering
Department of Energy and Process Engineering

NTNU
Norwegian University of
Science and Technology

NTNU
Norwegian University of Science and Technology

Thesis for the Degree of Philosophiae Doctor

Faculty of Engineering
Department of Energy and Process Engineering

ISBN 978-82-326-5828-2 (printed ver.)
ISBN 978-82-326-6402-3 (electronic ver.)
ISSN 1503-8181 (printed ver.)
ISSN 2703-8084 (online ver.)

Doctoral theses at NTNU, 2022:18

Printed by NTNU Grafisk senter

PREFACE

This thesis is submitted to the Norwegian University of Science and Technology in partial fulfilment of the requirements for the degree of Doctor of Philosophy (PhD).

This work was carried out at the Department of Energy and Process Engineering, Norwegian University of Science and Technology, Trondheim, Norway. The work was under the supervision of Professor Natasa Nord from the Norwegian University of Science and Technology and the co-supervision from Senior Scientist Tianzhen Hong from the Lawrence Berkeley National Laboratory, the U.S.

This PhD project was under financial support by the Research Council of Norway through the FRIPRO/FRINATEK program, project number 262707.

PREFACE

ACKNOWLEDGMENTS

It was a great achievement for me to finish the journey as a PhD candidate. Throughout the last four years, I have received a great deal of support, assistance, encouragement, inspiration, and companionship, which have allowed me to go through all the ups and downs.

Firstly, I would like to thank my supervisor, Professor Natasa Nord, for all her trust, understanding, patience, and scientific and personal advice. I highly appreciate her continued financial support, which has allowed me to concentrate on my research and accomplish the work in a methodical and leisurely manner. Most importantly, her characters of hard-working, motivated, and determined, makes her a role model for me, inspiring me to keep going during times of doubt and distress.

I would like to acknowledge my co-supervisor, Senior Scientist Tianzhen Hong, for his support during my guest research at the Berkeley Lab. I appreciate all his valuable guidance throughout my PhD program and the opportunities he provided for me to advance my research.

Thank Daniel Rohde for opening the door of the Modelica language, which contributed to establishing the study's core technologies. Furthermore, the shared value of the Modelica community inspired me throughout the PhD period.

I would like to express my gratitude to my colleagues and friends at NTNU, Trondheim, and Berkeley for all the memorable moments.

Finally, my heartfelt thanks to my wife, Juan Hou, and my son, Jixi Li. Thank you, Juan, for being a project partner, a control theory lecturer, a Modelica model co-developer, an editor, and a proofreader. Thank you, Jixi, for joining the family and brightening everyday life. Being husband and father is gratifying and challenging while motivating me to keep going.

Trondheim, Norway
October 5, 2021
Haoran Li

ACKNOWLEDGMENTS

ABSTRACT

With the growing integration of renewable energies into district heating (DH) systems, some heat users are installing on-site renewable-based distributed heat sources (DHSs), unlocking the possibility for heat users to supply heat to central DH systems. Representing new types of energy participants in future sustainable DH systems, these heat users integrated with DHSs are called heat prosumers due to their dual role of producer and consumer. The emergence of heat prosumers breaks the spatial barriers of utilizing non-dispatchable renewable energies in DH systems. Moreover, it transforms conventional unidirectional DH systems into future bidirectional DH systems, making the heat supply of DH systems more flexible, resilient, and competitive. However, the development of heat prosumers is facing numerous challenges. One of these challenges is the incompatibility between the bidirectional heat supply and unidirectional heating markets. Even though several DH companies have implemented bidirectional heat pricing models that allow heat prosumers to sell their excess heat at market prices, the vast majority of DH companies continue to use unidirectional heat pricing models, making it impossible for heat prosumers to profit from supplying heat to central DH systems. The facing challenge hinders the development of heat prosumers, posing barriers for the transition to future sustainable DH systems.

This thesis, therefore, aimed to address the facing challenge by improving heat prosumers' economic performance under unidirectional heating markets through optimal design and optimal operation. With a focus on DH systems in Scandinavia, this thesis tackled economic and technological issues, providing solutions for both the supply and demand sides. To achieve the goal, a step-by-step study was carried out, guided by five research questions.

Question 1: What are crucial factors that impact heat consumers' heating costs in current Scandinavian heating markets? Literature reviews revealed that heat use and peak load are crucial factors that impact heat consumers' heating costs in Scandinavian heating markets. Therefore, reducing heat use and shaving peak load are two possible ways to improve heat prosumers' economic performance under current unidirectional heating markets. Introducing thermal energy storage (TES) is a proven approach to achieve the above goals. TES may temporarily store surplus heat from DHSs for later use, allowing more heat from the DHSs, while less heat from the central DH system to be used. Meanwhile, by charging and discharging

the TES before and during peak hours, it may shave the peak load by shifting parts of the heat load from peak hours to non-peak hours. However, implementing TESs at large scales for DH systems is investment intensive and may demand extremely long payback periods. To solve this problem, the following three research questions, Questions 2-4, were proposed, addressing the challenges of optimal design and operation for heat-prosumer-based DH systems with TES.

Question 2: Which TES solution is superior for heat-prosumer-based DH systems? To answer this question, three candidate systems that represented typical TES solutions were proposed and modelled. These candidate systems integrated short-term water tank thermal energy storage (WTTES), seasonal borehole thermal energy storage (BTES), and both short-term WTTES and seasonal BTES, respectively. In addition, the model was developed with high detail on model components such as DHSs, substations, distribution networks, buildings, and TESs, using the Modelica modelling language and Modelica libraries. A case study on the DH system at a university campus in Norway showed that WTTES was superior to BTES regarding the following aspects. Firstly, compared to BTES, WTTES required a lower initial investment while achieving the same level of heating cost saving. Furthermore, WTTES had a payback period of fewer than ten years, it was superior to BTES, which might be up to twenty years.

Question 3: What is the economically optimal size for the selected TES? To answer this question, an economic optimization problem was formulated to minimize the heating cost of heat-prosumer-based DH systems integrated with the selected TES - WTTES. The impacts of storage capacity on heat prosumers' performance were explored by solving the optimization problem while sweeping the storage size parameter. Different from the detailed simulation model used for Question 2, this part created a simplified optimization model using the Modelica programming language, intending to be computational tractability and numerical stability. The case study on the campus DH system showed that medium storage sizes, equivalent to storage capacities ranging from twelve hours to one day, might be good choices, offering a reasonable trade-off between initial investment and heating cost saving.

Question 4: What is the economically optimal distribution temperature for heat-prosumer-based DH systems with TES? To answer this question, four distribution temperature scenarios were created, including three benchmark scenarios that represented the 2^{nd}, 3^{rd}, or 4^{th} generation DH systems, and an improved scenario with a wide distribution temperature range that crossed all the benchmark scenarios. The four scenarios specified the storage size equivalent to twelve

hours' storage capacity for their WTTESs, according to the optimal storage sizes identified by Question 3. The impacts of distribution temperature on the heat prosumers' performance were investigated by solving the economic optimization problem formulated in Question 3 under different distribution temperatures. The case study on the campus DH system showed that decreasing the distribution temperature reduced the distribution heat loss and cut the heat-use-related heating costs, however, it reduced the peak load shaving effect of TESs, resulting in higher peak-load-related heating costs for heat prosumers. By making a trade-off between these two sides, the improved scenario achieved the optimal economic performance with the lowest total heating cost.

By addressing Questions 2-4, solutions on the supply side were provided. A parallel study was conducted to tackle issues on the demand side, motivated by the last research question. *Question 5: How can rule-based control strategies be used to operate heating systems inside buildings?* To answer this question, six rule-based control scenarios were proposed, with proportional-integral (PI) controllers used to approach the lowest possible supply temperature, weather compensation (WC)-based controllers used to calculate the theoretical lowest supply temperature, and PI controllers used to obtain a low reference return temperature. A model was developed with high details on model components such as building envelopes, radiator-based space heating systems, weather, and controllers. A case study on a typical Norwegian space heating system revealed that reducing the supply temperature and reducing the return temperature are contradictory goals. Moreover, it was better to apply operation strategies that aim to lower the supply temperature rather than to lower the return temperature. Otherwise, an extremely high supply temperature was required to achieve the low return temperature due to the limited heating capacity of radiators.

In conclusion, this study provided a practical solution to heat prosumers' incompatibility problem that exists between the bidirectional heat supply and the unidirectional heating markets. It was a systematic approach to integrate TESs into heat prosumers and to design and operate heat-prosumer-based DH systems with TESs optimally. This study might contribute to the development of heat prosumers and the transition to more sustainable DH systems.

ABSTRACT

LIST OF PUBLICATIONS

Paper 1:

Li H, Nord N. Transition to the 4th generation district heating-possibilities, bottlenecks, and challenges. Energy Procedia. 2018;149:483-98. The 16th International Symposium on District Heating and Cooling.

Paper 2:

Li H, Hou J, Hong T, Ding Y, Nord N. Energy, economic, and environmental analysis of integration of thermal energy storage into district heating systems using waste heat from data centres. Energy. 2021;219:119582.

Paper 3:

Li H, Hou J, Tian Z, Hong T, Nord N, Rohde D. Optimize heat prosumers' economic performance under current heating price models by using water tank thermal energy storage. Energy. 2022;239:122103.

Paper 4:

Li H, Hou J, Hong T, Nord N. Distinguish between the economic optimal and lowest distribution temperatures for heat-prosumer-based district heating systems with short-term thermal energy storage. Submitted to Journal of Energy (Status: Under review).

Paper 5:

Li H, Nord N. Operation strategies to achieve low supply and return temperature in district heating system. E3S Web Conf. 2019;111:05022. The 13th REHVA World Congress CLIMA 2019.

Paper 6:

Li H, Hou J, Nord N. Using thermal storages to solve the mismatch between waste heat feed-in and heat demand: a case study of a district heating system of a university campus. Energy Proceedings. 2019;04. The 11th International Conference on Applied Energy.

Paper 7:

Li H, Hou J, Ding Y, Nord N. Techno-economic analysis of implementing thermal storage for peak load shaving in a campus district heating system with waste heat from the data centre. E3S Web Conf; 2021;246: 09003. The 10th International SCANVAC Cold Climate Conference.

Paper 8:

Li H, Hou J, Nord N. Optimize prosumers' economic performance by using water tank as thermal energy storage. The 17th International Symposium on District Heating and Cooling.

ABBREVIATIONS

BTES	Borehole thermal energy storage
CAD	Computer-aided design
CAO	Computer-aided operation
DC	Data centre
DH	District heating
DHS	Distributed heat source
DHW	Domestic hot water
EDC	Energy demand component
FDC	Flow demand component
FXC	Fixed component
HE	Heat exchanger
HP	Heat pump
LDC	Load demand component
MS	Main substation
PI	Proportional-integral
R^2	Coefficients of determination
R2R mode	Extracts the water from the return line and then feeds it back to the return line after the heating process
SH	Space heating
TES	Thermal energy storage
WC	Weather compensation
WTTES	Water tank thermal energy storage

LIST OF CONTENTS

LIST OF TABLES

LIST OF TABLES

LIST OF FIGURES

LIST OF FIGURES

1 INTRODUCTION

The transition to future sustainable energy systems is challenging the current heat supply and heat pricing modes of district heating (DH) systems. In conventional DH systems, both heat supply and pricing modes are unidirectional. The typical paradigm is that DH companies supply heat to end-users, meanwhile, end-users pay heating bills to DH companies. Under these unidirectional modes, all end-users play a single role, i.e., the consumer. However, with the rapid integration of renewable energies, DH systems' heat supply becoming increasingly flexible and end users' role is transforming. Some end-users introduce on-site renewable-based distributed heat sources (DHSs) and have the ability to deliver heat to the central DH network. These end-users are called heat prosumers due to their dual role of producer and consumer. The emergence of heat prosumers is making DH systems more resilient and flexible. Moreover, it transforms the mode of heat supply from unidirectional to bidirectional. This transformation, however, is facing unprecedented challenges. One challenge comes from the incompatibility between the bidirectional heat supply and the unidirectional heating markets. Most of the current heating markets only support the unidirectional heat supply from DH companies to end-users. Therefore, heat prosumers, as end-users, hardly gain any economic benefit from their heat supply to the central DH system. The facing incompatibility is hindering the development of heat prosumers, posing a barrier for the transition to future sustainable DH systems.

This thesis, therefore, aims to break the barrier by improving heat prosumers' economic performance through optimal design and operation techniques under the current unidirectional heating markets. With a special focus on DH systems in Scandinavia, this thesis tackles economic and technological challenges, providing solutions for heating systems on both the supply and demand sides.

1.1 Motivation

In the European Union (EU), buildings are responsible for approximately 40% of total energy use and 36% of greenhouse gas emissions [1]. Space heating (SH) and domestic hot water (DHW) systems, as essential parts of building energy systems, play an important role in buildings' energy use. For example, in the residential sector of the EU countries, about 80% of the energy use is for SH and DHW [2, 3]. DH systems make it possible to satisfy buildings' heat demand in an environment-friendly and energy-efficient way [4]. Moreover, compared with

alternative heating technologies, DH is competitive, especially for urban areas with concentrated heat demand. Nowadays, about 80,000 DH systems are working successfully worldwide, thereof about 6,000 DH systems are in Europe [5]. Moreover, for some countries, the national heat market share of DH can reach 60% [5-7]. However, DH systems' competitiveness is weakened by several challenges, such as the considerable distribution heat loss caused by high distribution temperature and the shrinking heat market due to the improving building energy efficiency [4]. To deal with these challenges and stay competitive, the current second and third generation DH systems are transitioning to the fourth and fifth generation DH systems [8-11]. The transition includes decreasing distribution temperature and upgrading infrastructure, and hence reduces the distribution heat loss and opens the door to more affordable heat sources such as renewable energies.

In future DH systems, renewable energies may be integrated into the user side as DHSs, besides being integrated into the central network as centralized heating plants. These heat users with DHSs are called heat prosumers due to their dual roles of producer and consumer. As consumers, they are supplied with heat by central heating plants as in the conventional DH systems; while, as producers, they can deliver heat to the central network. The emergence of heat prosumers makes it possible to break the spatial barriers of utilizing renewable energies in DH systems. Moreover, it can transform the conventional unidirectional DH system into the future bidirectional DH system and make the heat supply more flexible and resilient. In addition, as active participants, heat prosumers will contribute to the development of smart DH systems within the vision of smart energy systems. However, the development of heat prosumer is facing significant challenges. One challenge is the incompatibility between the bidirectional heat supply and the unidirectional heating markets. Most of the current heating markets in Scandinavia only support the unidirectional heat supply from DH companies to end-users. Therefore, heat prosumers, as end-users, hardly gain any economic benefit from their heat supply to the central DH system. This facing incompatibility is hindering the development of heat prosumers in DH systems, posing a barrier to the transition to more sustainable DH systems in the future. Therefore, research is needed to improve heat prosumers' economic performance under unidirectional heating markets, and thus promote the development of heat prosumers during this transition period of the DH system and finally pave the way for the future 100% sustainable DH system.

INTRODUCTION

The widely used heat pricing models in the current Scandinavian heating markets charge the heating cost based on the heat use and the peak load [12]. Therefore, the two possible ways to improve heat prosumers' economic performance: 1) increasing heat prosumers' self-utilization rate of heat supply from DHSs, and 2) shaving prosumers' peak load. Introducing thermal energy storage (TES) is a possible solution with a proven ability to achieve the above goals. Firstly, TESs can increase heat prosumers' self-utilization rate of heat supply from DHSs by temporarily storing the surplus heat [13-17]. The reversed heat supply from the prosumer to the central DH network due to the existence of surplus heat is reduced, and more heat from the DHSs is utilized by the prosumer itself. Secondly, TESs can shave prosumers' peak load by shifting parts of the central DH system's heat supply from peak hours to non-peak hours [18-20]. However, introducing TESs into DH systems is investment intensive, and it may have the economic risk of unreasonable long payback periods [21]. Therefore, research is needed for the proper design and operation of heat-prosumer-based DH systems with TESs.

Moreover, introducing TESs may impact the economically optimal distribution temperature of DH systems. Previous studies have been dedicated to enhancing DH systems' economic performance by improving their energy efficiency, which can be achieved by lowering the distribution temperature [22]. However, DH systems' economic performance depends not only on energy efficiency but also on the peak load. The peak load may have a considerable amount of influence over DH systems' investments as well as operating costs. For the investment, peak load determines the capacities of heating plants and distribution networks. Higher peak loads always mean higher capacities of heat generation and distribution, and hence higher investment for DH systems. For the operation cost, the peak load is generally covered by peak load heating plants which always have higher operating costs than baseload heating plants. Studies on heat pricing models in Sweden revealed that the peak-load-related heating cost is the second most significant component after the heat-use-related heating cost [12, 23]. Decreasing distribution temperature, which is driving the development of DH systems, may reduce the peak load shaving effect of TESs, resulting in higher peak-load-related heating costs for heat users. Decreases in the charging temperature of TESs along with the decreasing distribution temperature of DH systems will reduce the TES storage temperature as well as the storage capacity of TESs. The peak load shaving effect of TESs, which is positively correlated to the storage temperature and the storage capacity, would be impaired. Therefore, there is a trade-off between the improving energy efficiency of DH systems and the reducing peak load shaving

effect of TESs when decreasing the distribution temperature. Given the significant economic importance of DH systems' energy efficiency and peak load, further research is needed to understand how distribution temperature influences these two factors, and hence the overall economic performance of heat-prosumer-based DH systems with TESs.

Finally, besides the above-mentioned issues on the supply side of DH systems, the operation of the demand side, the heating system inside buildings, is crucial as well. Previous studies have focused on decreasing the operating temperatures on the demand side and proposed feasible measures to achieve it, including improving system control, renovating building envelopes, and replacing critical radiators and thermostatic valves [24-32]. Reducing the operating temperatures, supply and return temperatures, are two goals pursued in these studies, both of which may benefit the supply side of DH systems. Reducing the supply temperature might increase the output of solar thermal panels, raise the coefficient of performance of heat pumps (HPs), and increase the power to heat ratio of combined heat and power plants [33]. In addition, reducing the return temperature could decrease the costs of heat generation and distribution. Low return temperatures are particularly important to some DH companies, and they employ incentive tariffs to encourage their customers to reduce their return temperatures [34]. However, reducing the supply temperature and reducing the return temperature on the demand side are contradictory goals, because the mean water temperature should be constant to maintain a radiator's thermal output at a certain level when the indoor air temperature is fixed, as presented by the standard EN 442-2 [35]. Therefore, a decrease in the supply temperature would be offset by an increase in the return temperature. Further research is needed to properly operate the heating systems on the demand side, making a suitable trade-off between the reduced supply temperature and the increased return temperature.

To achieve the above goals, a study that covered both the supply and demand sides of the DH system, addressing economic and technological issues was conducted. Firstly, the heat pricing mechanisms of the current heating markets in Scandinavia were investigated to formulate the economic boundary of this study. Secondly, different TES solutions including short-term and seasonal TESs were introduced to improve prosumers' economic performance. Afterwards, methods for optimal design and operation of heat-prosumer-based DH systems with TESs were developed. Finally, the optimal distribution temperature for heat-prosumer-based DH systems with TES was identified. Moreover, the operation of the SH system inside buildings was analysed.

1.2 Research questions and research tasks

The following research questions and tasks are proposed as a step-by-step approach to achieve the thesis's aim.

Question 1: **What are crucial factors that impact heat consumers' heating costs in current Scandinavian heating markets?**

Task 1.1: Identify crucial factors based on literature reviews.

Task 1.2: Establish the study's economic boundaries by creating a generalized heat pricing model that incorporates the identified critical factors.

Question 2: Which TES solution is superior for heat-prosumer-based DH systems?

Task 2.1: Propose candidate solutions for heat-prosumer-based DH systems integrating with different TESs.

Task 2.2: Build models for individual candidate solutions and perform yearly simulations.

Task 2.3: Select a superior solution by comparing candidate solutions' energy and economic performance.

Question 3: What is the economically optimal size for the selected TES?

Task 3.1: Formulate an economic optimization problem for a heat-prosumer-based DH system that is integrated with the selected TES.

Task 3.2: Solve the optimization problem while sweeping TES's size parameter to obtain yearly operating trajectories for the heating system under varied storage capacities.

Task 3.3: Identify the economically optimal size by comparing the system's economic performance under different storage capacities.

Question 4: What is the economically optimal distribution temperature for heat-prosumer-based DH systems with TES?

Task 4.1: Solve the proposed optimization problem under the benchmark and improved scenarios, where the distribution temperatures represent different generation DH systems and future DH systems with the highest distribution temperature flexibility, respectively.

Task 4.2: Identify the economically optimal distribution temperature by comparing the economic performance of different scenarios.

Task 4.3: Distinguish between the economically optimal distribution temperature and the lowest distribution temperature to guide future DH systems' distribution temperature development.

Question 5: How can rule-based control strategies be used to operate heating systems inside buildings?

Task 5.1: Propose candidate rule-based control strategies for SH systems, aiming at low supply or low return temperatures.

Task 5.2: Select suitable control strategies by comparing candidate strategies' performance on supply and return temperatures.

The above research questions and tasks are logically connected and organized in Figure 1-1.

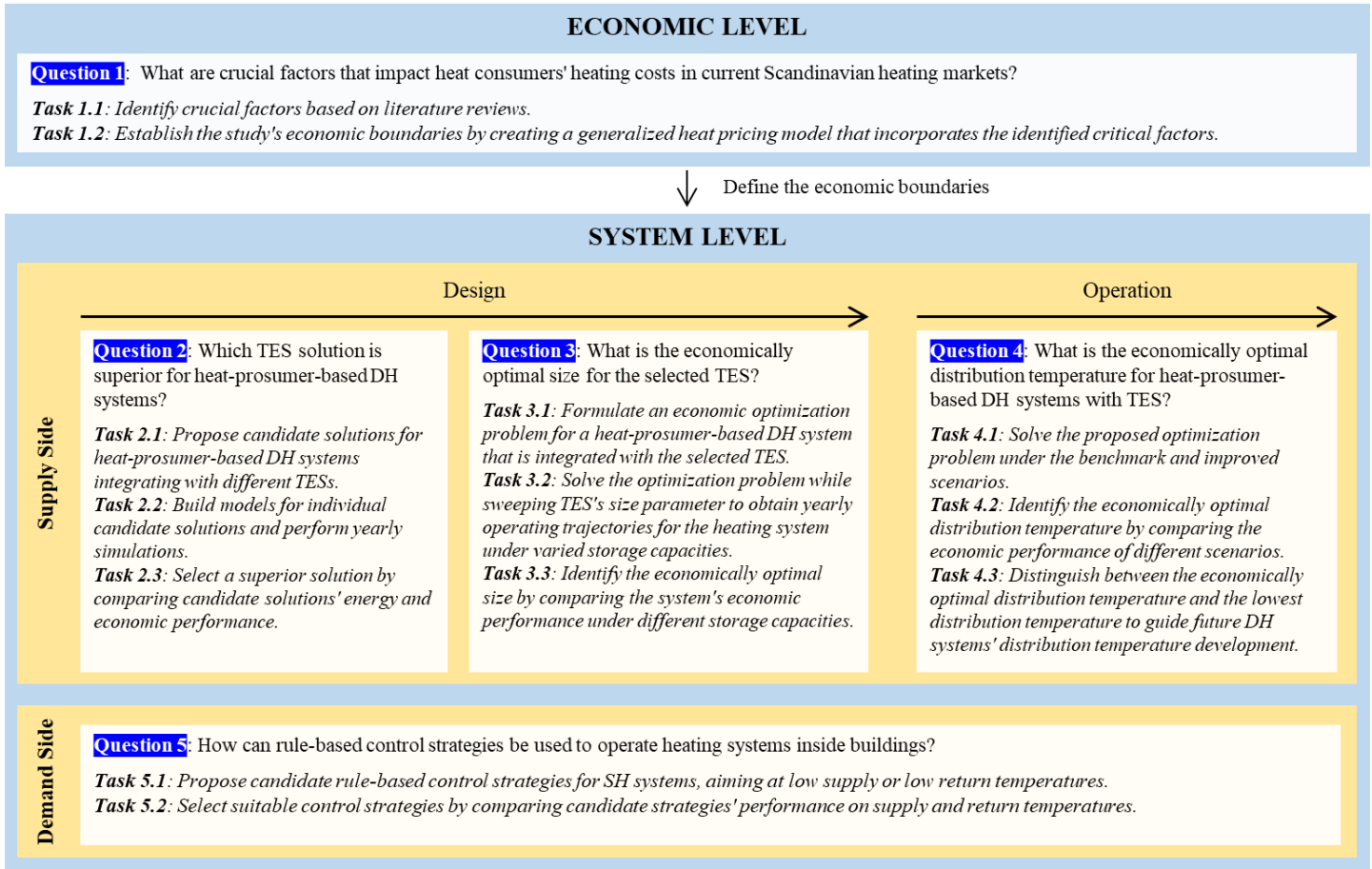

Figure 1-1. Connection and organization of the research questions

1.3 Structure of the thesis

The main body of the thesis is illustrated in Figure 1-2. Chapter 2 introduces the techno-economic background of the study. Chapter 3 presents the research methodology, including the candidate systems for heat-prosumer-based DH systems with TESs, as well as system modelling, simulation, and optimization methods. Chapter 4 describes the case studies of a university campus DH system and a typical Norwegian SH system. The key results of the study are presented and explained in Chapter 5. Chapter 6 outlines the main conclusions, acknowledges the major limitations, and gives recommendations for future research.

As presented in Figure 1-2, the first research question, **Question 1**, which functions as the economic boundary of the study, is answered in Chapter 2. In addition, the addressing of the other research questions, from **Question 2** to **Question 5,** constitutes the content from Chapter 3 to Chapter 5 of the thesis.

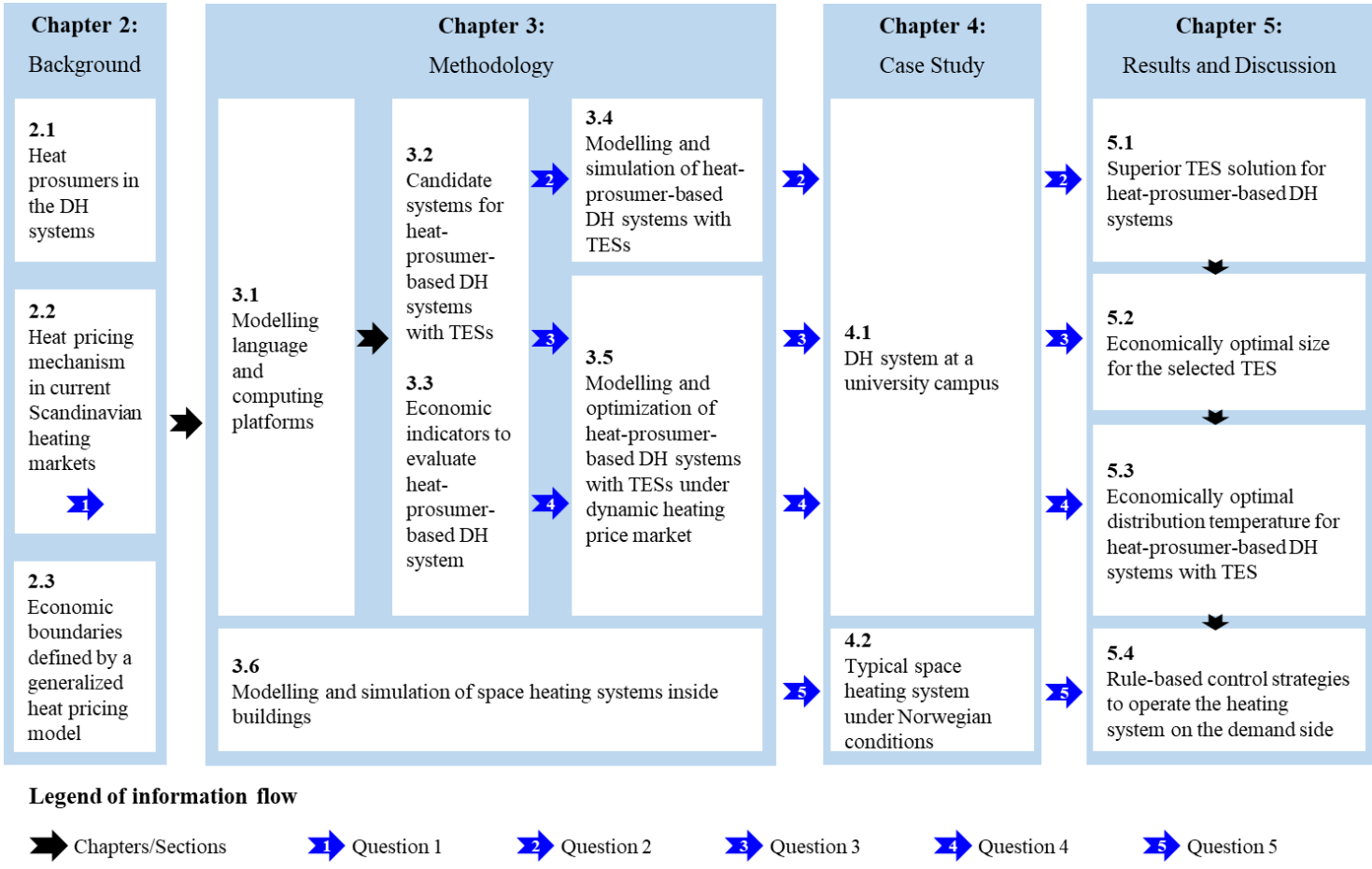

Figure 1-2. Structure and information flow from Chapter 2 to Chapter 5 of the thesis

1.4 List of publications

The type of this thesis is the paper collection. The thesis is built on the foundation of three journal publications and five conference papers. Figure 1-3 depicts an overview of the articles. It distinguishes between fundamental and supporting papers here, with fundamental papers addressing key research questions and supporting papers presenting preparatory work for the fundamental papers. The papers that make up this thesis, along with the author's contributions, are listed below.

Fundamental papers:

Paper 1:

Li H, Nord N. Transition to the 4th generation district heating-possibilities, bottlenecks, and challenges. Energy Procedia. 2018;149:483-98. The 16th International Symposium on District Heating and Cooling.

Contribution: The type of this paper is Review Article. The author made the literature search, data analysis, and original draft preparation. Natasa Nord reviewed and commented on the work.

Paper 2:

Li H, Hou J, Hong T, Ding Y, Nord N. Energy, economic, and environmental analysis of integration of thermal energy storage into district heating systems using waste heat from data centres. Energy. 2021;219:119582.

Contribution: The type of this paper is Full Length Article. The author made the methodology, formal analysis, and investigation. The conceptualization and the original draft preparation were done in collaboration with Juan Hou. Natasa Nord, Tianzhen Hong, and Yuemin Ding reviewed and commented on the work.

Paper 3:

Li H, Hou J, Tian Z, Hong T, Nord N, Rohde D. Optimize heat prosumers' economic performance under current heating price models by using water tank thermal energy storage. Energy. 2022;239:122103.

Contribution: The type of this paper is Full Length Article. The author made the formal analysis and investigation. The conceptualization was done in collaboration with Tianzhen Hong. The methodology and original draft preparation were done in collaboration with Juan Hou. Daniel Rohde assisted in computer code. Natasa Nord, Tianzhen Hong, Zhiyong Tian, and Daniel Rohde reviewed and commented on the work.

Paper 4:

Li H, Hou J, Hong T, Nord N. Distinguish between the economic optimal and lowest distribution temperatures for heat-prosumer-based district heating systems with short-term thermal energy storage. Submitted to Journal of Energy (Status: Under review).

Contribution: The type of this paper is Full Length Article. The author did the conceptualization, formal analysis, and investigation. The methodology and original draft preparation were done in collaboration with Juan Hou. Natasa Nord and Tianzhen Hong reviewed and commented on the work.

Paper 5:

Li H, Nord N. Operation strategies to achieve low supply and return temperature in district heating system. E3S Web Conf. 2019;111:05022. The 13th REHVA World Congress CLIMA 2019.

Contribution: The type of this paper is Full Length Article. The author did the conceptualization, formal analysis, methodology, investigation, and original draft preparation. Natasa Nord reviewed and commented on the work.

Supporting papers

Paper 6:

Li H, Hou J, Nord N. Using thermal storages to solve the mismatch between waste heat feed-in and heat demand: a case study of a district heating system of a university campus. Energy Proceedings. 2019;04. The 11th International Conference on Applied Energy.

Contribution: The type of this paper is Full Length Article. The author did the conceptualization, formal analysis, methodology, and investigation. The original draft

preparation was done in collaboration with Juan Hou. Natasa Nord reviewed and commented on the work.

Paper 7:

Li H, Hou J, Ding Y, Nord N. Techno-economic analysis of implementing thermal storage for peak load shaving in a campus district heating system with waste heat from the data centre. E3S Web Conf; 2021;246: 09003. The 10th International SCANVAC Cold Climate Conference.

Contribution: The type of this paper is Full Length Article. The author did the conceptualization, formal analysis, methodology, and investigation. The original draft preparation was done in collaboration with Juan Hou. Natasa Nord and Yuemin Ding reviewed and commented on the work.

Paper 8:

Li H, Hou J, Nord N. Optimize prosumers' economic performance by using water tank as thermal energy storage. The 17th International Symposium on District Heating and Cooling.

Contribution: The type of this paper is Full Length Article. The author did the conceptualization, formal analysis, methodology, and investigation. The original draft preparation was done in collaboration with Juan Hou. Natasa Nord reviewed and commented on the work.

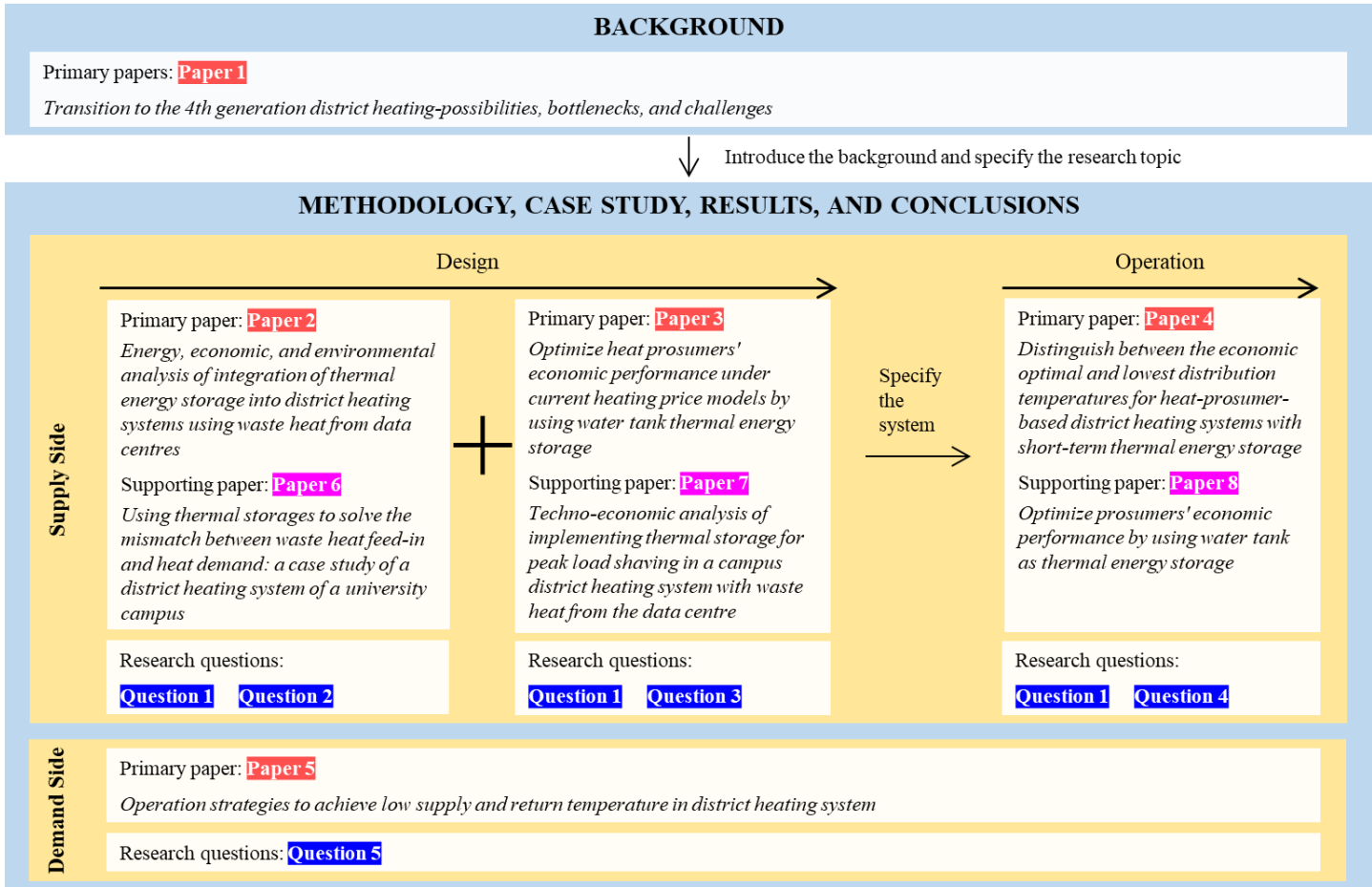

Figure 1-3. Overview of the publications collected in this thesis and their connections with the research questions

Additional papers:

Collaboration within the research project *Understanding Behaviour of District Heating Systems Integrating Distributed Sources* leads to further publications:

Paper 9:

Hou J, Li H, Nord N, Huang G. Model predictive control under weather forecast uncertainty for HVAC systems in university buildings. Energy and Buildings. 2021;20:111793.

Contribution: The type of this paper is Full Length Article. The author assisted in the creation of models, reviews, and commentary.

Paper 10:

Hou J, Li H, Nord N. Optimal control of secondary side supply water temperature for substation in district heating systems. E3S Web Conf. 2019;111:06015. The 13th REHVA World Congress CLIMA 2019.

Contribution: The type of this paper is Full Length Article. The author assisted in the review and commentary.

Paper 11:

Hou J, Li H, Nord N. Non-linear model predictive control for the space heating system of buildings in Norway. The 16th Conference on Sustainable Development of Energy, Water and Environment Systems.

Contribution: The type of this paper is Full Length Article. The author assisted in the review and commentary.

Paper 12:

Hou J, Li H, Nord N. Nonlinear model predictive control for the space heating system of a university building in Norway. Submitted to Journal of Energy (Status: Under review).

Contribution: The type of this paper is Full Length Article. The author assisted in the creation of models, reviews, and commentary.

2 BACKGROUND

This chapter introduces the thesis' economic and technological backgrounds. Firstly, the development of heat prosumers in the DH system is introduced. Following this, the pricing mechanism of the Scandinavian heating market is studied, leading to the answer to the first research question, **Question 1**. Finally, a generalized heat pricing model is developed to define the study's economic boundaries.

2.1 Heat prosumers in the DH system

In the energy sector, prosumers refer to the participants that can both produce and consume energy. Most of these prosumers are electricity prosumers coming from the power system, however, an increasing number of heat prosumers are starting to appear in the DH system in recent years, due to the trend of integrating renewable-based DHSs at the end-user side.

Heat prosumers can be classified into individual prosumers and community prosumers, based on the scale of connected end-users, i.e., a single building or a cluster of buildings. As shown with the upper right of Figure 2-1, an individual prosumer has a single building as the end-user. It may be a building installed with solar panels, a food store with waste heat from the refrigeration system, or an industrial building with waste heat from the production process. Individual prosumers facilitate the bidirectional heat flow between these individual buildings and the central DH network. Consequently, it makes it possible for small heat users to participate in the activities of the DH system actively, through controlling the heat production and consumption in real-time.

Similarly, a community prosumer integrates a cluster of buildings as the end-users. These buildings either belong to the same energy service agency or are geographically close and share common interests and goals. The block in the lower right of Figure 2-1 illustrates a community prosumer. The community prosumer may have a single DHS or multiple DHSs, meanwhile, the type of DHS may be renewable-based heating sources or fossil fuel-based heating plants. Some examples of DHSs for community prosumers are solar thermal plants, waste heat recovery facility of a data centre (DC), or micro combine heat and power plant. Different from the individual prosumer connecting the building to the central DH network directly, the community prosumer integrates a cluster of buildings into a regional micro-network and connects the

micro-network to the central DH network via the main substation (MS). Therefore, the community prosumer can be managed as a whole and act as a single heat participant in the DH system. The heat flow between the central DH system and the community prosumer is usually considerable, and hence the activity of the community prosumer may have an enormous impact on the central DH system.

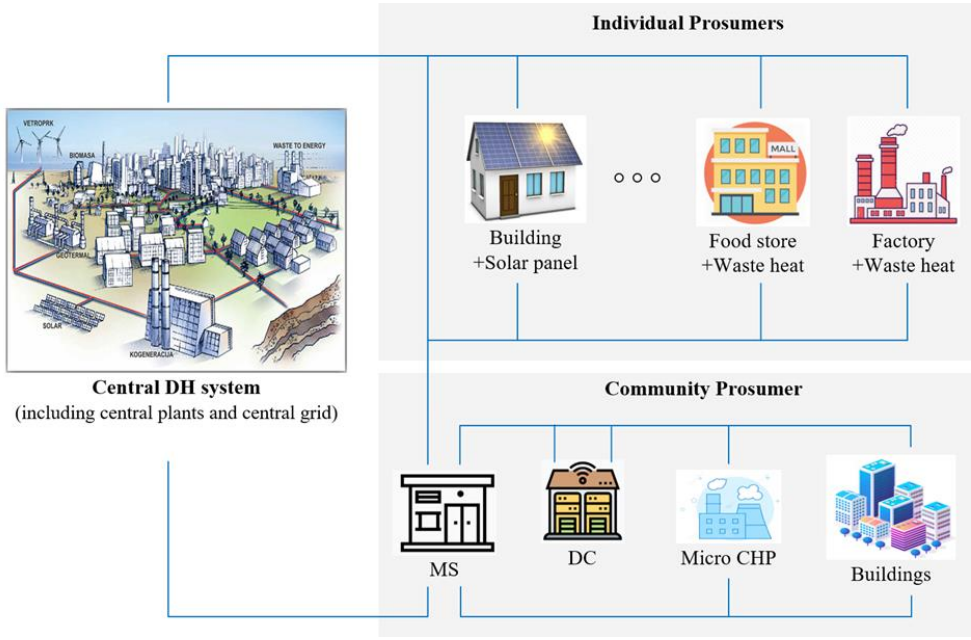

Figure 2-1. Schematic illustrates heat prosumers in a DH system (source: Paper 3)

There is a growing interest in heat prosumers in DH systems. Recent research has proposed methods to design and operate heat prosumers and demonstrated the economic benefits of introducing prosumers in DH systems. Marguerite et al. introduced a tool to optimize the design and operation of prosumer [36]. Nielsen et al. [37] and Brand et al. [38] investigated the impacts of prosumers on DH systems. Huang et al. reviewed the applications of DCs as prosumers in DH systems [39], and Kauko et al. studied the impacts of DCs and supermarkets as prosumers in DH systems [40]. Furthermore, some pioneer projects have successfully implemented heat prosumers in the real world. Open District Heating, led by the Swedish energy company Stockholm Exergi, is one of the leading projects [41]. In the project, excess heat mainly from DCs and supermarkets is sold to the central DH network at market prices. GleSYS is one

customer of the Open District Heating project. Excess heat from GleSYS's DC is delivered to the central DH network at a capacity of 1 MW, satisfying the heat demand of more than 1,000 apartments nearby. GleSYS makes a considerable long-term profit by selling the excess heat, meanwhile, it contributes to reducing carbon dioxide emissions in Stockholm, Sweden.

2.2 Heat pricing mechanism in current Scandinavian heating markets

Despite several DH companies providing "open" markets for customers - such as Stockholm Exergi who offers market prices for its customers to sell their excess heat under the project Open District Heating, most of the DH companies still maintain "close" heating markets that do not support the reverse heat supply from customers to the central DH network. Moreover, in most cases, heat pricing models applied to heat prosumers are the same as those applied to general heat users. In this thesis, these "close" heating markets applied to heat prosumers are called unidirectional heating markets, because they were developed in the conventional DH systems with unidirectional heat supply and have not been updated to address the new situation of bidirectional heat supply for heat-prosumer-based DH systems.

Based on the review article [12], the heat pricing models in the Scandinavian countries may include four components: energy demand component (EDC), load demand component (LDC), fixed component (FXC), and flow demand component (FDC). The EDC is charged based on heat users' heat use. It aims to cover the production cost, which mainly refers to the fuel cost. The LDC is usually charged according to the heat user's peak load. It reflexes DH companies' investment cost for new facilities, depreciation of existing facilities, and operating cost to maintain a certain level of heat generation capacity, etc. Generally, the FXC is also charged according to heat users' peak load. It is the connecting fee for heat users to stay in the heating network. The FDC is charged based on the volume of the circulating heat carrier, i.e. hot water. It aims to cover the electricity cost for heat delivery, meanwhile, it stimulates the lower return temperature. Among these four components, LDC and EDC are crucial, regarding both their existence and their proportion in a heat pricing model [12]. For example, based on a survey of heating bills in Sweden as presented in Figure 2-2, all the heating bills have the EDC and about 87% of the heating bills have the LDC. These two components together account for 96% of the total heating cost on average. In contrast, just about half of the heating bills have FXC and FDC, and the average share of the two components is less than 4%.

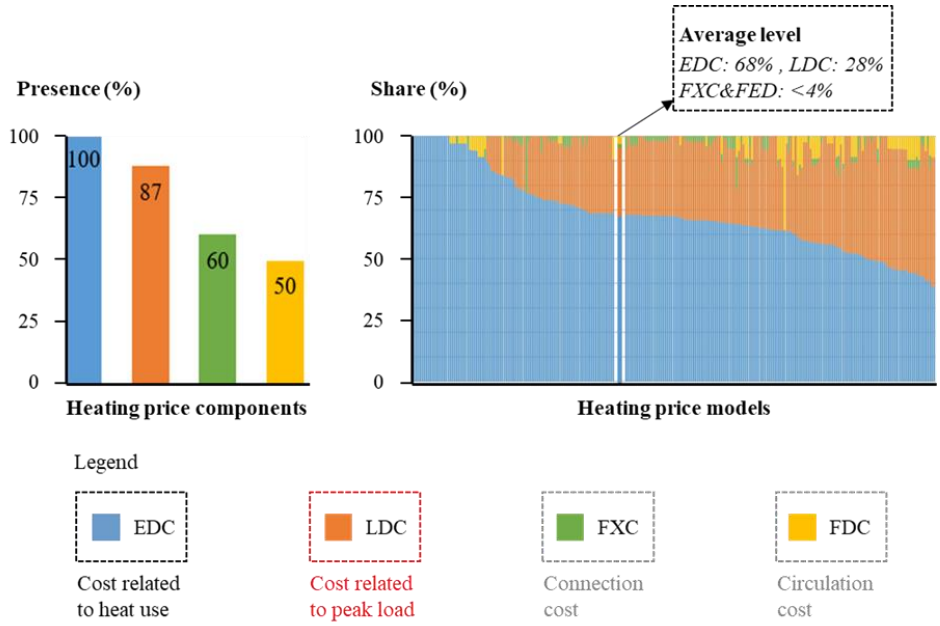

Figure 2-2. Presence and share of price components for investigated heating price models (source: Paper 4)

Based on the above explanation, the first research question of this thesis can be answered:

Question 1: What are crucial factors that impact heat consumers' heating costs in current Scandinavian heating markets?

Answer: Heat use and peak load, which determine the EDC and LDC heating cost, respectively.

2.3 Economic boundaries defined by a generalized heat pricing model

To establish generalized and simplified economic boundaries for this study, a generalized heat pricing model, which incorporates the identified critical factors, is developed. As presented in Equation (2-1), the generalized heat pricing model includes the EDC and LDC heating costs as:

$$C_{tot} = C_{ldc} + C_{edc} \quad (2\text{-}1)$$

where C_{tot} is the total heating cost, C_{ldc} and C_{edc} are the LDC and EDC heating costs, respectively.

The EDC, C_{edc}, depends on heat use flow rate and real-time heating price as defined in Equation (2-2):

$$C_{edc} = \int_{t_0}^{t_f} EP(t) \cdot \dot{Q}(t) dt \tag{2-2}$$

where $\dot{Q}(t)$ is the heat flow rate supplied to the heat user and $EP(t)$ is the EDC heating price.

The LDC, C_{ldc}, depends on the peak load and price of the peak load as calculated in Equation (2-3):

$$C_{ldc} = LP \cdot \dot{Q}_{pea} \tag{2-3}$$

where LP is the LDC heating price, and $\dot{Q}_{pea}$ is the yearly peak load according to [42, 43].

BACKGROUND

3 METHODOLOGY

This chapter explains the methodology of the thesis. Section 3.1 introduces the computing tools used in this study, including modelling language and computing platforms. Section 3.2 proposes candidate systems for heat-prosumer-based DH systems that featured different TES solutions. Section 3.3 introduces indicators to evaluate the economic performance of these candidate systems. Section 3.4 presents the modelling and simulation method that supported the evaluation and selection of the candidate systems. Section 3.5 introduces the modelling and optimization method that facilitated the optimal operation and sizing of the selected system. Finally, Section 3.6 explains the modelling and simulation method that assisted in investigating the operation of the heating system at the demand side.

3.1 Modelling language and computing platforms

The main tasks of this study were computer-aided design (CAD) and computer-aided operation (CAO) of heat-prosumer-based DH systems with TESs. The key features of this study are summarized as follows:

- A wide range of research, covering both the supply and demand sides of the DH system, as well as their control systems.
- A whole process of study, including concept design, system modelling, simulation, optimization, system evaluation, and optimal sizing.

To accomplish the above tasks, the selected modelling language and computing platforms should have the following merits:

- Modelling language: The capability of modelling complex thermal systems, and a given preference to those modelling languages with relevant libraries.
- Computing platform: The compatibility with the selected modelling language; the capability to conduct both simulation and optimization; and the ability to compute large-scale complex dynamic systems using state-of-the-art algorithms.

- General merits: The interaction with at least one general-purpose programming language that scripts and automates the compilation, simulation, optimization, results logging, and data visualization processes.

Based on the above-required merits, Modelica language was chosen as the modelling language, Dymola was selected as the modelling and simulation environment, JModelica.org was used as the optimization platform, and Python was applied as the general-purpose programming language. Meanwhile, the open-source libraries *Modelica Standard Library* and *Modelica IBPSA Library* were used to build the system model. These computing tools are briefly introduced as follows.

The Modelica language is a non-proprietary, object-oriented, and equation-based modelling language to model complex physical systems [44]. Its features make it capable of modelling building energy and control systems. Firstly, Modelica is a high-level modelling language rather than a conventional programming language. It allows people to focus on high-level mathematical descriptions of component behaviours without extensive knowledge of computer science. Secondly, Modelica can model systems in most engineering domains, e.g. hydraulic, thermal, and control systems. Therefore, the building energy and control systems can be seamlessly modelled in a single language. Moreover, Modelica has a wide range of open-source libraries, e.g. *Modelica Standard Library* developed by the Modelica Association [45] and *Modelica IBPSA Library* developed through the organization of IBPSA Project 1 [46], codifying best practices for modelling building and control systems at both urban and building scales. Thirdly, Modelica is object-oriented. New models can be built by modifying existing models, therefore, repetitive work can be avoided when building models for multiple scenarios.

Dymola is a complete environment for model creation, testing, simulation, and post-processing [47]. The merits of Dymola are listed as follows. Firstly, Dymola's intuitive modelling mode makes it convenient to model physical systems through drag-and-drop processes. Secondly, Dymola has high and robust performance for computing Modelica based models.

JModelica.org is a platform for numerically solving large-scale dynamic optimization problems that are described in Modelica language [48]. Some advantages of JModelica.org are listed as follows. Firstly, JModelica.org integrates many prominent software packages in the dynamic optimization platform. It has state-of-the-art techniques to transcribe and solve optimization

problems. Secondly, JModelica.org supports the interaction with Python. Thus, the compilation, simulation, optimization, results logging, and data visualization processes can be scripted and automated in a Python interface.

3.2 Candidate systems for heat-prosumer-based DH systems with TESs

In the candidate system design phase, three types of candidate systems were developed to integrate TESs into heat-prosumer-based DH systems. These candidate systems offered several TES solutions, including short-term TES, seasonal TES, and a combination of short-term and seasonal TES. In this phase, suitable TES technologies were identified through a literature review. As explained in the report from the International Energy Agency [49], the widely recognized and commonly used TESs for DH systems are water tank thermal energy storage (WTTES), borehole thermal energy storage (BTES), pit thermal energy storage, and aquifer thermal energy storage. In this study, WTTES was chosen as the short-term TES due to its merits such as:

- Wide applicability that does not subject to geological conditions [50, 51].
- High storage efficiency with well-insulated envelopes [49].
- High-performance on load shifting and peak shaving due to high charging and discharging heat flow rate [49].
- Small installation space because of the high specific heat capacity of water [49].

Meanwhile, BTES was chosen as the seasonal TES because of the following reasons:

- It can easily scale up its storage size to adapt to the expansion of DH systems [49].
- It can be easily integrated with surroundings, e.g. being installed under playgrounds, under parks, and inside building foundations [14].
- Low specific storage cost, especially for large scale installations [49].

Besides the above candidate systems, a reference system that presented the situation before introducing any TES was proposed. The reference system was used as a benchmark. Figure 3-1 illustrates the candidate systems and the reference system. A brief description of these systems is given as follows.

The reference system *REF* presented a typical heat-prosumer-based DH system without any TES. The main components were MS, DHS, and buildings. The MS connected the heat prosumer's regional DH system with the central DH system, meanwhile, it separated the hydraulic conditions of these two systems. The MS had two functions. Firstly, it supplemented the heat supply from the DHS. Secondly, it boosted the supply temperature of the heat prosumer's regional DH system to the required level. The DHS was a low-temperature heat source based on renewables or waste heat. It was integrated into the prosumer's regional DH system by the R2R mode, i.e., extracts the water from the return line and then feeds it back to the return line after the heating process. The R2R mode was used because it is preferable for low-temperature heat sources [4]. The buildings, as introduced in Section 2.1, can be a cluster of buildings or a single building.

The candidate system *REF+WT* integrated a WTTES into the reference system. The WTTES functioned as the short-term TES. It aimed to relieve the mismatch between buildings' heat demand and DHS's heat supply, meanwhile, it serviced for the peak load shaving.

The candidate system *REF+BTES* integrated a BTES system, including an HP, a heat exchanger (HE), and a borehole field, into the reference system. The BTES system functioned as the seasonal TES and it aimed to transfer DHS's surplus heat from the non-heating season to the heating season. The HE of the BTES system was used to charge the surplus heat into the borehole field during the non-heating season, while the HP of the BTES system was used to discharge the stored heat from the borehole field during the heating season.

The candidate system *REF+WT+BTES* integrated both a WTTES and a BTES system into the reference system. It took advantage of the two types of TES systems. The following functions were achieved by this system: relieving the short-term mismatch, shaving the peak load, and transferring the surplus heat from the non-heating season to the heating season.

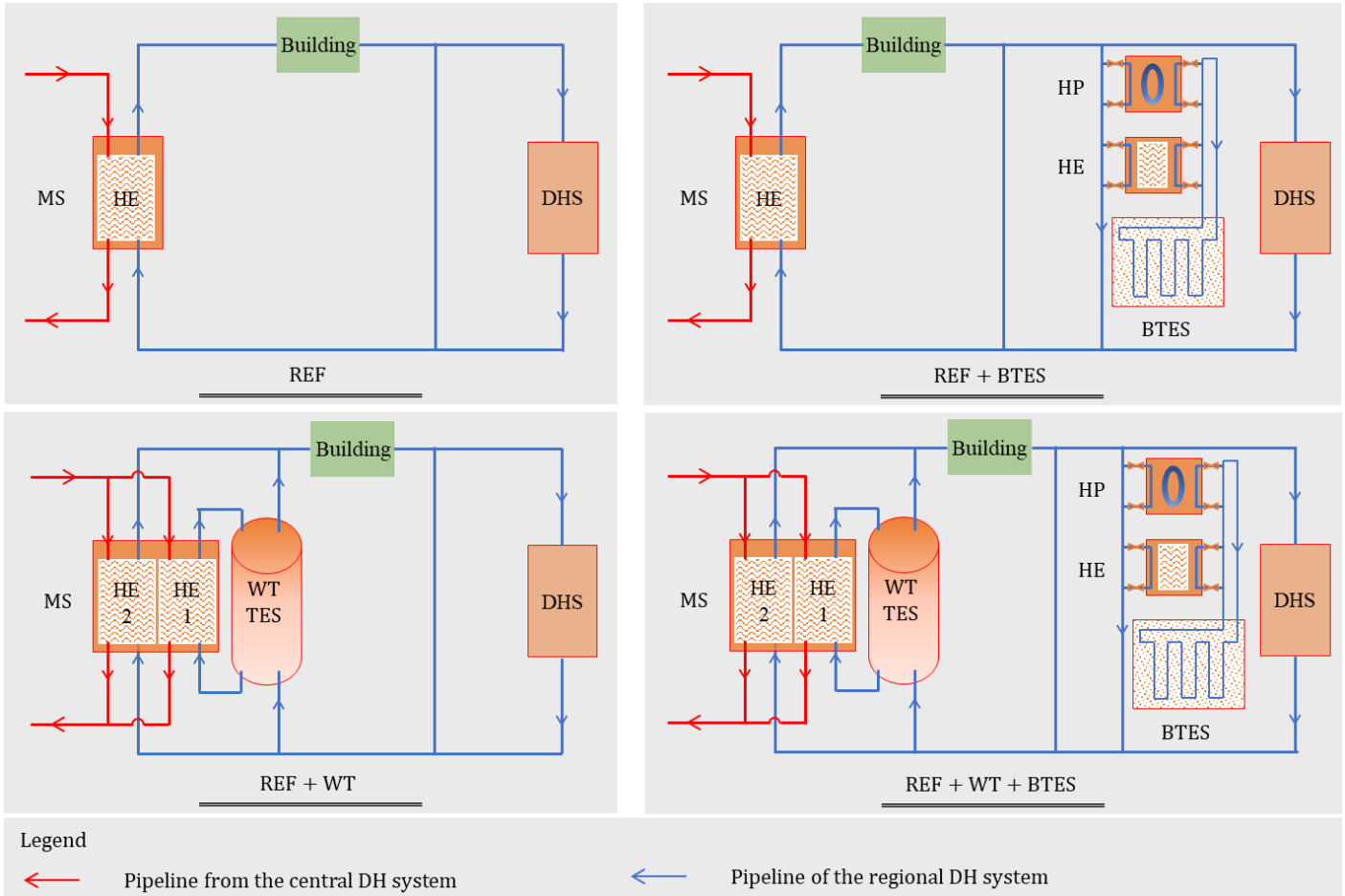

Figure 3-1. Schematic illustrates the candidate systems for heat-prosumer-based DH systems with TESs

3.3 Economic indicators to evaluate heat-prosumer-based DH system

This section introduces indicators to evaluate the economic performance of the heat-prosumer-based DH system. These indicators include the initial investment of TESs, the energy bills of heat prosumers, and the payback period of TESs.

3.3.1 Initial investment for introducing TESs

The initial investment required for a TES system varies with the storage type and strongly depends on the storage size. Figure 3-2 illustrates the relationship between the initial investment and the size of a WTTES and a BTES system. The solid black dots in Figure 3-2 represent the previous projects [49]. Figure 3-2 shows that power functions approximate the relationship very well, with coefficients of determination (R^2) higher than 0.8 and no obvious overfitting. In this study, the power functions were used to estimate the initial investment for the TES system.

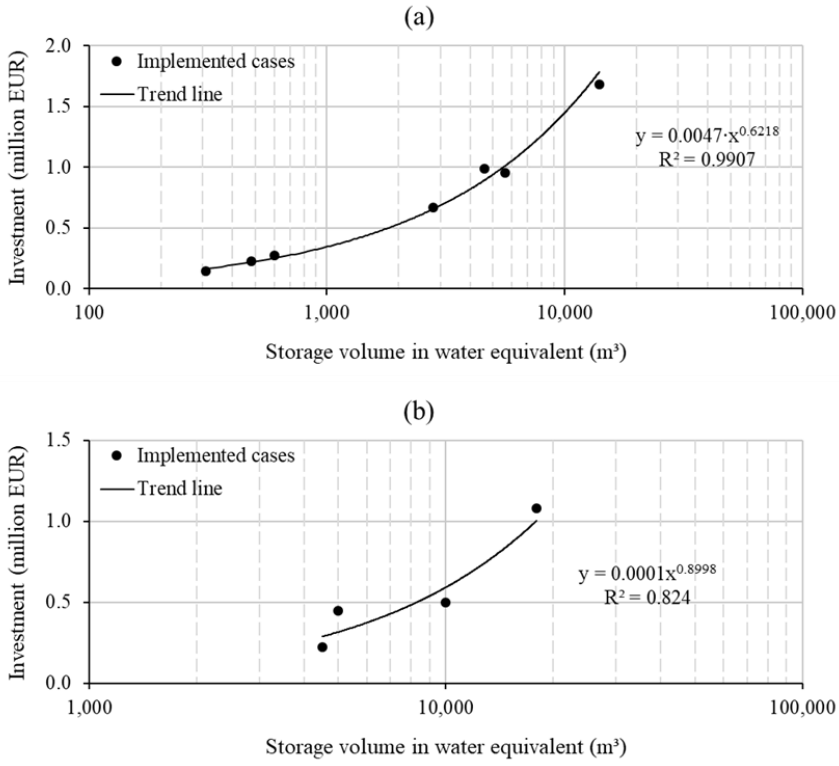

Figure 3-2. Investment for TESs under different storage volume in water equivalent, (a) WTTES and (b) BTES (source: Paper 2)

For the BTES system, the initial investment of HP was also considered. The unit cost of the HP was assumed to be 0.8 million EUR/MW, based on a report that studied large scale HPs for DH systems [52].

3.3.2 Energy bill for heat-prosumer-based DH system

The energy costs included the heating and electricity bills. The heating bill contains two parts: EDC and LDC, as presented in Equation (2-1) by the generalized heat pricing model from Section 2.

Similarly, the electricity bill includes a fixed part and a variable part, while the fixed part in Norway is determined by electricity use. However, a simplified electricity bill calculation method was proposed in Equation (3-1). This method assumed that the electricity bill contained only the variable part, and it was a function of electricity use. The equivalent electricity price is calculated by dividing the total electricity cost (including fixed and variable parts) by the electricity use, the value of which was estimated using the national statistics data. The equivalent electricity cost was calculated as:

$$B_{elec} = E_{elec} \cdot P_{elec} \tag{3-1}$$

where B_{elec} is the electricity cost, E_{elec} is the electricity use, and P_{elec} is the equivalent electricity price.

3.3.3 Payback period for introducing TESs

The payback period is the time taken to fully recover the initial investment. It is one of the most commonly used methods for evaluating initial investments [53]. The payback period PB is calculated using the following equation:

$$B_{sav} \cdot \frac{(1+i)^{PB} - 1}{i \cdot (1+i)^{PB}} - Invt = 0 \tag{3-2}$$

where B_{sav} is the annual energy bill saving. $Invt$ is the initial investment of the TES. i is the prevailing interest rate.

3.4 Modelling and simulation of heat-prosumer-based DH systems with TESs

This section briefly introduces the method to address the second research question - **Question 2**: Which TES solution is superior for heat-prosumer-based DH systems? A more comprehensive description of the methods can be found in **Paper 2**.

Firstly, detailed Modelica models were developed for the candidate systems and the reference system proposed in Section 3.2. These models were obtained by connecting model components, including the MS, buildings, DHS, WTTES, and BTES system. The *Modelica Standard Library* [54] and the *Modelica Library of IBPSA Project 1* [55] were used to build these model components. Afterwards, the developed models were simulated in the Dymola environment, and the results were evaluated using the proposed indicators in Section 3.3. The information on the model components and the simulation scenarios are presented in the text below.

3.4.1 Main substation model

The MS connected the central DH system to the regional DH system. It had two functions. First, it supplemented the heat supply when the DHS could not cover the heat demand. Second, it further boosted the supply temperature when the supply temperature from the DHS was insufficient for the building system. The MS component was assembled by the following elements: HE, connecting pipelines of the central DH system, and connecting pipelines of the prosumer's regional DH system. The model structure is illustrated in Figure 3-3.

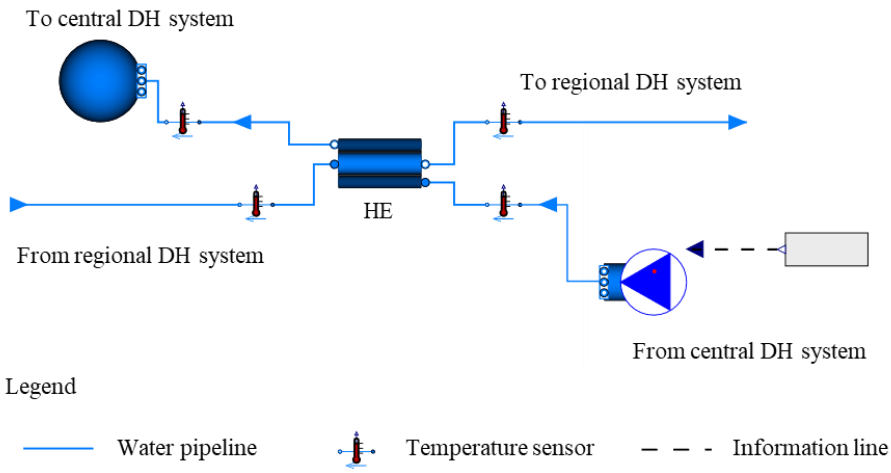

Figure 3-3. Main substation model (source: Paper 2)

3.4.2 Buildings model

A single-equivalent building model was used to represent the overall performance of all the buildings. The properties of the equivalent building were obtained by summing or averaging the properties of individual buildings. For example, the area of the exterior wall of the equivalent building was calculated by summing the corresponding values for all the buildings, and the U-value of the exterior wall of the equivalent building equalled the weighted average value of the corresponding values of all the buildings. The equivalent building model enabled increased computational efficiency, while maintaining simulation accuracy. As illustrated in Figure 3-4, the building model contained six modules: building envelope, internal heat gain, SH system, DHW system, ventilation system, and weather.

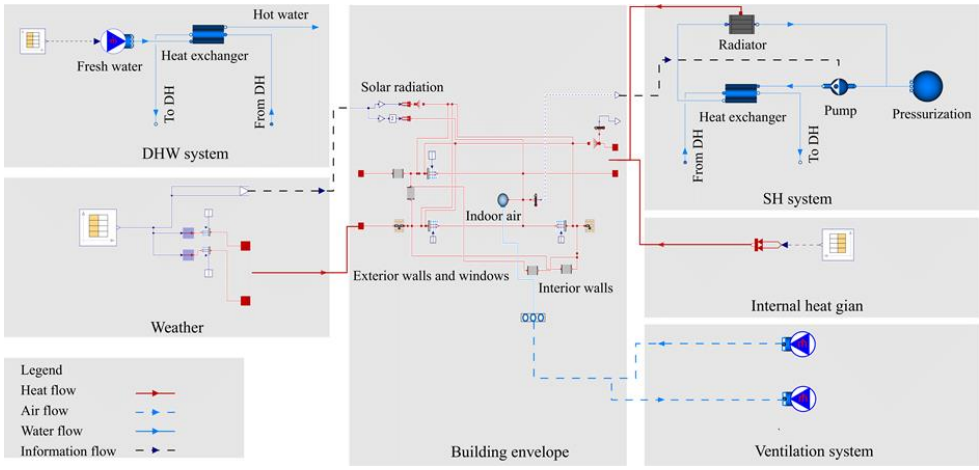

Figure 3-4. Buildings model (source: Paper 2)

3.4.3 Distributed heat source model

In this study, a waste heat recovery facility for a DC was selected as the example DHS. The reason for this was because a real DH system with a DC as the DHS is located at the author's university, and detailed measurement data could be achieved from the university's energy management platform. The model structure of the DC waste heat recovery system is illustrated in Figure 3-5. The key components were an HP and a cooling tower. The HP connected DC's cooling system to the campus DH system. Its evaporator side produced chilled water for the cooling system, meanwhile, its condenser side fed waste heat into the campus DH system. The

cooling tower was used to guarantee the safe operation of DC's cooling system. It started to work when the incoming water temperature at the condenser side exceeded the safety level.

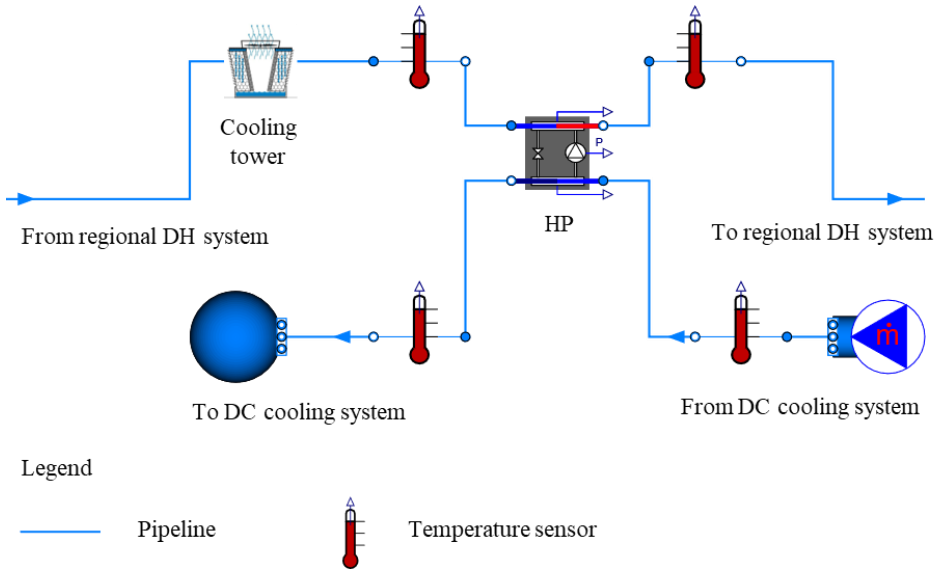

Figure 3-5. DC waste heat recovery system model (source: Paper 2)

3.4.4 Thermal energy storage systems model

A WTTES model and a BTES system model were developed. To achieve high charging and discharging heat flow rate, a direct connected WTTES, without HE to transfer heat between the water of the DH network and the water inside the tank, was used. As illustrated in Figure 3-6, the WTTES model used several sections to represent stratification, and the thermal dynamics of each section were described by the laws of energy conservation.

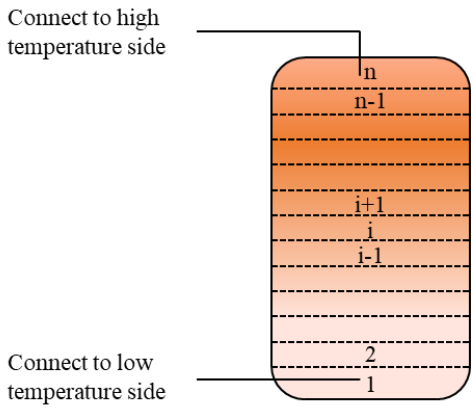

Figure 3-6. WTTES model (based on the user's guide of the AixLib library [56])

In addition, as illustrated in Figure 3-7, the key components of the BTES system model were HP, water pump, pressurization system, and BTES (borehole field). The borehole field consisted of parallel-connected U-tube borehole heat exchangers, with a uniform depth and distance. The borehole field model calculated the thermal dynamics using an axial discretized resistance-capacitance network.

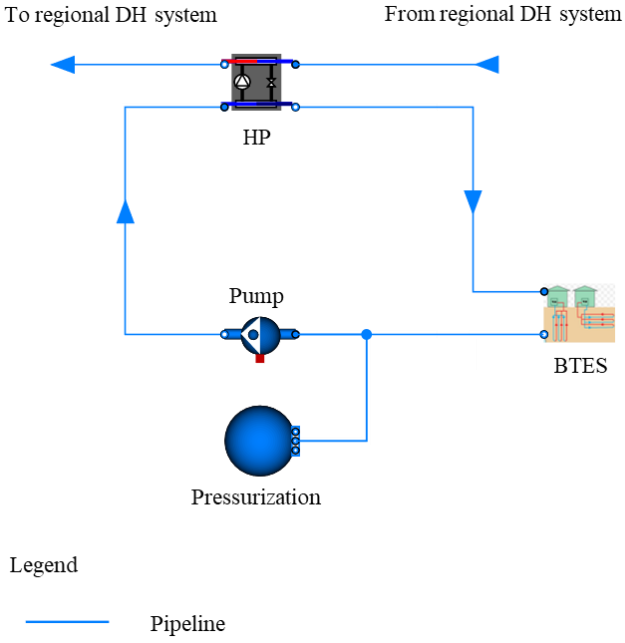

Figure 3-7. BTES system model (source: Paper 2)

3.4.5 Simulation scenarios

Four simulation scenarios were designed, representing the proposed candidate systems and the reference system in Section 3.2. The system models of these scenarios were built using the model components described in Sections 3.4.1-3.4.4. The operation strategies of these scenarios were introduced as follows.

The reference scenario *Ref* was used as the benchmark. The control system of this scenario included two levels: the heat source level and the building level. As illustrated in Figure 3-8, the heat source level was serviced for the MS and the DHS (waste heat recovery facility of the DC). For the control system of the MS, a proportional-integral (PI) controller was used to track the reference signal of the secondary side supply temperature by adjusting the primary side water flow rate. The reference signal of the secondary side supply temperature was generated by a weather compensation (WC)-based controller. The PI controller in combination with the WC-based controller performed the tasks using a PI function and a WC function, respectively. For the control system of the DC, a PI controller was used to track the reference signal of the evaporator side outlet temperature by adjusting the HP's power input. The reference signal of the evaporator side outlet temperature was determined by the cooling system of the DC. The building level control system, as illustrated in Figure 3-9, served for the SH system and the DHW system inside the building. There was one building substation consisting of two HEs, one was for the SH system and the other one was for the DHW system. For the control system of the SH system, a PI controller was used to track the reference signal of the secondary side supply temperature by adjusting the primary side water flow rate. The reference signal of the secondary side supply temperature was generated by a WC-based controller. In addition, a PI controller was used to track the reference signal of the indoor air temperature by adjusting the secondary side water flow rate. For the control system of the DHW system, a PI controller was used to track the reference signal of the tap water side outlet temperature by adjusting the DH side water flow rate.

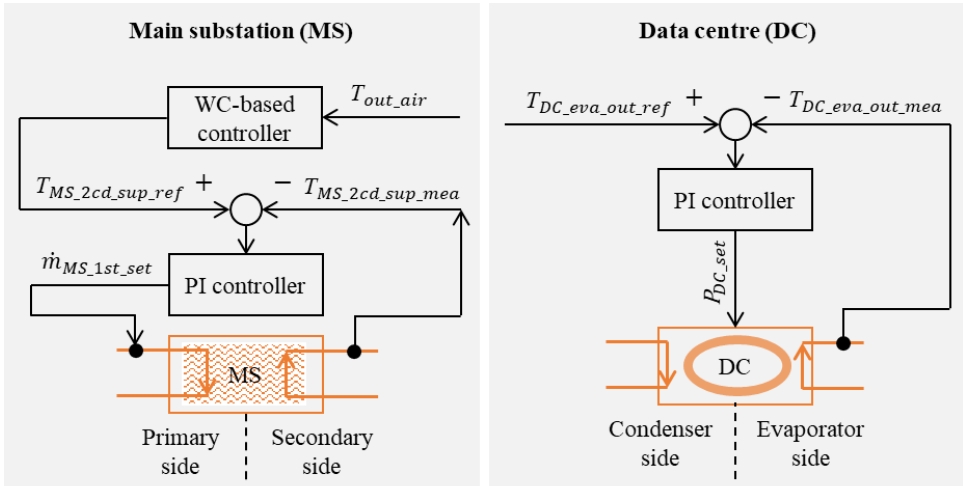

Legend:

T_{out_air}	outdoor air temperature
$T_{MS\_2cd\_sup\_ref}$	reference signal of the secondary side supply temperature of the MS
$T_{MS\_2cd\_sup\_mea}$	measured value of the secondary side supply temperature of the MS
$\dot{m}_{MS\_1st\_set}$	setting signal of the primary side water flow rate of the MS

Legend:

$T_{DC\_eva\_out\_ref}$	reference signal of the evaporator side outlet temperature of the DC
$T_{DC\_eva\_out\_mea}$	measured value of the evaporator side outlet temperature of the DC
P_{DC_set}	setting signal of the HP's power input of the DC

Figure 3-8. Heat source level control system (based on Paper 2)

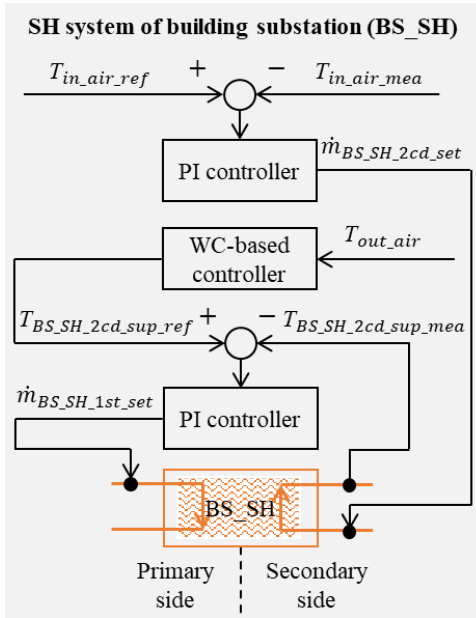

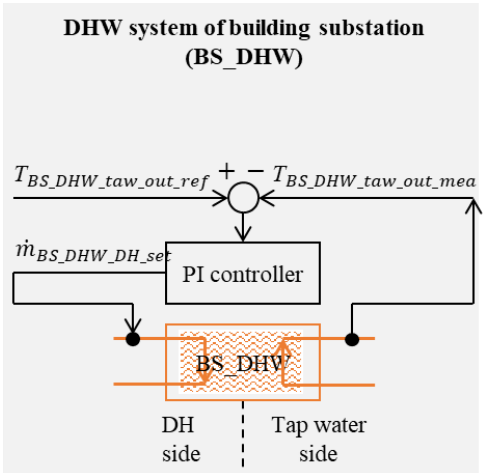

Legend:

T_{out_air}	outdoor air temperature
$T_{in\_air\_ref}$	reference signal of the indoor air temperature
$T_{in\_air\_mea}$	measured value of the indoor air temperature
$\dot{m}_{BS\_SH\_2cd\_set}$	setting signal of the secondary side water flow rate of the BS_SH
T_{out_air}	outdoor air temperature
$T_{BS\_SH\_2cd\_sup\_ref}$	reference signal of the secondary side supply temperature of the BS_SH
$T_{BS\_SH\_2cd\_sup\_mea}$	measured value of the secondary side supply temperature of the BS_SH
$\dot{m}_{BS\_SH\_1st\_set}$	setting signal of the primary side water flow rate of the BS_SH

Legend:

$T_{BS\_DHW\_taw\_out\_ref}$	reference signal of the tap water side outlet temperature of the BS_DHW
$T_{BS\_DHW\_taw\_out\_mea}$	measured value of the tap water side outlet temperature of the BS_DHW
$\dot{m}_{BS\_DHW\_DH\_set}$	setting signal of the DH side water flow rate of the BS_DHW

Figure 3-9. Building level control system (based on Paper 2)

Scenario *Ref+WT* presented the candidate system with the WTTES. Compared with the control system of the reference scenario, a TES level with the control system for the WTTES was added. As illustrated in Figure 3-10, the control system of WTTES used a switch controller to switch the signals between the heating season and the non-heating season. In both the heating season and the non-heating season, a PI controller was used for shifting the heat load. However, in the non-heating season, a PI controller was used to solve the mismatch problem by adjusting the charging and discharging water flow rate, based on the deviation between the measured buildings' heat demand and DC's waste heat supply. In the heating season, a PI controller was used to shave the peak load above the predefined threshold by adjusting the charging and discharging water flow rate. In addition, the charging process on the source side and the discharging process on the user side were not conducted simultaneously i.e. a charging process on the source side meant no action on the user side and vice versa. These opposite signals were generated by the control component of the signal processing block by reversing the input signal to get the output signal.

Scenario *Ref+BTES* presented the candidate system with the BTES. Compared with the control system of the reference scenario, a TES level with the control system for the BTES was added. As illustrated in Figure 3-10, the control system of BTES used a switch controller to switch the signals between the heating and non-heating seasons. During the heating season, a PI controller was used to shave the MS's heat load to a predefined threshold by adjusting the HP's power input. However, during the non-heating season, the HP was on the OFF status with a power input of zero. In addition, an ON-OFF controller was used to manipulate the status of HE's water valves, with the ON and OFF statuses for the non-heating and heating season, respectively. Meanwhile, a NOT gate controller was used to manipulate the status of HP's water valves by reversing the status signal coming to the HE's water valves.

Scenario *Ref+WT+BTES* presented the candidate system with both the WTTES and the BTES system. Compared with the control system of the reference scenario, a TES level with the control systems for the WTTES and the BTES was added. The control logic of the TES level was identical to Scenarios *Ref+WT* and *Ref+BTES*, except for the predefined thresholds. As illustrated in Figure 3-11, the peak load was divided into two parts: the upper and bottom parts. The upper-part peak load appeared only at peak hours and was shaved by the WTTES; while the bottom-part peak load could last for several days and was shaved by the BTES system.

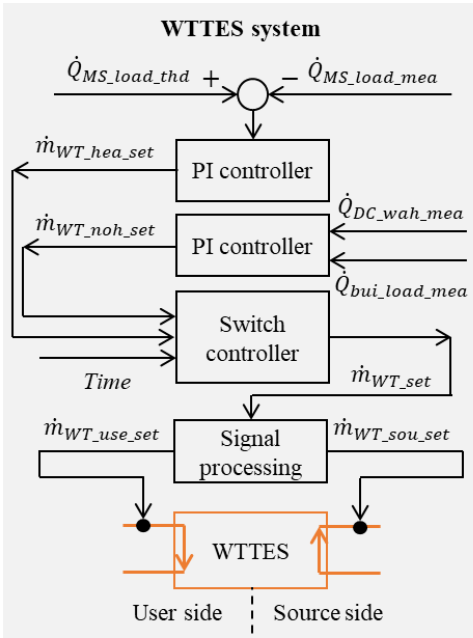

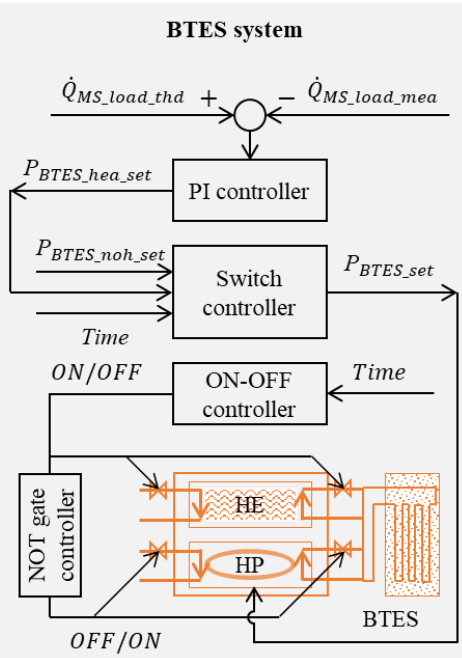

Legend:

$\dot{Q}_{MS\_load\_thd}$	threshold of the MS heat load
$\dot{Q}_{MS\_load\_mea}$	measured value of the MS heat load
$\dot{m}_{WT\_hea\_set}$	setting signal of the water flow rate of the WTTES in the heating season
$\dot{Q}_{DC\_wah\_mea}$	measured value of the DC waste heat supply
$\dot{Q}_{bui\_load\_mea}$	measured value of the buildings heat load
$\dot{m}_{WT\_noh\_set}$	setting signal of the water flow rate of the WTTES in the non-heating season
$\dot{m}_{WT\_set}$	setting signal of the water flow rate of the WTTES
$\dot{m}_{WT\_use\_set}$	setting signal of the user side water flow rate of the WTTES
$\dot{m}_{WT\_sou\_set}$	setting signal of the source side water flow rate of the WTTES

Legend:

$\dot{Q}_{MS\_load\_thd}$	threshold of the MS heat load
$\dot{Q}_{MS\_load\_mea}$	measured value of the MS heat load
$P_{BTES\_hea\_set}$	setting signal of the HP's power input in the heating season
$P_{BTES\_noh\_set}$	setting signal of the HP's power input in the non-heating season
P_{BTES_set}	setting signal of the HP's power input

Figure 3-10. TES level control system (based on Paper 2)

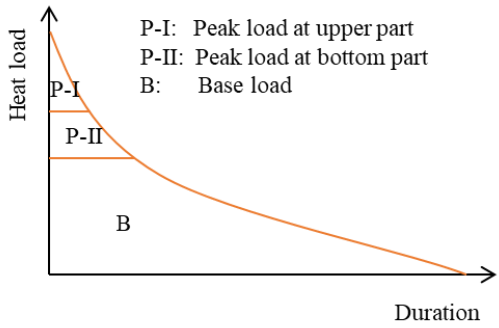

Figure 3-11. Heat load duration curve

3.5 Modelling and optimization of heat-prosumer-based DH systems with TESs under dynamic heating price market

This section followed the research results of Section 3.4, by which the WTTES was identified as a preferred TES solution. It introduces the methods to address the third and fourth research questions- **Question 3** and **Question 4**, which is "What is the economically optimal size for the selected TES?" and "What is the economically optimal distribution temperature for heat-prosumer-based DH systems with TES?", respectively. A comprehensive description of the work is presented in **Paper 3** and **Paper 4**.

Firstly, an economic optimization problem was formulated to minimize the energy cost of heat-prosumer-based DH systems with WTTESs. Afterwards, the size parameter of WTTES was swept when solving the optimization problem to obtain the optimal storage size considering the trade-off between the payback period and the heating cost saving. Finally, the optimal distribution temperature for the heat-prosumer-based DH system with the WTTES was investigated. Different from the detailed model used for the simulation task in Section 3.4, this section developed a simplified Modelica model for optimization, aiming to achieve high computational tractability and numerical stability. The developed simplified model was processed in the JModelica.org platform facilitating the optimization task.

3.5.1 Formulation of the optimization problem

As introduced in Section 2.2, the developed generalized heat pricing model included the EDC and the LDC, which were determined by heat use and peak load, respectively. To optimize prosumers' economic performance, the optimal operation strategy should minimize prosumers'

heat use from the central DH system by increasing the self-utilization rate of the heat supply from the prosumer's DHSs, meanwhile, it should minimize the prosumers' peak load. In addition, the operation should track the reference indoor temperature by minimizing the deviation between the simulated indoor temperature and its reference value. To achieve the above goals, a multi-objective dynamic optimization problem was formulated as Equations (3-3), (3-4), (3-5), (3-6), and (3-7):

Minimize:

$$\int_{t_0}^{t_f} EP(t) \cdot \dot{Q}(t)dt + LP \cdot \dot{Q}_{pea} + W \cdot \int_{t_0}^{t_f} (T_{ia}(t) - T_{ia}^{ref}(t))^2 \cdot dt \quad (3\text{-}3)$$

subject to:

$$\dot{Q}(t) \leq \dot{Q}_{pea} \quad (3\text{-}4)$$

$$F(t, \boldsymbol{z}(t)) = 0 \quad (3\text{-}5)$$

$$F_0(t_0, \boldsymbol{z}(t_0)) = 0 \quad (3\text{-}6)$$

$$z_L \leq \boldsymbol{z}(t) \leq z_U \quad (3\text{-}7)$$

where the first and second term of Equation (3-3) is the EDC and the LDC heating cost, respectively. The last term of Equation (3-3) is the deviation between the achieved indoor temperature and its reference value, which aims to take the advantage of building thermal inertia by softening the constraint of the indoor temperature. $EP(t)$ and LP is the heating price for the EDC and the LDC, respectively. $\dot{Q}(t)$ is the heat supply flow rate from the central DH system to the heat prosumer and $\dot{Q}_{pea}$ is the corresponding peak load. $T_{ia}(t)$ and $T_{ia}^{ref}(t)$ are the achieved indoor temperature and its reference value, respectively. Equation (3-5) defines the dynamics of the heat-prosumer-based DH system with WTTES, and Equation (3-6) specifies the initial conditions of this system. $\boldsymbol{z} \in \mathbb{R}^{n_z}$ are the time-dependent variables, including the manipulated variables $\boldsymbol{u} \in \mathbb{R}^{n_u}$, the differential variables $\boldsymbol{x} \in \mathbb{R}^{n_x}$, and the algebraic variables $\boldsymbol{y} \in \mathbb{R}^{n_y}$. $z_L \in [-\infty, \infty]^{n_z}$ and $z_U \in [-\infty, \infty]^{n_z}$ represent the lower bounds and upper bounds, respectively.

This dynamic optimization problem contained manipulated variables that represented heat-supply-side and heat-demand-side management. For the heat-supply-side management that aimed to optimize the DH system's distribution temperature, the manipulated variables were the supply temperature and the water mass flow rate of the MS. For the heat-demand-side

management that responded to the heat-supply-side management, the manipulated variables were the water mass flow rate of the buildings and the heat flow rate from the radiator to the buildings. In addition, to conduct the optimal sizing of TES, in **Paper 3** different size parameters for the WTTES were swept and the optimization problem was computed multiple times.

As introduced above, the optimization problem used a simplified model. The system dynamics defined in Equation (3-5) included the dynamics of the building, WTTES, and pipelines. The energy and mass flow exchanged between these components were described by Equations (3-8), (3-9), (3-10), (3-11), and (3-12) as:

$$\dot{Q}(t) = \dot{Q}_{HE1} + \dot{Q}_{HE2} \tag{3-8}$$

$$\dot{Q}_{HE1} + \dot{Q}_{HE2} + \dot{Q}_{DHS} = \dot{Q}_{Bui} + \dot{Q}_{TES} + \dot{Q}_{loss,TES} + \dot{Q}_{loss,pip} \tag{3-9}$$

$$\dot{Q}_{HE1} = c \cdot \dot{m}_{HE1} \cdot (T_{HE1,sup} - T_{HE1,ret}) \tag{3-10}$$

$$\dot{Q}_{HE2} = c \cdot \dot{m}_{HE2} \cdot (T_{HE2,sup} - T_{HE2,ret}) \tag{3-11}$$

$$\dot{Q}_{DHS} = c \cdot \dot{m}_{DHS} \cdot (T_{DHS,sup} - T_{DHS,ret}) \tag{3-12}$$

where $\dot{m}_{HE1}$, $\dot{m}_{HE2}$, and $\dot{m}_{DHS}$ are the mass flow rates of HE1, HE2, and DHS, respectively. $\dot{Q}_{HE1}$, $\dot{Q}_{HE2}$, and $\dot{Q}_{DHS}$ are the heat flow rates of HE1, HE2, and DHS, respectively. $\dot{Q}_{TES}$ is the charging (positive values) and discharging (negative values) heat flow rate of the WTTES. $\dot{Q}_{Bui}$ is the heat demand of buildings. $\dot{Q}_{loss,TES}$ and $\dot{Q}_{loss,pip}$ are the heat loss from the WTTES and pipelines, respectively. $T_{HE1,sup}$, $T_{HE2,sup}$, and $T_{DHS,sup}$ are the supply water temperature of HE1, HE2, and DHS, respectively. $T_{HE1,ret}$, $T_{HE2,ret}$, and $T_{DHS,ret}$ are the return water temperature of HE1, HE2, and DHS, respectively. c is the specific heat capacity of water.

The modelling methods of individual components are briefly introduced in the following sections.

3.5.2 Simplified model for the buildings

The simplified buildings model included two parts: 1) an equality constraint that defined the correlation between buildings' heating demand, water flow rate, and water temperature as Equation (3-13); and 2) inequality constraints that defined the bounds of water flow rate and water temperature as Equations (3-14), (3-15), and (3-16).

$$\dot{Q}_{Bui} = c \cdot \dot{m}_{Bui} \cdot (T_{sup} - T_{ret}) \quad (3\text{-}13)$$

$$\dot{m}_{Bui,L} \leq \dot{m}_{Bui} \leq \dot{m}_{Bui,U} \quad (3\text{-}14)$$

$$T_{sup,L} \leq T_{sup} \leq T_{sup,U} \quad (3\text{-}15)$$

$$\Delta T_{Bui,L} \leq \Delta T_{Bui} = T_{sup} - T_{ret} \leq \Delta T_{Bui,U} \quad (3\text{-}16)$$

where $\dot{Q}_{Bui}$ is the buildings' heat demand including demand for the SH and the DHW system. $\dot{m}_{Bui}$ and ΔT_{Bui} are the mass flow rate and the temperature difference of the water at the primary side of the building's substation, respectively. T_{sup} and T_{ret} are the supply and return temperature of the water at the primary side of the building's substation, respectively. $\Delta T_{Bui,L}$, $T_{sup,L}$, and $\dot{m}_{Bui,L}$ are the lower bounds of ΔT_{Bui}, T_{sup}, and $\dot{m}_{Bui}$, respectively. $\Delta T_{Bui,U}$, $T_{sup,U}$, and $\dot{m}_{Bui,U}$ are the upper bounds of ΔT_{Bui}, T_{sup}, and $\dot{m}_{Bui}$, respectively. c is the specific heat capacity of water.

The lower bound of the supply temperature, $T_{sup,L}$, should be high enough for the SH system and the DHW system to keep a comfortable indoor temperature and avoid hygiene issues, as defined in Equation (3-17). The lower bound of the supply temperature was defined by Equation (3-18) for the SH system [57], and the lower bound of the supply temperature for the DHW system was 60℃ as defined in Equation (3-19), which is required by European standard CEN/TR16355 [58]. In addition, the upper bound for the supply temperature was determined by the supply temperature of the central DH system, which was deduced through measured data.

$$T_{sup,L} = max(T_{sup,SH,L}, T_{sup,DHW,L}) \quad (3\text{-}17)$$

$$T_{sup,SH,L} = T_{ia} + 0.5 \cdot (T_{sup,SH,des} + T_{ret,SH,des} - 2 \cdot T_{ia,des}) \cdot \left(\frac{T_{ia,des} - T_{oa}}{T_{ia,des} - T_{oa,des}}\right)^{1/b} + 0.5 \cdot (T_{sup,SH,des} - T_{ret,SH,des}) \cdot \left(\frac{T_{ia,des} - T_{oa}}{T_{ia,des} - T_{oa,des}}\right) \quad (3\text{-}18)$$

$$T_{sup,DHW,L} = 60℃ \quad (3\text{-}19)$$

where $T_{sup,SH,L}$ and $T_{sup,DHW,L}$ are the lower bound of the supply temperature for the SH and the DHW system, respectively. T_{ia} and T_{oa} are the indoor and the outdoor temperature, respectively. $T_{sup,SH}$ and $T_{ret,SH}$ are the supply and the return temperature of the SH system, respectively. b is a parameter depending on the characteristic of the radiator. The subscript des refers to the design conditions.

The lower bound of the water mass flow rate $\dot{m}_{Bui,L}$ is zero, and the upper bound of the water mass flow rate $\dot{m}_{Bui,U}$ is constrained by the capacity of the distribution system. In this study, the upper bound of the water mass flow rate $\dot{m}_{Bui,U}$ was obtained by the measurement data. In addition, the characteristics of the system and equipment determine the feasible region of the water temperature difference as described in Equation (3-16). In this study, the lower bound of the water temperature difference $\Delta T_{Bui,L}$ was zero, and the upper bound of the water temperature difference $\Delta T_{Bui,U}$ was obtained by the linear regression using the measured data as:

$$\Delta T_{Bui,U} = a_0 + a_1 \cdot T_{sup} \tag{3-20}$$

where a_0 and a_1 are parameters.

The buildings' heat demand, $\dot{Q}_{Bui}$, includes the heat demand for the SH and the DHW system as calculated in Equation (3-21).

$$\dot{Q}_{Bui} = \dot{Q}_{SH} + \dot{Q}_{DHW} \tag{3-21}$$

where $\dot{Q}_{SH}$ and $\dot{Q}_{DHW}$ are the heat demand of SH and DHW systems, respectively. $\dot{Q}_{SH}$ can be further divided into the demand for the radiator heating system $\dot{Q}_{rad}$ and the demand for the ventilation system $\dot{Q}_{ven}$, as described in Equation (3-22).

$$\dot{Q}_{SH} = \dot{Q}_{rad} + \dot{Q}_{ven} \tag{3-22}$$

Considering the thermal inertia of buildings, a simplified-lumped-capacity model derived from resistance-capacitance networks analogue to electric circuits was used to describe the building dynamics, as defined in Equations (3-23), (3-24), and (3-25).

$$C_{env} \cdot \frac{dT_{env}}{dt} = \frac{T_{ia} - T_{env}}{R_{i,e}} + \frac{T_{oa} - T_{env}}{R_{o,e}} \tag{3-23}$$

$$C_{ia} \cdot \frac{dT_{ia}}{dt} = \frac{T_{ma} - T_{ia}}{R_{i,m}} + \frac{T_{env} - T_{ia}}{R_{i,e}} + \frac{T_{oa} - T_{ia}}{R_{win}} + \frac{T_{oa} - T_{ia}}{R_{ven}} + \dot{Q}_{rad} + \dot{Q}_{ven} + \dot{Q}_{in} \tag{3-24}$$

$$C_{ma} \cdot \frac{dT_{ma}}{dt} = \frac{T_{ia} - T_{ma}}{R_{i,m}} \tag{3-25}$$

where C and R represent the heat capacitance and resistance, T is the temperature. Subscripts env, ia, oa, ma, win, and ven denote building envelopes (including exterior walls and roofs), indoor air, outdoor air, internal thermal mass, window, and ventilation (including infiltration

and mechanical ventilation), respectively. In addition, $R_{i,e}$ is the heat resistance between the indoor air and the building envelopes, $R_{o,e}$ is the heat resistance between the outdoor air and the building envelopes, and $R_{i,m}$ is the heat resistance between indoor air and interior thermal mass. $\dot{Q}_{in}$ is the internal heat gains. All the introduced heat capacitances, thermal resistances, temperatures, and heat flow rates in Equations (3-23), (3-24), and (3-25) are marked in Figure 3-13.

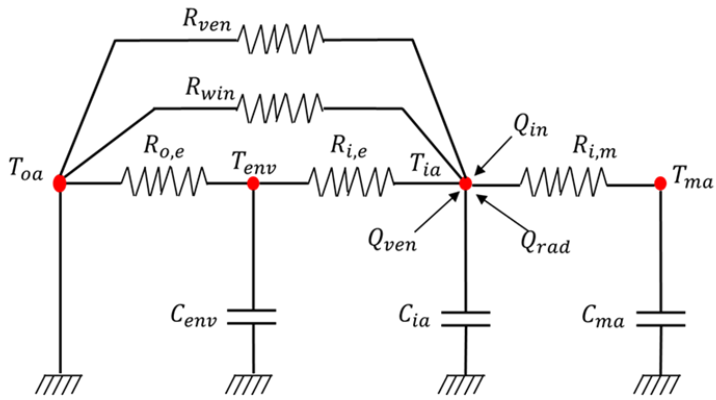

Figure 3-12. Schematic of the simplified-lumped-capacity building model (source: Paper 3)

3.5.3 Simplified model for the water tank thermal energy storage

A one-dimensional and uniform-grid model was used to describe the dynamics of the WTTES. The model divided the tank into *n* sections as shown in Figure 3-13. The thermal dynamics of each section were described as Equations (3-26) and (3-27).

$$c \cdot \rho \cdot A_{XS} \cdot \Delta x \cdot \frac{dT_i}{dt} = c \cdot \dot{m}_{use} \cdot (T_{i-1} - T_i) + c \cdot \dot{m}_{sou} \cdot (T_{i+1} - T_i) - U \cdot P \cdot \Delta x \cdot (T_i - T_{amb}) + \frac{\varepsilon \cdot A_{XS}}{\Delta x} \cdot (T_{i+1} - 2 \cdot T_i + T_{i-1}) \quad (3\text{-}26)$$

$$\dot{q}_{loss,TES,i} = U \cdot P \cdot \Delta x \cdot (T_i - T_{amb}) \quad (3\text{-}27)$$

where, T_i is the water temperature of the ith node. A_{XS} and P are the cross-sectional area and the perimeter of the tank, respectively. Δx is the length of each section. $\dot{m}_{sou}$ and $\dot{m}_{use}$ are the water mass flow rate from the heat source side and the user side, respectively. T_{amb} is the ambient temperature. U is the U-value of the tank wall. ε is a parameter representing the

combined heat transfer effect of water through diffusion, conduction, and mixing due to turbulent flow. $\dot{q}_{loss,TES,i}$ is the heat loss of the ith section. ρ is the density of water.

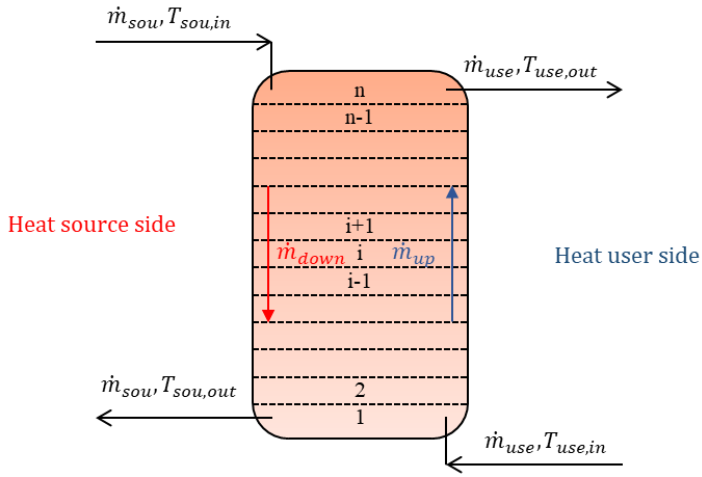

Figure 3-13. Diagram illustrates the spatial discretization for a thermocline tank (source: Paper 3)

3.5.4 Simplified model for the pipelines

The pipelines model described the heat loss to the ground, including the heat loss from the supply pipes and return pipes. The model is presented as Equations (3-28), (3-29), and (3-30).

$$\dot{Q}_{loss,pip} = \dot{Q}_{loss,pip,sup} + \dot{Q}_{loss,pip,ret} \tag{3-28}$$

$$\dot{Q}_{loss,pip,sup} = L \cdot \pi \cdot d \cdot \frac{(R_g + R_i) \cdot \Delta T_{pip,sup} - R_c \cdot \Delta T_{pip,ret}}{(R_g + R_i)^2 - {R_c}^2} \tag{3-29}$$

$$\dot{Q}_{loss,pip,ret} = L \cdot \pi \cdot d \cdot \frac{(R_g + R_i) \cdot \Delta T_{pip,ret} - R_c \cdot \Delta T_{pip,sup}}{(R_g + R_i)^2 - {R_c}^2} \tag{3-30}$$

where $\dot{Q}_{loss,pip}$, $\dot{Q}_{loss,pip,sup}$, and $\dot{Q}_{loss,pip,ret}$ are the total heat loss from pipes, the heat loss from supply pipes, and the heat loss from return pipes, respectively. L is the route length for the pair of pipes. d is the outer pipe diameter. R_i, R_g, and R_c are the resistances for insulation, ground, and coinciding, respectively, and they can be obtained by Equations (3-31), (3-32), and (3-33). In addition, $\Delta T_{pip,sup}$ and $\Delta T_{pip,ret}$ are the temperature difference for the supply pipe and the return pipe, and can be obtained by Equations (3-34) and (3-35):

$$R_i = \frac{d}{2 \cdot \lambda_i} \cdot ln\frac{D}{d} \quad (3\text{-}31)$$

$$R_g = \frac{d}{2 \cdot \lambda} \cdot ln\frac{4 \cdot h}{D} \quad (3\text{-}32)$$

$$R_c = \frac{d}{2 \cdot \lambda} \cdot ln(((\frac{2 \cdot h}{s})^2 + 1)^{0.5}) \quad (3\text{-}33)$$

$$\Delta T_{pip,sup} = T_{pip,sup} - T_{grou} \quad (3\text{-}34)$$

$$\Delta T_{pip,ret} = T_{pip,ret} - T_{grou} \quad (3\text{-}35)$$

where D is the outer insulation diameter, h is the distance between the pipe centres and the ground surface, s is the distance between pipe centres, and λ and λ_i are the heat conductivity for the ground and insulation. In addition, T_{grou} is the ground temperature. $T_{pip,sup}$ and $T_{pip,ret}$ are the water temperature in the supply pipe and the return pipe, respectively.

3.5.5 Simulation scenarios

Two groups of simulation scenarios were proposed to address the research questions **Question 3** and **Question 4**, respectively.

To identify the economically optimal size of the WTTES, a group of scenarios were designed with different storage capacities of WTTES. The storage capacity meant the maximum discharging time for a WTTES under the discharging heat flow rate equals buildings' annual average heat demand. Eight scenarios including the reference scenario were proposed as listed in Table 3-1. The reference scenario, *Ref*, represented the DH system without any TES. The other scenarios represented the WTTES solutions with storage capacities ranging from three hours to one week. The WTTESs were cylinder-shaped. All the tanks had the same height, while the diameters were modified to provide certain storage capacities.

Table 3-1. Information for the scenarios with different storage capacities (source: Paper 3)

Scenario abbreviation	**Storage capacity** (hour)
Ref	N/A
3 h	3
6 h	6
12 h	12
1 d	24
3 d	72
5 d	120
7 d	168

In addition, to identify the economically optimal distribution temperature of heat-prosumer-based DH systems with TES, another group of scenarios were designed. These scenarios used an identical operation strategy proposed in Section 3.5.1, while applying different levels of the distribution temperatures. The basic information of these scenarios is presented in Table 3-2, and the corresponding supply temperatures are illustrated in Figure 3-15. The upper bound in Figure 3-15 was determined by the supply temperature of the central city DH system, and the lower bound was obtained by Equation (3-17). As presented in Table 3-2, Scenarios *H-Temp*, *M-Temp*, and *L-Temp* presented the distribution temperature levels of the 2nd, 3rd, and 4th generation DH systems, respectively. These three scenarios were used as the benchmarks. In contrast, Scenario *Op-Temp* had the highest flexibility in the distribution temperature, and it was an improved scenario compared to the benchmark scenarios. Simulation outputs obtained from the scenario *Op-Temp* were designed to compare with the benchmark scenarios, and the comparison results were used to conclude the research.

Table 3-2. Information for the scenarios with different distribution temperatures (source: Paper 4)

Abbreviation	Feasible region of the supply temperature	Note
Op-Temp	Region Op-Temp in Figure 3-15, ranging from 50℃ to 120℃.	This scenario had the largest feasible region with the highest flexibility in supply temperature. It was an improved scenario that obtained the ***Economically Optimal Distribution Temperature***.
H-Temp	Region H-Temp in Figure 3-15, ranging from 100℃ to 120℃.	This scenario had a high supply temperature that represented 2nd generation DH systems. It was a benchmark scenario.
M-Temp	Region M-Temp in Figure 3-15, ranging from 80℃ to 100℃.	This scenario had a medium supply temperature that represented 3rd generation DH systems. It was a benchmark scenario.
L-Temp	Region L-Temp in Figure 3-14, ranging from 50℃ to 80℃.	This scenario had a low supply temperature that represented 4th generation DH systems. It was a benchmark scenario, which obtained the ***Lowest Distribution Temperature***.

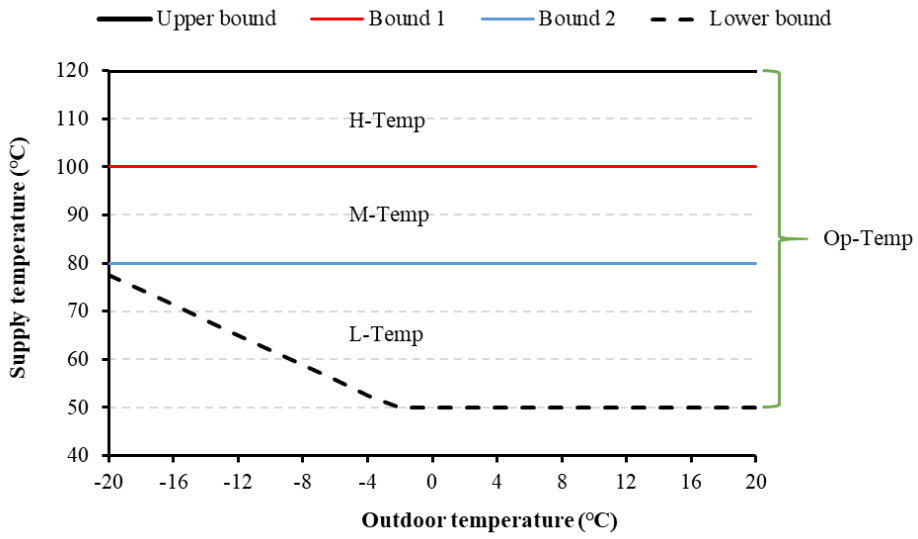

Figure 3-14. Feasible region of supply temperature for the four scenarios (source: Paper 4)

3.6 Modelling and simulation of space heating systems inside buildings

This section introduces the methods to address the last research question - **Question 5**: How can rule-based control strategies be used to operate heating systems inside buildings? A comprehensive description of the work is presented in **Paper 5**.

Firstly, a detailed Modelica model was developed to support the simulation of the demand side. The model components included building envelopes and an SH system. The *Modelica Standard Library* [54] and the *Modelica Library of IBPSA Project 1* [55] were used to build these model components. Afterwards, simulations were conducted in the Dymola environment, and the simulation results were used to map the correlation between the supply temperature and the return temperature of the SH system. The following parts will briefly introduce the above steps.

3.6.1 Building envelope model

The building envelope model described the dynamics of building envelopes, including heat transfer between neighbouring rooms, heat gain from solar radiation, heat gain from radiators, heat loss to the outdoor environment, and heat loss from infiltration. The model is illustrated in Figure 3-15. In this model, the apartment was assumed of 70 m^2 and with five rooms, including a living room, a children room, a bedroom, a bathroom, and a kitchen. Detailed information on these assumptions is explained in Section 4.2.

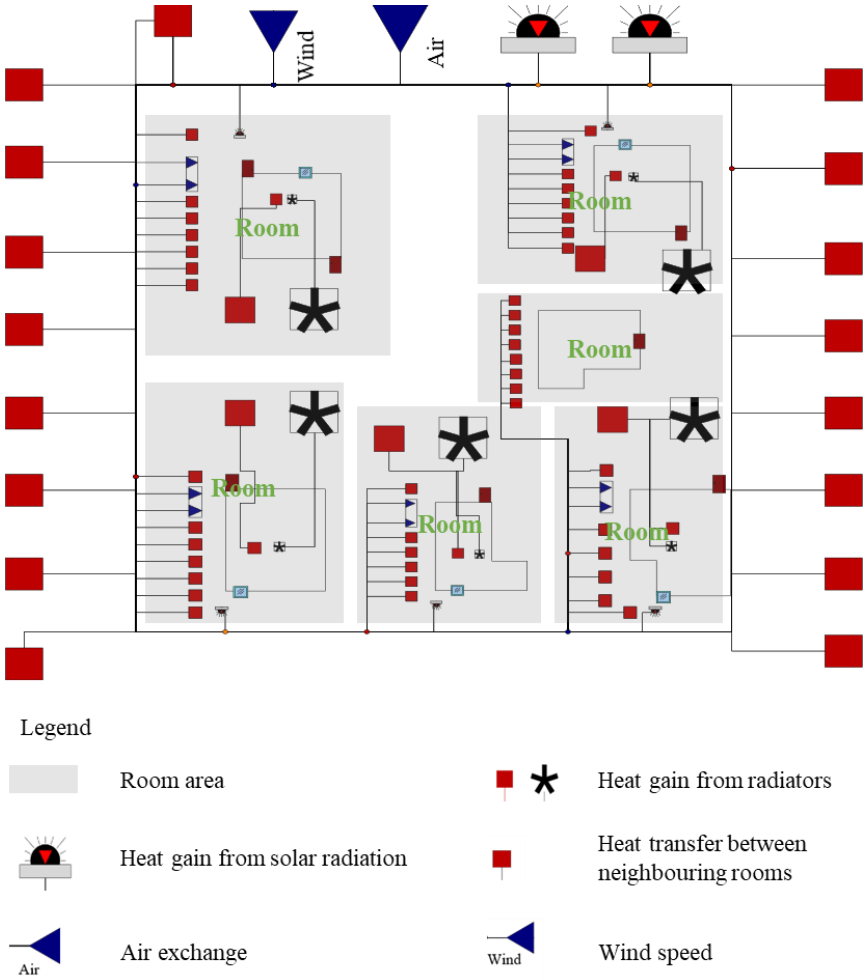

Figure 3-15. Building envelopes model (source: Paper 5)

3.6.2 Space heating system model

The SH system model defined the dynamics of the SH system inside buildings. The main components included radiators, thermostatic valves, and pipelines. The model structure is illustrated in Figure 3-16. In the model, the supply water from the building substation went through the radiators, afterwards, the return water from the radiators went back to the building substation. The thermostatic valves received the indoor air temperature signal and adjusted their opening.

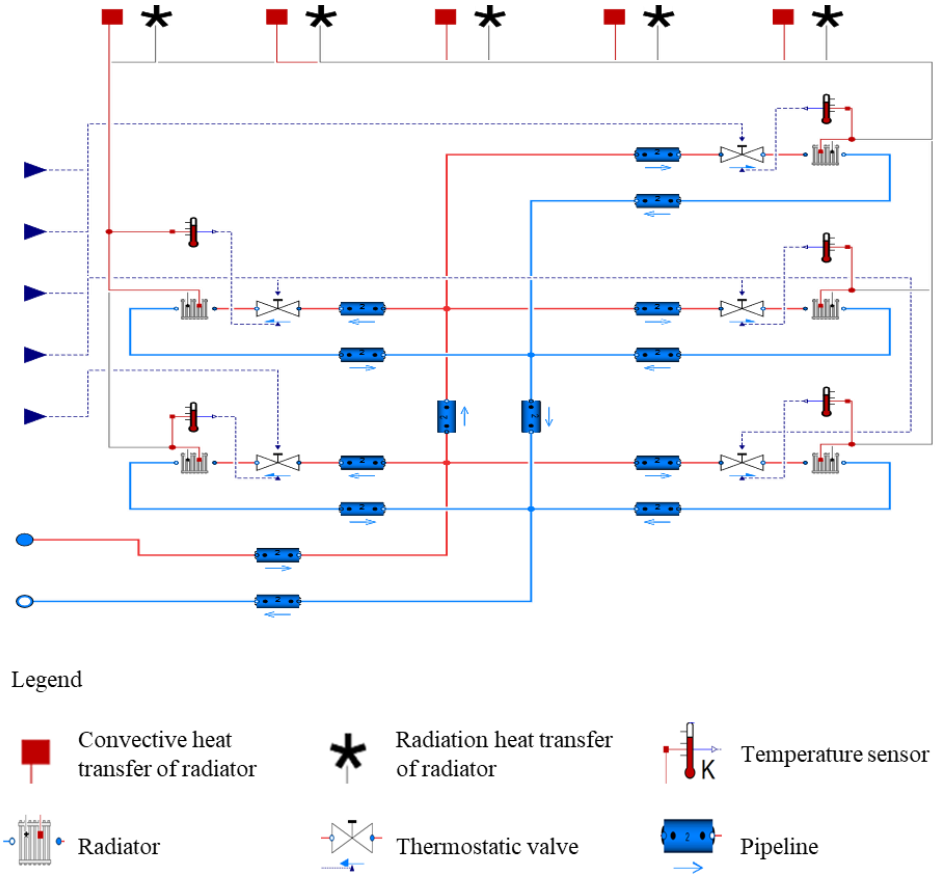

Figure 3-16. SH system model (source: Paper 5)

3.6.3 Simulation scenarios

To test different control strategies and map the correlation between the supply temperature and the return temperature of the SH system, six simulation scenarios that aimed at different goals, i.e., achieving the low supply temperature or the low return temperature, were developed. The control frameworks of these scenarios were divided into two levels: the building level and the room level. The building level control was to provide the setting value for the secondary side supply temperature of the building substation. The room level control aimed to maintain the reference indoor temperature by adjusting the water mass flow rate of the radiator. All these control strategies kept a constant pressure difference at the secondary side of the building substation. The control strategies of these scenarios are briefly explained as follows.

The control strategy of Scenario *TS_PI_NL* is illustrated in Figure 3-17. For the building level control, a PI controller was used to track the reference signal of the indoor temperature by adjusting the secondary side supply temperature. For the room level control, a PI controller was used to track the modified reference signal of the indoor temperature by manipulating the opening of the water valve of the radiator. The modified reference indoor temperature used in the room level control was slightly higher than the one used in the building level control, therefore, the setting temperature at the secondary side of the building substation was always insufficient for the radiator, and hence the radiator water valve was kept fully open during the whole process. This scenario featured the lowest possible supply temperature accompanied by the highest possible water flow rate.

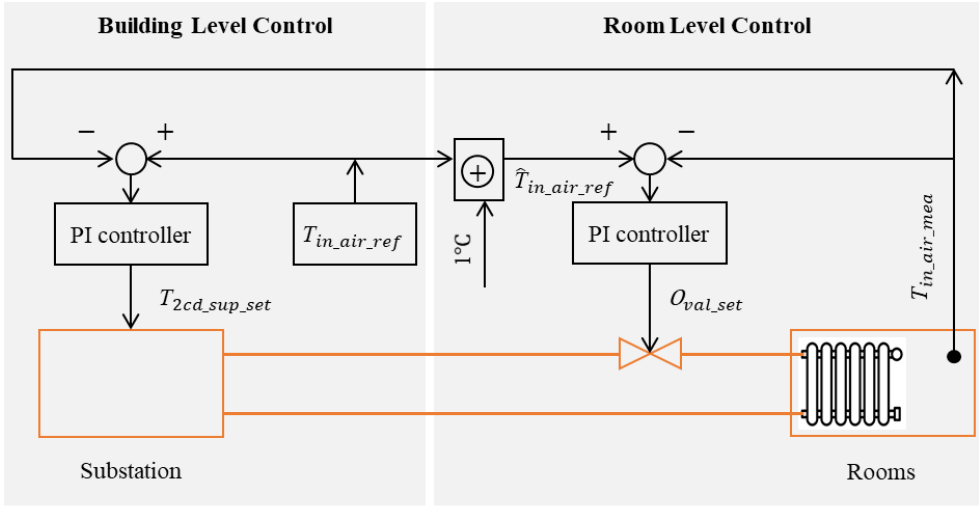

Legend:

$T_{in\_air\_ref}$	reference signal of the indoor air temperature
$\hat{T}_{in\_air\_ref}$	modified reference signal of the indoor air temperature
$T_{in\_air\_mea}$	measured value of the indoor air temperature
$T_{2cd\_sup\_set}$	setting signal of the secondary side supply temperature of the building substation
O_{val_set}	setting signal of the opening of the water valve

Figure 3-17. Control strategies for Scenarios *TS_PI_NL* and *TS_PI_WL* (based on Paper 5)

The control strategy of Scenario *TS_TC_NL* is illustrated in Figure 3-18. Different from the building level control of Scenario *TS_PI_NL* using a feedback controller, it applied a feedforward controller to compute the setting signal of the secondary side supply temperature. The feedforward controller, namely the WCC-based controller, calculated the theoretical lowest supply temperatures under different outdoor temperatures based on a function that considered the behaviours of the building and radiators. In addition, different from the room level control of Scenario *TS_PI_NL* using the modified reference indoor temperature, this scenario used the original reference indoor temperature. Therefore, the opening of the water valve was adjusted according to the measured indoor temperature. This scenario featured the theoretical lowest supply temperature with a high water flow rate. However, since the WCC-based controller considered neither building dynamics nor internal/solar heat gain, the theoretical lowest supply temperature was always higher than the one observed in Scenario *TS_PI_NL*.

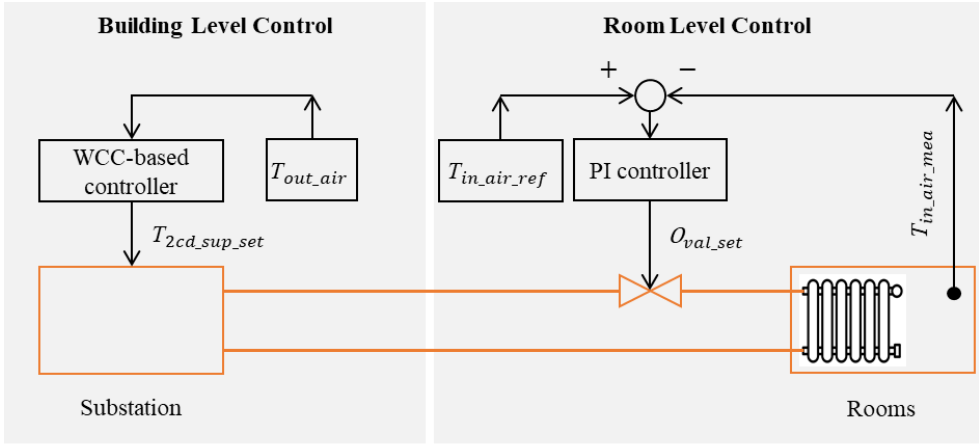

Legend:

T_{out_air}	outdoor air temperature
$T_{in\_air\_ref}$	reference signal of the indoor air temperature
$T_{in\_air\_mea}$	measured value of the indoor air temperature
$T_{2cd\_sup\_set}$	setting signal of the secondary side supply temperature of the building substation
O_{val_set}	setting signal of the opening of the water valve

Figure 3-18. Control strategies for Scenarios *TS_TC_NL* and *TS_TC_WL* (based on Paper 5)

The control strategy of Scenario *TR_PI_TC* is illustrated in Figure 3-19. Similar to the building level control of Scenario *TS_PI_NL*, it used a feedback controller to compute the setting signal of the secondary side supply temperature. However, the controlled variable was the return temperature. This control strategy aimed to achieve low return temperatures by using low reference values. In addition, for the room level control, it was identical to Scenario *TS_TC_NL* that used a PI controller to track the reference indoor temperature. This scenario featured a low return temperature.

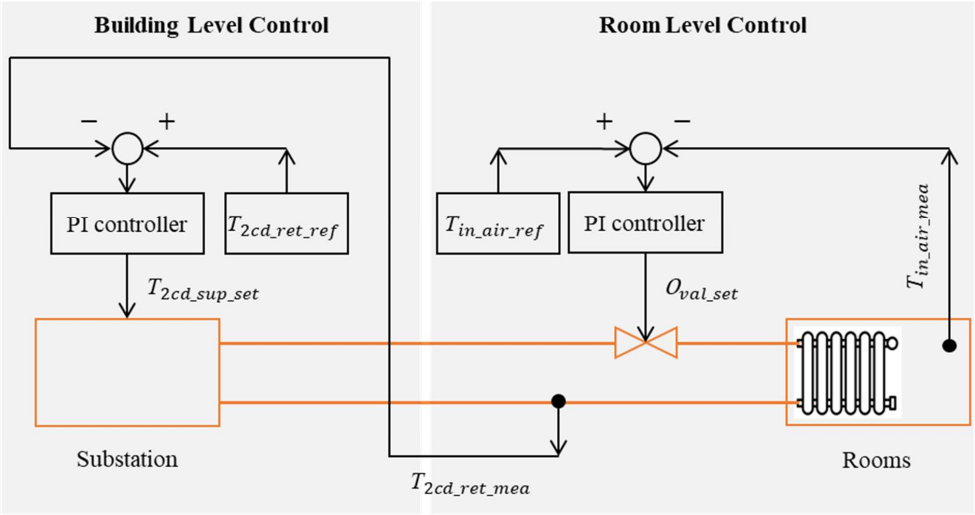

Legend:

$T_{2cd\_ret\_ref}$	reference signal of the secondary side return temperature of the building substation
$T_{in\_air\_ref}$	reference signal of the indoor air temperature
$T_{in\_air\_mea}$	measured value of the indoor air temperature
$T_{2cd\_sup\_set}$	setting signal of the secondary side supply temperature of the building substation
O_{val_set}	setting signal of the opening of the water valve

Figure 3-19. Control strategies for Scenarios *TR_PI_TC* and *TR_PI_TV* (based on Paper 5)

The control strategy of Scenarios *TS_PI_WL* and *TS_TC_WL* was identical to that of Scenarios *TS_PI_NL* and *TS_TC_NL*, respectively, except that a lower bound was added to restrict the setting signal of the secondary side supply temperature in the building level control. This lower bound was defined based on the European standard CEN/TR16355 [58], which requires the

minimum supply temperature to avoid legionella issues of the DHW system. In addition, the control strategy of Scenario *TR_PI_WC* was identical to that of Scenario *TR_PI_NC*, except that the reference return temperature was adjusted from a constant value to a variable that was negatively correlated to the outdoor temperature.

METHODOLOGY

4 CASE STUDY

This chapter briefly introduces the case studies of the thesis. Firstly, the case study of a DH system at a university campus in Norway is introduced. This campus DH system was used for the study of the supply side of heat-prosumer-based DH systems. Afterwards, the case study of a typical SH system for Norwegian apartments is described. This typical SH system was used for the study of the demand side of heat-prosumer-based DH systems.

4.1 DH system at a university campus

A campus DH system in Trondheim, Norway, was chosen as the case study. As illustrated in Figure 4-1, the campus DH system is a prosumer with DHS and heat users. The DHS is the university DC, which recovers the condensing waste heat from its cooling system. The heat users are buildings at the campus with a total building area of 300,000 m^2. The campus DH system is connected to the central DH system via the MS. According to the measurements from June 2017 to May 2018, the total heat supply for the campus DH system was 32.8 GWh. About 80% of the heat supply came from the central DH system through the MS. The other 20% came from the waste heat recovery from the DC.

The campus DH system demonstrates the potential of heat-prosumer-based DH systems that utilize DCs' waste heat, which reaps significant economic and social benefits. However, the system is facing the following problems: 1) the mismatch between the heat supply from DC and the heat demand of buildings; and 2) high peak load, which results in a large amount of money paid for it. As shown in Figure 4-2 (a), the building heat demand fluctuated between 0 MW to 14 MW for the studied year, in contrast, the waste heat recovery was more stable with an almost constant heat flow rate of 1 MW. The mismatch between the waste heat recovery and the building heat demand results in surplus waste heat recovery that cannot be utilized by the campus DH system, especially during the warm period. As shown in Figure 4-2 (b), about 1.7 GWh out of 8.7 GWh recovered waste heat became surplus heat supply, accounting for 20% of the total waste heat recovery. The surplus waste heat is supplied to the central DH system through the MS, however, the university does not get any benefit from this heat supply, because the local heat pricing models have not yet supported the reverse heat supply from heat users to the central DH system. In addition, as shown in Figure 4-2 (a), the building heat demand was not equally distributed and there were peak loads. The maximum building heat demand was 14

MW and it was about four times higher than the annual average level. The heat pricing model used by the local DH company considers the peak loads, and about 20% of the university's heating cost is linked to the peak load.

Considering the above facing problems, this thesis provides solutions to improve the economic performance of the campus DH system, by introducing TES and optimizing the operation of the campus DH system as described in Chapter 3. Detailed information on this campus DH system, including the building properties and the local heat pricing model, can be found in **Paper 2**, **Paper 3**, and **Paper 4**.

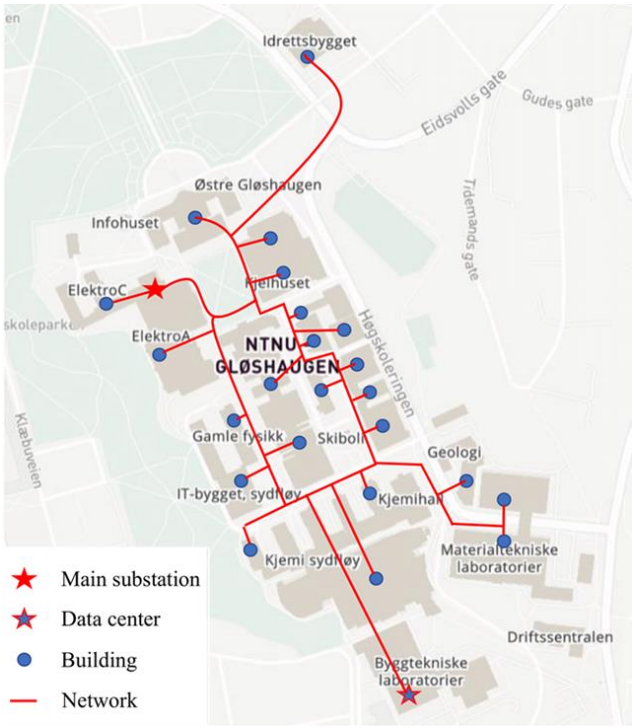

Figure 4-1. Campus district heating system (source: Paper 2, Paper 3, and Paper 4)

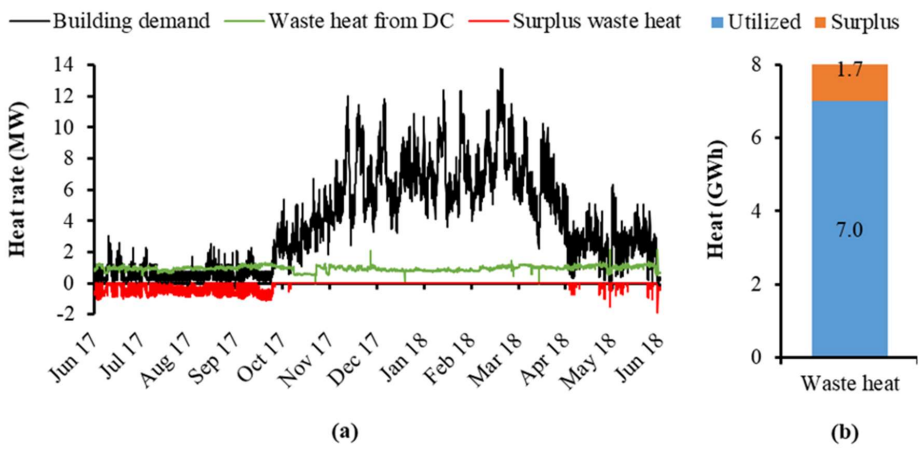

Figure 4-2. Heat demand and waste heat supply (source: Paper 4)

4.2 Typical space heating system under Norwegian conditions

To study the demand side, a typical SH system was proposed based on the conditions of the Norwegian apartments. The following two steps were conducted to design this typical SH system. Firstly, a reference apartment was developed. Based on the data from Statistics Norway [59], the Norwegian statistics bureau, an apartment built around the 1970s or 1980s, of 60-79 m^2, and with 4-6 rooms can represent the conditions of a typical apartment in Norway [60, 61]. Therefore, the reference apartment was assumed of 70 m^2 and with five rooms, including a living room, a children room, a bedroom, a bathroom, and a kitchen. In addition, the thermal properties of the reference apartment were set according to the Norwegian building code TEK69. Secondly, a typical SH system was developed to service the reference apartment. The principles to design this typical SH system were 1) each room had one radiator located under the exterior window of the room, and 2) the radiators were sized with oversizing ranging from 15% to 25% according to the investigation research [27].

The reference apartment and the typical SH system are illustrated in Figure 4-3. The rooms' heat loads under the design outdoor temperature and the radiators' heating capacities under the design condition are presented in **Table 4-1**. More detailed information on the typical SH system and the reference apartment can be found in **Paper 5**.

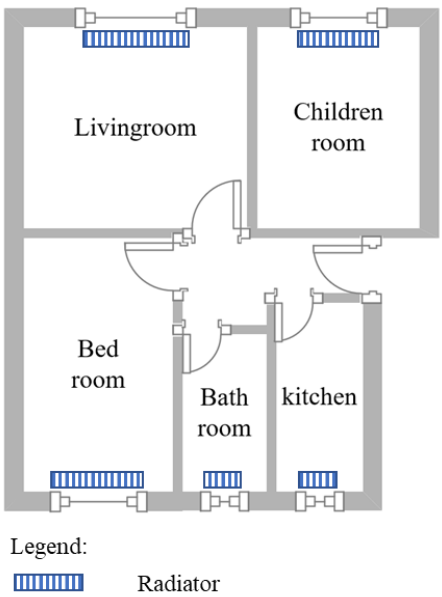

Figure 4-3. Reference apartment (based on Paper 5)

Table 4-1. Heat loads of rooms and heating capacities of radiators.

Room	**Heat load under design outdoor temperature** (W)	**Radiator's heating capacity under design conditions** (W)	**Radiator oversizing** (%)
Living room	770	874	14
Children room	520	608	17
Bedroom	520	608	17
Bathroom	352	431	22
Kitchen	360	415	15

5 RESULTS AND DISCUSSION

This chapter explains the key findings of the thesis, moreover, research questions from **Question 2** to **Question 5** are answered. The findings addressed optimal design and operation of heat-prosumer-based DH systems, taking into account both the supply and demand sides. Therefore, a whole package of solutions that aimed to improve heat-prosumer-based DH systems' economic performance under unidirectional heating markets is presented.

5.1 Superior TES solution for heat-prosumer-based DH systems

This section summarizes the key findings of the research in Section 3.4 on the economic performance of the candidate systems. To begin, the peak loads and energy uses of the four scenarios introduced in Section 3.4.5 are compared. These scenarios included the reference scenario, *Ref*, that represented the system before introducing any TES, and three improved scenarios, *Ref+WT*, *Ref+BTES*, and *Ref+WT+BTES*, that represented the systems after integrating a WTTES, a BTES system, and both a WTTES and a BTES system, respectively. Following this, the results on the economic performance of these scenarios are investigated, assisting the analysis of the impacts of the TES solutions on the performance of heat-prosumer-based DH systems. Finally, this section answers the second research question of this thesis- **Question 2**: Which TES solution is superior for heat-prosumer-based DH systems? More detailed results can be found in **Paper 2**.

5.1.1 Candidate systems' energy performance on peak load and energy use

Figure 5-1 presents the heat load duration curves for the four scenarios, which is used for the analysis of the peak load. Figure 5-2 illustrates the energy use of the four scenarios, which is for the analysis of the energy use.

From Figure 5-1, it can be found that compared with the reference scenario (*Ref*), the scenario that introduced a WTTES (*Ref+WT*) shaved the peak load significantly from 11.7 MW to 8.2 MW, a shaving of 30%. However, as shown in Figure 5-2, introducing a WTTES did not bring any benefit on energy use saving, as observed that there was no obvious difference in annual heat use and electricity use between Scenario *Ref+WT* and *Ref*. In contrast, it can be found that introducing a BTES system reduced the annual heat use from 25.1 GWh to 22.8 GWh, a saving of 9% when comparing Scenario *Ref+BTES* to Scenario *Ref*. However, Scenario *Ref+BTES*

achieved less peak load shaving effect than Scenario *Ref+WT*, with a peak load shaving of 14% from 11.7 MW to 10.0 MW. Moreover, introducing the BTES system caused an extra electricity use of 0.9 GWh per year due to the introduction of the ground source HP. In addition, Scenario *Ref+WT+BTES* achieved high performance on both the peak load shaving and heat use saving. Compared to Scenario *Ref*, it shaved the peak load from 11.7 MW to 7.5 MW, a shaving of 36%, which was the best peak load shaving effect among all the scenarios with TES. Meanwhile, it reduced the annual heat use from 25.1 GWh to 23.0 GWh, a saving of 9%, which was the second-best heat use saving effect after Scenario *Ref+BTES*. However, same as Scenario *Ref+BTES*, introducing the BTES system increased the annual electricity use by 0.9 GWh due to the introduction of the ground source HP.

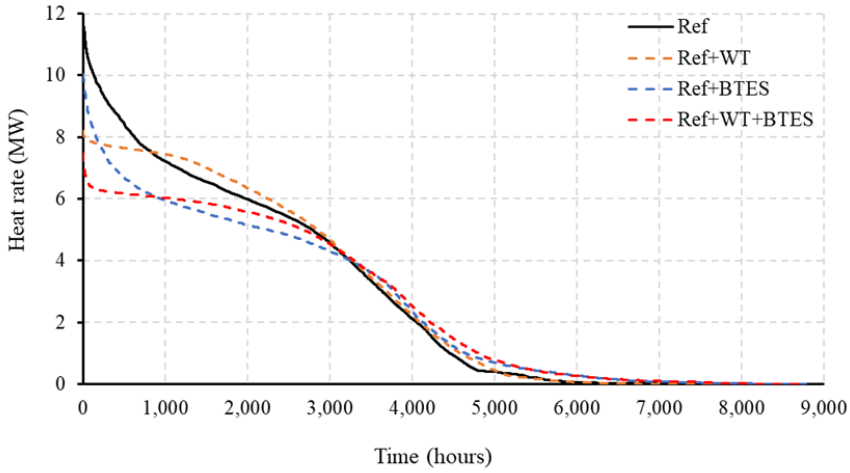

Figure 5-1. Heat load duration diagram for the four scenarios (source: Paper 2)

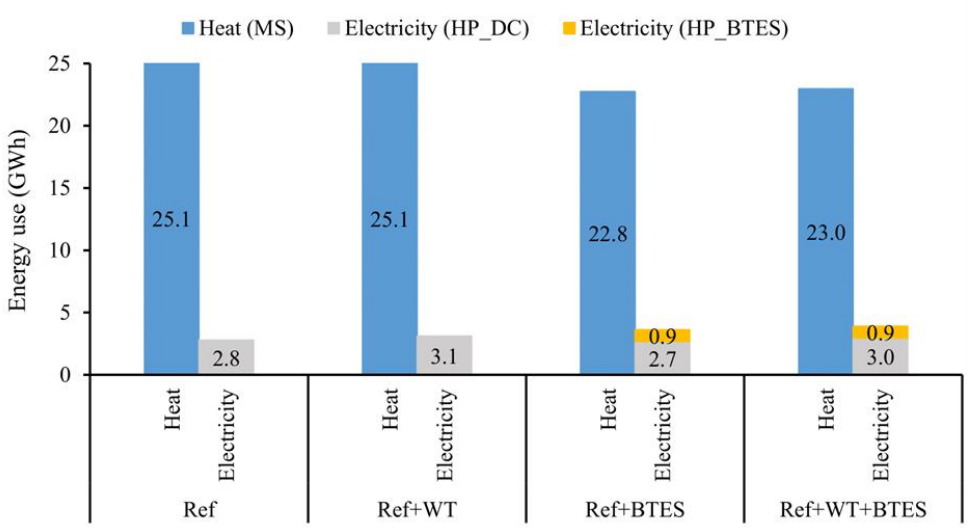

Figure 5-2. Annual heat and electricity use for the four scenarios (source: Paper 2)

5.1.2 Candidate systems' economic performance on energy cost and payback period

The initial investment of different TES solutions is shown in Figure 5-3. The resulting energy bills of the four scenarios are presented in Figure 5-4, and the payback periods for different TES solutions are shown in Figure 5-5. From Figure 5-3, it can be found that introducing a WTTES had the lowest investment of 11.9 million NOK[1]. Introducing a BTES system would increase the investment to 18.6 million NOK, an increase of 56% compared to the WTTES. The scenario with both the WTTES and the BTES system had the highest investment of 30.6 million NOK, an increase of 156% compared to the WTTES scenario.

Moreover, as shown in Figure 5-4, both the WTTES and the BTES system could save energy bills. Scenario *Ref+WT* saved 5% of the annual energy bill compared to the reference scenario (*Ref*). This saving arose only due to the reduction of the LDC heating cost, which was brought by the peak load shaving effect of the WTTES. Similarly, Scenario *Ref+BTES* saved 6% of the annual energy bill. This bill saving came from the reduction in both the LDC and EDC of the heating cost, which was caused by the peak load shaving and mismatch reliving effects of the BTES system, respectively. Moreover, Scenario *Ref+WT+BTES* achieved the highest energy

[1] The currency rate between NOK and EUR can be found from https://www.xe.com/, in this study 1 EUR=10 NOK.

bill saving, reducing the bill by 8%, due to the full use of the advantages of both the WTTES and the BTES system.

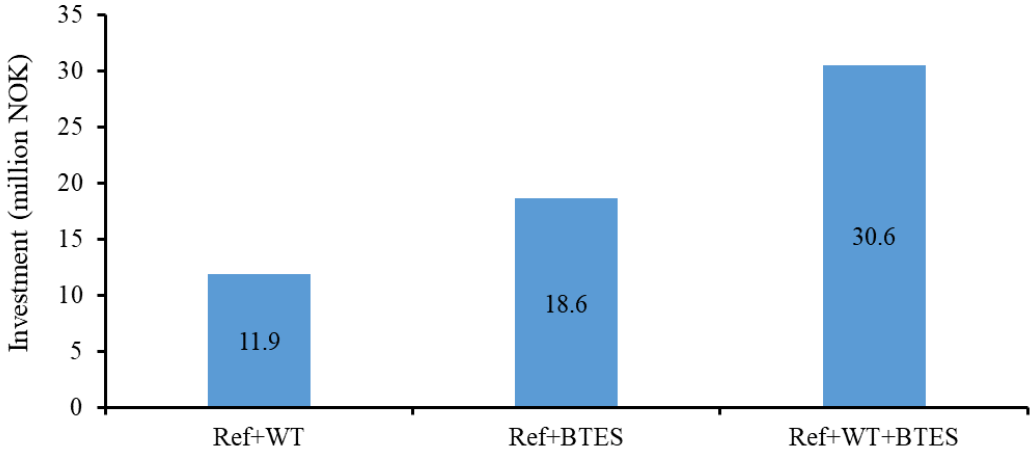

Figure 5-3. Investment for TES scenarios (based on Paper 2)

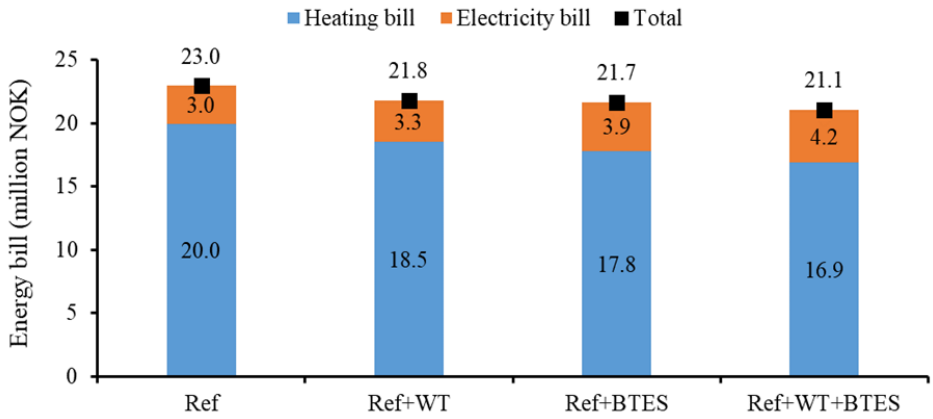

Figure 5-4. Annual heat and electricity bills for the four scenarios (source: Paper 2)

In addition, as shown in Figure 5-5, Scenario *Ref+WT* had the shortest payback period of 12 years. In contrast, Scenario *Ref+BTES* and *Ref+WT+BTES* had longer payback periods of 17 and 20 years, respectively, although they had better annual energy bill savings. These long payback periods were due to the high initial investment of the BTES system.

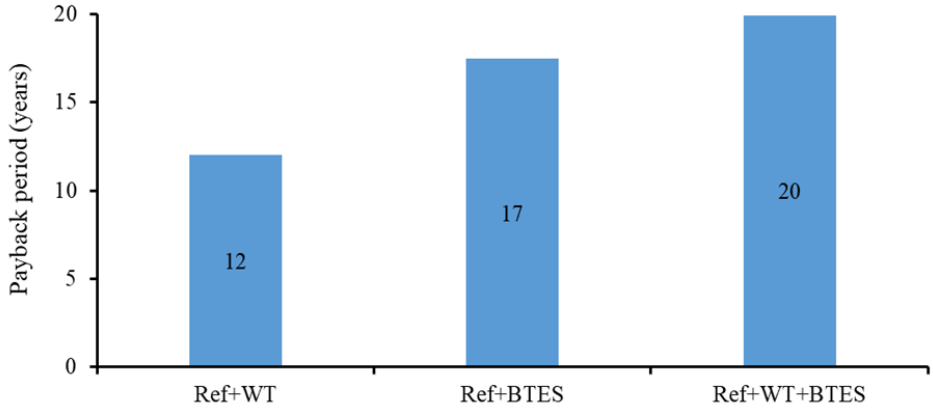

Figure 5-5. Payback period for the three TES scenarios (source: Paper 2)

5.1.3 Answer to Question 2

Based on the above findings, the overall economic performance of different scenarios is presented in Figure 5-6. Accordingly, the second research question can be answered.

Question 2: Which TES solution is superior for heat-prosumer-based DH systems?

Answer: The superior TES solution is determined by the economic conditions as well as the economic strategies of the heat prosumer. For the situation with limited investment and a propensity for a short payback period, introducing a WTTES may be a superior TES solution. However, for the situation with ample investment and a propensity for low operating cost, introducing both a WTTES and a BTES system may be a superior TES solution. Moreover, introducing a BTTS system may be a compromised solution that could reduce the energy cost considerably, while demanding a moderate amount of investment and recovering the investment within 20 years as well.

This study preferred the solution that demanded less investment, while receiving a considerable amount of energy-cost-saving, therefore, the candidate system with WTTES, *Ref+WT*, was selected.

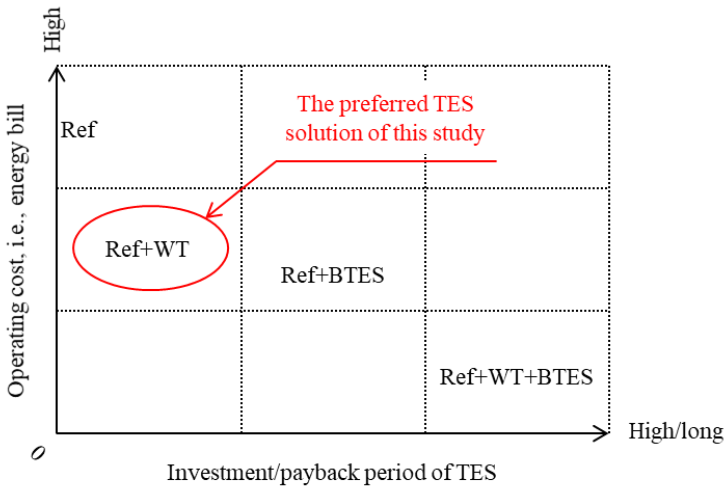

Figure 5-6. Economic performance of different scenarios (based on Paper 2)

5.2 Economically optimal size for the selected TES

This section summarizes the key findings of the research in Section 3.5 on the economic performance of the selected candidate system, *Ref+WT*, under different storage sizes. To begin, the peak loads and energy uses of the eight scenarios mentioned in **Table 3-1** are compared. These scenarios included the reference scenario, *Ref*, that represented the system before introducing any TES, and seven improved scenarios, *3 h*, *6 h*, *12 h*, *1 d*, *3 d*, *5 d*, and *7 d*, that represented the systems after integrating a WTTES with a storage capacity ranging from three hours to seven days. Following this, the results on the economic performance of these scenarios are investigated, assisting the analysis of the impacts of the storage size on the performance of heat-prosumer-based DH systems. Finally, this section answers the third research question of this thesis - **Question 3**: What is the economically optimal size for the selected TES? More detailed results can be found in **Paper 3**.

5.2.1 WTTES's energy performance under different storage size

Figure 5-7 presents the heat load duration of the selected candidate system, *Ref+WT*, under different storage sizes. This figure is used for the analysis of the peak load. Figure 5-8 illustrates the corresponding heat uses, which is for the analysis of the heat use.

From Figure 5-7, it can be found that compared to the reference scenario, *Ref*, part of the heat load for the scenarios with WTTES was shifted from the peak hours (the area highlighted with

red colour) to the non-peak hours (the area highlighted with green colour). This load shifting contributed to the peak load shaving effect. Therefore, all the scenarios with WTTES had a lower peak load compared to the reference scenario. Furthermore, the load shifting effect was more significant for the scenarios with the larger WTTES. The maximal peak load shaving effect was achieved with Scenario *7 d*, which had the largest WTTES. The peak load was shaved from 10.8 MW to 6.6 MW, a reduction of 39%. In contrast, the scenario with the smallest WTTES, *3 h*, had minimal peak load shaving, a reduction of only 4%.

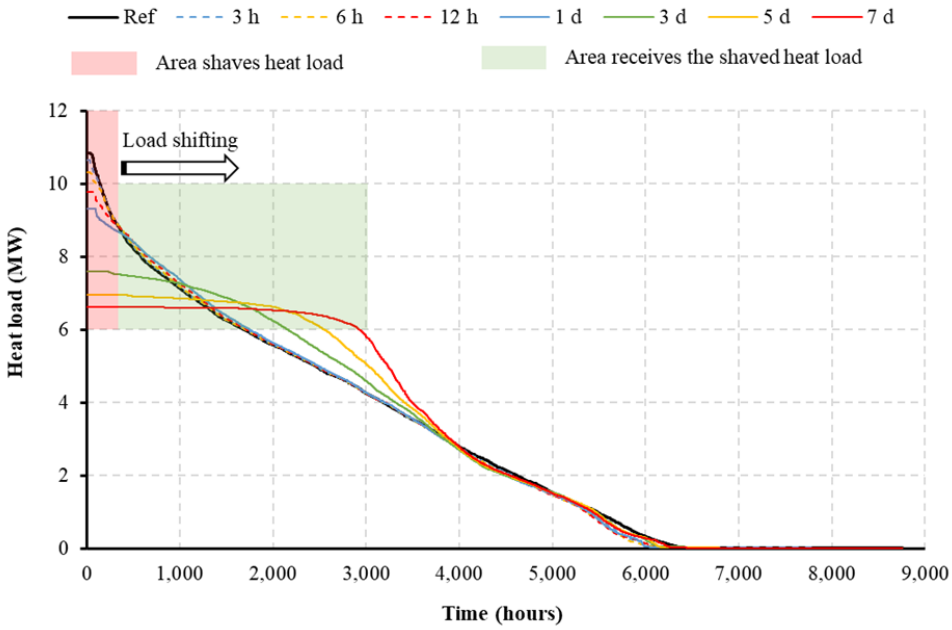

Figure 5-7. Heat load duration diagram for the WTTES scenarios with different storage sizes (source: Paper 3)

In addition, as shown in Figure 5-8, results revealed that the scenarios with the medium size WTTES (*3 h*, *6 h*, *12 h*, and *1 d*) had minimal heat use, about 26.1 GWh, a heat use saving of 0.4 GWh compared to the reference scenario, *Ref*. However, the scenarios with the larger WTTES (*3 d*, *5 d*, and *7 d*) had higher heat use and hence less heat use saving. These results were due to the larger WTTES showing better performance on the mismatch relieving, and the waste heat self-utilization rate was increased. However, the larger WTTES had higher heat loss to the environment because of its larger heat transfer area. The overall heat use saving performance of the WTTES depended on the sum of the above two effects. For the smaller

WTTES, the mismatch relieving effect dominated the overall heat use performance. In contrast, for the larger WTTES, the heat loss effect dominated the overall heat use performance. Consequently, in this study, the WTTESs with three hours to one day's storage capacity were the optimal storage size in terms of heat use saving.

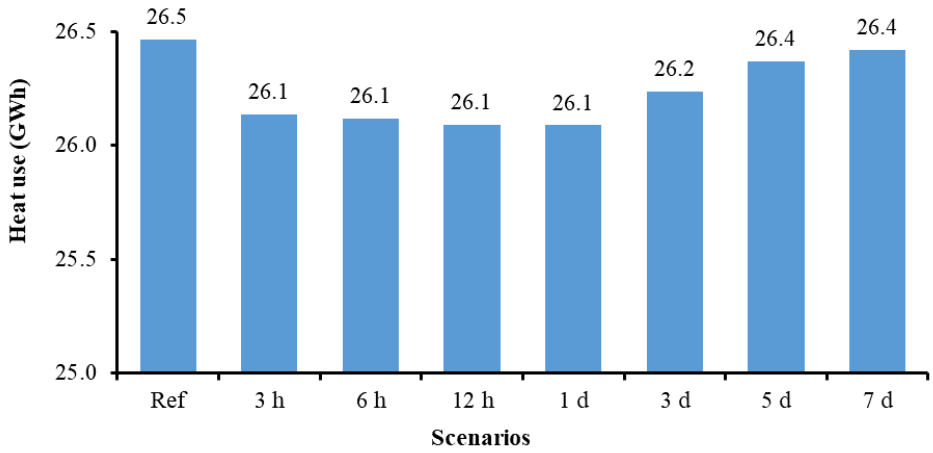

Figure 5-8. Annual heat use for the WTTES scenarios with different storage sizes (source: Paper 3)

5.2.2 WTTES's economic performance under different storage size

The initial investment of WTTESs with different storage sizes is shown in Figure 5-9. The resulting heating bills are given in Figure 5-10, and the payback periods of WTTESs under different storage sizes are shown in Figure 5-11.

From Figure 5-9, it can be observed that the initial investment of WTTESs increased with the increasing storage size. From Scenario *3 h* to Scenario *7 d*, the initial investment increased from 1.3 million NOK to 16.2 million NOK, an increase of more than tenfold.

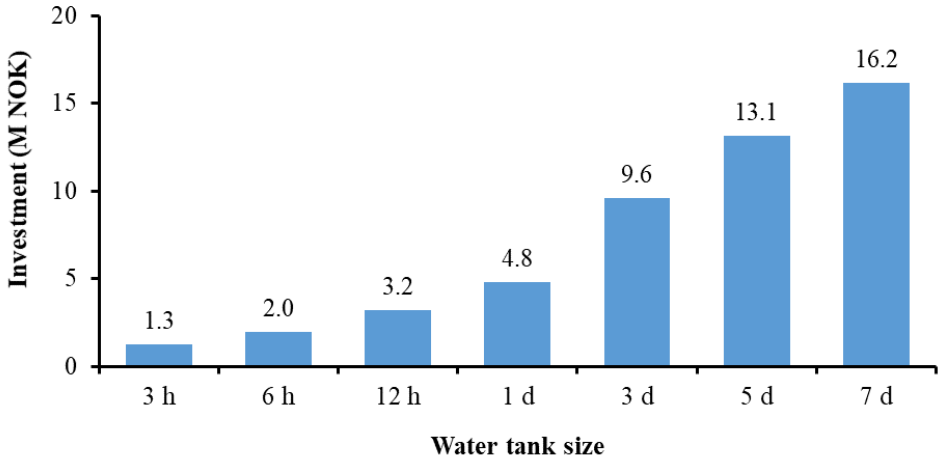

Figure 5-9. Investment for the WTTESs with different storage sizes (based on Paper 3)

In addition, from Figure 5-10, it can be found that: 1) the heating cost saving mainly came from the LDC, and 2) the larger WTTES brought more significant heating cost savings. The annual EDC heating costs for the proposed scenarios were 15.4±0.1 million NOK, and the difference among these scenarios were less than 1%. In contrast, the annual LDC heating cost ranged from 4.7 million NOK to 2.8 million NOK with the increasing storage capacity of the WTTES, meaning a maximum difference of 39%. This significant reduction in the LDC contributed to the total heating cost saving. As increasing the storage capacity of the WTTES, the annual heating cost saving increased from 0.4 million NOK to 1.9 million NOK, meaning a saving of 2%-9%. In this study, despite the waste heat self-utilization rate was increased, the relieving mismatch problem played a limited role in heating cost saving due to the original high waste heat self-utilization rate. However, for other cases with lower waste heat self-utilization rates, the relieving mismatch problem may contribute more to heating cost savings.

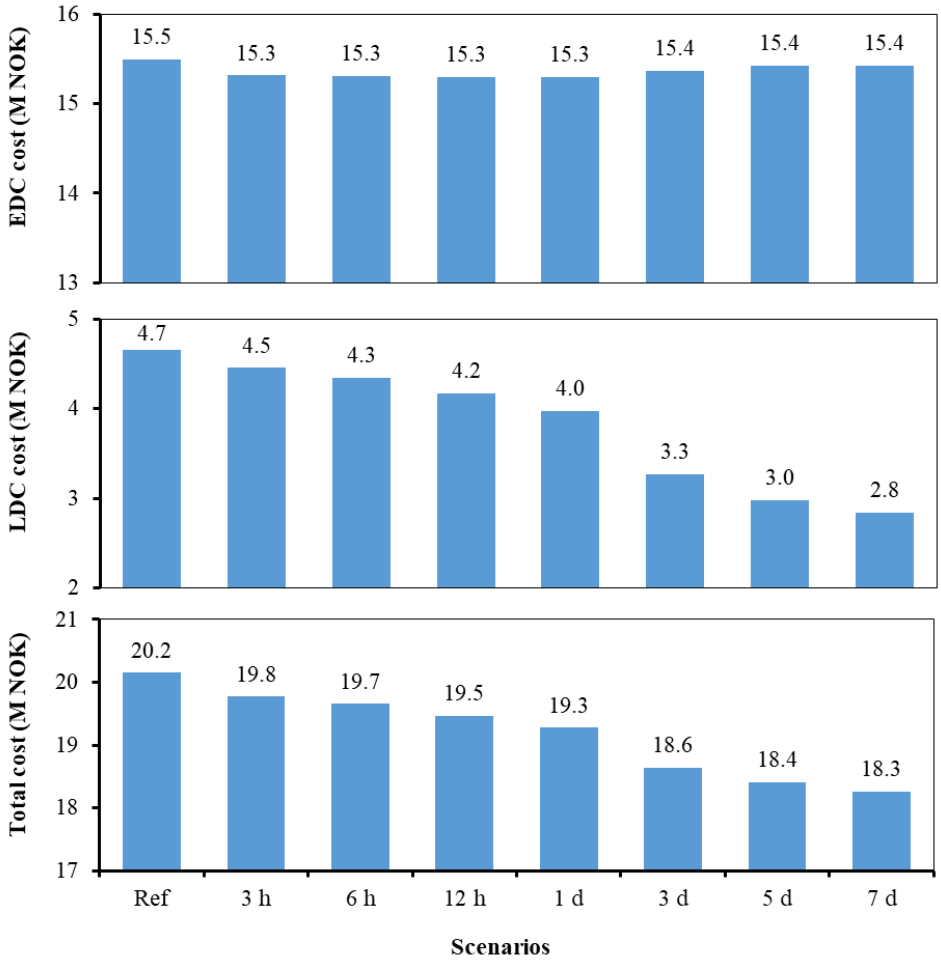

Figure 5-10. Annual heat bills for the WTTES scenarios with different storage sizes (source: Paper 3)

Moreover, from Figure 5-11, it can be seen that the payback periods ranged from four years to ten years with the increasing WTTES storage size. Although the scenario with the largest WTTES needed the longest payback period, it achieved the highest heating cost saving. In contrast, the scenario with the smallest WTTES saved the lowest heating cost, while its payback period was the shortest. Therefore, the prosumer should make a trade-off between the payback period and the heating cost saving based on its own economic situation.

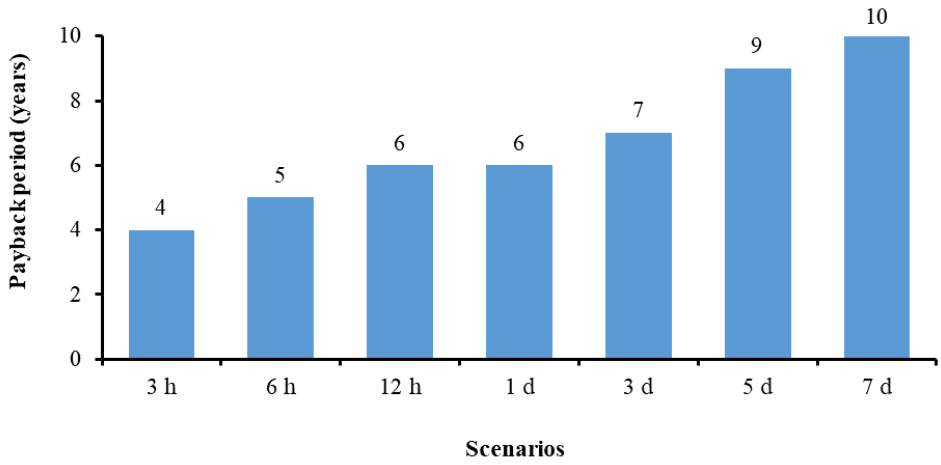

Figure 5-11. Payback period for the WTTESs with different storage sizes (source: Paper 3)

5.2.3 Answer to Question 3

Based on the above findings, the overall economic performance of the selected candidate system *Ref+WT* under different storage sizes are presented in Figure 5-12. Accordingly, the third research question can be answered.

Question 3: What is the economically optimal size for the selected TES?

Answer: There is a trade-off between increasing investment (payback period) and reducing operating costs. Therefore, the optimal storage size is impacted by the weighting of these two sides. On one hand, larger WTTESs lead to lower operating costs, but they demand more initial investments and thus longer payback periods. On the other hand, smaller WTTESs require less initial investments and have shorter payback periods, but they are less effective in cutting heating costs.

This study preferred a compromise strategy that took into account the investment (payback time) and the operational costs equally. As a result, the medium storage size of twelve-hour storage capacity was chosen.

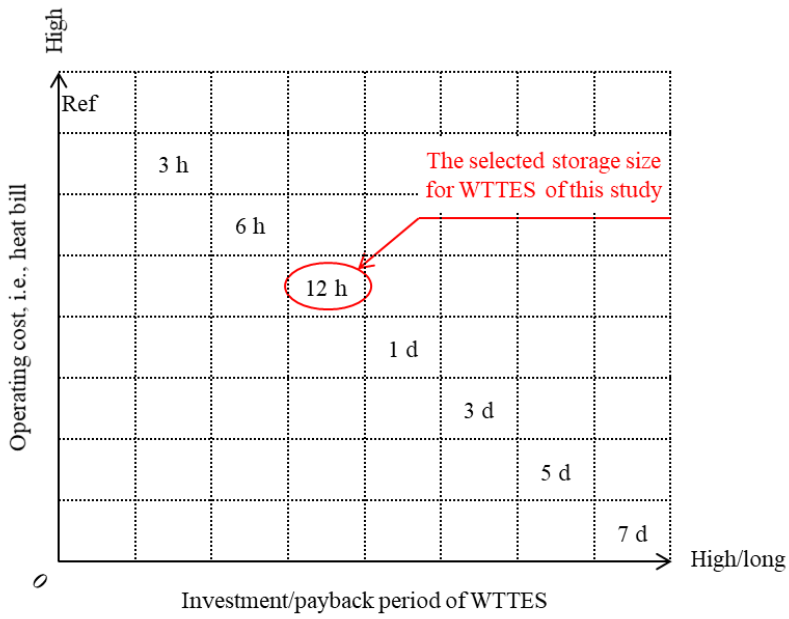

Figure 5-12. Economic performance of the WTTES scenarios with different storage sizes (based on Paper 3)

5.3 Economically optimal distribution temperature for heat-prosumer-based DH systems with TES

This section summarizes the key findings of the research in Section 3.5 on the economic performance of the candidate system *Ref+WT* under different distribution temperatures. To begin, the optimal distribution temperatures of the four scenarios mentioned in Table 3-2 are compared. These scenarios included three benchmark scenarios, *H-Temp*, *M-Temp*, and *L-Temp*, that represented the distribution temperature levels of the 2nd, 3rd, and 4th generation DH systems, respectively; and the improved scenario, *Op-Temp*, that had the highest flexibility in the distribution temperature crossing all the benchmark scenarios. Following this, the results on the energy and economic performance of these scenarios are investigated, assisting the analysis of the impacts of the distribution temperature on the performance of heat-prosumer-based DH systems with TES. Finally, this section answers the fourth research question of this thesis - **Question 4**: What is the economically optimal distribution temperature for heat-prosumer-based DH systems with TES? More detailed results can be found in **Paper 4**.

5.3.1 Optimal distribution temperatures for different generation DH systems

The optimized operation trajectories, including the water mass flow rates and water temperatures, of the campus DH system under different scenarios, can be found in **Paper 4**. The following common phenomena were observed: 1) for the campus DH system, low supply and low return temperatures were preferred and high temperatures only existed during the peak periods; 2) for the WTTES during the warm periods, which were from June to October of 2017 and from April to June of 2018, the WTTES served for the mismatch relieving, while the charging and discharging processes were controlled based on the states and degree of the mismatch; and 3) for the WTTES during the cold period, which was from October of 2017 to April of 2018, the WTTES served for the peak load shaving, and the charging process mainly happened at the beginning of the peak periods. The first phenomenon can be explained by that the low supply and return temperatures could reduce the distribution heat loss of the campus DH system. The second phenomenon was due to the warm period only suffered the mismatch problem and relieving the mismatch could bring heat use saving for the campus DH system. The last phenomenon was due to charging at the beginning of the peak periods could serve for the peak load shaving, meanwhile, keeping the low storage temperatures during non-peak periods could reduce unnecessary storage heat loss.

Despite the above-mentioned shared phenomena, the optimized distribution temperatures achieved by these scenarios varied substantially in terms of the supply temperature. Firstly, it can be observed from Figure 5-13 that compared to the benchmark scenarios, *H-Temp*, *M-Temp*, and *L-Temp*, the improved scenario, *Op-Temp*, had the widest distribution range on the supply temperature, ranging from 120℃ to 50℃ and crossing all the benchmark scenarios. This wide distribution can be explained by that Scenario *Op-Temp* took full advantage of its high flexibility on the supply temperature to obtain optimal economic performance. Moreover, it can be found in Figure 5-14 that the annual average supply temperatures varied substantially among scenarios, ranging from 109℃ to 59℃. However, different from the supply temperature, the return temperatures were highly consistent among scenarios, ranging from 40℃ to 60℃ and with an annual average value of about 45℃.

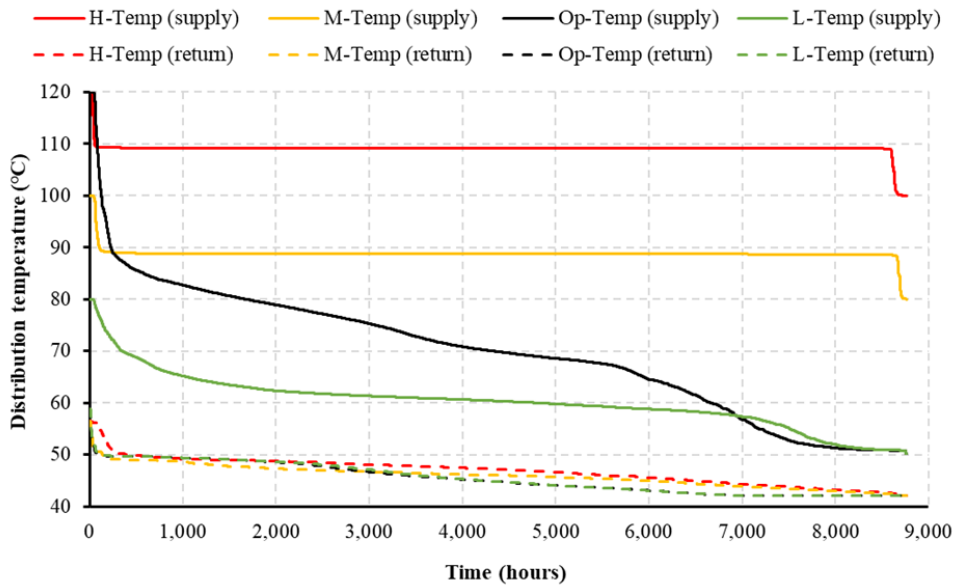

Figure 5-13. Duration diagram of the distribution temperature of the four scenarios, the supply temperature means the one with higher values among the supply temperature of HE1 and HE2 (source: Paper 4)

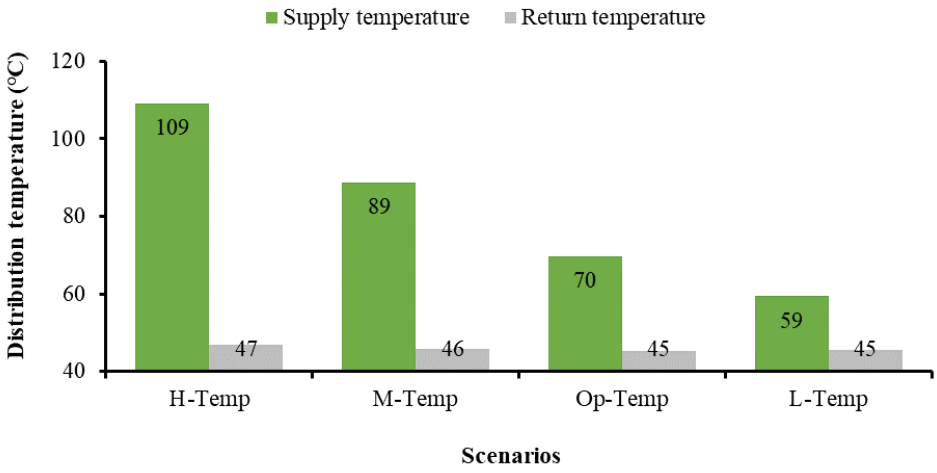

Figure 5-14. Annual average distribution temperatures of the four scenarios, scenarios were sorted based on the annual average supply temperature from the highest to the lowest from the left side to the right side (source: Paper 4)

5.3.2 Heat-prosumer-based DH systems' energy performance in different distribution temperature

Section 5.3.1 showed that the distribution temperatures for different scenarios can be distinguished by their supply temperatures. Therefore, figures in the following Sections 5.3.2 and 5.3.3 sort the scenarios based on the annual average supply temperature, from the highest to the lowest, i.e. with the order *H-Temp*, *M-Temp*, *Op-Temp*, and *L-Temp* from the left side to the right side. Figure 5-15 presents the heat load duration for the campus DH system under different scenarios. Figure 5-16 illustrates the corresponding heat uses.

In Figure 5-15, the results show that decreasing the distribution temperature reduced the peak load shaving effect of the WTTES, and thus increased the peak load of the benchmark scenarios. As shown by the area highlighted with pink colour in Figure 5-15, the peak load of the benchmark scenarios presented a rising trend from 10.8 MW to 11.5 MW from Scenarios *H-Temp* and *M-Temp* to Scenario *L-Temp*. However, this reduced peak load shaving effect was effectively avoided by the improved scenario, *Op-Temp*. Even with a low distribution temperature, the peak load of Scenario *Op-Temp* was around 10.5 MW, which was the lowest of all the scenarios.

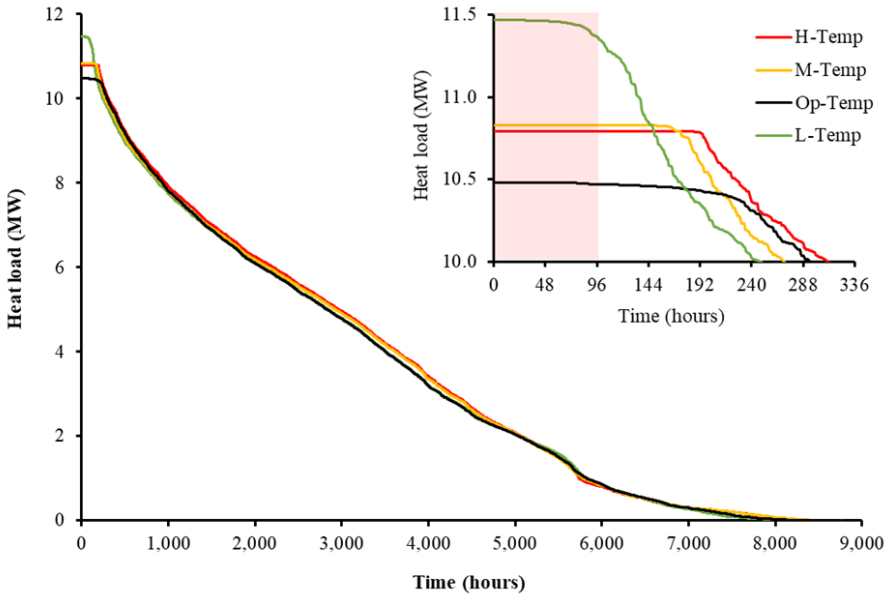

Figure 5-15. Heat load duration diagram for the scenarios with different distribution temperatures (source: Paper 4)

In addition, as shown in Figure 5-16, it can be found that the total annual heat use decreased from 31.1 GWh to 30.4 GWh with the decreased distribution temperature. Moreover, the improved scenario, *Op-Temp*, had the least heat use, which was the same as the scenario with the lowest distribution temperature, *L-Temp*.

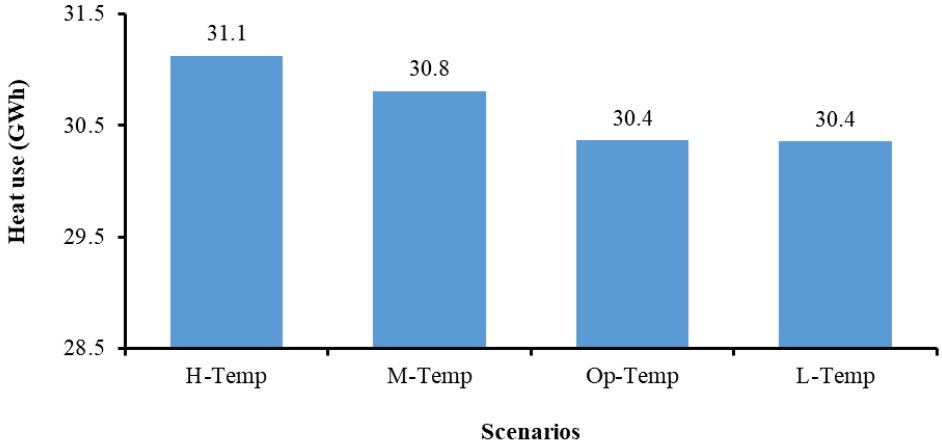

Figure 5-16. Annual heat use for the scenarios with different distribution temperatures (source: Paper 4)

5.3.3 Heat-prosumer-based DH systems' economic performance in different distribution temperature

The resulting heating bills for the scenarios with different distribution temperatures are presented in Figure 5-17. Results showed that the decreasing distribution temperature increased the annual LDC heating cost of the benchmark scenarios, with a rising from 4.6 million NOK to 4.9 million NOK from the high-temperature scenario, *H-Temp*, to the low-temperature scenario, *L-Temp*. However, this rising trend was effectively avoided by the improved scenario, *Op-Temp*. Even with a low distribution temperature, the annual LDC heating cost of Scenario *Op-Temp* was 4.5 million NOK, which was the lowest of all the scenarios. The obtained results on the annual LDC heating cost can be explained by the conditions of the peak load observed in Section 5.3.2 due to the positive correlation between them. In addition, the annual EDC heating cost decreased from 18.2 million NOK to 17.7 million NOK when decreasing the distribution temperature. Meanwhile, the improved scenario, *Op-Temp*, had the lowest annual EDC heating cost, which was the same as the scenario with the lowest distribution temperature,

L-Temp. Similarly, the obtained results on the annual EDC heating cost can be explained by the conditions of the annual heat use observed in Section 5.3.2 due to the positive correlation between them.

In addition, the improved scenario, *Op-Temp*, achieved the best performance with the lowest annual total heating cost of 22.2 million NOK. The scenario with the medium distribution temperature, *M-Temp*, followed this performance with a higher annual total heating cost of 22.6 million NOK. In contrast, the high-temperature scenario, *H-Temp*, and the low-temperature scenario, *L-Temp*, had the highest annual total heating costs of 22.8 and 22.7 million NOK, which were 0.6 and 0.4 million NOK higher than Scenario *Op-Temp*, accounting for an increase of 2% and 3%, respectively.

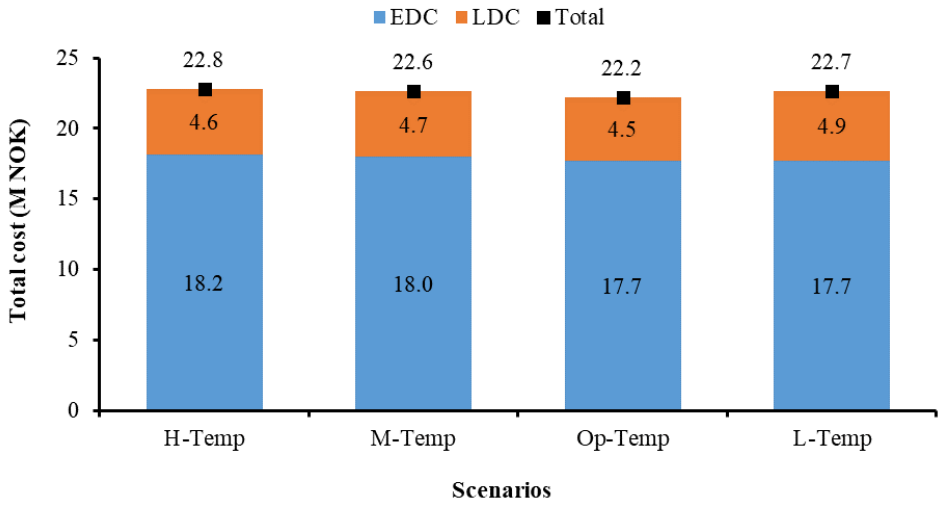

Figure 5-17. Annual heat bills for the scenarios with different distribution temperatures (source: Paper 4)

5.3.4 Answer to Question 4

Conclusions driven from the above analysis are as follows. Firstly, the distribution temperature could be distinguished by the supply temperature, because the supply temperature showed significant differences among scenarios in terms of the distribution range as well as the annual average value. In contrast, the corresponding conditions of the return temperature were highly consistent among scenarios. Secondly, as illustrated in Figure 5-18, for the benchmark scenarios, which represented the temperature levels from the 2nd to the 4th generation DH

systems, the annual average distribution temperature was negatively correlated with the peak load as well as the LDC heating cost, meanwhile, it was positively correlated with the heat use and the EDC heating cost. These correlations meant decreasing the annual average distribution temperature would reduce the heat use and save the EDC heating cost, while this decreased temperature may lead to higher peak load and more LDC heating cost. However, for the improved scenario, which had the highest flexibility in the distribution temperature, these two correlations disappeared. With an annual average distribution temperature between the scenarios that represented the 3rd and 4th generation DH systems, the improved scenario achieved the best energy performance with the lowest peak load and the least heat use, and thus the best economic performance with the lowest heating cost.

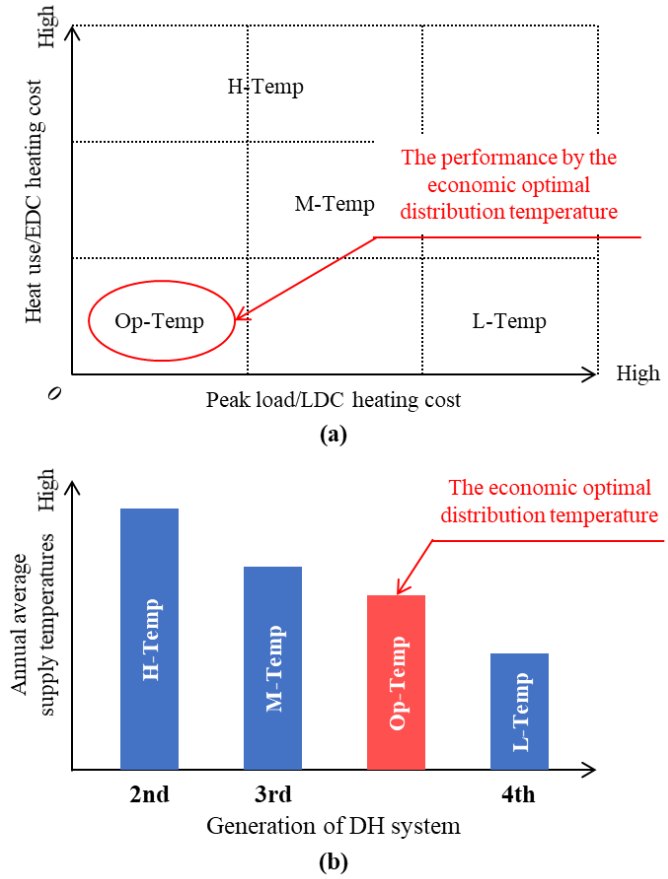

Figure 5-18. Performance of the campus DH system under different distribution temperatures (based on Paper 4)

Based on the above findings, the fourth research question can be answered.

Question 4: What is the economically optimal distribution temperature for heat-prosumer-based DH systems with TES?

Answer: A wider feasible region on the distribution temperature guarantees a better economic outcome for heat-prosumer-based DH systems with TES. Therefore, to improve the system's economic performance, the highest flexibility on the distribution temperature should be provided, unlocked by available DH technologies, i.e., the 2nd, 3rd, and 4th generation DH technologies for DH systems using hot water as the medium.

This study had an economically optimal distribution temperature distributed crossing the 2nd, 3rd, and 4th generation DH systems, with an annual average supply temperature between the 3rd and 4th generation DH systems.

5.4 Rule-based control strategies to operate the heating system on the demand side

This section summarizes the key findings of the research in Section 3.6 on the operation of the SH system inside buildings. To begin, the supply and return temperatures of the six scenarios mentioned in Section 3.6.3 are compared. These scenarios included Scenarios *TS_PI_NL* and *TS_PI_WL* using PI controllers to approach the lowest possible supply temperature, Scenarios *TS_TC_NL* and *TS_TC_WL* using WCC-based controllers to calculate the theoretical lowest supply temperature, and Scenarios *TR_PI_TC* and *TR_TC_WL* using PI controllers to obtain the low reference return temperature. Following this, the results assisted to map the correlation between the supply temperature and the return temperature of the SH system. Finally, this section answers the last research question of this thesis - **Question 5**: How can rule-based control strategies be used to operate heating systems inside buildings? More detailed results can be found in **Paper 5**.

5.4.1 Correlation between the supply and return temperature of the SH system

The obtained results on the supply and return temperatures are presented in Figure 5-19, and the boxplot for these temperatures is given in Figure 5-20. Based on the results in Figure 5-19 and Figure 5-20, it was discovered that the four scenarios aiming for the low supply temperatures achieved expected results, with medians below 60℃ and just a few occasions

above 70℃. These scenarios were associated with relatively high return temperatures, with medians of around 45℃. In contrast, the two scenarios aiming for the low return temperatures achieved low return temperatures of lower than 40℃ for most of the time, with medians of 30℃ and 37℃, respectively. However, these scenarios had extraordinarily high supply temperatures, with medians of 94℃ and 72℃, respectively, and maximums of 130℃ and 111℃.

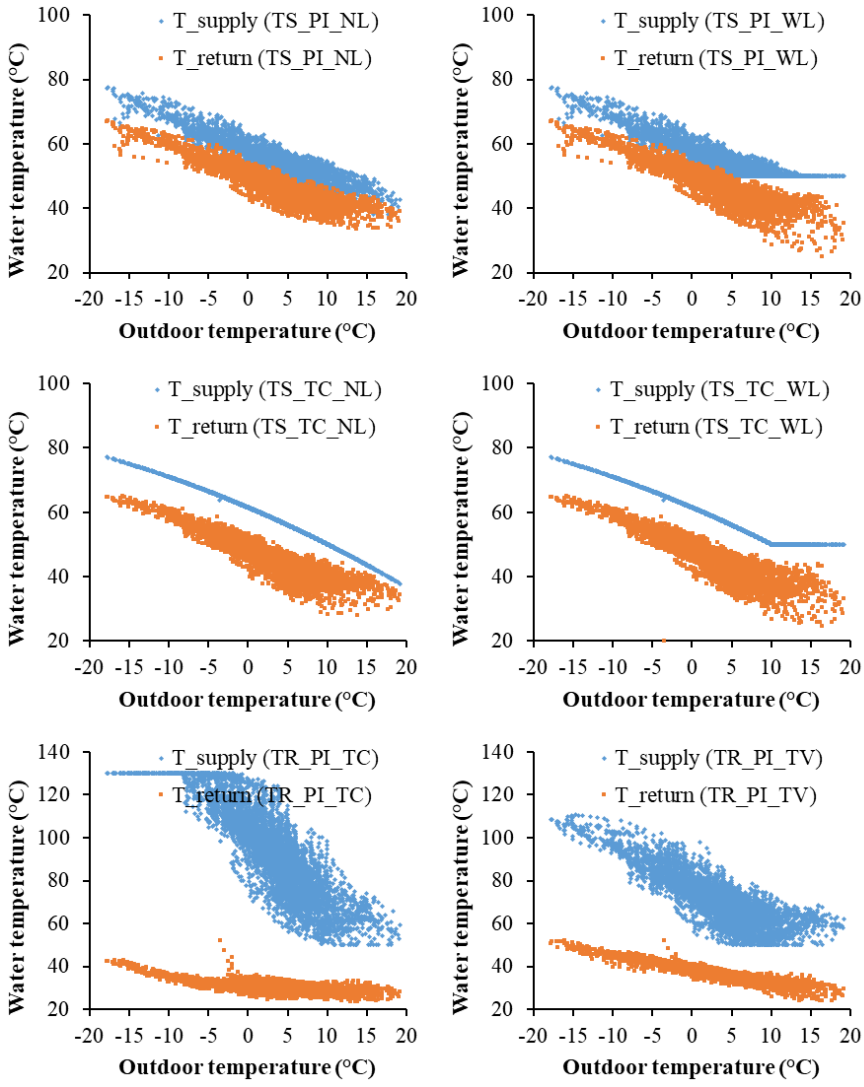

Figure 5-19. Supply and return temperature during the heating season plotted against the outdoor temperature (source: Paper 5)

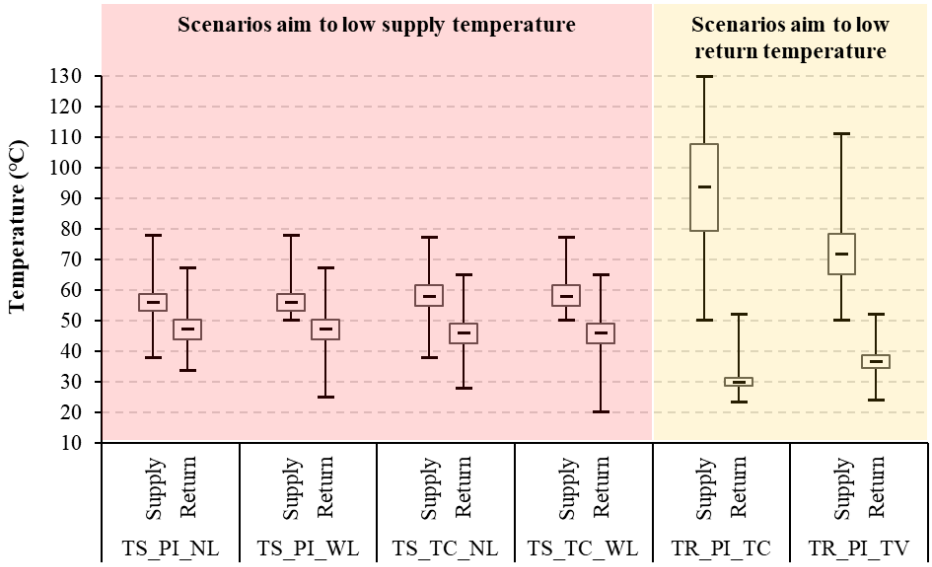

Figure 5-20. Boxplot for the supply and return temperature (based on Paper 5)

The above analysis reveals a negative correlation between the supply temperature and the return temperature, which is further illustrated in Figure 5-21. It was discovered that a second-order polynomial equation could accurately represent the correlation, with an R^2 of 0.9996 and no evident overfitting in the plot. This negative correlation can be explained by Equations (5-1) and (5-2) from the standard EN 442-2 [35]. As shown by Equation (5-1), the mean water temperature should be constant to maintain the radiator's thermal output at a certain level, when the indoor air temperature is fixed. As a result, a decrease in the supply temperature would be offset by an increase in the return temperature, as shown by Equation (5-2).

$$\dot{Q}_{rad} = K_m \cdot (T_{mea} - T_{ia})^n \tag{5-1}$$

$$T_{mea} = \frac{T_{sup} + T_{ret}}{2} \tag{5-2}$$

where K_m and n are parameters that are determined by the characteristics of the radiator. T_{mea} is the mean water temperature.

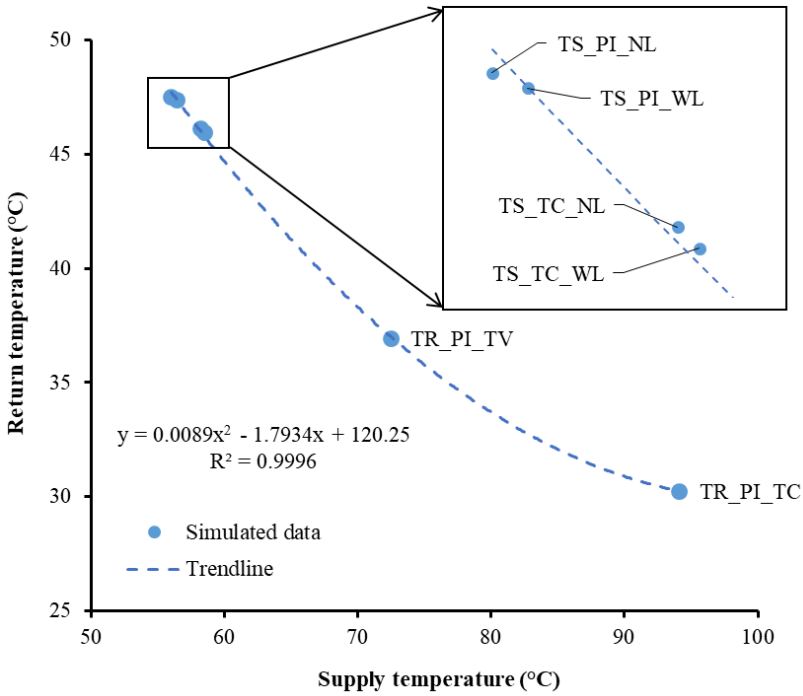

Figure 5-21. Correlation between the average supply and return temperature (based on Paper 5)

5.4.2 Answer to Question 5

Based on the above findings, the temperature performance of different operation strategies is presented in Figure 5-22. Accordingly, the last research question can be answered.

Question 5: How can rule-based control strategies be used to operate heating systems inside buildings?

Answer: There is a trade-off between reducing the supply temperature and increasing the return temperature. Using the PI controller or the WCC-based controllers to approach the lowest possible supply temperature can achieve low supply temperatures, while it results in relatively high return temperatures. In contrast, using the PI controllers to track the reference low return temperatures can achieve low return temperatures. However, these strategies may result in extremely high supply temperatures.

This study preferred the former group of strategies, which used the PI and WCC-based controllers to approach the lowest possible supply temperatures because they can achieve the low supply temperatures while maintaining acceptable return temperatures.

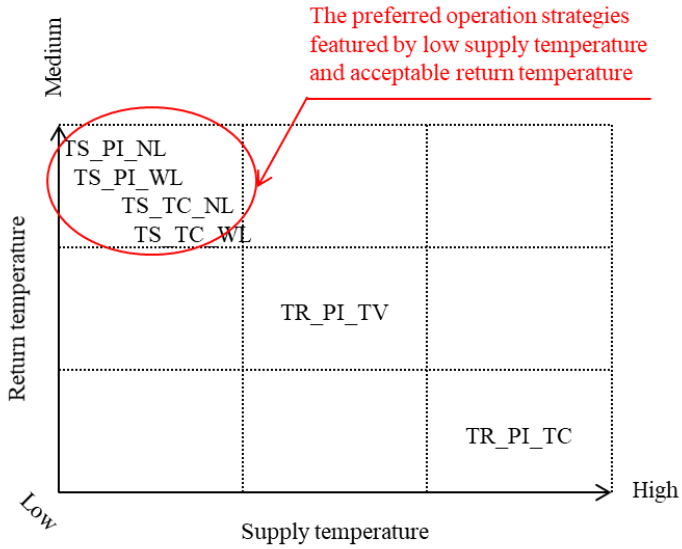

Figure 5-22. Temperature performance of different operation strategies (based on Paper 5)

6 CONCLUSIONS

This chapter summarizes the key findings of this thesis. The main conclusions are presented in Section 6.1. The limitations of the studies are acknowledged in Section 6.2. Recommendations for future research are given in Section 6.3.

6.1 Concluding remarks

This thesis aimed to improve heat prosumers' economic performance under current unidirectional heating markets. With a specific focus on DH systems in Scandinavia, this study addresses economic and technological issues, proving solutions on optimal design and operation, involving heating systems on both the supply and demand sides. The following are the most important conclusions:

Firstly, heat use saving and peak load shaving are two possible and effective solutions that improve heat prosumers' economic performance in terms of reducing heating costs, because heat use and peak load were identified as the most crucial factors that impact heat users' heating costs in the current heat pricing models in the Scandinavian countries.

NOTE:

The identified components of heat pricing models in the Scandinavian countries include EDC, LDC, FXC, and FDC. EDC and LDC, which are determined by heat users' heat use or peak load, play the most significant roles in heat pricing models. These two components combined may account for up to 95% of heat users' total heating costs. In contrast, FXC and FDC, which are linked to other factors such as circulating water flow rate, are less important. These two components may account for less than 5% of heat users' total heating costs.

Secondly, a systematic approach, including optimal selection and sizing of TESs as well as optimal operation of the heat-prosumer-based DH system with TES, may improve heat prosumers' economic performance under current unidirectional heating markets, thus prompt heat prosumers' development in the transition period of the DH system. The case study indicated that introducing the WTTES could cut the heating cost by 2%-9%, with acceptable payback periods ranging from 4 years to 10 years depending on the storage capacity of TESs.

NOTE:

Regarding the selection of TESs, the WTTES may be preferable to BTES. In comparison to the latter, the former requires a smaller initial investment but achieves the same level of heating cost savings. Furthermore, whereas the latter has extremely long payback periods of up to 20 years, the former has far shorter and more acceptable payback periods, less than 10 years under optimal operation.

Regarding the sizing of the WTTESs, heat prosumers must make a trade-off between increasing the investment (payback period) and reducing the operating costs, considering their economic conditions and strategies. Medium storage sizes, with storage capacities ranging from 12 hours to one day, might be a good compromise, providing considerable improvements on heat prosumers' energy and economic performance without requiring a high initial investment.

Thirdly, the economically optimal distribution temperature of the heat-prosumer-based DH systems with TES distinguishes from the lowest distribution temperature featured by the 4th generation DH systems. Decreasing the distribution temperature will reduce the distribution heat loss thus improving the energy efficiency and cutting the heat-use-related heating costs. However, it may reduce the peak load shaving effect of the TESs, resulting in higher peak-load-related heating costs for heat prosumers. Therefore, the economically optimal distribution temperature, which facilitates the minimized total heating cost, makes a trade-off between these two sides. The case study showed that, compared to the lowest distribution temperature, the economically optimal distribution temperature had a higher annual average supply temperature of 70°C. Moreover, this supply temperature had the highest flexibility, crossing the temperature levels of the 2nd, 3rd, and 4th generation DH systems.

NOTE:

Higher flexibility in distribution temperature ensures higher economic performance for the heat-prosumer-based DH systems with TESs. In the future, DH systems should be designed and operated more intelligently. Firstly, the system design should take advantage of the current DH technologies to enable great flexibility in the distribution temperature, including the supply and return temperature. The system operation should then optimize the heating system's conditions in real-time, making the most of the provided temperature flexibility.

Lastly, to operate SH systems inside buildings, it is better to apply operation strategies that aim at low supply temperatures rather than at low return temperatures. Otherwise, extremely high

supply temperatures are required to achieve the low return temperature. The case study found that using the PI and WCC-based controllers to approach the lowest possible supply temperature achieved expected results, with the median supply temperature below 60℃ and just a few occasions above 70℃, meanwhile, the obtained return temperatures were acceptable with medians of about 45℃.

NOTE:

Reducing the supply temperature and reducing the return temperature are contradictory goals. This dilemma makes it impossible to find proper solutions without broadening the scope into the entire DH system. The operating conditions on the demand side (heating systems inside buildings) impact the conditions on the supply side (the connected DH system). Therefore, evaluating the supply side's energy and economic performance may guide finding the optimal supply and return temperature at the demand side.

6.2 Limitation

The first limitation comes from the economic boundary. The optimization problem in Section 3.5 only applies to heat pricing models that calculate the LDC heating cost using the measured peak load. However, DH companies may use another variable, i.e. flow capacity, to calculate the LDC heating cost instead of peak load [62, 63]. Equation (6-1) presents one widely used method to calculate the flow capacity, in which the flow capacity is obtained by dividing the heat use over a certain period by a predefined category number [62]. The period might be a whole year, in which case the flow capacity represents heat users' annual heat use; alternatively, the period could be the winter season, in which case the flow capacity reflects heat users' peak load. However, due to the installation of smart meters and the trend of digitalization, an increasing number of DH companies are starting to utilize real-time measurement for charging heat bills. Therefore, the developed method in this research adopted the heat pricing models using the measured peak load to calculate heat users' LDC heating cost.

$$flow\ capacity = \frac{heat\ use\ over\ a\ certain\ period}{category\ number} \tag{6-1}$$

Moreover, the specified conditions of the case study may limit the applicability of the research, especially for the findings on the economic optimal distribution temperature. The conditions of DH systems vary from case to case, and some changing factors may impact the results

significantly. As discussed in **Paper 4**, the share of the LDC heating cost in the heat pricing model and the linear heat density of the DH system are two crucial factors needed to be considered, when investigating the economically optimal distribution temperature. Raising the share of the LDC heating cost motivates heat users to shave their peak load, and thus increases the economically optimal distribution temperature, because the TESs need higher charging temperatures to achieve larger peak load shaving capacities. In addition, decreases in the linear heat density would be detrimental to the heat distribution and result in higher distribution heat loss, consequently, the economically optimal distribution temperature should be reduced to maintain the same level of the heating cost. Figure 6-1 illustrates how these two factors drive the economically optimal distribution temperature. The orange rectangles in the upper left corner and the green rectangles in the bottom right corner locate the situations with the high and the low economically optimal distribution temperatures, respectively. The current DH systems mainly use hot water as the medium, therefore the high and low distribution temperatures in Figure 6-1 may belong to the 2nd and the 4th generation DH system, respectively. The blue rectangles represent the situations with medium economically optimal distribution temperatures, which may belong to the 3rd generation DH system.

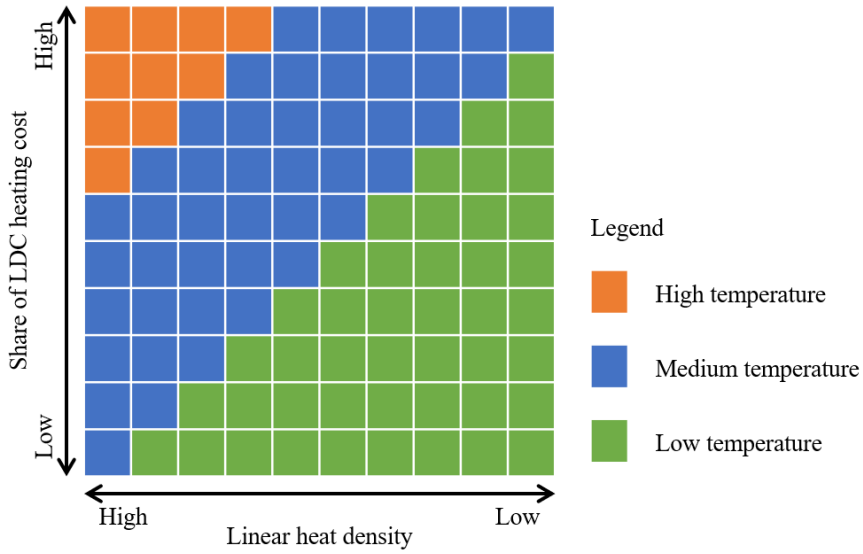

Figure 6-1. Roadmap for the economically optimal distribution temperature (based on Paper 4)

Last but not least, thermal couplings between the supply and demand sides should be handled more meticulously by the optimization problem. The supply and demand sides of DH systems each have their individual goals, but their operation should be coordinated to achieve global optimums for the entire DH systems. Precisely describing thermal couplings between these two sides is crucial to facilitate this coordination process in an optimization framework. To represent these thermal couplings, the optimization problem in Section 3.5 used a simplified technique, i.e., utilizing bounds to constrain the supply side's supply temperature and temperature difference. Using bounds to constrain these temperatures, however, is insufficient to describe the thermal couplings. These couplings, as shown in Figure 6-2, are the results of a complicated heat transfer process that is influenced by operating variables on both sides, such as water temperatures and flow rates. Nonlinear equations are required to describe this process, such as using the Number of Thermal Units Method. These nonlinear equations, on the other hand, may reduce computationally efficiency and cause numerical instabilities for the optimization problem. Moreover, obtaining the variables on the demand side used by these nonlinear equations, which must take into account weather conditions as well as thermal dynamics of buildings and heating systems as illustrated in Figure 6-2, might add to the optimization problem's complexity.

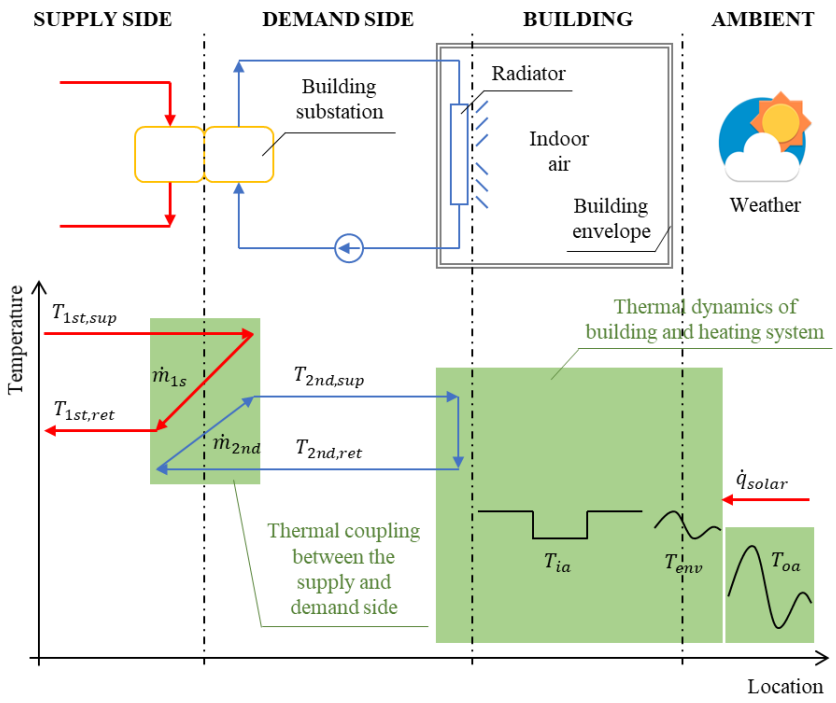

Figure 6-2. Thermal couplings between the supply side and the demand side

6.3 Future research

Based on the presented research findings and acknowledged limitations, possible future studies are recommended as follows.

Firstly, given the importance of distribution temperature in the development of DH systems, an elaborated roadmap that illustrates the correlations between the economically optimal distribution temperature and crucial factors is needed. The roadmap will assist the design and operation of heat-prosumer-based DH systems, as well as provide individual guidelines for heat prosumers in specific situations. Furthermore, the roadmap might aid DH companies in developing new heat pricing models, promoting the development of heat prosumers, and facilitating the transition to future DH systems.

In addition, a multi-level optimization framework is also demanded, in which the optimization of the entire DH system is divided into three levels: heat sources, TESs, and buildings. The multi-level optimization framework minimizes the total energy cost, while satisfying individual

demands and restrictions. It makes a significant contribution by overcoming the disadvantages of the centralized optimization framework developed in this thesis, such as high computational burden and limited flexibility and scalability.

CONCLUSIONS

BIBLIOGRAPHY

[1] In focus: Energy efficiency in buildings, https://ec.europa.eu/info/news/focus-energy-efficiency-buildings-2020-feb-17_en#:~:text=Collectively%2C%20buildings%20in%20the%20EU,%2C%20usage%2C%20renovation%20and%20demolition, accessed September 2020.

[2] Heating and cooling, https://ec.europa.eu/energy/topics/energy-efficiency/heating-and-cooling_en?redir=1, accessed September 2020.

[3] Mapping and analyses of the current and future (2020-2030) heating/cooling fuel deployment (fossil/renewables), https://ec.europa.eu/energy/studies/mapping-and-analyses-current-and-future-2020-2030-heatingcooling-fuel-deployment_en, accessed September 2020.

[4] Li H, Nord N. Transition to the 4th generation district heating - possibilities, bottlenecks, and challenges. Energy Procedia. 2018;149:483-98.

[5] Werner S. International review of district heating and cooling. Energy. 2017;137:617-31.

[6] Åberg M, Fälting L, Lingfors D, Nilsson AM, Forssell A. Do ground source heat pumps challenge the dominant position of district heating in the Swedish heating market? Journal of Cleaner Production. 2020;254:120070.

[7] Connolly D, Lund H, Mathiesen BV, Werner S, Möller B, Persson U, et al. Heat Roadmap Europe: Combining district heating with heat savings to decarbonise the EU energy system. Energy Policy. 2014;65:475-89.

[8] Buffa S, Cozzini M, D'Antoni M, Baratieri M, Fedrizzi R. 5th generation district heating and cooling systems: A review of existing cases in Europe. Renewable and Sustainable Energy Reviews. 2019;104:504-22.

[9] Christian Holmstedt Hansen OG, Hanne Kortegaard Støchkel, and Nina Detlefsen. The competitiveness of district heating compared to individual heating. 2018.

[10] Dalla Rosa A, Li H, Svendsen S, Werner S, Persson U, Ruehling K, et al. IEA DHC Annex X report:Toward 4th Generation District Heating. Experience and Potential of Low-Temperature District Heating2014.

[11] Persson U, Werner S. Heat distribution and the future competitiveness of district heating. Applied Energy. 2011;88(3):568-76.

[12] Song J, Wallin F, Li H. District heating cost fluctuation caused by price model shift. Applied Energy. 2017;194:715-24.

[13] Tian Z, Perers B, Furbo S, Fan J. Thermo-economic optimization of a hybrid solar district heating plant with flat plate collectors and parabolic trough collectors in series. Energy Conversion and Management. 2018;165:92-101.

[14] Shah SK, Aye L, Rismanchi B. Seasonal thermal energy storage system for cold climate zones: A review of recent developments. Renewable and Sustainable Energy Reviews. 2018;97:38-49.

[15] Köfinger M, Schmidt RR, Basciotti D, Terreros O, Baldvinsson I, Mayrhofer J, et al. Simulation based evaluation of large scale waste heat utilization in urban district heating networks: Optimized integration and operation of a seasonal storage. Energy. 2018;159:1161-74.

[16] Rohde D, Andresen T, Nord N. Analysis of an integrated heating and cooling system for a building complex with focus on long–term thermal storage. Applied Thermal Engineering. 2018;145:791-803.

[17] Rohde D, Knudsen BR, Andresen T, Nord N. Dynamic optimization of control setpoints for an integrated heating and cooling system with thermal energy storages. Energy. 2020;193:116771.

[18] Verrilli F, Srinivasan S, Gambino G, Canelli M, Himanka M, Del Vecchio C, et al. Model Predictive Control-Based Optimal Operations of District Heating System With Thermal Energy Storage and Flexible Loads. IEEE Transactions on Automation Science and Engineering. 2017;14(2):547-57.

[19] Verda V, Colella F. Primary energy savings through thermal storage in district heating networks. Energy. 2011;36(7):4278-86.

[20] Harris M. Thermal Energy Storage in Sweden and Denmark: Potentials for Technology Transfer. IIIEE Master thesis. 2011.

[21] Li H, Hou J, Hong T, Ding Y, Nord N. Energy, economic, and environmental analysis of integration of thermal energy storage into district heating systems using waste heat from data centres. Energy. 2021;219:119582.

[22] Lund H, Werner S, Wiltshire R, Svendsen S, Thorsen JE, Hvelplund F, et al. 4th Generation District Heating (4GDH) Integrating smart thermal grids into future sustainable energy systems. Energy. 2014;68:1-11.

[23] Larsson O. Pricing models in district heating, Master thesis, 2011.

[24] Brand M, Svendsen S. Renewable-based low-temperature district heating for existing buildings in various stages of refurbishment. Energy. 2013;62:311-9.

[25] Østergaard DS, Svendsen S. Costs and benefits of preparing existing Danish buildings for low-temperature district heating. Energy. 2019;176:718-27.
[26] Østergaard DS, Svendsen S. Replacing critical radiators to increase the potential to use low-temperature district heating – A case study of 4 Danish single-family houses from the 1930s. Energy. 2016;110:75-84.
[27] Østergaard DS, Svendsen S. Are typical radiators over-dimensioned? An analysis of radiator dimensions in 1645 Danish houses. Energy and Buildings. 2018;178:206-15.
[28] Østergaard DS, Svendsen S. Experience from a practical test of low-temperature district heating for space heating in five Danish single-family houses from the 1930s. Energy. 2018;159:569-78.
[29] Jangsten M, Kensby J, Dalenbäck JO, Trüschel A. Survey of radiator temperatures in buildings supplied by district heating. Energy. 2017;137:292-301.
[30] Nord N, Ingebretsen M, Tryggestad I. Possibilities for Transition of Existing Residential Buildings to Low Temperature District Heating System in Norway. Conference Possibilities for Transition of Existing Residential Buildings to Low Temperature District Heating System in Norway. p. 22-5.
[31] Li H, Nord N. Operation strategies to achieve low supply and return temperature in district heating system. E3S Web Conf. 2019;111:05022.
[32] Hou J, Li H, Nord N. Optimal control of secondary side supply water temperature for substation in district heating systems. E3S Web Conf. 2019;111:06015.
[33] Li H, Nord N. Transition to the 4th generation district heating-possibilities, bottlenecks, and challenges. Energy Procedia. 2018;149:483-98.
[34] Tunzi M, Østergaard DS, Svendsen S, Boukhanouf R, Cooper E. Method to investigate and plan the application of low temperature district heating to existing hydraulic radiator systems in existing buildings. Energy. 2016;113:413-21.
[35] CEN. EN 442-2: Radiators and Convectors–Part 2: Test Methods and Rating. 2003.
[36] Marguerite C, Schmidt R-R, PARDO GARCIA N. Concept development of an industrial waste heat based micro DH network. Conference Concept development of an industrial waste heat based micro DH network. LESO-PB, EPFL, p. 597-602.
[37] Nielsen S, Möller B. Excess heat production of future net zero energy buildings within district heating areas in Denmark. Energy. 2012;48(1):23-31.

[38] Brand L, Calvén A, Englund J, Landersjö H, Lauenburg P. Smart district heating networks – A simulation study of prosumers' impact on technical parameters in distribution networks. Applied Energy. 2014;129:39-48.

[39] Huang P, Copertaro B, Zhang X, Shen J, Löfgren I, Rönnelid M, et al. A review of data centers as prosumers in district energy systems: Renewable energy integration and waste heat reuse for district heating. Applied Energy. 2020;258:114109.

[40] Kauko H, Kvalsvik KH, Rohde D, Nord N, Utne Å. Dynamic modeling of local district heating grids with prosumers: A case study for Norway. Energy. 2018;151:261-71.

[41] Open District Heating, https://www.opendistrictheating.com/, accessed May 2021.

[42] Sernhed K, Gåverud H, Sandgren A. Customer perspectives on district heating price models. International Journal of Sustainable Energy Planning and Management. 2017;13:47-60.

[43] Song J, Wallin F, Li H, Karlsson B. Price Models of District Heating in Sweden. Energy Procedia. 2016;88:100-5.

[44] The Modelica Association, https://www.modelica.org/, accessed Jan 2021.

[45] Modelica Standard Library, https://github.com/modelica/ModelicaStandardLibrary, last access May 2021.

[46] IBPSA Project 1, https://ibpsa.github.io/project1/index.html, accessed May 2021.

[47] DYMOLA Systems Engineering, https://www.3ds.com/products-services/catia/products/dymola/, Last accessed May 2021.

[48] Magnusson F, Åkesson J. Dynamic optimization in jmodelica. org. Processes. 2015;3(2):471-96.

[49] Mangold D, Deschaintre L. Task 45 Large Systems Seasonal thermal energy storage Report on state of the art and necessary further R+ D. International Energy Agency Solar Heating and Cooling Programme. 2015.

[50] Bott C, Dressel I, Bayer P. State-of-technology review of water-based closed seasonal thermal energy storage systems. Renewable and Sustainable Energy Reviews. 2019;113:109241.

[51] Pinel P, Cruickshank CA, Beausoleil-Morrison I, Wills A. A review of available methods for seasonal storage of solar thermal energy in residential applications. Renewable and Sustainable Energy Reviews. 2011;15(7):3341-59.

[52] Clausen KS, From N, Hofmeister M, Paaske BL, Flørning J. Large heat pump projects in the district heating system (in Danish). Copenhagen: Danish Energy Agency; 2014.

[54] Modelica Standard Library, https://github.com/modelica/ModelicaStandardLibrary. Last accessed 2020.

[55] IBPSA Project 1, https://ibpsa.github.io/project1/index.html. Last accessed 2020.

[56] AixLib.Fluid.Storage.UsersGuide. 2019.

[57] He P, Sun G, Wang F, Wu H, Wu X. Heating engineering (in Chinese): China Architecture & Building Press, 2009.

[58] CEN. CEN/TR16355 Recommendations for prevention of Legionella growth in installations inside buildings conveying water for human consumption. 2012.

[59] Statistics Norway, https://www.ssb.no/en, accessed Sep 2021.

[60] Housing conditions, survey on living conditions, https://www.ssb.no/en/bygg-bolig-og-eiendom/statistikker/bo. 2019.

[61] AS P, AS E. Potential and barrier study- Energy efficiency of Norwegian buildings (in Norwegian). 2012.

[62] Larsson O. Pricing models in district heating 2011.

[63] Frederiksen S, Werner S. District heating and cooling: Studentlitteratur Lund, 2013.

BIBLIOGRAPHY

APPENDIX- PUBLICATIONS

This section contains the publications that make up the thesis.

APPENDIX- PUBLICATIONS

APPENDIX- PUBLICATIONS

PAPER 1

Li H, Nord N. Transition to the 4th generation district heating-possibilities, bottlenecks, and challenges. Energy Procedia. 2018;149:483-98. The 16th International Symposium on District Heating and Cooling.

APPENDIX- PUBLICATIONS

Available online at www.sciencedirect.com

ScienceDirect

Energy Procedia 149 (2018) 483–498

Energy Procedia

www.elsevier.com/locate/procedia

16th International Symposium on District Heating and Cooling, DHC2018, 9–12 September 2018, Hamburg, Germany

Transition to the 4th generation district heating - possibilities, bottlenecks, and challenges

Haoran Li[a]*, Natasa Nord[a]

[a]*Norwegian University of Science and Technology, Kolbjørn Hejes v 1B, Trondheim, NO-7491, Norway*

Abstract

The 4th generation district heating (DH) will be available in the coming years. However, the transition from the current 2nd or 3rd generation DH is a challenging task. This article reviewed the technical issues associated with the transition: supplying low temperature to buildings, integrating various heat sources and thermal storages, and developing smart DH systems. Possibilities, bottlenecks, and challenges of the transition were discussed. The conclusion was that the transformation should be conducted carefully and gradually. Comprehensive consideration such as the energy status, system conditions, and operation customs must be taken into account.

Keywords: 4th generation distrcit heating, transition, challenges, low temperature district heating, various heat sources, thermal storage, smart district heating system;

1. Introduction

District heating (DH) is an energy service, which moves the heat from available heat sources to customers. The fundamental idea of DH is to use local fuel or heat resources, which would otherwise be wasted, to satisfy local customer heat demands, by using heat distribution networks [1].

· Corresponding author. Tel.: +47-48670533.
E-mail address: haoranli@ntnu.no

10.1016/j.egypro.2018.08.213

In historical development of DH, three generations of DH developed successively. The 1st generation DH systems used steam as the heat carrier. Typical components were steam pipes in concrete ducts, steam traps, and compensators. Almost all DH systems established until 1930 used this technology. The 2nd generation DH systems used pressurized hot water as the heat carrier, with supply temperatures mostly higher than 100℃. Typical components were water pipes in concrete ducts, large tube-and-shell heat exchangers, and material-intensive, large, and heavy valves. These systems emerged in the 1930s and dominated all new systems until the 1970s. The 3rd generation DH systems still use pressurized water as the heat carrier, but the supply temperatures are often below 100 ℃. Typical components are prefabricated, pre-insulated pipes directly buried into the ground, compact substations using plate stainless steel heat exchangers, and material lean components. The systems was introduced in the 1970s and took a major share of all extensions in the 1980s and beyond [2].

The direction of development for these three generations has been in favor of lower distribution temperature, material-lean components, and prefabrication. On the basis of the trends identified above, the future DH technology should include lower distribution temperatures, assembly-oriented components, and more flexible materials [1]. The revolutionary temperature level, with supply temperature below 50~60℃, will become the most important feature of the 4th generation DH. The energy supply system, end users, and occupants will benefit from the low temperature level. A brief summary of those benefits are shown in Table 1.

Table 1. Major advantages with lower distribution temperatures.

Objects	Advantages	References
Flue gas condensation from combustion of biomass and waste	Higher output capacity (25~40%) from direct condensation of the fuel moisture in biomass fuels and waste	[1]
Geothermal energy and industrial residual heat with medium temperature	Higher output capacity (50~100%) from available medium-temperature (70~100℃) water flow	[1]
Solar energy	Higher output capacity from connected solar heat collectors	[1]
Steam based combined heat and power (CHP) plant	Higher power-to-heat ratios in the same CHP plant design, results more electricity generation at the same heat demand	[1]
Heat pump (HP)	Higher coefficient of performance, since both pressure and temperature can be lower in the HP condenser	[3]
Heat storage	Increased capacities in water-based heat storages managing both supply and demand variations, reduce heat losses from thermal storage units	[1, 3]
Network	Higher distribution efficiency due to less heat loss from the network	[3]
Network	Lower risk of pipe leakages due to thermal stress, and the corresponding maintenance costs are reduced as well	[3]
Network	Possibility to use plastic pipes in distribution areas with low pressures	[3]
Network	Lower risk of water boiling in the network, which means lower risk of two-phase-flow in pumps and fast moving water walls	[3]
Building	Better match the future building heat demand and heat temperature requirement	[3]
Occupant	Eliminate the potential risk of scalding human skin due to water leakages	[3]

In addition, the 4th generation DH will take advantage of various heat sources, different level thermal storages, modern measuring equipment, and advanced information technology, to make itself more flexible, reliable, intelligent, and competitive.

This article reviews the technical issues associated with transition to the future DH. The studies on transition to the low temperature DH (LTDH) systems are summarized in Section 2.1. The knowledge of integrating various heat sources and thermal storages are presented in Section 2.2 and Section 2.3, respectively. The idea of smart DH system is shown in Section 2.4. Further, some facing challenges and possible solutions for the future DH are discussed in Section 3. Finally, the conclusions for transition to the future DH are proposed in Section 4.

2. Transition to the future district heating

Characterized by low temperature, various heat sources, thermal energy storage (TES), intelligent management, and integration with smart energy system, the 4th generation DH will be available in the coming years. However, the transition from the current 2nd or 3rd generation DH to the future 4th generation DH is a challenging task. This section reviews the following technical issues associated with transition to the 4th generation DH: suppling low temperature to new and existing buildings, integrating various heat sources including renewable sources and recycled sources, different TES technologies, and smart DH systems. In addition, the bottlenecks and challenges of the transition are presented together with potentials solutions.

2.1. Transition to the low temperature district heating system

2.1.1. Temperature level of the current system

For the DH system using pressurized hot water as the heat carrier, the water is heated up to the supply temperature at the heat supply units, and cooled down to the return temperature at the customer substations. The supply temperature is decided by the heat provider, while the return temperature is the aggregated result from all cooling processes at the customer substations. The supply and return network temperatures are not standardized, they will depend on the local conditions [1].

An overview of annual average temperature level of 142 Swedish and 207 Danish DH systems is provided in Fig. 1 [4]. Fig. 1 shows that Swedish and Danish DH systems can be regarded as the 3rd generation DH system with respect to their temperature levels. The average network temperatures in Sweden and Denmark are compared with six other European DH systems in Fig. 2. Fig. 2 shows that the temperature levels of Riga, Warsaw, and Poznan DH systems are similar to the Swedish and Danish systems and they can be also classified as the 3rd generation DH system. However, for Geneva and Brescia systems, the temperature level are relative high, with annual average supply temperatures close to or above 100°C, and with return temperatures range from around 60°C to 80°C. Therefore, these systems may be regarded as the 2nd generation DH system [5].

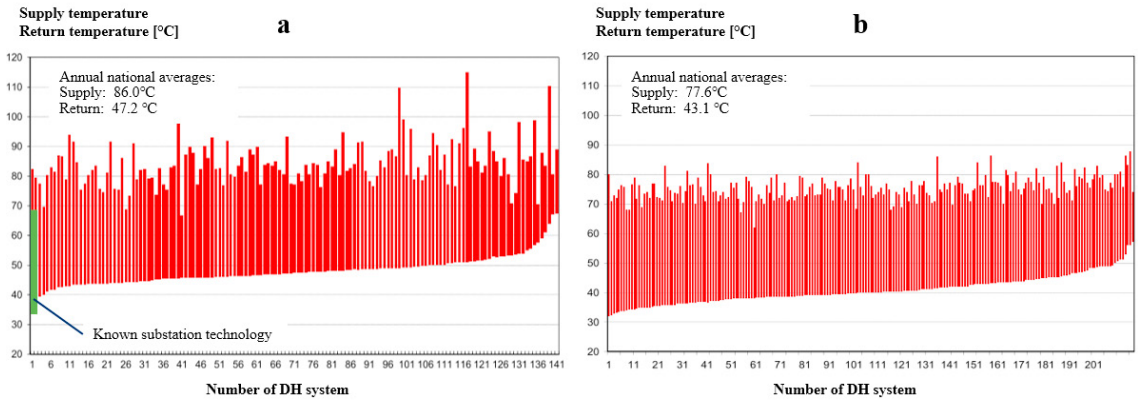

Fig. 1. Overview of heat distribution temperatures in different DH systems. (a) 142 Swedish DH systems, (b) 207 Danish DH systems [4]

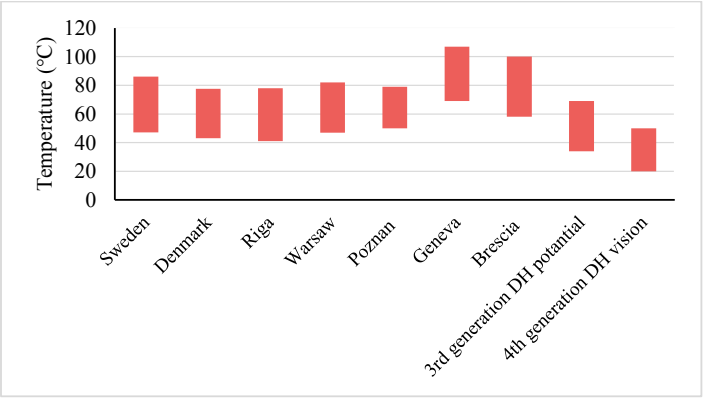

Fig. 2. Typical distribution temperatures for various systems

2.1.2. Transition to the low temperature district heating system

The possibilities to achieve lower temperature level are summarized in the final report of International Energy Agency Technology Collaboration on District Heating and Cooling including Combined Heat and Power (IEA DHC) Annex XI - Transformation Roadmap from High to Low Temperature District Heating Systems [5] . In this report, the transition processes to the low temperature DH are explained in two steps. In the first step, the temperature potential of the current DH system will be fulfilled, with the measures of eliminating system errors and improving system control. In the second step, the temperature level will be further reduced, by the means of enhancing the heat transfer performance of heat exchangers, and improving the design of substations. The renovation of buildings will be conducted along the two steps when it is necessary. These necessary actions for the transition are explained in the text below.

Eliminating system errors and improving system control is a highly important task to reduce the temperature in a DH system. The green bar at the left of Fig. 1 (a) shows the theoretical annual supply and return temperatures of 69 and 34°C for a typical error-free substation with the current substation technology [1]. During 2009, the Marstal DH system in Denmark had an annual average supply and return temperature of 74 and 36°C, very near to the theoretical temperature level. The Marstal DH management has thus proved that it is possible to operate a DH system very near to the theoretical supply and return temperatures [1]. However, Most Swedish DH systems have substantially higher return temperature than their potentials, especially the systems located to the right of Fig. 1 (a). The causes and possible solutions for the difference between actual and theoretical return temperature are summarized in Table 2.

Table 2. Causes and possible solutions for the difference between actual and theatrical return temperature.

Causes		Possible solutions	References
Short-circuit flows	Intentional short-circuit flows to maintain a minimum supply temperature, or to avoid network work freezing	Suitable controlled by thermostatic valves, or introduce innovative systems to avoid bypass flow	[1, 6]
	Unintentional short-circuit flows from remnants of construction, or from the connection mistake	Improve the construction quality	
Low supply temperature	Substation control with high flows to compensate the low supply temperature	Apply intentional short-circuit flows, or use three pipe system with two supply pipes and one return pipe	[1, 5]
Errors in customer heating systems	Missing thermostatic valves in space heating (SH) system, missing hot water circulation in domestic hot water (DHW) system, and using three-way diverting valves in the SH system	Add thermostatic valves in SH system, put the temperature sensor of DHW near or in the heat exchanger, and replace three-way diverting valves with two-way valves	[1, 5]

Causes		Possible solutions	References
	Too small heat emitting surfaces in SH, ventilation and DHW system, which results in a large flow and low cooling	Choose suitable heat emitting surfaces	
Errors in customer substations	Set point errors, sometimes the secondary set point temperature is higher than the primary supply temperature, giving full primary flow	Intelligent control which can ignore impossible control situations	[1, 4, 7]
	Malfunction errors, such as leaking valves, defective valve motors, and malfunctioning temperature transmitters, fouled heat transfer areas for heat exchangers	Use high quality equipment, apply fault detection technology, and regular maintenance	
	Design errors, such as too large valves, wrongly assembled temperature transmitters, and wrong valve motors chosen, parallel flow installations for heat exchangers, and wrong heat exchanger size chosen, deviations from recommended substation configurations	Improve the design quality, apply the prefabricated equipment	

Domestic hot water (DHW) preparation requires certain temperature levels and thereby influence the substation layout and component sizes. The Number of Thermal Units (NTU) indicates the heat transfer ability of heat exchangers. With a fixed heat exchange capacity, larger NTU allows a heat exchanger to operate with lower temperature difference. Meanwhile, larger NTU implies an increased heat exchanger area, which leads to an increased investment cost. For a heat exchanger for DHW preparation, the NTU value is 3.2, with the primary and secondary inlet/outlet temperature as 60°C/25°C and 10°C/50°C, which are recommended by Euroheat and Power [8]. For the low temperature systems with the primary and secondary inlet/outlet temperature as 50°C/20°C and 14°C /47°C, the NTU value should be doubled to 7.6 [5].

For the ultra-low-temperature DH systems, whose supply temperature can be 46°C most of the year, supplementary heating devices are recommended to guarantee comfortable and hygienic DHW [9-11]. Some examples for such application are shown in Fig. 3. In Fig. 3 (a), the DHW is stored in the storage tank and used directly. The DHW is preheated by the DH and further heated by the electric heater. The layout difference between Fig. 3 (a) and Fig. 3 (b) is that Fig. 3 (b) has a heat exchanger after the storage tank, and the DH water is stored in the tank. In Fig. 3 (c), the DHW is preheated by DH through a heat exchanger. The temperature could be comfortable for taking a shower, but considering the requirement for hotter DHW for washing purposes in the kitchen, an instantaneous electric heater is installed on the DHW pipe to the kitchen taps. Fig. 3 (d) has the same layout as Fig. 3 (c), except that an electric heater is used to heat up the total DHW flow. In Fig. 3 (e), a micro HP and a storage tank are installed before the heat exchanger, and one stream of the DH supply is used as the heat source for the HP.

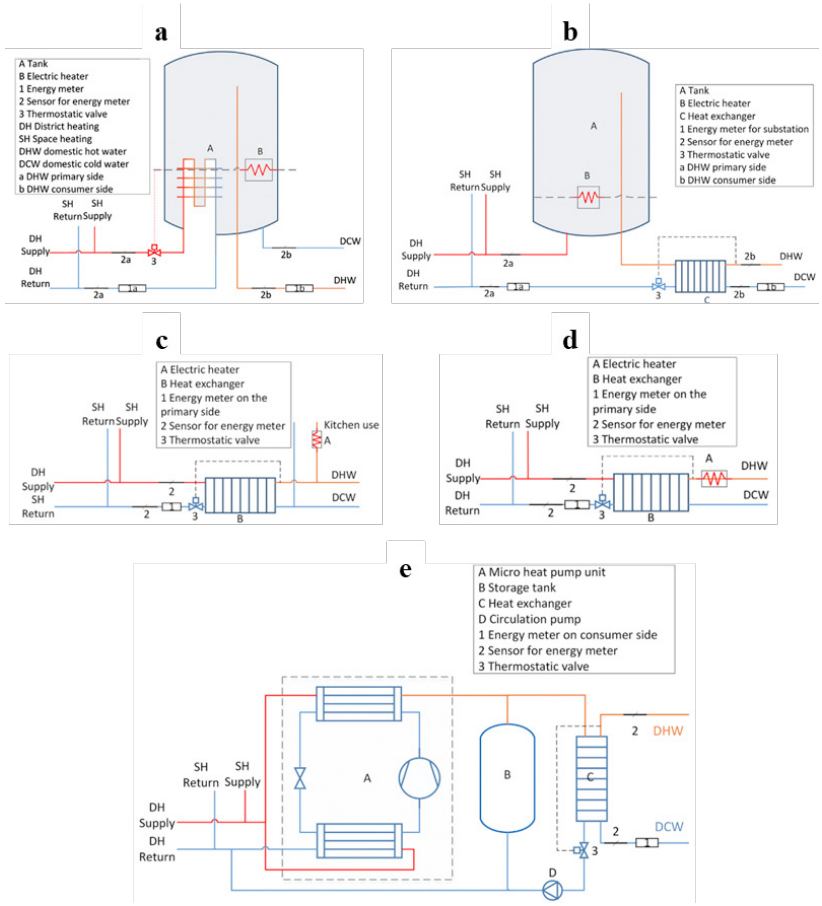

Fig. 3. Different layouts of substations for DHW with supplementary heating devices. (a) substation with tank, (b) substation with tank and heat exchanger, (c) substation with heat exchanger and supplementary heater for kitchen use, (d) substation with heat exchanger and supplementary heater for the total DHW flow, (e) substation with HP, tank and heat exchanger [10].

Building space heat (SH) demand will change in the future and thereby the temperature requirements will change. For newly built buildings and future buildings, 50°C supply temperature to the SH system is enough, with floor heating or low-temperature radiators, and there is still the option to boost the supply temperature during the coldest periods. In fact, the DH supply temperature can be even lower, but it needs supplementary heating system to heat up DHW as explained previously [12].

Low-energy buildings comprise only a small share of the building stock, while the majority are older buildings with considerably higher heat demand. The older buildings will continue to make up a large share of the building stock for many years (for Denmark and Norway, the share will be about 85-90% [13] and 50% [14] in 2030, respectively). Existing buildings are usually equipped with SH systems designed with supply temperatures around 70°C or higher and thereby a reduction of the supply temperature would be expected to cause discomfort for the occupants [12]. However, studies show that houses from the 70s or 80s without any renovation are possible to be heated with the low supply temperature of 50°C most of the year, and only limited time the supply temperature has to be above 60°C. If original windows of the houses are replaced, it is possible to decrease the supply temperature below 60°C for almost the entire year. Further, when the renovated houses replace their SH systems with low-temperature radiators, they may be supplied year around with the supply temperature of 50°C [12, 15].

2.2. Integrating various heat sources into district heating system

There is a huge potential to supply DH systems with heat from various renewable sources, such as industrial waste heat (IWH), solar thermal energy, and geothermal energy. The main advantage of LTDH system is its easier integration and higher efficiency when utilize renewable energy and waste heat (REWH). When the temperature of REWH is higher than the return temperature of a DH system, the resource can be used directly, otherwise the temperature must be upgraded with a HP [16].

Availability is one critical aspect of REWH. Some resources, such as solar and wind, are intermittent and not dispatchable. The hourly and seasonal distribution of those resources may be counter to the distribution of heat demands. In addition, some resources, such as IWH, may be subject to interruptions due to the operating hours of industrial facilities [16]. One common solution is to combine REWH with TES and dispatchable heat sources [1, 17-19].

2.2.1. Methods for heat sources feed-in

There are mainly three ways to feed-in heat sources into DH grids: 1) extraction from the return line and feed-in into the supply line, 2) extraction from the return line and feed-in into the return line, and 3) extraction from the supply line and feed-in into the supply line. The features, advantages, and disadvantages of those variants are summarized in Table 3 [14].

Table 3. The features, advantages and disadvantages of various connection variants.

Connection variants	Features	Advantages	Disadvantages
Extraction from the return line and feed-in into the supply line	The temperature difference is dependent on operating conditions and grid operator. The pressure difference is high, and depends on the actual location in the grid	The return temperature is unchanged, which avoids temperature the strain on return pipes, and the influence of heat extraction efficiency of other heat sources	High energy demand for the mandatory feed-in pumps
Extraction from the return line and feed-in into the return line	The temperature rise is commonly set by the DH operator, the pressure difference is relatively low	It is preferable for heat sources with high efficiencies for lower temperatures	The return temperature is raised, which increases the grid heat loss, and influence the efficiency of other heat sources
Extraction from the supply line and feed-in into the supply line	The temperature increase is prescribed by the grid operator, the pressure difference is relatively low	—	The supply temperature is raised, which increases the grid heat loss, and influence the efficiency of other heat sources

2.2.2. Heat recycling from industrial processes

Recycling heat from industrial processes represents one of the main strategic opportunity for DH, in line with the basic idea of using heat that would otherwise be wasted. In Sweden, recycling of IWH makes up around 6% of the total energy supply to DH networks in 2010. For Danish DH systems, the proportion is about 2%~3%. The DH system in Gothenburg, Sweden, obtains 1112 GWh waste heat from two oil refineries. This gave approximately 27% of heating demand in 2010 [1].

The IWHs are heterogeneous and of various grades. The high-grade IWHs, such as steam and combustible gas, mostly be exploited within the factory, for power generation. However, the low-grade IWHs, with the temperature mostly between 30°C and 200°C, are likely discarded into the environment. There are several technical issues for recycling IWH for DH use: the long distance delivery of IWH to end users, and peak load-shaving of DH system [20].

Long distance delivery for waste heat: Industrial plants are usually far away from DH users, the recommended radius for IWH based DH is 5~10 km for a small-scale town and 20~30 km for a large-or-medium-scale city, due to the investment of transmission network and heat loss during the transmission. However, such a radius might vary with different economic conditions [21].

To decrease the energy use of distribution pumps and thereby the distribution losses, the temperature difference between the supply and return temperature should be increased. As the advantages of LTDH, the reasonable solution is to reduce the return temperature. Several potential techniques to obtain higher temperature difference are shown in Fig. 4, which includes cascade heating technology, absorption heat pump (AHP) technology, and HP technology.

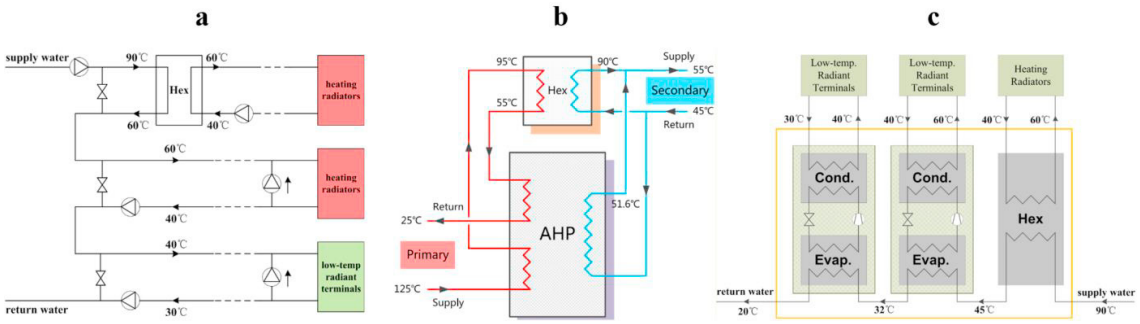

Fig. 4. Scheme of different IWH transition techniques. (a) typical cascade heating system, (b) substation/building entrance AHP system, (c) substation/building entrance electrically driven HP system [20].

In Fig. 4 (a), cascade heating technology supplies heat to the indirectly connected radiators, directly connected radiators, and directly connected low-temperature heating terminals (e.g. floor heating), in sequence. Commonly, the return temperature can be reduced to 30°C or even less by this technology. In Fig. 4 (b), water on the primary side firstly flows into AHP to drive the machine, AHP extracts heat from return water of heat exchanger. After AHP, the water go through the heat exchanger and AHP successively. The final return water can be 25°C. The limitation of this technology is the supply temperature should be high enough to drive AHP. In Fig. 4 (c), supply water firstly transfers heat to heating radiators through a heat exchanger, afterword, the water provides heat to several low-temperature heating terminals by HPs, until the final return temperature become 20°C or even lower [21].

Peak load-shaving in DH systems: An IWH based DH system is complex with respect to the coordination between IWH productions and DH heat demands. Waste heat from industrial processes is constantly fluctuating, and may even come to a temporary stop, depending on the production schedules [21]. However, the heat demand of a DH system changes continuously and smoothly according to the weather conditions [21] and the occupant behaviors [22].

For the above reason, IWH can never serve as the sole heat source, specific control and peak load-shaving strategies should be applied, as shown in In Fig. 5. In Fig. 5 (a), IWH is able to serve the maximum heat load, and cooling towers (CTs) have to operate all the time except the coldest days to release heat to the environment. Opposite, in Fig. 5 (c), IWH serves as the base load. Thus, the peak load-shaving strategies have to be implemented to make up the difference between the total load and the base load. Fig. 5 (b) illustrates a case between these extremes, in which both the CTs and peak-shaving strategies are necessary. To achieve a high IWH recovery ratio, it is appropriate for the IWH to serve as the base load as in Fig. 5 (c). Fig. 5 (d) shows an ideal operation strategy, which takes the fluctuation of IWH into consideration. In this case, IWH together with other heat sources provide the base load, and the peak load-shaving strategy works at the coldest time in winter [21].

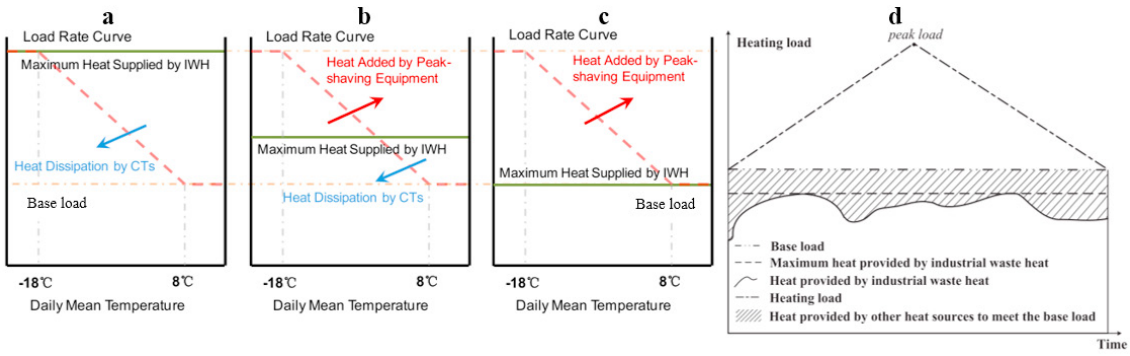

Fig. 5. Regulation and peak load-shaving of IWH based DH system. (a) IWH is able to serve the maximum heat load, (b) a moderate operation strategy with both the peak load-shaving equipment and CTs, (c) IWH serves as the base load, (d) an ideal operation strategy taking the fluctuation of IWH into consideration [20].

2.2.3. Solar district heating

In an international context, solar DH is still in development stage, and it is difficult to ascertain its long-term prospects. There have been interesting developments in a number of countries in Europe, especially in Austria, Denmark, Germany, and Sweden. Recently, companies from these countries have succeeded in contracting for large plants in Asia [1].

The contribution of solar heat to the total heat load can be various from system to system. A large solar thermal plant can be used as a preheater with solar fraction up to 5%. A 100%-coverage of the summer heat load is usually reached with a solar fraction of about 15% on an annual basis. Solar fraction of up to 50% of the annual heat load have been demonstrated for systems using large seasonal heat storages, charging the summer solar heat for the heating period in winter [23].

Solar DH can be provided in a centralized manner with a large array of ground-based collectors, or in a decentralized manner with rooftop-mounted collectors on the buildings that are connected to a DH network, mixed alternatives are also possible, depend on the situation of the projects [1, 19]. Several typical applications of solar DH are presented in Table 4.

Table 4. Typical applications of solar DH.

Location	Solar fraction/ Solar capacity (%/MW_{th})	Other heat sources	DH supply/return temperature (°C)	Thermal storage	Type of integration	Reference
Vallda Heberg (Sweden)	10~20/ 0.2~2	Wood-pellet boiler	—	Buffer storage tank	Centralized	[23]
Crailsheim (Germany)	20~50/ 2~20	Main DH system	65/40	Inter-seasonal borehole heat storage	Centralized	[23]
Gothenburg (Sweden)	100/ 0.2~2	Main DH system	65~100/-	No heat storage	Decentralized	[23]
Büsingen (Germany)	15~20/ 0.5~50	Biomass boiler	75~80/50	—	Centralized	[23]
Braedstrup (Denmark)	10~50/ 0.5~50	CHP, HP and electro-boiler	70~75/30	Multifunctional heat storage	Centralized	[23]
Wels (Austria)	10/ 0.5~10	Main DH system	70~120/-	No heat storage	Decentralized	[23]
Marstal (Denmark)	30/ 13	Oil boiler	—	Two small and one large buffer storages	Centralized	[1]

Location	Solar fraction/ Solar capacity (%/MW_{th})	Other heat sources	DH supply/return temperature (°C)	Thermal storage	Type of integration	Reference
Lyckebo (Sweden)	-/ 3	Biomass boiler	—	Rock cavern hot water storage	Centralized	[1]

The major technical limitation for solar DH is the low energy production density, which means the large areas for placing the solar collectors. In the future, solar thermal energy will continue to be a complementary option [23]. However, the developing technology will bring some possibilities for DH. In the decentralized solar DH systems, there is a possibility that buildings can be either 'importers' or 'exporters' of solar heat energy, or both, depending on the time of the year. Flexibility in this respect offers a prospect for maximizing the use of solar energy, but makes its management difficult. There is another possibility that a large, inter-seasonal storage can be combined with the decentralized solar energy, so that in the summer season all (or most) connected buildings act as 'exporters'.

2.2.4. Geothermal district heating

Geothermal energy has enormous potentials; meanwhile, utilization of geothermal energy produces minimal environmental impact. To varying degrees, exploitable geothermal energy is available all around the world. In spite of the impressive size of this energy source, it currently accounts for only a small fraction of the word energy supply. Intensive initial cost, exploration risk, and human-induced earthquakes are the major obstacle to utilize geothermal energy. In addition, there is also the resource problem- once a geothermal well is set up at a given location, the amount of extracted heat tends to decay gradually, makes it felt to a significant degree after one or few decades, while the DH network is still functioning [1].

Deep geothermal systems use heat from 500~5000 m depth; shallow geothermal systems provide heat from less than 300 m depth. High temperature geothermal energy can be used in conventional ways for electricity generation and for direct heat utilization. Ambient heat stored at shallow depths, and aquifer thermal energy stores in ground water layers can be extracted with ground source heat pump (GSHP) and applied for SH and DHW [24].

Several typical applications of geothermal DH are presented in Table 5.

Table 5. Typical applications of geothermal DH.

Location	Type of system	Geothermal fraction /Geothermal capacity (%/MW_{th})	Other heat sources	Geothermal or DH temperature (°C)	Reference
Paris (France)	1.5~1.8 km depth wells	-/ 250	Fossil fuel boilers	Geo: 70	[25]
Ferrara (Italy)	1 km depth wells	80/ 14	Waste-to-energy plant, backup stations, solar heating station, thermal storage, and organic rankine cycle electricity generation	Geo: 100~105	[25]
Beijing (China)	3 km depth wells	100/ -	No other heat source	Geo: 75	[25]
Ontario (Canada)	213 m depth boreholes	—	—	—	[26]
Malmö (Sweden)	90 m depth wells	-/ 1.3	GSHP, boiler	—	[26]
Bucharest (Romani)	70 and 170 m depth wells	100/ 0.39	GSHP	DH: 40/35	[26]

2.3. Thermal energy storages in district heating system

TES can be divided into inter-seasonal storage and short-term storage. Inter-seasonal storage is still in a development phase, while, short-term storage can be made with well-proven technology. However, the dividing line is not sharp; the largest facilities used for short-term storage in large networks could provide inter-seasonal storage in

small systems [1]. In addition, as the end users of DH systems- buildings can also function as TES, due to their thermal inertia. Sometimes, building inertia TES is able to moderate short-term daily net load variations to the same degree compared with hot water tank, while, with much lower investment cost [27].

One purpose of short-term storage is to shift loads away from peak demand hours to lower demand hours. Another purpose is to provide rapid heat or cold supply to meet sudden load changes, which is not capable for heat generating equipment, or to avoid losses associated with quick starts and stops of the generating equipment. A further function of short-term heat storage is to allow for boosted electric power output from some type of CHP plants, which are characterized by a reduced output at increased heat extraction [1, 28].

The objective of inter-seasonal storage is usually either to store collected solar heat for winter heating, or to act as the heating and cooling source as well as thermal storage for GSHP [29].

There are three available technologies for TES: sensible heat storage, latent heat storage, and chemical storage. Sensible heat storage is a comparatively mature technology that has been implemented and evaluated in many large-scale demonstration projects. Latent heat and chemical storage have much higher energy storage densities than sensible storage, and seldom suffer from heat loss problems. However, the latter two technologies are currently still in the stages of material investigations and lab-scale experiments [30]. The detail comparison of those three technologies are shown in Table 6.

Table 6. Comparison of the three available technologies for TES [30].

	Sensible	Latent	Chemical
Storage medium	Water, gravel, pebble, soil...	Organics, inorganics	Metal chlorides, metal hydrides...
Type	Water, rock, and ground based system	Active and passive storage	Thermal sorption and chemical reaction
Advantage	Environmentally friendly, cheap material, relative simple system, easily control, and reliable	Higher energy density than sensible heat storage, and provide thermal energy at constant temperature	Highest energy density, compact system, and negligible heat losses
Disadvantage	Low energy density, huge volumes required, self-discharge and heat losses problem, high cost of site construction, and geological requirements	Lack of thermal stability, crystallization corrosion, and high cost of storage material	Poor heat and mass transfer property under high density condition, uncertain cyclability, and high cost of storage material
Present status	Large-scale demonstration projects	Laboratory-scale prototypes	Laboratory-scale prototypes
Future work	Optimization of control strategy to advance the solar fraction and reduce the power consumption, optimization of storage temperature to reduce heat losses, and simulation of ground based system with the consideration of affecting factors	Screening for better suited phase change material materials with higher heat of fusion, optimal study on store process and concept, and further thermodynamic and kinetic study, noble reaction cycle	Optimization of the particle size and reaction bed structure to get constant heat output, optimization of temperature level during charging/discharging process, screening for more suitable and economical materials, and further thermodynamic and kinetic study, noble reaction cycle

2.4. Smart district heating system

The transformation toward the future renewable energy system poses challenge for all the sub-systems. Facing the challenge, all the sub-systems should benefit from the use of modern information and communication technologies, and uprated themselves to become smart systems [31].

The smart DH system consists of three essential parts: physical network (PN), internet of things (IoT), and intelligent decision system (IDS). PN includes pipes, heating equipment, local meters, and control devices. IoT is the network of sensors, data collecting and transmission devices, and other items, which enables these objects to be connected and exchange data. IDS makes the optimal decisions based on collected data, heat demands, and system responds [32]. One example for the smart DH concept is shown in Fig. 6.

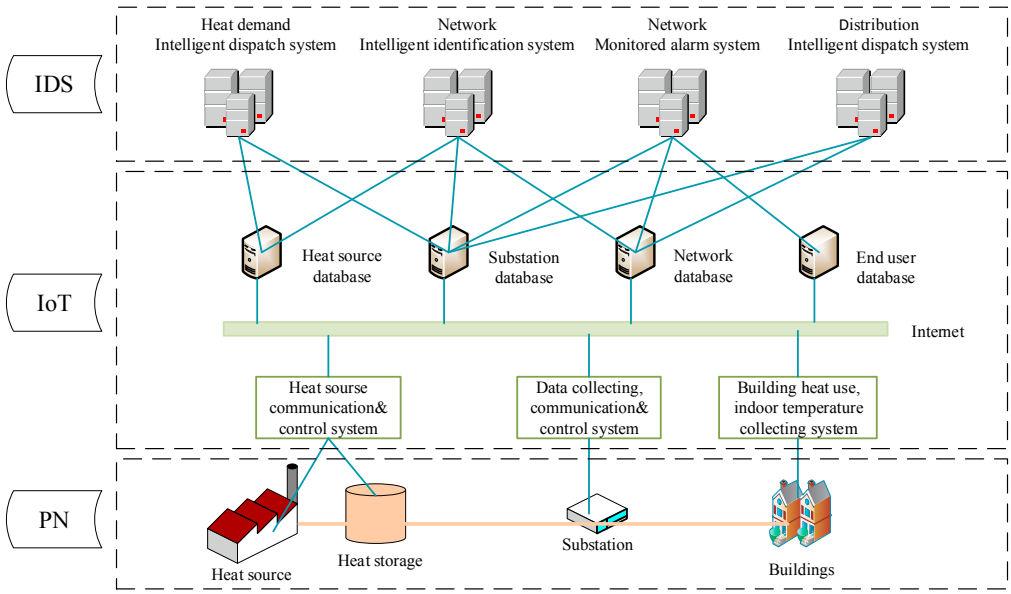

Fig. 6. Concept of smart DH system [33].

The final goal of the smart DH system is to become an essential part of the future smart and renewable energy system. In the future energy system, the focus is on the integration of the electricity, heating, cooling, and transport sectors, and on the use of flexibility in demands and various storages of different sectors. To enable this, the smart DH system must be able to coordinate with other sectors in the energy system [2, 34].

3. Facing challenges for the future district heating system

3.1. Heat losses through distribution network

Reducing heat losses in DH networks is one of the main challenges for the future DH system, because it will reduce the primary energy use and infrastructure investments. Heat loss in DH networks accounts for a relatively high share of heat supply [35], and it will become more significant for the future DH with decreased heat demand.

Real measurement data for heat losses for several DH systems are organized in Table 7. Except the three Swedish cases, all the cases are LTDH demonstration projects. From Table 7, it is obviously that the heat loss in DH networks should not be underestimated, even for the systems with the low temperature and newly upgraded networks. Ten of thirteen systems have a heat losses over 15%, and seven systems have a heat losess over 20%. For the system in Rotskär, the heat losses are up to 32%.

Table 7. Heat losses and detail information of several DH systems.

Location	Construction or upgrade year	Linear heat density MWh/(m·a)	Supply/Return temperature (°C)	Heat loss share (%)	Reference
Slough (UK)	2009~2010	0.319	52/32	28	[14]
Taastrup (Denmark)	2012	—	55/40	13~14	[14]
Lystrup (Denmark)	2008~2009	0.31	55/25	17	[36]
Samsø island (Denmark)	2005	—	—	20~24	[36]
Spjald (Denmark)	1998	0.57	65/32~39	26	[5]
Tarm (Denmark)	1995	0.66	65 /36	17	[5]

Location	Construction or upgrade year	Linear heat density MWh/(m·a)	Supply/Return temperature (°C)	Heat loss share (%)	Reference
Bramminge (Denmark)	—	—	68/-	20	[5]
Middelfart (Denmark)	—	0.72	68/44	19	[5]
Munich (Germany)	2006	1.43	55/30	3	[3]
Okotok (Canada)	2005~2007	0.7	40/35	5~13	[3]
Prästmarken (Sweden)	1995~2004	0.5	75/50	24	[37]
Munksundet (Sweden)	1997	0.84	70/40	22	[37]
Rotskär (Sweden)	2002	0.49	80/-	32	[37]

Some potential solutions to reduce the distribution heat loss are summarized in Table 8.

Table 8. Potential solutions to reduce the distribution heat loss.

Object	Solutions	Limitation	Project applications	Reference
Network	Install pipes inside buildings, to decrease the length of network and utilize heat loss for SH	Not welcomed by DH companies and customers	Peter Freuchenvej	[37]
Network	House-to-house connection, to decrease the length of service pipes	Not welcomed by DH companies and customers	Cederborg, Nordgren, Gudmundsson	[37]
Network	Three or four media pipes, to shut down one or two pipes in summer	—	Experiment in Nykøbing Falster	[37]
Network	Use booster pumps, to reduce the dimension of pipes	—	Widely used	[37, 38]
Network	Apply branched network with bypass units instead of looped network	Results in high return temperature	Widely used	[38]
Pipe	Improve the insulation of pipes	—	Widely used	[37]
Pipe	Pre-insulated twin pipes or triple pipes	—	Widely used	[1, 37, 39]
Pipe	Prevent over dimensioning of pipes	—	Widely used	[38]
Pipe	Use buffer tanks for DHW production, to reduce the dimension of pipes	Legionella problem with LTDH system	Widely used	[38]
DH system	Leakage detection to avoid hot water loss	—	Widely used	[40]
Substation	Fault detection to avoid any malfunction	—	Widely used	[1, 4, 7]

3.2. Decreased heat demands in the future district heating

The competitiveness of DH systems may be decreased when heat demands are expected to decrease in the future. One study, based on 83 DH systems in European cities shows that there is a lower risk for reduced competitiveness for large cities and inner city areas, however, the areas with low heat density will lose competitiveness in the future [41].

The experiences gained from different projects show that DH systems with low heat demand density require careful plan and design to achieve good economy. In some cases, innovative solutions have been applied and gained extra rewards. With those solutions, it is believed that DH may supply the areas with heat density of 10 kWh/(m^2·a), or linear heat density of 0.3 MWh/(m·a) [37]. Some potential measures to apply DH in low heat density areas are shown in Table 9.

Table 9. Potential measures to apply DH to low heat density areas.

Classification	Solutions	Limitation	Reference
Heat source	Use IWH, waste incineration and other cheap heat sources	—	[41]
System design	Optimized network layout with less pipeline length, to get higher linear heat density	—	[42]

Classification	Solutions	Limitation	Reference
System design	Low pressure and low temperature systems with direct connection of SH system	Hydraulic interaction between DH system and SH system	[1, 37]
System design	Reduce pipe dimensions by applying DHW tanks	Legionella problem with LTDH system	[37]
System design	Reduce pipe dimensions by applying booster pumps	—	[37]
System design	House-to-house connection to decrease the length of service pipes	Not welcomed by DH companies and customers	[37]
System design	Three or four media pipes, to shut down one or two pipes in summer	—	[37]
System design	Install pipes inside the buildings, to decrease the length of network and utilize heat loss for SH	Not welcomed by DH companies and customers	[37]
System design	Increase the degree of connection		[37]
Pipe	Improve the insulation of pipes		[37]
Pipe	Pre-insulated twin pipes or triple pipes		[37]
Pipe	Prevent over dimensioning of pipes		[38]
DH system	Leakage detection to avoid hot water loss		[40]
Substation	Fault detection to avoid any malfunction		[1, 4, 7]
Civil works	Reduce the ground cover		[37]
New loads	Supply household equipment previously supplied by electricity	Conflict with traditional practices	[37]

4. Conclusion

Transition to the 4th generation DH is a challenge issue. The process requires the upgrades of DH system and the collaboration with other energy systems. In addition, buildings may also need some refurbishment to coordinate the changes of those systems. The final goal of the transition is to make the future DH system more flexible, reliable, intelligent, and competitive, and become an essential part of the future smart and renewable energy system.

The upgrades of DH system involve the physical system as well as the virtual system. For the physical system, the transition will focus on lowering the system temperature levels, and integrating various heat sources and thermal storages. Two steps will be conducted to lower the temperature level. The first step is to achieve the temperature potentials of the current DH system by the means of eliminating system errors and improving system control. The second step is to further reduce the temperature levels through enhancing heat transfer performance of heat exchangers and improving system design. The renovation of buildings may also be conducted through those two steps when it is necessary. Various heat sources and different level TESs will be integrated into the future DH system. Transition to 4th generation DH should take into consideration all the consisting issues such as way of heat feed-in, type of heat sources and TESs, distribution heat losses, the design of DH system, and operation strategies. Finally, the decisions should be made depending on the local natural and economic conditions.

For the virtual system, transition to 4th generation DH will be based on the intelligent physical system, which is able to measure, transmit information, collect data, and control. In addition, IDS will become more powerful with advanced functions in the future DH system, such as the reliability assessment, accident analysis, accident alarm, operation evaluation, operation supervision, and operation optimization.

The large share of distribution heat loss and the decreasing heat demand are two challenges the future DH systems are going to face. The potential solutions involve innovating system design, upgrading physical and virtual system, integrating cheap heat sources, and introducing new heat loads.

The conclusion of this study is that even enjoying the developing trend of the 4th generation DH, transition to 4th generation DH should be conducted carefully and gradually. Comprehensive consideration must be took into, focus on the energy status, condition of existing systems, and the operation custom in different areas or countries. In addition, the technologies for the future system need further development, and the operation as well as management strategies should be innovated.

Acknowledgements

The authors gratefully acknowledge the support from the Research Council of Norway through the research project Understanding behaviour of district heating systems integrating distributed sources under FRIPRO/FRINATEK program (the project number 262707).

References

[1] S. Frederiksen, S. Werner, District Heating and Cooling, Studentlitteratur, 2013.
[2] H. Lund, S. Werner, R. Wiltshire, S. Svendsen, J.E. Thorsen, F. Hvelplund, B.V. Mathiesen, 4th Generation District Heating (4GDH) Integrating smart thermal grids into future sustainable energy systems, Energy, 68 (2014) 1-11.
[3] A.D. Rosa, H. Li, S. Svendsen, S. Werner, U. Persson, K. Ruehling, C. Felsmann, M. Crane, R. Burzynski, C. Bevilacqua, Annex X Final report: Towards 4th Generation DH Experiences with and Potential of Low Temperature DH, in, IEA DHC/CHP, 2014.
[4] H. Gadd, S. Werner, Achieving low return temperatures from district heating substations, Applied energy, 136 (2014) 59-67.
[5] H. Averfalk, S. Werner, C. Felsmann, K. Rühling, R. Wiltshire, S. Svendsen, H. Li, J. Faessler, F. Mermoud, L. Quiquerez, Annex XI final report: Transformation Roadmap from High to Low Temperature District Heating Systems, in, IEA DHC/CHP, 2017.
[6] D. Schmidt, A. Kallert, M. Blesl, S. Svendsen, H.W. Li, N. Nord, K. Sipila, Low Temperature District Heating for Future Energy Systems, in: Enrgy Proced, 2017, pp. 26-38.
[7] K. Yliniemi, Fault detection in district heating substations, in, Luleå tekniska universitet, 2005.
[8] Euroheat & Power: Home, in.
[9] X. Yang, H. Li, S. Svendsen, Energy, economy and exergy evaluations of the solutions for supplying domestic hot water from low-temperature district heating in Denmark, Energy conversion and management, 122 (2016) 142-152.
[10] X. Yang, H. Li, S. Svendsen, Evaluations of different domestic hot water preparing methods with ultra-low-temperature district heating, Energy, 109 (2016) 248-259.
[11] X. Yang, S. Svendsen, Achieving low return temperature for domestic hot water preparation by ultra-low-temperature district heating, Energy Procedia, 116 (2017) 426-437.
[12] M. Brand, S. Svendsen, Renewable-based low-temperature district heating for existing buildings in various stages of refurbishment, Energy, 62 (2013) 311-319.
[13] H. Lund, B. Möller, B.V. Mathiesen, A. Dyrelund, The role of district heating in future renewable energy systems, Energy, 35 (2010) 1381-1390.
[14] IEA, Future low temperature district heating design guidebook, in: D. Schmidt, A. Kallert (Eds.), International Energy Agency Technology Collaboration Programme on District Heating and Cooling including Combined Heat and Power, AGFW-Project Company Stresemannallee, Germany, 2017.
[15] N. Nord, M. Ingebretsen, I. Tryggestad, Possibilities for Transition of Existing Residential Buildings to Low Temperature District Heating System in Norway, in: Proceedings of the 12th REHVA World Congress, Aalborg, Denmark, 2016, pp. 22-25.
[16] M. Spurr, T.S.E. Moe, M. Lehtmets, Annex X Final Report: Economic and Design Optimization in Integrating Renewable Energy and Waste Heat with District Energy Systems, in, 2014.
[17] F.M. Rad, A.S. Fung, Solar community heating and cooling system with borehole thermal energy storage – Review of systems, Renewable and Sustainable Energy Reviews, 60 (2016) 1550-1561.
[18] C. Winterscheid, J.-O. Dalenbäck, S. Holler, Integration of solar thermal systems in existing district heating systems, Energy, 137 (2017) 579-585.
[19] M. Rämä, S. Mohammadi, Comparison of distributed and centralised integration of solar heat in a district heating system, Energy, 137 (2017) 649-660.
[20] H. Fang, J. Xia, Y. Jiang, Key issues and solutions in a district heating system using low-grade industrial waste heat, Energy, 86 (2015) 589-602.
[21] H. Fang, J. Xia, K. Zhu, Y. Su, Y. Jiang, Industrial waste heat utilization for low temperature district heating, Energy policy, 62 (2013) 236-246.

[22] N. Nord, T. Tereshchenko, L.H. Qvistgaard, I.S. Tryggestad, Influence of occupant behavior and operation on performance of a residential Zero Emission Building in Norway, Energy and Buildings, 159 (2018) 75-88.
[23] T. Pauschinger, Solar thermal energy for district heating, Advanced District Heating and Cooling (DHC) Systems. Woodhead Publishing Series in Energy, (2015) 99-120.
[24] R.E.T.D.I.A.a.t.R.E.W.P.o.t.I.E. Agency, Renewables for heating and cooling, in, Paris, France, 2007.
[25] R. Bertani, 4 - Deep geothermal energy for heating and cooling A2 - Stryi-Hipp, Gerhard, in: Renewable Heating and Cooling, Woodhead Publishing, 2016, pp. 67-88.
[26] J.F. Urchueguia, 5 - Shallow geothermal and ambient heat technologies for renewable heating A2 - Stryi-Hipp, Gerhard, in: Renewable Heating and Cooling, Woodhead Publishing, 2016, pp. 89-118.
[27] D. Romanchenko, J. Kensby, M. Odenberger, F. Johnsson, Thermal energy storage in district heating: Centralised storage vs. storage in thermal inertia of buildings, Energy Conversion and Management, 162 (2018) 26-38.
[28] V. Verda, F. Colella, Primary energy savings through thermal storage in district heating networks, Energy, 36 (2011) 4278-4286.
[29] A.V. Novo, J.R. Bayon, D. Castro-Fresno, J. Rodriguez-Hernandez, Review of seasonal heat storage in large basins: Water tanks and gravel–water pits, Applied Energy, 87 (2010) 390-397.
[30] J. Xu, R.Z. Wang, Y. Li, A review of available technologies for seasonal thermal energy storage, Solar Energy, 103 (2014) 610-638.
[31] H. Lund, Renewable energy systems: a smart energy systems approach to the choice and modeling of 100% renewable solutions, Academic Press, 2014.
[32] X. Fang, Requirement of smart heating for heating enterprises and related enterprises, Gas & heat, 38 (2018).
[33] P. Zou, Heating Engineering, China Architecture & Building Press, Beijing, 2018.
[34] B.V. Mathiesen, H. Lund, D. Connolly, H. Wenzel, P.A. Østergaard, B. Möller, S. Nielsen, I. Ridjan, P. Karnøe, K. Sperling, Smart Energy Systems for coherent 100% renewable energy and transport solutions, Applied Energy, 145 (2015) 139-154.
[35] R. Lund, S. Mohammadi, Choice of insulation standard for pipe networks in 4 th generation district heating systems, Applied Thermal Engineering, 98 (2016) 256-264.
[36] A. Dalla Rosa, The Development of a New District Heating Concept, in, Ph. D. thesis, Technical University of Denmark, Kgs. Lyngby, Denmark. Google Scholar, 2012.
[37] H. Zinko, B. Bøhm, H. Kristjansson, U. Ottosson, M. Rämä, K. Sipilä, District heating distribution in areas with low heat demand density, in: H. Zinko (Ed.), IEA 2008.
[38] H.İ. Tol, S. Svendsen, Improving the dimensioning of piping networks and network layouts in low-energy district heating systems connected to low-energy buildings: A case study in Roskilde, Denmark, Energy, 38 (2012) 276-290.
[39] A. Dalla Rosa, H. Li, S. Svendsen, Method for optimal design of pipes for low-energy district heating, with focus on heat losses, Energy, 36 (2011) 2407-2418.
[40] S. Zhou, Z. O'Neill, C. O'Neill, A review of leakage detection methods for district heating networks, Applied Thermal Engineering, (2018).
[41] U. Persson, S. Werner, Heat distribution and the future competitiveness of district heating, Applied Energy, 88 (2011) 568-576.
[42] N. Nord, E.K.L. Nielsen, H. Kauko, T. Tereshchenko, Challenges and potentials for low-temperature district heating implementation in Norway, Energy, 151 (2018) 889-902.

PAPER 2

Li H, Hou J, Hong T, Ding Y, Nord N. Energy, economic, and environmental analysis of integration of thermal energy storage into district heating systems using waste heat from data centres. Energy. 2021;219:119582.

APPENDIX- PUBLICATIONS

Energy 219 (2021) 119582

Contents lists available at ScienceDirect

Energy

journal homepage: www.elsevier.com/locate/energy

Energy, economic, and environmental analysis of integration of thermal energy storage into district heating systems using waste heat from data centres

Haoran Li [a, *], Juan Hou [a], Tianzhen Hong [b], Yuemin Ding [a], Natasa Nord [a]

[a] Department of Energy and Process Technology, Norwegian University of Science and Technology (NTNU), Kolbjørn Hejes Vei 1 B, Trondheim, 7491, Norway
[b] Building Technology and Urban Systems Division, Lawrence Berkeley National Laboratory, One Cyclotron Road, Berkeley, CA, 94720, USA

ARTICLE INFO

Article history:
Received 28 April 2020
Received in revised form
7 December 2020
Accepted 9 December 2020
Available online 16 December 2020

Keywords:
Mismatch problem
Peak load
Borehole thermal energy storage
Water tank
Energy bill
CO_2 emissions

ABSTRACT

Data centres produce waste heat, which can be utilized in district heating systems. However, the mismatch between data centres' heat supply and district heating systems' heat demands limits its utilization. Further, high peak loads increase the operation cost of district heating systems. This study aimed to solve these problems by introducing thermal energy storages. A water tank and a borehole thermal energy storage system were selected as the short-term and long-term thermal energy storage, respectively. Energy, economic, and environmental indicators were introduced to evaluate different solutions. The case study was a campus district heating system in Norway. Results showed that the water tank could shave the peak load by 31% and save the annual energy cost by 5%. The payback period was lower than 15 years when the storage efficiency remained higher than 80%. However, it had no obvious benefits in terms of mismatch relieving and CO_2 emissions reduction. In contrast, the borehole thermal energy storage increased the waste heat utilization rate to 96% and reduced the annual CO_2 emissions by 8%. However, the payback period was more than 17 years. These results provide guidelines for the retrofit of district heating systems, where data centres' waste heat is available.

1. Introduction

The fundamental idea of district heating (DH) is to utilise local resources that would otherwise be wasted to satisfy local heat demand [1]. Suitable resources include waste incineration, geothermal energy, solar thermal energy, and waste heat [2–8]. Among these, waste heat plays an important role in current DH systems. In the countries of the European Union, about 72% of the heat supply comes from waste heat [9]. Moreover, the current DH systems are facing a transformation to the fourth generation DH, which will decrease temperature levels dramatically. The decrease in temperature will bring huge potential for waste heat utilization in DH systems [10–14].

Waste heat can come from industrial processes, combined heat and power plants, and large electricity users [15–17]. Waste heat from data centres (DCs) is a promising heat resource, especially for the Nordic countries [18]. First, DCs are energy-intensive facilities and the amounts of electricity used globally by DCs have grown significantly in recent years. Up to 2010, DCs accounted for 1.3% of the world's electricity use. However, this proportion is increasing, with an annual growth rate of 25% [19]. Second, a large proportion of this electricity is converted into waste heat [20,21]. For a typical DC, about half of the electricity used ultimately becomes waste heat. Third, the equally spread load profile and waste heat generation make DCs a reliable heat source [17]. Finally, many DCs are built close to an existing DH network. Therefore, it is possible to feed the DCs' waste heat into the nearby DH networks [18].

Studies have showed that it is technically and economically feasible to recycle waste heat for DH systems usage. According to a review by Ebrahimi et al., techniques for recycling waste heat from a DC include absorption cooling, electricity generation, and DH [22]. Wahlroos et al. studied one Finnish DH system with waste heat recovery from a DC. The results showed that operation cost savings of 0.6–7.3% could be made after recycling waste heat from the DC [17]. Similarly, Davies et al. investigated a DH system in London. The results showed that waste heat recovery from a DC reduced the annual operational cost by $373,634-$876,000 [23]. Kauko et al. studied a Norwegian DH system. Their results showed that heat

* Corresponding author.
E-mail address: haoranli@ntnu.no (H. Li).

https://doi.org/10.1016/j.energy.2020.119582

Nomenclature

BTES	Borehole thermal energy storage
COP	Coefficient of performance
CT	Cooling tower
DH	District heating
DHW	Domestic hot water
DC	Data centre
HP	Heat pump
MS	Main substation
SH	Space heating
TES	Thermal energy storage
WT	Water tank

demand was reduced by 13% by recycling waste heat from a DC and two food stores [24]. However, there are some challenges hindering the utilization of waste heat from DCs for DH systems. One is the mismatch between DCs' waste heat supply and DH systems' heat demand [25]. The available waste heat from a DC depends on its load profile, which is usually spread equally. Therefore, the waste heat generated by DCs is at almost a constant rate [17,26]. In contrast, the heat demand in buildings is related to outdoor air temperature and occupant behaviour, which is full of fluctuations and uncertainties [27]. The resulting heat demand varies with the season, and even changes within one day. The difference between waste heat generation and heat demand leads to a mismatch between heat supply and heat demand. The mismatch problem would reduce the waste heat utilization rate and limit the economic and environmental benefits of utilizing DCs' waste heat [18].

One way to solve the mismatch in a DH system is to introduce thermal energy storage (TES). In a review by Shah et al., borehole thermal energy storage (BTES) was found to be an appropriate solution to solve the mismatch for solar DH systems in cold climates [28]. Rohde et al. studied an integrated heating and cooling system in Norway. BTES was proposed to solve the mismatch between heat supply (from solar collectors and the condensing heat) and heat demand [29,30]. Köfinger et al. studied a DH system with industrial waste heat recovery in Austria. Pit thermal energy storage was used to shift industrial waste heat from summer to autumn or winter, and supplied heat during peak hours [31]. Similarly, Moser et al. explored the use of large-scale (seasonal) heat storage to shift industrial waste heat from summer to winter and thereby made the feed-in of waste heat economically more attractive [32]. Tian et al. studied a hybrid solar DH system with both TES and back up boilers in Denmark. A water tank (WT) was applied as a short-term TES to relieve the mismatch between the heat supply from a solar heating plant and the heat demand in buildings [6].

Finally, peak load is an important issue in DH systems. Higher peak load will increase the initial investment and operation cost of a DH system. A survey shows that 87% of the current heating price models in Sweden take into account heat users' peak load [33]. These price models divide the heating bill into two parts: fixed and variable [34–37]. The fixed part is charged based on the peak load, and it accounts for 10–50% of the total heating bill [33]. Therefore, shaving the peak load will bring significant economic benefits for heat users.

Introducing TES is one way to shave the peak load in a DH system. Verda et al. studied the idea of using a WT to shave the peak load of a DH system in Italy. The WT was charged at night and shaved the peak load in the morning. The results showed that peak load shaving led to a reduction of 12% and 5% for the annual fuel use and fuel cost, respectively [38]. Harris investigated the DH systems in Sweden and found that almost all heating plants used WTs to shave the peak load. This measure reduced the installed capacity and improved the operation efficiency of heating plants [39]. Verrilli et al. proposed an optimal control strategy to reduce the operation and maintenance cost of a DH plant in Finland. The control strategy took advantage of the load shifting effect of WT and saved the cost by 8% [40]. Jebamalai et al. investigated the benefits of placing WTs in a DH system to decrease its peak load. The results showed that the centralized WT could reduce the total network investment cost by 4%, the substation level WT could reduce the costs by 5%, and the building level WT could reduce the costs up to 7% [41].

In summary, introducing TES is an effective way for mismatch relieving and peak load shaving in DH systems. However, to the best of the author's knowledge, there is limited research considering the two performance indicators of TES at the same time, especially for the DH systems with heat supply from DCs. Further research is needed to evaluate the system performance in terms of energy, economic, and environmental indicators after introducing TESs. Therefore, this study aimed to solve the mismatch problem and shave the peak load for the DH systems, where DCs supply waste heat, by introducing TESs. Different scenarios with the short-term or long-term TESs were proposed. Energy, economic, and environmental indicators were introduced to evaluate the system performance. The novelty of this study is summarized as followed: 1) This research focused on improving the utilization of DCs' waste heat in DH systems by introducing TESs, which is rarely addressed by existing studies. 2) Considering pricing schemes of DH, joint management of mismatch relieving and peak load shaving of TESs were investigated to optimize the economic performance. 3) For completeness of performance evaluation, research into both short-term and long-term TESs was conducted from aspects of energy efficiency, economic profits, and environmental impacts. 4) Sensitivity study of thermal storage efficiency was conducted to draw generalized conclusions on utilizing various TESs for waste heat supply from DCs.

The remainder of this article is organised as follows. Section 2 introduces the case study as the background for the system model. Section 3 presents the analysed scenarios, modelling approach, and methods used for economic and environmental analysis. Section 4 shows the model validation and simulation results. Section 5 presents the sensitivity analysis to investigate the impacts of TES storage efficiency. Finally, in Section 6, conclusions are presented.

2. Description of the case study

A campus DH system in Norway was chosen as the case study. The topology of the system is presented in Fig. 1. The system supplies heat to a total building area of 300,000 m^2, and the main functions of these buildings are education, offices, laboratories, and sports [42,43]. The campus DH system is connected to the city DH system by the main substation (MS). Apart from the heat supply from the city DH system, part of the annual heat supply comes from waste heat recovered from the university's DC. The current campus DH system faces two problems: 1) the mismatch between the heat supply from DC and the heat demand in buildings; 2) the higher peak load, which results in a large amount of money paid for it.

Fig. 2 shows the hourly mismatch between building heat demand and DC waste heat supply. During the non-heating season, the building heat demand came only from the domestic hot water (DHW) system. The heat demand ranged from 0.2 to 3.1 MW, which depended on occupant behaviour. During the heating season, the building heat demand came from both DHW needs and space heating (SH) system, which was negatively correlated with the

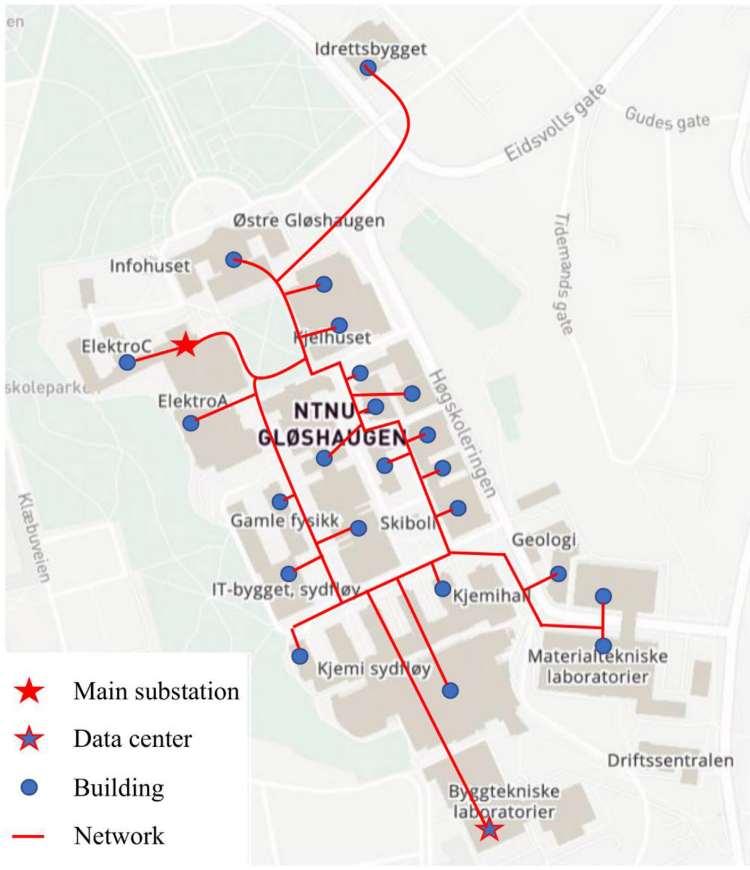

Fig. 1. Campus district heating system.

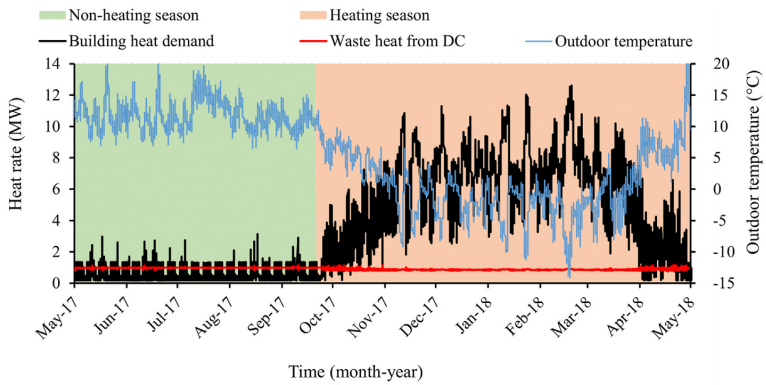

Fig. 2. Hourly building heat demand and data centre waste heat supply for the year 2017–2018.

outdoor temperatures. The heat demand ranged from 0.2 to 12.6 MW. In contrast, the DC waste heat supply was stable throughout the year, around 0.9 MW, see the red line in Fig. 2.

Fig. 3 illustrates the seasonal mismatch between building heat demand and DC waste heat supply. During the non-heating season, the supplied waste heat exceeded the heat demand. The total DC waste heat supply was 3.4 GWh, which was 1.4 GWh higher than the building heat demand, as shown in Fig. 3 at the left hand side.

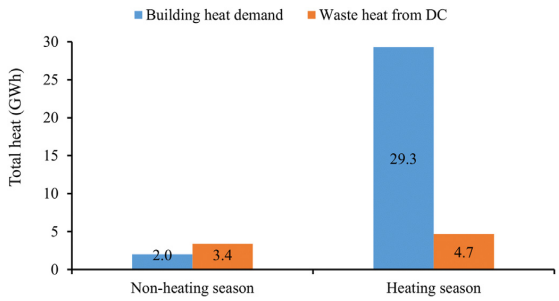

Fig. 3. Total building heat demand and data centre waste heat supply for the year 2017–2018.

During the heating season, the DC waste heat supply was far from satisfying the building heat demand. The waste heat supply was 4.7 GWh, while the building heat demand was 29.3 GWh, as shown in Fig. 3 at the right hand side.

In addition, as shown in Fig. 2, the building heat demand was not equally distributed and there were peak loads for both the heating and non-heating seasons. The maximum building heat demand was 12.6 MW during the heating season, which was about two times higher than the average value of 5.5 MW. Similarly, the maximum building heat demand was 3.1 MW during the non-heating season, which was about five times higher than the average value of 0.6 MW. The local DH company charges for heating based on heat use and peak load. The university pays about 4.7 million NOK[1] for the peak load each year. The money paid for the peak load accounts for 23% of the total heating bill.

3. Method

Three TES configurations were proposed to solve the mismatch problem and shave the peak load for the DH system, where the waste heat from the DCs was available. In addition, a reference scenario presenting the current campus DH system, was used as the benchmark to evaluate the system performance of the three TES scenarios. In total, the four scenarios were simulated in the Dymola platform. Finally, their system performance was evaluated and compared in terms of energy, economic, and environmental indicators. Detailed information on the research scenarios, modelling approach, and economic and environmental analysis methods are introduced in this section.

3.1. Suggested scenarios to include TESs

Fig. 4 shows schematics of the four scenarios. The reference scenario, *Ref*, presented the current campus DH system, see Fig. 4 a). In this scenario, the city DH system acted as the basic heat source and supplied heat through the MS. Meanwhile, the DC functioned as an additional heat source. The condensing heat of the DC cooling system was fed into the return line of the campus DH ring. This scenario suffered from the mismatch and high peak load problems, as introduced in Section 2.

The scenario *Ref* + *WT* integrated a WT into the reference scenario *Ref*, see Fig. 4 b). The volume of the WT was chosen as 8,000 m^3, which was able to supply heat to the campus DH system for two days. The WT functioned as the short-term TES. It aimed to relieve the mismatch between the DC waste heat supply and the building heat demand during the non-heating season. The WT operated in charging mode when the DC waste heat supply was higher than the building heat demand, otherwise, it operated in discharging mode. During the heating season, the WT was used to shave the peak load. It operated in discharging mode during the peak load hours, otherwise, it operated in charging mode.

The scenario *Ref* + *BTES* integrated a BTES system, that included a heat pump (HP) and a borehole field, into the reference scenario *Ref*, see Fig. 4 c). The borehole field contained 240 single U-tube boreholes. The depth of the boreholes was 55 m, and the distance between each borehole was 3 m. All boreholes were connected in parallel. The borehole field was sized with a charging rate of 1.1 MW, which was 80% of the maximum heat rate of the waste heat supply [44]. During the non-heating season, the BTES system operated in charging mode, storing the surplus waste heat supplied by the DC. In charging mode, the HP was not in operation, and the BTES system and DC were connected in series. During the heating season, the BTES system switched to discharging mode. However, it operated only during the peak load hours. In discharging mode, the long-term TES system and the DC were connected in parallel, working together to supply heat to the campus DH system.

The scenario *Ref* + *WT* + *BTES* integrated both a WT and a BTES system into the reference scenario *Ref* , see Fig. 4 d). During the non-heating season, the WT was used to solve the hourly mismatch problem. In addition, the BTES system operated in charging mode to solve the seasonal mismatch problem. As presented in Fig. 3, about 1.4 GWh excess waste heat was supplied during the non-heating season. The BTES system was used to shift this part of waste heat to the heating season. During the heating season, the WT and BTES worked together to shave the peak load. The charging and discharging strategies were the same as in scenarios *Ref* + *WT* and *Ref* + *BTES*.

3.2. Modelling approach for the campus DH system

The Dymola model of the campus DH system is presented in Fig. E1 of Appendix E. The model has the following components: buildings, DC, WT, BTES, and MS. The approach used to model these components is explained in this section and the key parameter settings are presented in Table A.1, B.1, C.1, C.2, C.3 and D.1 of Appendices A-D.

3.2.1. Building model

A single-equivalent building model was used to represent the overall performance of all the buildings on campus. The properties of the equivalent building were determined by summing or weighting the average properties of individual buildings. For example, the area of the exterior wall of the equivalent building was calculated by summing the corresponding values for all the buildings, and the U-value of the exterior wall of the equivalent building equalled the weighted average value of the corresponding values of all the buildings. The equivalent building model enabled increased computational efficiency, while maintaining high simulation accuracy. As shown in Fig. 5, the building model contained six modules: building envelope, internal heat gain, SH system, DHW system, ventilation system, and weather.

The building envelope module was developed based on the *TwoElements* component of the *Buildings* library [45]. It used an RC thermal network to represent the thermal process. Detailed information about this component can be found in Ref. [46]. The internal heat gain module defined the heat rate of the internal heat gain from the building's equipment, lighting, and occupants. The ventilation system module represented the building's ventilation system and specified its airflow rate and heat recovery efficiency.

[1] The currency rate between NOK and EUR can be found from https://www.xe.com/, in this study 1 EUR = 9.5 NOK.

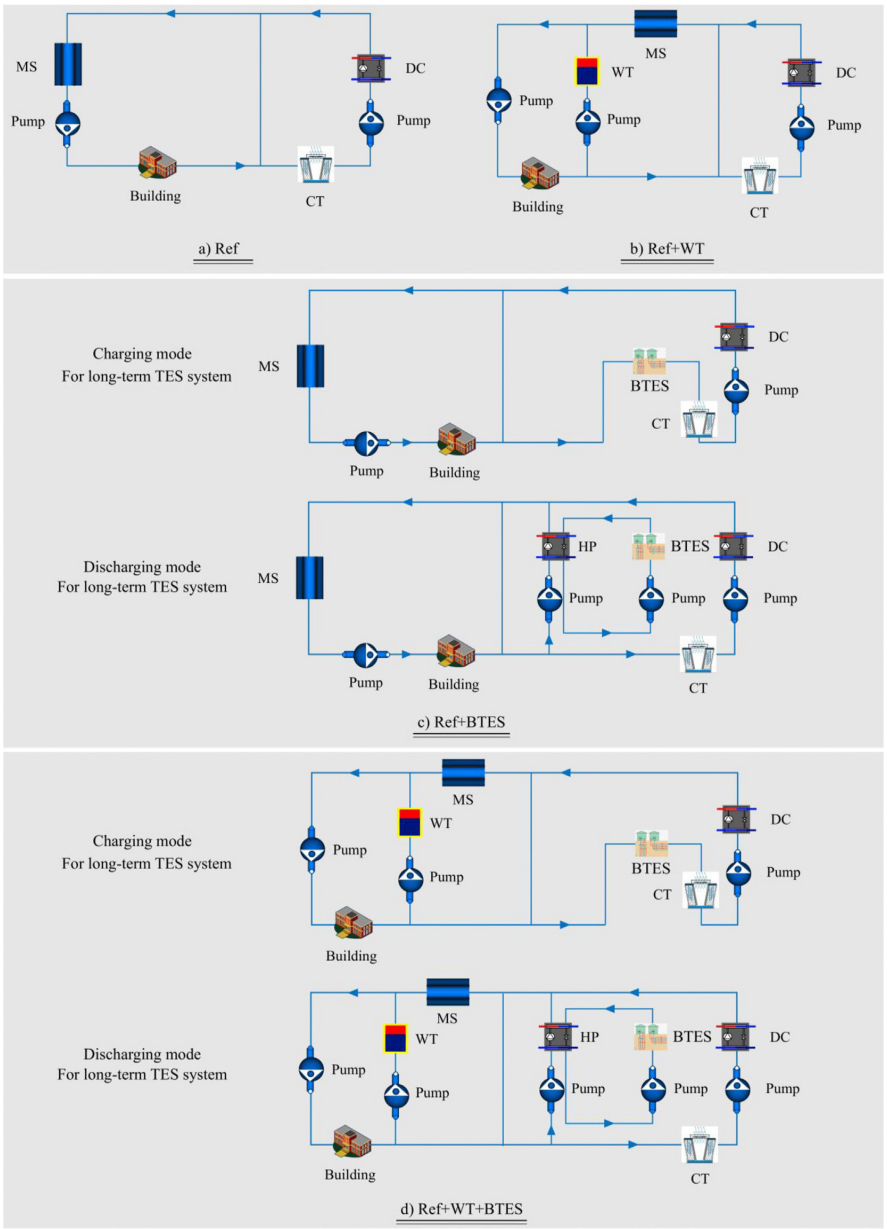

Fig. 4. Schematics of the four scenarios.

The SH and DHW system modules represented the SH and DHW systems of the buildings. The main components of these modules included radiator, pumps, heat exchangers, water taps, and pressurization systems. All these components came from the *Modelica Standard Library* [47] and libraries from IBPSA Project 1 [48].

3.2.2. Data centre model

The DC model is shown in Fig. 6. The key components were the HP and the cooling tower (CT). The HP connects the DC cooling system to the campus DH system. Its evaporator side produces chilled water for the cooling system, while its condenser side feeds waste heat into the campus DH system. The HP model was built based on the *Carnot_y* component in the *IDEAS* library [49]. This calculates the coefficient of performance (COP) based on the nominal COP, Carnot efficiency, and part-load efficiency. Detailed information on the *Carnot_y* component can be found in Ref. [50].

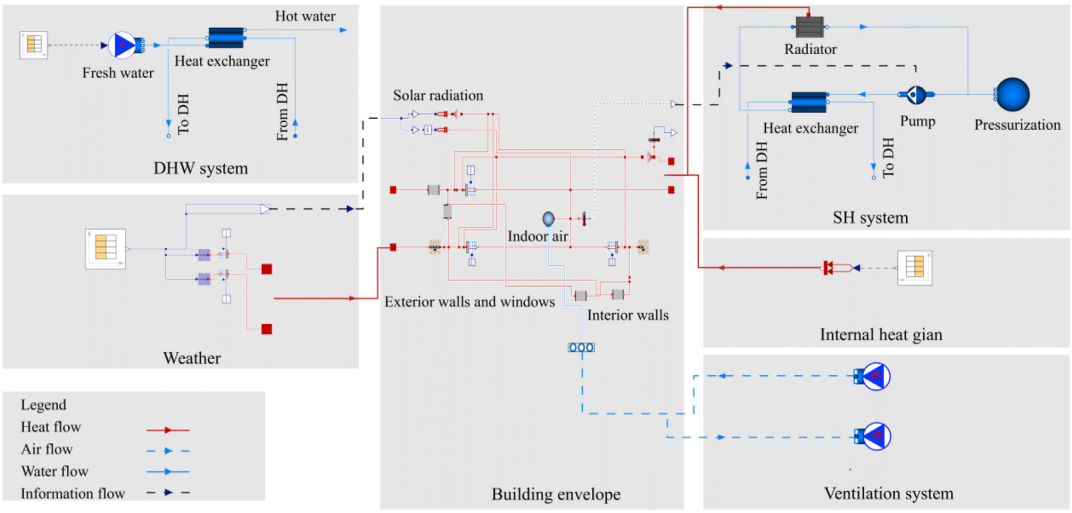

Fig. 5. Building model.

The CT is used to guarantee the safe operation of the DC cooling system. It starts to work when the incoming water temperature at the condenser side exceeds the safety level.

3.2.3. Water tank and borehole thermal energy storage system model

The WT model came from the *StratifiedEnhanced* component of the *AixLib* library [51]. The model used several sections to represent stratification, and the thermal process of each section was described by the laws of energy conservation. Detailed information about the model can be found in Ref. [52].

The BTES system model is shown in Fig. 7. Its key components were BTES and HP. The BTES model was developed based on the *OneUTube* component of the *IDEAS* library. The model calculated the thermal processes using an axial discretized resistance-capacitance network. Detailed information on the BTES model can be found in Ref. [53].

3.2.4. Main substation model

The MS connects the city DH system to the campus DH system. The MS has two functions. First, it supplements the heat supply when waste heat cannot cover the heat demand. Second, it further boosts the supply temperature when the supply temperature from the DC is insufficient for the building system. As shown in Fig. 8, the key component of the MS model was the heat exchanger. The heat exchanger model was based on the *BasicHX* component of the *Modelica Standard Library* [54].

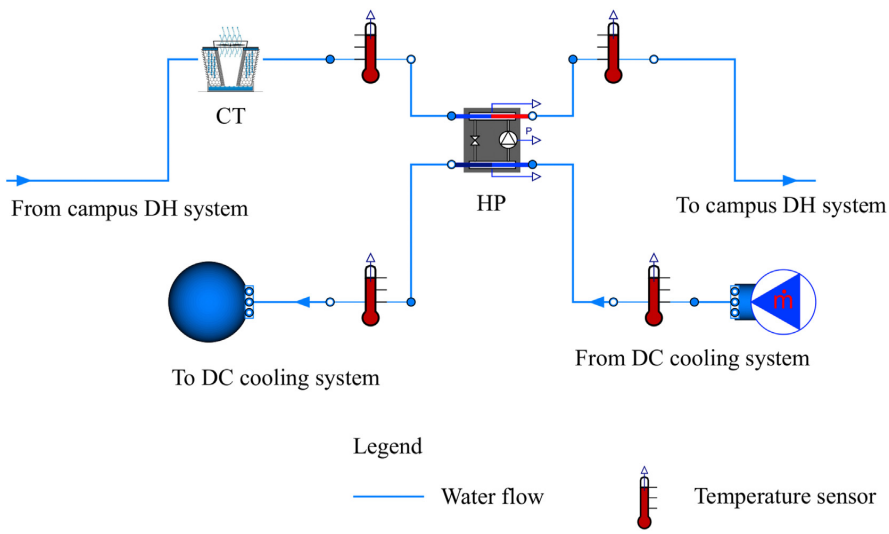

Fig. 6. Data centre model.

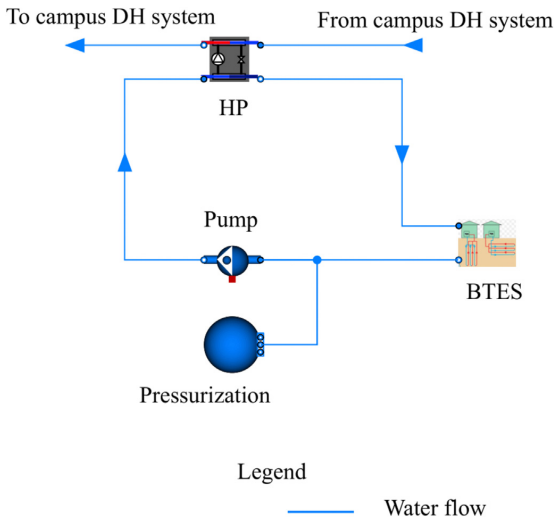

Fig. 7. Borehole thermal energy storage system model.

3.3. Method for economic analysis

3.3.1. Initial investment for a TES system

The initial investment required for a TES system varies with the storage type and depends strongly on the storage size. Fig. 9 illustrates the relationship between initial investment and size for a WT and a BTES system. The solid black dots in Fig. 9 represent previous projects [55]. The figure shows that power functions approximate the relationship very well, with coefficients of determination (R^2) higher than 0.8 and no obvious overfitting. In this study, the power functions were used to estimate the initial investment for the TES system. For the BTES system, initial investment in the HP was also considered. The unit cost of the HP was assumed to be 0.8 million EUR/MW, based on a report that studied large scale HPs for DH systems [56].

3.3.2. Calculation of energy bill

The energy bill includes the heating and electricity bills, which are explained as follows.

The heating bill contains two parts: fixed and variable, as presented in Eq. (1).

$$B_{heat(tot)} = B_{heat(fix)} + B_{heat(\mathrm{var})} \tag{1}$$

where $B_{heat(tot)}$ is the total heating cost, $B_{heat(fix)}$ is the fixed part, and $B_{heat(var)}$ is the variable part.

The fixed part is calculated in Eq. (2) as follows:

$$B_{heat(fix)} = \dot{Q}_{peak,sum} P_{heat(fix,sum)} + \dot{Q}_{peak,win} P_{heat(fix,win)} \tag{2}$$

where $\dot{Q}_{peak,sum}$ and $\dot{Q}_{peak,win}$ are the peak load for the summer and winter seasons, respectively. $P_{hit(fix,sum)}$ and $P_{heat(fix,win)}$ are the unit fixed heating price for the summer and winter seasons, respectively.

The variable part is calculated in Eq. (3) as:

$$B_{heat(\mathrm{var})} = Q_{heat} P_{heat(\mathrm{var})} \tag{3}$$

where Q_{heat} is the total heat use, and $P_{heat(var)}$ is the variable heating price. The unit fixed and variable heating price was obtained from the local DH company, Statkraft Varme, in Trondheim [57,58].

The electricity bill includes also a fixed part and a variable part. However, the fixed part in Norway is determined by the electricity use. However, a simplified electricity bill calculation method was proposed in Eq. (4). This method assumed that the electricity bill contained only the variable part, and it was a function of electricity use. The equivalent electricity price was calculated as:

$$B_{elec} = E_{elec} P_{elec} \tag{4}$$

where B_{elec} is the electricity cost, E_{elec} is the electricity use, and P_{elec} is the equivalent electricity price. The equivalent electricity price is equal to the total electricity cost (including the fixed and variable parts) divided by the electricity use. In this study, the equivalent electricity price was 1.07 NOK/kWh.

3.3.3. Calculation of the payback period

The payback period is the time taken to fully recover the initial investment. It is one of the most commonly used methods for evaluating initial investments [59]. The payback period *PB* is calculated using Eq. (5):

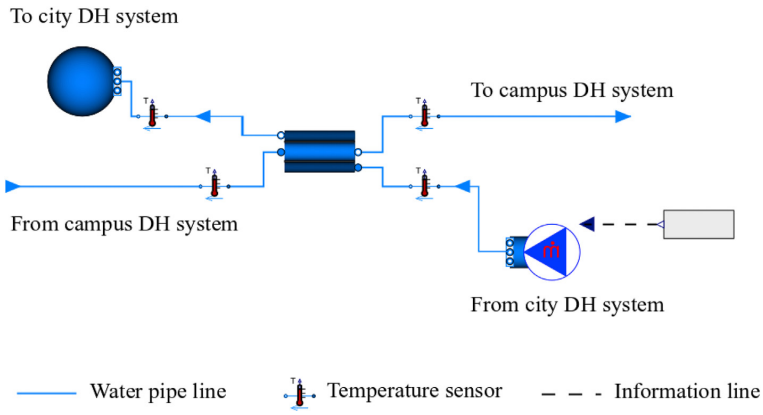

Fig. 8. Main substation model.

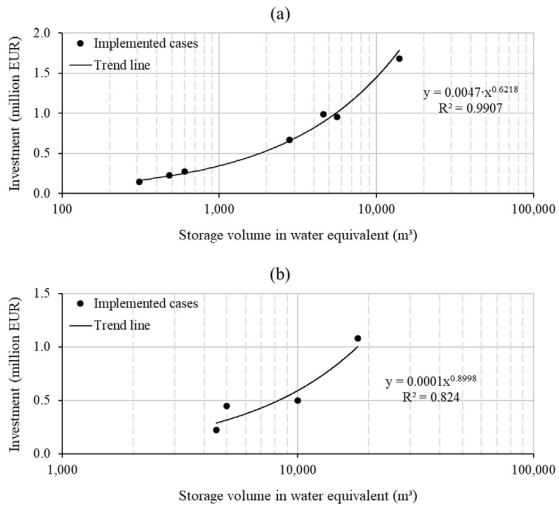

Fig. 9. Investment in thermal energy storage with different sizes, (a) water tank and (b) borehole thermal energy storage.

$$B_{sav}\frac{(1+i)^{PB}-1}{i(1+i)^{PB}} - Invt = 0 \quad (5)$$

where B_{sav} is the annual energy bill saving. $Invt$ is the initial investment. i is the prevailing interest rate, for which 2% was used in this study [60].

3.4. Method for environmental analysis

The increase in global average temperatures is attributed to an increase in greenhouse gas emissions, especially CO_2 [61]. Therefore, this study used CO_2 emissions as an indicator to evaluate environmental impact.

As shown in Eq. (6), a CO_2 emission factor is used to calculate CO_2 emissions as:

$$EM_{CO2} = E \times EF \quad (6)$$

where EM_{CO2} is the CO_2 emission, E is heat or electricity use, and EF is the CO_2 emission factor for heat or electricity.

The reference value for the CO_2 emission factor for heat was obtained from the local DH company as 51.8 g/kWh [57]. This value considers the entire life-cycle emissions of all types of fuel, including waste incineration, biomass, liquefied petroleum gas, etc. The reference value for the CO_2 emission factor for electricity was 18.9 g/kWh [62]. This low value is attributed to the high proportion of renewable electricity in Norway. About 98% of electricity is from hydropower and wind power.

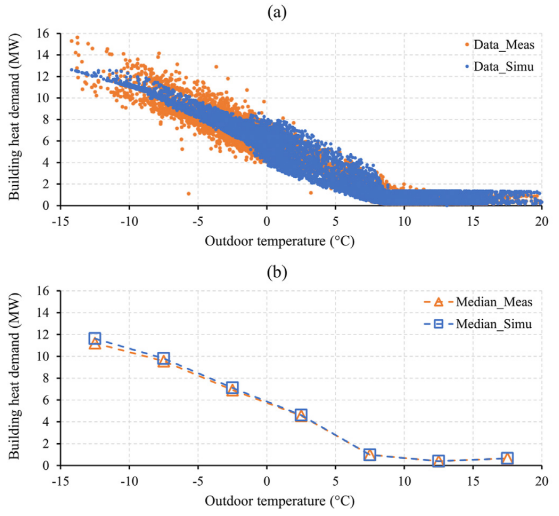

Fig. 10. Simulated and measured hourly building heat demand plotted against outdoor temperature, (a) original simulated and measured data, and (b) medians with an interval of 5 °C and their trend lines.

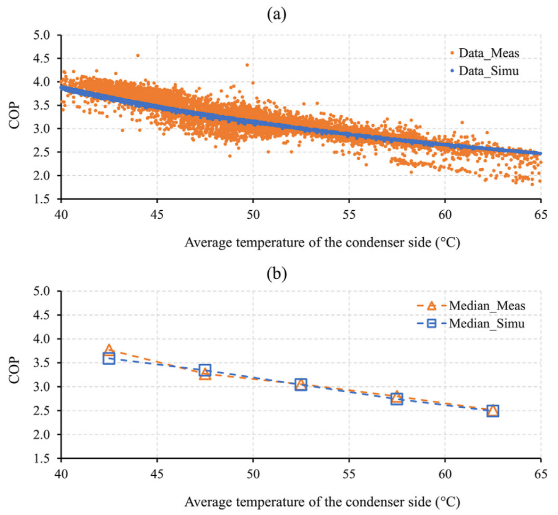

Fig. 11. Simulated and measured COP plotted against the average water temperature of the condenser side, (a) original simulated and measured data, and (b) medians with an interval of 5 °C and their trend lines.

4. Results

This section first presents the model validation, then evaluates

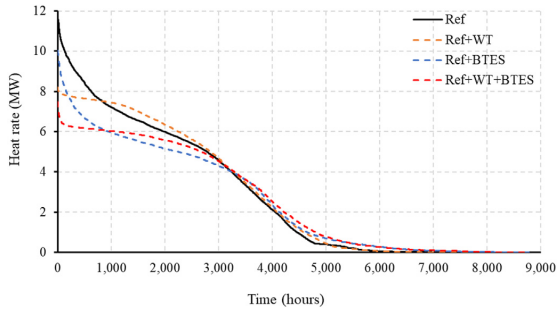

Fig. 12. Heat load duration diagram for the four scenarios.

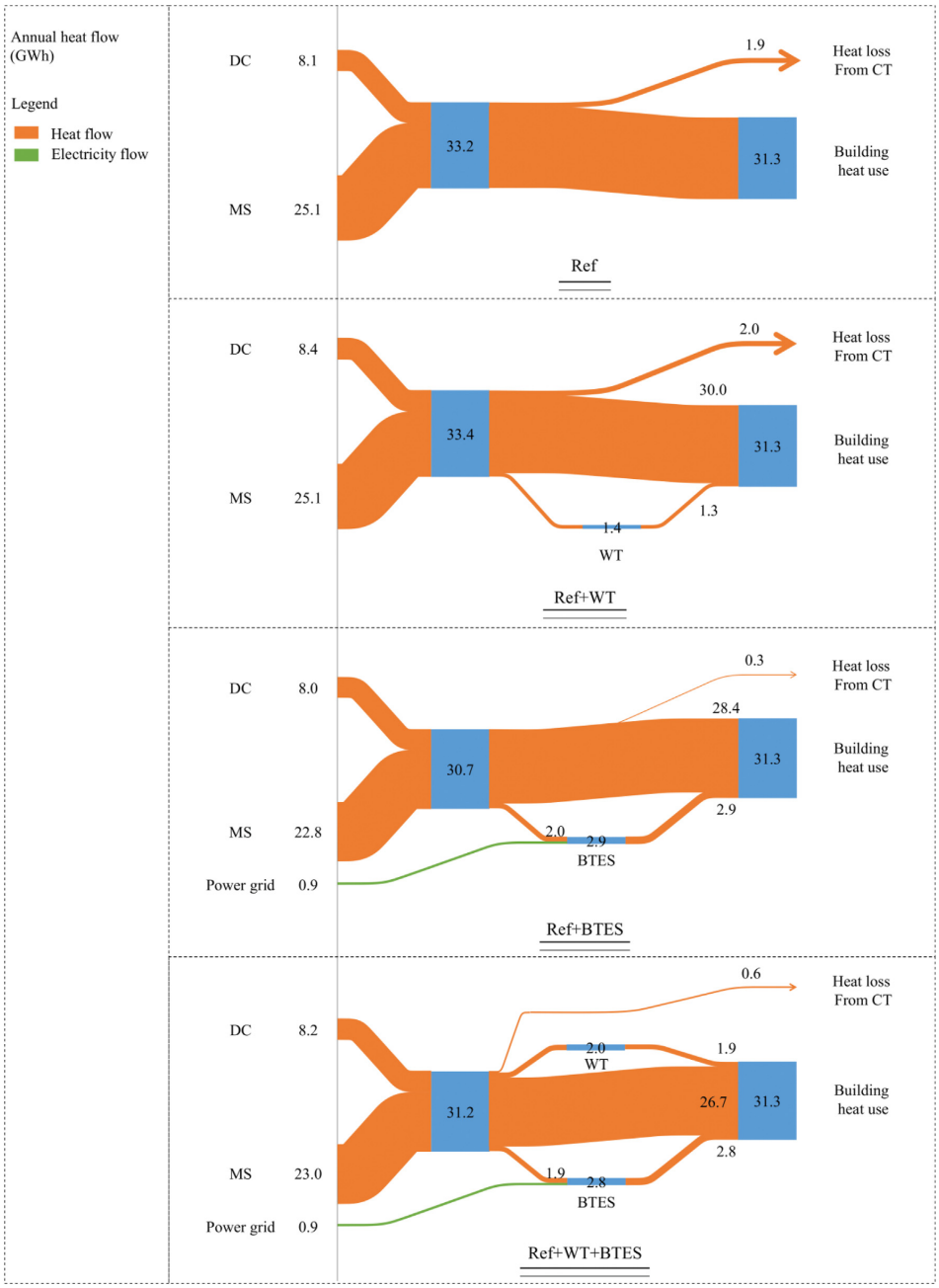

Fig. 13. Annual heat flow for the four scenarios.

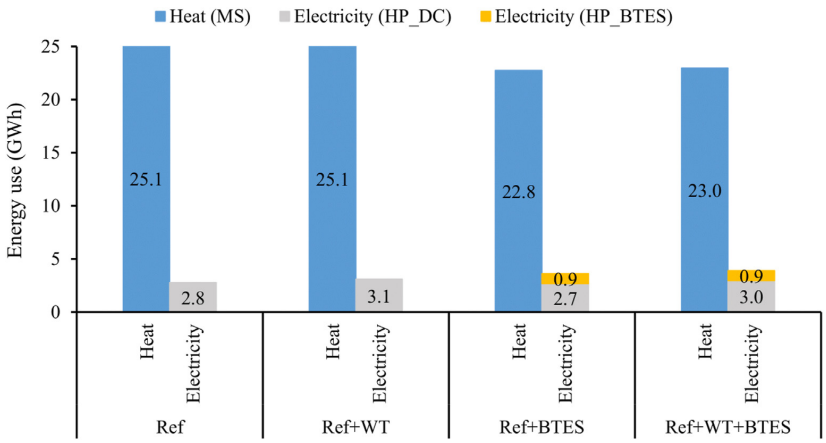

Fig. 14. Annual heat supply and electricity use for the four scenarios.

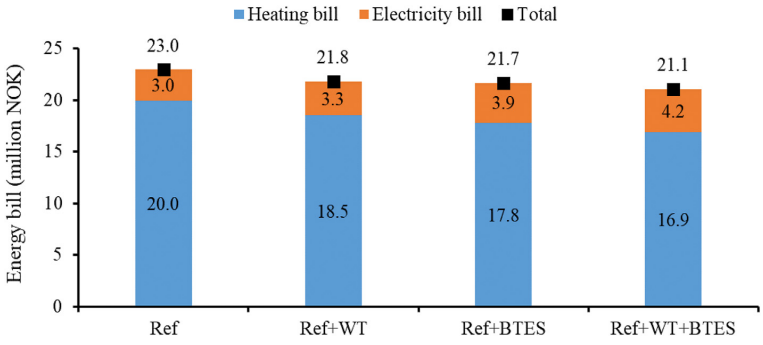

Fig. 15. Annual heat and electricity bills for the four scenarios.

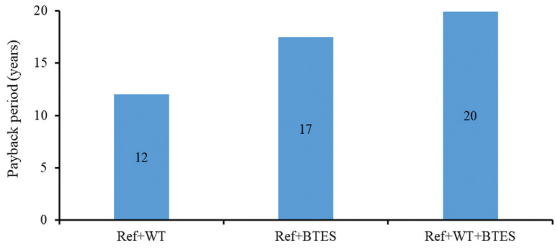

Fig. 16. Payback period for the three TES scenarios.

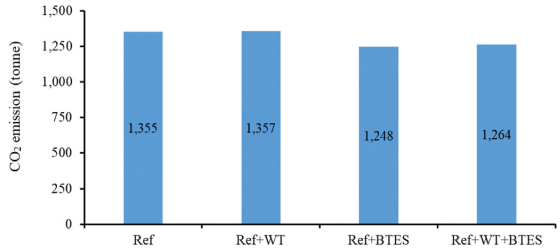

Fig. 17. Annual CO_2 emissions for the four scenarios.

the three TES scenarios based on energy, economic, and environmental analyses.

4.1. Model validation

The building and HP models were validated by the measured data from the campus energy management platform. The validation of the building model is presented in Fig. 10. The simulated and measured hourly building heat demands exhibited a similar pattern. During the heating season, the building heat demand was negatively correlated with the outdoor temperature. However, this correlation disappeared during the non-heating season. In addition, the median of the simulated building heat demand matched the measured value at the same interval. The errors of these medians were within ±4%. Similarly, the simulated total building heat demand also matched the measured data, which were 31.3 GWh and 31.4 GWh, respectively. The error in the total building heat demand was within ±1%.

For a typical water source HP, the COP is a function of condensation and evaporation temperatures. These cannot be measured

Table 1
Scenarios of sensitivity analysis.

Name	WT efficiency (%)	BTES efficiency (%)
Ref + WT	100	–
Ref + WT9	90	–
Ref + WT8	80	–
Ref + WT7	70	–
Ref + WT6	60	–
Ref + WT5	50	–
Ref + BTES	–	100
Ref + BTES9	–	90
Ref + BTES8	–	80
Ref + BTES7	–	70
Ref + BTES6	–	60
Ref + BTES5	–	50

directly, but the water temperatures on the condenser and evaporator sides can be used instead. In this study, the influence of the evaporation temperature was ignored because the water temperature on the evaporator side remained approximately constant (with inlet and outlet temperatures of 11 and 7 °C, respectively). Therefore, the relationship between the COP and the water temperature at the condenser side was used to validate the HP model. Fig. 11 presents the validation of the HP model. Please note that the average water temperature at the condenser side refers to the average value of the inlet and outlet water temperatures. The simulated COP agreed very well with the measured COP. They exhibited the same trend, with the COP decreasing when the water temperature increased at the condenser side. Meanwhile, the median of the simulated and measured COP was calculated at the same interval. The errors of those medians were within ± 5%.

4.2. Evaluating the TES scenarios by energy analysis

This section evaluates the TES scenarios based on energy analysis. Fig. 12 illustrates the heat load duration curves of the campus DH system, which was used to evaluate the peak load shaving effect. Fig. 13 and Fig. 14 show the heat balance and energy use, which were used to evaluate the mismatch reliving effect. Please note that the heat load refers to the heat rate of heat supply from the MS. The heat loss refers to the amount of heat removed by the CT as a result of the mismatch problem. During the non-heating season, more waste heat was supplied than the building heat demand, and this surplus waste heat would ultimately become heat loss. In addition, the additional pumping electricity use for TESs was not accounted for in this study, because it was negligible compared to the HP electricity use. For a typical DH system, the demand for electricity for pumping is only about 0.5% of the heat delivery [1].

As shown in Fig. 12, the WT contributed to a significant peak load shaving effect. The peak load of the scenario *Ref* + *WT* dropped to around 8.1 MW, a reduction of almost 30% compared to the reference scenario *Ref*. However, introducing the *WT* did not relieve the mismatch problem and consequently did not reduce the MS heat supply. As shown in Figs. 13 and 14, the scenario *Ref* + *WT* even showed a slightly higher heat loss than the reference scenario *Ref*. This was because the DC waste heat supply increased with the introduction of the *WT*. During the *WT* charging process, the outlet water from the *WT* and the return water from the building mixed together, and then became the inlet water for the HP of the DC. The outlet temperature from the *WT* was usually higher than the return temperature from the building, so the *WT* charging process increased the inlet temperature of the HP. This increased temperature led to a higher condensation temperature and a lower COP for the HP. Therefore, more waste heat was generated to produce the same amount of cooling.

However, the BTES system almost solved the mismatch problem and saved a considerable amount of MS heat supply. As shown in Fig. 13, the scenario *Ref* + *BTES* reduced the heat loss by 83% compared to the reference scenario *Ref*. The surplus waste heat was stored by the BTES system during the non-heating season and then supplied to the building during the heating season. This long-term heat storage shifted the waste heat from non-heating season to heating season, and thus increased the waste heat utilization rate from 77% to 96%. Consequently, as shown in Fig. 14, the annual heat supply from MS was reduced by 10%. In addition, the BTES system also brought a remarkable peak load shaving effect, although this was less significant than in the case of the WT. As shown in Fig. 12, the peak load of the scenario *Ref* + *BTES* was 15% lower than the reference scenario *Ref*.

The scenario *Ref* + *WT* + *BTES*, which combined a WT and a BTES system, had the most complex system, as shown in Fig. 4. The peak load shaving effect achieved the best performance due to the combination of WT and BTES, a reduction of 37%, as illustrated in Fig. 12. However, the mismatch relieving effect was worse than the scenario *Ref* + *BTES*. The heat loss and the MS heat supply were reduced by 68% and 9%, respectively, as presented in Fig. 14.

In addition, both the *WT* and *BTES* scenarios used more electricity than the reference scenario. As shown in Fig. 14, the scenario *Ref* + *WT* increased electricity use by 12%. This was because the WT charging process led to a higher condensation temperature for the HP in the DC, and thus increased HP electricity use, as explained above. Similarly, the *Ref* + *BTES* scenario increased electricity use by 30%. This was caused by the additional electricity use of the HP in the BTES system, which was 0.9 GWh per year. The scenario *Ref* + *WT* + *BTES* resulted in the largest increase in electricity use, amounting to 40%. This was because it not only increased electricity use from the HP in the DC but also resulted in additional electricity use by the HP in the BTES system.

4.3. Evaluating the TES scenarios by economic analysis

This section evaluates the TES scenarios based on economic analysis. As shown in Fig. 15, both the WT and the BTES system could save energy bills. The scenario *Ref* + *WT* saved 5% of the annual energy bill compared to the reference scenario *Ref*. This saving arose only due to the reduction in the fixed part of the heating bill, which was brought by the peak load shaving effect of the WT. Similarly, the scenario *Ref* + *BTES* saved 6% of the annual energy bill. This bill saving came from the reduction in both the fixed and variable parts of the heating bill, which was caused by the peak load shaving and mismatch reliving effects of the BTES. In addition, the scenario *Ref* + *WT* + BTES achieved the highest energy bill saving, reducing the bill by 8%. This was because it made full use of the advantages of both the WT and BTES.

Fig. 16 presents the payback period of the three TES scenarios. The scenario *Ref* + *WT* had the shortest payback period of 12 years. In contrast, the *Ref* + *BTES* and *Ref* + *WT* + *BTES* scenarios presented longer payback periods of 17 and 20 years, respectively, although they had better annual energy bill savings. These long payback periods were due to the high initial investment.

4.4. Evaluating the TES scenarios by environmental analysis

This section evaluates the TES scenarios based on environmental analysis. As shown in Fig. 17, the BTES system effectively reduced CO_2 emissions. The *Ref* + *BTES* and *Ref* + *WT* + *BTES* scenarios reduced the annual CO_2 emissions by 8% and 7%, respectively. This significant reduction was for two reasons. First, the BTES system almost solved the mismatch problem and consequently saved a considerable amount of MS heat supply. Second, the CO_2 emission

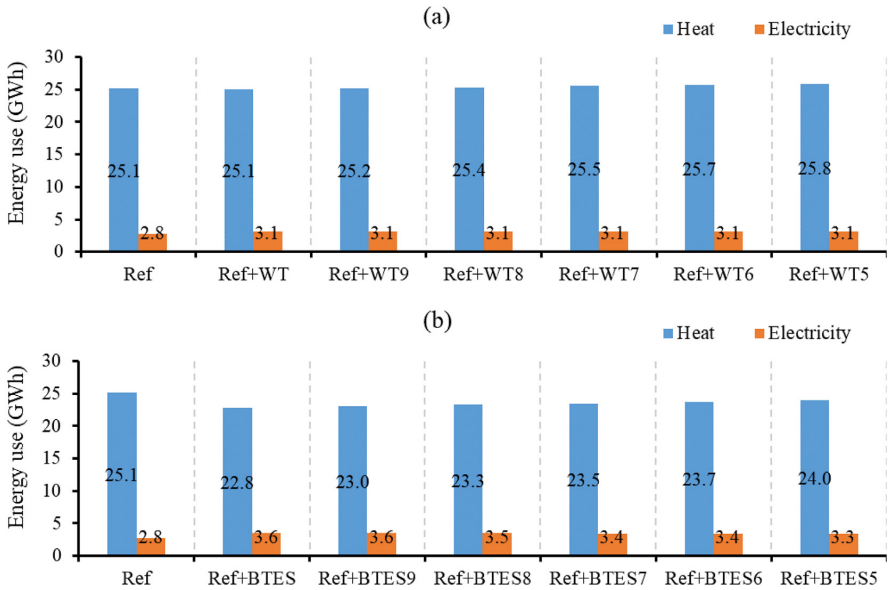

Fig. 18. Annual energy use for the water tank scenarios (a) and the borehole thermal energy storage scenarios (b).

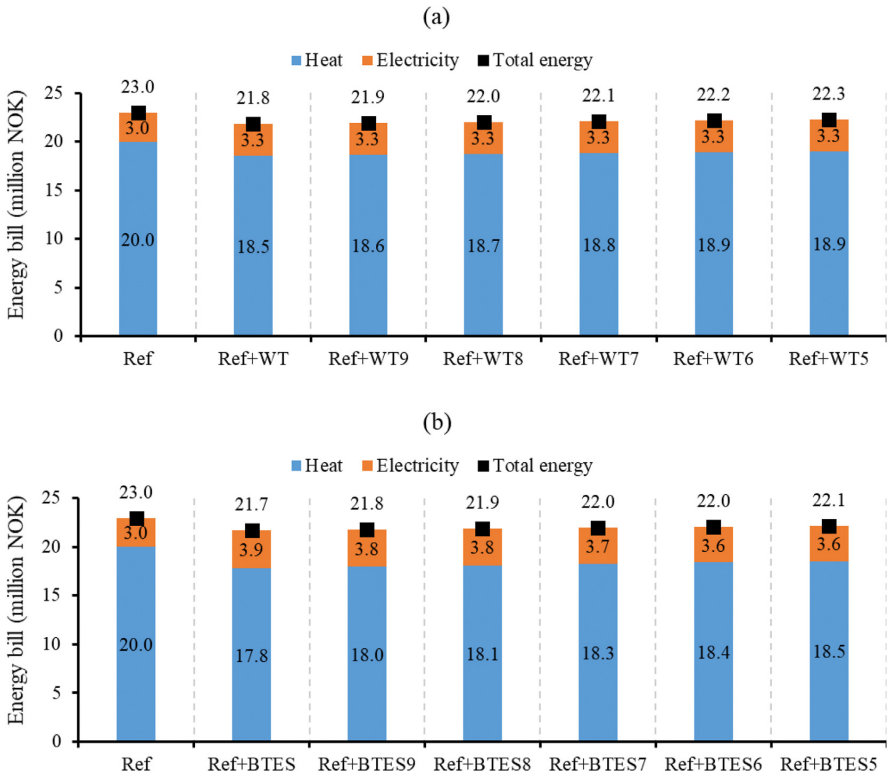

Fig. 19. Annual energy bill for the water tank scenarios (a) and the borehole thermal energy storage scenarios (b).

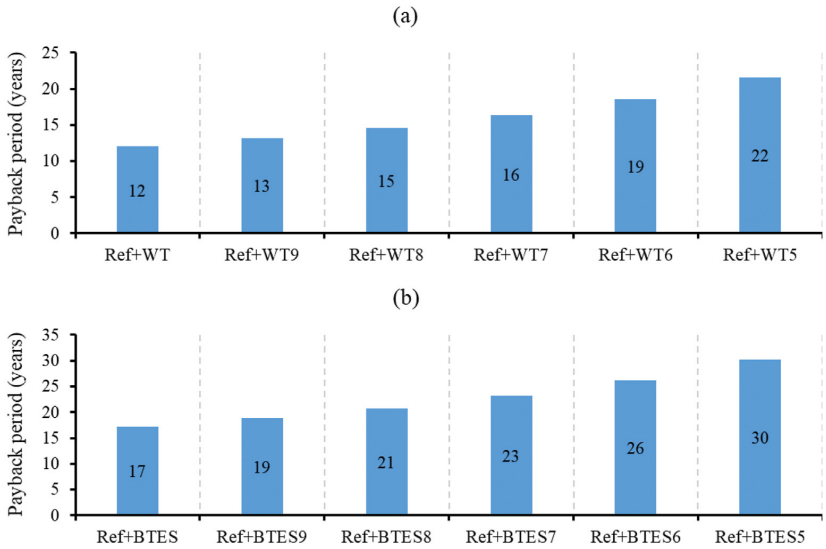

Fig. 20. Payback period for the water tank scenarios (a) and the borehole thermal energy storage scenarios (b).

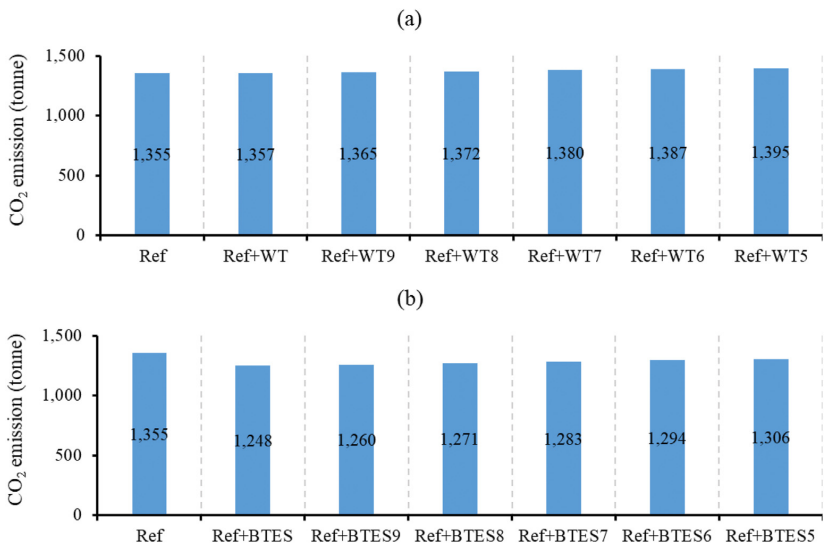

Fig. 21. Annual CO_2 emission for the water tank scenarios (a) and the borehole thermal energy storage scenarios (b).

factor for electricity was much smaller than that for heat, even though electricity use increased with the introduction of BTES. Therefore, the decrease in the CO_2 emissions from heat was much larger than the increase in CO_2 emissions from electricity. In contrast, the WT did not bring any benefits in terms of reducing CO_2 emissions, because it had no obvious heat-saving effect.

5. Sensitivity analysis of thermal energy storage efficiency

The results from Section 4 assumed that the TES has a storage efficiency of 100%. However, the storage efficiency ranges from 50% to 100% for the WT and BTES, based on a report from the International Energy Agency on large scale TESs [55]. The storage efficiency

of TESs differs from case to case and even changes with time. For example, the storage efficiency of BTES is highly related to its local geological condition. The storage efficiency of WT may reduce after several years' operation due to the moistened insulation. Therefore, it is necessary to conduct a sensitivity study to investigate the impacts of storage efficiency on different TESs, and thus provide more generalized suggestions on choosing different TESs. This section conducts a sensitivity analysis of storage efficiency. The study was conducted based on the principle of energy balance, which meant that heat loss from the TES would be supplemented by the MS. The annual MS heat supply and electricity use for the *Ref* + *WT* and *Ref* + *BTES* scenarios was used as the benchmark, which is presented in Fig. 14.

Table 1 presents the scenarios used for sensitivity analysis. The sensitivity analysis did not include the scenario with both the WT and BTES. The scenario *Ref* + *WT* + *BTES* did not achieve the best performance in terms of energy saving and CO_2 emissions reduction, even though it had the most complex system and the highest initial investment.

Fig. 18 shows the variation in the annual energy use as the storage efficiency of the TES varies. The MS heat supply increased with the decreased storage efficiency of the WT and BTES. In the WT scenarios, the annual MS heat supply would increase by 0.6% if the storage efficiency decreased by 10%. When the storage efficiency declined to less than 90%, the WT scenarios would require more MS heat supply than the reference scenario. In the BTES scenarios, the annual MS heat supply increased by 1.1% when the storage efficiency decreased by 10%. However, the BTES scenarios still had 5% less MS heat supply than the reference scenario, even when the storage efficiency dropped to 50%. In addition, the lower storage efficiency could reduce the electricity use for the BTES scenarios, because less stored heat was recovered by the HP of the BTES system.

Fig. 19 presents the variation in the annual energy bill as the storage efficiency of the TES varies. The annual energy bill would increase by 0.4% when the storage efficiency of the WT and BTES declined by 10%. However, the annual energy bills were still saved by 3–4%, even when the storage efficiency of the WT and BTES dropped to 50%. The increased annual energy bill led to a longer payback period for both the WT and BTES scenarios. As illustrated in Fig. 20, the payback period would increase by 2–4 years when the storage efficiency of the WT and BTES decreased by 10%. The WT scenarios would have a reasonable payback period of fewer than 15 years, if the storage efficiency remained higher than 80%. In contrast, the BTES scenarios presented a longer payback period of more than 17 years. The payback period could even be up to 30 years if the storage efficiency dropped to 50%.

Fig. 21 presents the variation in the annual CO_2 emissions as the storage efficiency of the TES varies. The lower storage efficiency increased the CO_2 emissions in both the WT and BTES scenarios. When the storage efficiency decreased by 10%, the increase was about 0.5% for the WT scenarios and 0.9% for the BTES scenarios. However, the BTES scenarios could always maintain lower CO_2 emissions compared to the reference scenario. The reduction of CO_2 emissions was around 4%, even when the storage efficiency dropped to 50%.

6. Conclusion

Three TES scenarios were proposed to address the mismatch problem and shave the peak load for the DH system, where the waste heat from data centre was available. The system performance was evaluated in terms of energy, economic, and environmental indicators. A campus DH system in Norway was selected as the case study.

The WT scenario was able to shave the peak load by up to 31%, which saved the annual energy bill by 5%. Meanwhile, the payback period was fewer than 15 years when the storage efficiency remained higher than 80%. However, introducing the WT had no obvious benefits in terms of mismatch relieving and CO_2 emissions reduction.

In contrast, the BTES scenario was able to improve the system performance substantially in terms of mismatch reliving and CO_2 emissions reduction. The waste heat utilization rate was increased from 77% to 96%, and the CO_2 emissions was reduced by up to 8%. In addition, the BTES also shaved the peak load by 15%, although this was less remarkable than the reduction achieved by the WT. Consequently, the annual energy bill was saved by 6% due to the mismatch reliving and peak load shaving. However, the BTES scenario presented a longer payback period of more than 17 years.

The scenario with both the WT and the BTES, had the most complex system and the highest initial investment. However, the system did not achieve the best performance in terms of energy saving and CO_2 emissions reduction. In addition, it had the longest payback period of 19 years, even without considering any heat loss.

These results provide guidelines for the retrofit of district heating systems, where data centres' waste heat is available.

Credit author statement

Haoran Li, Conceptualization, Methodology, Software, Validation, Writing – original draft. Juan Hou, Conceptualization, Software, Writing – original draft. Tianzhen Hong, Conceptualization, Writing – review & editing. Yuemin Ding, Conceptualization, Writing – review & editing. Natasa Nord, Conceptualization, Writing – review & editing, Supervision

Declaration of competing interest

The authors declare that they have no known competing financial interests or personal relationships that could have appeared to influence the work reported in this paper.

Acknowledgement

The authors gratefully acknowledge the support from the Research Council of Norway through the research project Understanding behaviour of district heating systems integrating distributed sources under the FRIPRO/FRINATEK program (project number 262707).

Appendix A. Parameters for the building model

Table A.1
Key parameters for the building model.

Category	Parameter	Value
Areas of building envelope (m^2)	Exterior wall	102,600
	Roof	75,400
	Ground floor	75,900
	Window	40,700
U-value of building envelope ($W/(m^2 \cdot K)$)	Exterior wall	0.48
	Roof	0.41
	Ground floor	0.17
	Window	2.07
Ventilation system	Air change rate (1/h)	2.45
	Heat recovery efficiency (%)	58
	Building air volume (m^3)	1,054,600

Appendix B. Parameters for the DC model

Table B.1
Key parameters for the heat pump component in the data centre model.

Category	Parameter	Value
Annual average conditions	Temperature difference on the evaporator/ condensation side (K)	−4/ 12
	Nominal mass flow rate on the evaporator/ condensation side (kg/s)	18/ 36
Baseline	Carnot effectiveness	0.4
Maximum capacity	Nominal compressor power (kW)	850

Appendix C. Parameters for the WT and BTES system model

Table C.1
Key parameters for the water tank model.

Parameter	Value
Height (m)	15
Volume (m^3)	8,000

Table C.2
Key parameters for the borehole thermal energy storage model.

Category	Parameter	Value
Bore field	Length/width (m)	69/27
	Number of boreholes	240
	Distance between two boreholes (m)	3
Borehole	Height (m)	55
	Radius (m)	0.063
Tube	Type	Single U
	Radius (m)	0.0167
	Thermal conductivity ($W/(m \cdot K)$)	0.39
	Thickness (m)	0.003
Filling material	Thermal conductivity ($W/(m \cdot K)$)	1.15
	Specific heat capacity ($J/(K \cdot kg)$)	800
	Density ($kg/(m^3)$)	1,600
Soil	Thermal conductivity ($W/(m \cdot K)$)	2.7 [63]
	Specific heat capacity ($J/(K \cdot kg)$)	840 [63,64]
	Density (kg/m^3)	2,800 [63,64]
	Temperature (°C)	5.0

Table C.3
Key parameters for the heat pump component in the borehole thermal energy storage system model.

Category	Parameter	Value
Annual average conditions	Temperature difference on the evaporator/ condensation side (K)	−4/ 12
	Nominal mass flow rate on the evaporator/ condensation side (kg/s)	14/ 28
Baseline	Carnot effectiveness	0.4
Maximum capacity	Nominal compressor power (kW)	680

Appendix D. Parameters for the MS model

Table D.1
Key parameters for the main substation model.

Parameter	Value
Heat transfer area (m^2)	420
Design capability (MW)	15.6

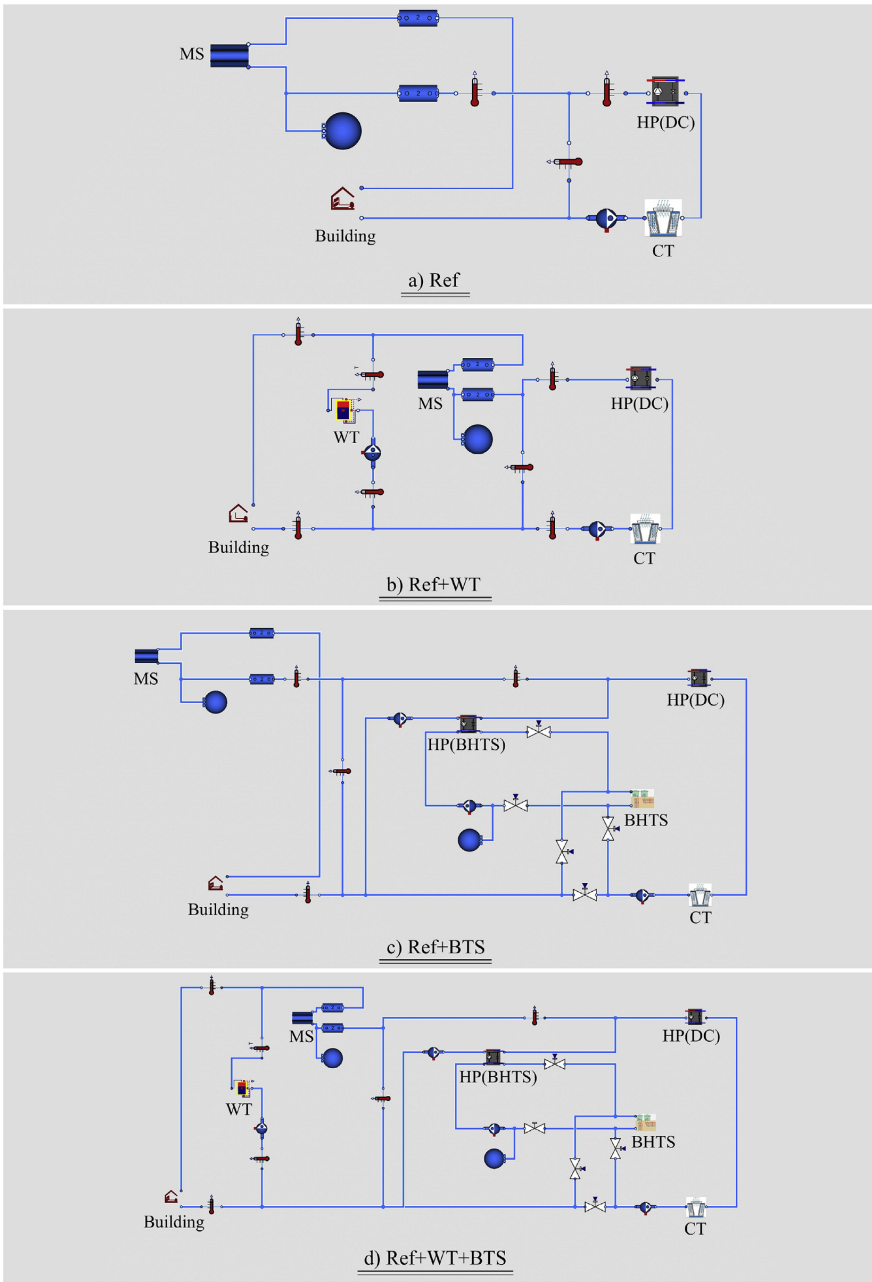

Fig. E1. Dymola models of the four scenarios.

References

[1] Frederiksen S, Werner S. District heating and cooling. Studentlitteratur Lund; 2013.
[2] Anderson A, Rezaie B. Geothermal technology: trends and potential role in a sustainable future. Appl Energy 2019;248:18–34.
[3] Holmgren K. Role of a district-heating network as a user of waste-heat supply from various sources – the case of Göteborg. Appl Energy 2006;83(12):1351–67.
[4] Li H, Nord N. Transition to the 4th generation district heating - possibilities, bottlenecks, and challenges. Energy Procedia 2018;149:483–98.

[5] Rezaie B, Rosen MA. District heating and cooling: review of technology and potential enhancements. Appl Energy 2012;93:2–10.
[6] Tian Z, Perers B, Furbo S, Fan J. Thermo-economic optimization of a hybrid solar district heating plant with flat plate collectors and parabolic trough collectors in series. Energy Convers Manag 2018;165:92–101.
[7] Tian Z, Zhang S, Deng J, Fan J, Huang J, Kong W, et al. Large-scale solar district heating plants in Danish smart thermal grid: developments and recent trends. Energy Convers Manag 2019;189:67–80.
[8] Tschopp D, Tian Z, Berberich M, Fan J, Perers B, Furbo S. Large-scale solar thermal systems in leading countries: a review and comparative study of Denmark, China, Germany and Austria. Appl Energy 2020;270:114997.
[9] Werner S. International review of district heating and cooling. Energy 2017;137:617–31.
[10] Lund H, Möller B, Mathiesen BV, Dyrelund A. The role of district heating in future renewable energy systems. Energy 2010;35(3):1381–90.
[11] Lund H, Østergaard PA, Chang M, Werner S, Svendsen S, Sorknæs P, et al. The status of 4th generation district heating: research and results. Energy 2018;164:147–59.
[12] Lund H, Werner S, Wiltshire R, Svendsen S, Thorsen JE, Hvelplund F, et al. 4th Generation District Heating (4GDH) Integrating smart thermal grids into future sustainable energy systems. Energy 2014;68:1–11.
[13] Upham P, Jones C. Don't lock me in: public opinion on the prospective use of waste process heat for district heating. Appl Energy 2012;89(1):21–9.
[14] Brand M, Svendsen S. Renewable-based low-temperature district heating for existing buildings in various stages of refurbishment. Energy 2013;62:311–9.
[15] Fang H, Xia J, Jiang Y. Key issues and solutions in a district heating system using low-grade industrial waste heat. Energy 2015;86:589–602.
[16] Koch K, Höfner P, Gaderer M. Techno-economic system comparison of a wood gas and a natural gas CHP plant in flexible district heating with a dynamic simulation model. Energy 2020;202:117710.
[17] Wahlroos M, Pärssinen M, Manner J, Syri S. Utilizing data center waste heat in district heating – impacts on energy efficiency and prospects for low-temperature district heating networks. Energy 2017;140:1228–38.
[18] Wahlroos M, Pärssinen M, Rinne S, Syri S, Manner J. Future views on waste heat utilization – case of data centers in Northern Europe. Renew Sustain Energy Rev 2018;82:1749–64.
[19] Koomey J. Growth in data center electricity use 2005 to 2010. 2011.
[20] Lu T, Lü X, Remes M, Viljanen M. Investigation of air management and energy performance in a data center in Finland: case study. Energy Build 2011;43(12):3360–72.
[21] Nadjahi C, Louahlia H, Lemasson S. A review of thermal management and innovative cooling strategies for data center. Sustainable Computing: Informatics and Systems 2018;19:14–28.
[22] Ebrahimi K, Jones GF, Fleischer AS. A review of data center cooling technology, operating conditions and the corresponding low-grade waste heat recovery opportunities. Renew Sustain Energy Rev 2014;31:622–38.
[23] Davies GF, Maidment GG, Tozer RM. Using data centres for combined heating and cooling: an investigation for London. Appl Therm Eng 2016;94:296–304.
[24] Kauko H, Kvalsvik KH, Rohde D, Nord N, Utne Å. Dynamic modeling of local district heating grids with prosumers: a case study for Norway. Energy 2018;151:261–71.
[25] Huang P, Copertaro B, Zhang X, Shen J, Löfgren I, Rönnelid M, et al. A review of data centers as prosumers in district energy systems: renewable energy integration and waste heat reuse for district heating. Appl Energy 2020;258:114109.
[26] Fiandrino C, Kliazovich D, Bouvry P, Zomaya AY. Performance and energy efficiency metrics for communication systems of cloud computing data centers. IEEE Transactions on Cloud Computing 2015;5(4):738–50.
[27] Noussan M, Jarre M, Poggio A. Real operation data analysis on district heating load patterns. Energy 2017;129:70–8.
[28] Shah SK, Aye L, Rismanchi B. Seasonal thermal energy storage system for cold climate zones: a review of recent developments. Renew Sustain Energy Rev 2018;97:38–49.
[29] Rohde D, Andresen T, Nord N. Analysis of an integrated heating and cooling system for a building complex with focus on long–term thermal storage. Appl Therm Eng 2018;145:791–803.
[30] Rohde D, Knudsen BR, Andresen T, Nord N. Dynamic optimization of control setpoints for an integrated heating and cooling system with thermal energy storages. Energy 2020;193:116771.
[31] Köfinger M, Schmidt RR, Basciotti D, Terreros O, Baldvinsson I, Mayrhofer J, et al. Simulation based evaluation of large scale waste heat utilization in urban district heating networks: optimized integration and operation of a seasonal storage. Energy 2018;159:1161–74.
[32] Moser S, Mayrhofer J, Schmidt R-R, Tichler R. Socioeconomic cost-benefit-analysis of seasonal heat storages in district heating systems with industrial waste heat integration. Energy 2018;160:868–74.
[33] Song J, Wallin F, Li H. District heating cost fluctuation caused by price model shift. Appl Energy 2017;194:715–24.
[34] Larsson O. Pricing models in district heating. 2011.
[35] Sjödin J, Henning D. Calculating the marginal costs of a district-heating utility. Appl Energy 2004;78(1):1–18.
[36] Liu W, Klip D, Zappa W, Jelles S, Kramer GJ, van den Broek M. The marginal-cost pricing for a competitive wholesale district heating market: a case study in The Netherlands. Energy 2019;189:116367.
[37] Björkqvist O, Idefeldt J, Larsson A. Risk assessment of new pricing strategies in the district heating market: a case study at Sundsvall Energi AB. Energy Policy 2010;38(5):2171–8.
[38] Verda V, Colella F. Primary energy savings through thermal storage in district heating networks. Energy 2011;36(7):4278–86.
[39] Harris M. Thermal energy storage in Sweden and Denmark: potentials for technology transfer. IIIEE Master thesis; 2011.
[40] Verrilli F, Srinivasan S, Gambino G, Canelli M, Himanka M, Del Vecchio C, et al. Model predictive control-based optimal operations of district heating system with thermal energy storage and flexible loads. IEEE Trans Autom Sci Eng 2017;14(2):547–57.
[41] Jebamalai JM, Marlein K, Laverge J. Influence of centralized and distributed thermal energy storage on district heating network design. Energy 2020;202:117689.
[42] Guan J, Nord N, Chen S. Energy planning of university campus building complex: energy usage and coincidental analysis of individual buildings with a case study. Energy Build 2016;124:99–111.
[43] Nord N, Sandberg NH, Ngo H, Nesgård E, Woszczek A, Tereshchenko T, et al. Future energy pathways for a university campus considering possibilities for energy efficiency improvements. Conference Future energy pathways for a university campus considering possibilities for energy efficiency improvements, vol. vol. 352. IOP Publishing, p. 12037.
[44] Lu Y. Design handbook for HVAC system (in Chinese). China Architecture & Building Press; 2007.
[45] Zuo W, Nouidui TS, Pang X. Modelica buildings library. Journal of Building Performance Simulation 2014;7(4):253–70.
[46] Buildings.ThermalZones.ReducedOrder.RC. https://simulationresearch.lbl.gov/modelica/releases/latest/help/Buildings_ThermalZones_ReducedOrder_RC.html#Buildings.ThermalZones.ReducedOrder.RC.TwoElements; 2020.
[47] Modelica standard library. https://github.com/modelica/ModelicaStandardLibrary; 2020.
[48] IBPSA project 1. https://ibpsa.github.io/project1/index.html; 2020.
[49] Reynders G, Baetens R, Picard D, Saelens D, Helsen L. Implementation and verification of the IDEAS building energy simulation library. Journal of Building Performance Simulation 2018;11(6):669–88.
[50] Annex60.Fluid.HeatPumps. 2020. http://www.iea-annex60.org/releases/modelica/1.0.0/help/Annex60_Fluid_HeatPumps.html#Annex60.Fluid.HeatPumps.Carnot_y. last accessed in December 2020.
[51] Modelica AixLib library. 2020. https://github.com/modelica-3rdparty/AixLib.
[52] AixLib.Fluid.Storage.UsersGuide. 2020. https://build.openmodelica.org/Documentation/AixLib.Fluid.Storage.UsersGuide.html. last accessed in December 2020.
[53] IBPSA.Fluid.Geothermal.Borefields.UsersGuide. 2020. https://build.openmodelica.org/Documentation/IBPSA.Fluid.Geothermal.Borefields.UsersGuide.html. last accessed in December 2020.
[54] Modelica.Fluid.Examples.HeatExchanger.BaseClasses.BasicHX. 2020. https://www.maplesoft.com/documentation_center/online_manuals/modelica/Modelica_Fluid_Examples_HeatExchanger_BaseClasses.html.
[55] Mangold D, Deschaintre L. Task 45 Large Systems Seasonal thermal energy storage Report on state of the art and necessary further R+ D. International Energy Agency Solar Heating and Cooling Programme. 2015.
[56] Clausen KS, From N, Hofmeister M, Paaske BL, Flørning J. Large heat pump projects in the district heating system (in Danish). Copenhagen: Danish Energy Agency; 2014.
[57] Statkraft Varme at tronheim. 2020. https://www.statkraftvarme.no/om-statkraftvarme/vare-anlegg/norge/trondheim/.
[58] Heating price at tronheim. https://www.statkraftvarme.no/globalassets/2-statkraft-varme/statkraft-varme-norge/om-statkraft-varme/prisark/20190901/fjernvarmetariff-trondheim-bt1.pdf; 2020.
[59] Jaluria Y. Design and optimization of thermal systems. CRC press; 2007.
[60] The policy rate. https://www.norges-bank.no/en/topics/Monetary-policy/Policy-rate/; 2020.
[61] CO_2 and greenhouse gas emissions. https://ourworldindata.org/co2-and-other-greenhouse-gas-emissions#global-warming-to-date; 2020.
[62] Electricity disclosure 2018. https://www.nve.no/norwegian-energy-regulatory-authority/retail-market/electricity-disclosure-2018/; 2020.
[63] Liebel HT. Influence of groundwater on measurements of thermal properties in fractured aquifers. 2012.
[64] Sibbet B, McClenahan D. Seasonal borehole thermal energy storage—guidelines for design & construction. Denmark: Natural Resources: Hvalsoe; 2015.

APPENDIX- PUBLICATIONS

PAPER 3

Li H, Hou J, Tian Z, Hong T, Nord N, Rohde D. Optimize heat prosumers' economic performance under current heating price models by using water tank thermal energy storage. Energy. 2022;239:122103.

APPENDIX- PUBLICATIONS

Energy 239 (2022) 122103

Contents lists available at ScienceDirect

Energy

journal homepage: www.elsevier.com/locate/energy

Optimize heat prosumers' economic performance under current heating price models by using water tank thermal energy storage

Haoran Li [a, *], Juan Hou [a], Zhiyong Tian [b], Tianzhen Hong [c], Natasa Nord [a], Daniel Rohde [d]

[a] Department of Energy and Process Technology, Norwegian University of Science and Technology, Kolbjørn Hejes vei 1 B, Trondheim, 7491, Norway
[b] School of Environmental Science and Engineering, Huazhong University of Science and Technology, Wuhan, PR China
[c] Building Technology and Urban Systems Division, Lawrence Berkeley National Laboratory, 1 Cyclotron Road, Berkeley, CA, 94720, USA
[d] SINTEF Energy Research, Sem Sælands vei 11, 7034, Trondheim, Norway

ARTICLE INFO

Article history:
Received 29 March 2021
Received in revised form
19 August 2021
Accepted 19 September 2021
Available online 22 September 2021

Keywords:
4th generation district heating
Thermal energy storage
Distributed heat sources
Heating price model
Peak load
Mismatch problem

ABSTRACT

Due to heat prosumers' dual roles of heat producer and heat consumer, the future district heating (DH) systems will become more flexible and competitive. However, the current heating price models have not yet supported the reverse heat supply from prosumers to the central DH system, which means the prosumers would gain no economic benefit from supplying heat to the central DH system. These unidirectional heating price models will reduce interest in prosumers, and thus hinder the promotion of prosumers in DH systems. This study aimed to optimize prosumers' economic performance under the current heating price models by introducing water tank thermal energy storage (WTTES). A dynamic optimization problem was formulated to explore prosumers' economic potentials. The size parameter of WTTESs was swept in prosumers to obtain the optimal storage size considering the trade-off between the payback period and the heating cost saving. The proposed method was tested on a campus DH system in Norway. The results showed that the prosumer's annual heating cost was saved up to 9%, and the investment of WTTES could be recovered in less than ten years. This study could provide guidelines on improving prosumers' economic performance and promote the development of prosumers during the transformation period of DH systems.

1. Introduction

Buildings account for a large share of total energy use and contribute to global warming considerably. In the European Union (EU), buildings are responsible for approximately 40% of total energy use and 36% of greenhouse gas emissions [1]. Space heating (SH) and domestic hot water (DHW) systems, as essential parts of building energy systems, play an important role in buildings' energy use. For example, in the residential sector of the EU countries, about 80% of the energy use is for SH and DHW [2,3]. District heating (DH) systems can satisfy buildings' heat demand in an energy-efficient and environment-friendly way [4]. Due to these merits, DH systems are competitive compared with alternative heating technologies, especially for urban areas with concentrated heat demand. Currently, more than four thousand DH systems are working successfully in Europe [5], and the national heat market share for DH systems can reach 60% for some areas [6–8]. However, DH systems' competitiveness is weakened by several challenges, such as the considerable distribution heat loss caused by high distribution temperature and the shrinking heat market due to the improving building efficiency [4]. To deal with these challenges and stay competitive, the current second and third generation DH systems are transforming to the fourth and fifth generation DH systems [9–12]. The transformation includes decreasing distribution temperature and upgrading infrastructure, and hence reduces the distribution heat loss and opens the door to more free heat such as renewables and waste heats.

For the future DH systems, renewables and waste heats may be integrated into the user side as distributed heat sources (DHSs) besides the central DH system. These end-users with DHSs are called heat prosumers due to their dual roles of producer and consumer. Fig. 1 illustrates examples of heat prosumers in a DH system. The block *Individual Prosumers* in the upper right of Fig. 1 shows different types of individual prosumers that integrated into the central DH system, these prosumers maybe a building installed with solar panels, a food store with waste heat from the

* Corresponding author.
E-mail address: haoranli@ntnu.no (H. Li).

https://doi.org/10.1016/j.energy.2021.122103

Nomenclature

CHP	Combine heat and power plant
CV(RMSE)	Coefficient of variation of the root mean square error
DC	Data centre
DH	District heating
DHW	Domestic hot water
DHS	Distributed heat source
EDC	Energy demand component
FDC	Flow demand component
FXC	Fixed component
HE	Heat exchanger
LDC	Load demand component
MS	Main substation
NLP	Nonlinear programming
NMBE	Normalized mean bias error
R2R	Extraction from the return line and feed into the return line
R2S	Extraction from the return line and feed into the supply line
S2S	Extraction from the supply line and feed into the supply line
SH	Space heating
TES	Thermal energy storage
WTTES	Water tank thermal energy storage

refrigeration system, or a factory with waste heat from the production process. In addition, the block *Community Prosumer* in the lower right of Fig. 1 presents a community prosumer with end-users and DHSs. These end-users are a cluster of buildings that may contain residential buildings and commercial buildings, and the DHSs may be a data centre (DC) with waste heat from its cooling system and a micro combine heat and power plant (CHP). Different from the individual prosumers connecting to the central DH system directly, the community prosumer is connected to the central DH system via the main substation (MS), and hence the management of the community DH system can be separated from the central DH system. For both the individual prosumers and the community prosumers, it allows bidirectional heat flow between the prosumers and the central DH system. Therefore, the prosumers may be supplied with heat from the central DH system during high heat demand periods, and feed surplus heat from their DHSs to the central DH system during low heat demand periods.

There is a growing interest in prosumers in DH systems. Nord et al. [13] and Lickleder et al. [14] proposed methods to model heat prosumer-based DH systems. Marguerite et al. introduced a tool to optimize the design and operation of prosumers [15]. Pipiciello et al. developed a new type of substation for heat prosumers in DH systems [16]. Nielsen et al. [17], Brand et al. [18], and Gross et al. [19] investigated the impacts of prosumers on DH systems. Huang et al. reviewed the applications of DCs as prosumers in DH systems [20], and Kauko et al. studied the impacts of DCs and supermarkets as prosumers in DH systems [21]. Previous research has proposed the methods to design and operate prosumers and demonstrated the economic benefits of introducing prosumers in

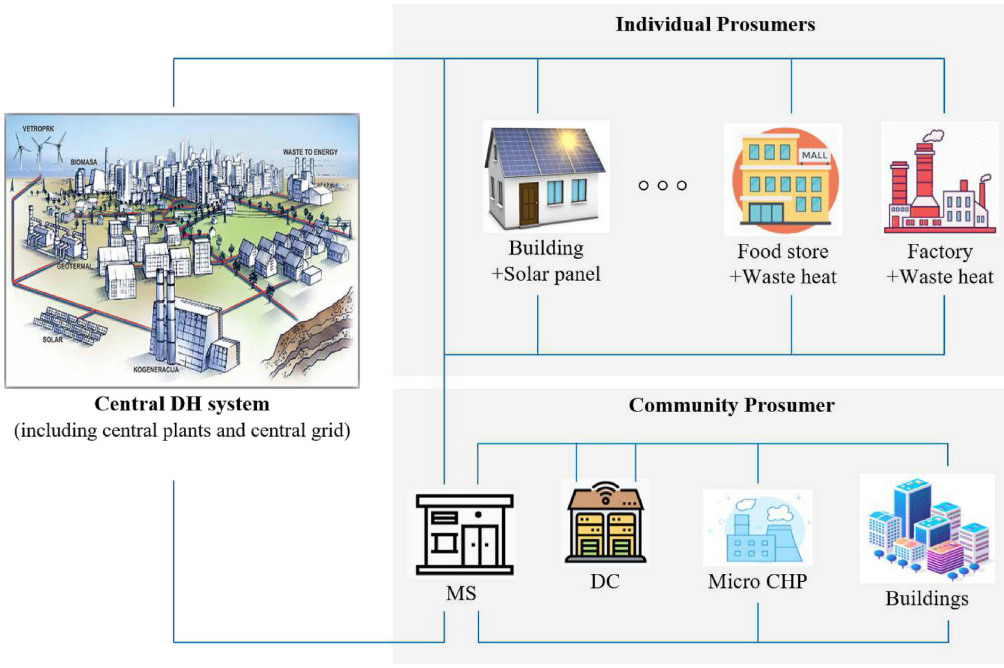

Fig. 1. Schematic illustrates examples of prosumers in a DH system.

DH systems. However, there is limited research focusing on optimizing prosumers' economic performance, especially under the current heating price models. During the transformation period of the DH system, despite some successful projects with bidirectional heating price models, the widely used heating price models have not supported the reverse heat supply from the heat prosumers to the central DH system, which means the prosumers would gain no economic benefit from supplying heat to the central DH system [22]. These unidirectional heating price models are reducing people's interest in heat prosumers, and thus hindering the promotion of prosumers in DH systems. Therefore, further research is needed to optimize prosumers' economic performance under the current widely used heating price models during the transformation period of the DH system.

The current widely used heating price models charge the heating cost of heat prosumers based on both the heat use and the peak load [22]. Therefore, the two possible ways to optimize heat prosumers' economic performance are: 1) increasing the self-utilization rate of heat supply from prosumers' DHSs, and hence reducing the heat supply from the central DH system, and 2) shaving prosumers' peak load by shifting parts of central DH system's heat supply from peak hours to non-peak hours. Thermal energy storages (TESs) have been proven to be good at achieving the above goals. Firstly, TESs may be used to relieve the mismatch between prosumers' heat supply from DHSs and buildings' heat demand [23–27]. Consequently, less heat is fed to the central DH system when surplus heat exists, and the self-utilization rate of the heat supply from prosumers' DHSs is increased. Secondly, TESs may shift the central DH system's heat supply from peak hours to non-peak hours, thereby shaving the peak load of the heat prosumers [28–30]. However, one barrier to the integration of TESs into prosumers is their high investment costs and the economic risk of long payback periods. Therefore, further research is needed to explore the economic feasibility of introducing TESs to prosumers under current heating price models.

This study aimed to break the above economic barrier through the optimal operation of heat prosumers with TESs and the optimal sizing of TESs. Firstly, a water tank thermal energy storage (WTTES) was chosen as short-term TES and integrated into a prosumer. Afterwards, a dynamic optimization problem was formulated aiming to explore the economic potential of the heat prosumer with TES. The economic performance of the prosumer with TES was evaluated in terms of heating cost saving and payback period. Finally, the size parameter of WTTES was swept to obtain the optimal storage size considering the trade-off between the payback period and the heating cost saving. The proposed method was tested on a campus DH system in Norway, which received heat from the central DH system, meanwhile, had its own DHS with waste heat recovery from the university DC. The main contributions of this study are summarized as the following. Firstly, the technical contribution is to support the transformation of current DH systems towards completely renewable-based DH systems with DHSs by optimizing prosumers' economic performance under the current heating price models, which is a practical but rarely addressed problem. Secondly, the scientific contribution is to use the technique of combining dynamic optimization and parameter' sweeping to explore prosumers' economic potentials considering the economic feasibility after introducing TESs. Thirdly, the practical contribution is to provide more comprehensive recommendations for heat prosumers and DH companies to understand the effect of the peak load definition on the economic performance of heat prosumers. This study provides guidelines on improving prosumers' economic performance during the transformation period of the DH system, and thus promote the development of the heat prosumers in DH systems.

The remaining of the article is organized as follows. Section 2 proposes a generalized heating price model based on the current widely used heating price models, afterwards introduces the system design and operation strategy aiming to optimize prosumers' economic performance under the generalized heating price model by using short-term TESs. Section 3 introduces the background of the case study, meanwhile provides information on research scenarios and simulation settings. Section 4 investigates and compares different scenarios' performance in terms of energy and economic indicators. Section 5 discusses the effects of the peak load definition on prosumers' economic performance and investigates the WTTESs' thermoclines during charging and discharging processes. Section 6 concludes this study.

2. Method

This section introduces the method to optimize prosumers' economic performance under current heating price models by using WTTESs. Firstly, a generalized heating price model is proposed based on the current widely used heating price models. Afterwards, considering the generalized heating price model, the system design for prosumers with the WTTESs and the optimization problem aiming to minimize the prosumers' heating cost are given. Meanwhile, the models and constraints used in the optimization problem are presented. Finally, the economic indicators used to evaluate prosumers' performance are introduced.

This study was based on numerical simulation. The DH system model was built using the Modelica language, which is an object-oriented language to conveniently model physical systems [31]. The optimization was performed with JModelica.org, which is an open-source platform for the simulation and optimization of complex dynamic systems [32]. For the optimization process based on the JModelica.org platform, the formulated infinite-dimensional optimization problem was transcribed into a finite-dimensional nonlinear programming (NLP) problem through Direct collocation [33]. Afterwards, the obtained NLP problem was solved by NLP solvers in the following steps. Firstly, the inequality constraints in the NLP problem were eliminated using the interior-point method [34]. Then a local optimum for the NLP was achieved by solving the first order Karush-Kuhn-Tucker condition, using iterative techniques through Newton's method.

2.1. Generalized heating price model

Although heating price models vary with local DH companies, a generalized heating price model was defined and was used in the optimization of prosumers' economic performance. This generalized heating price model was defined as suggested in the review paper of [22], where the current heating price models may include four components: fixed component (FXC), flow demand component (FDC), energy demand component (EDC), and load demand component (LDC). The FXC is paid to connect to the central DH system. The FDC is charged based on the volume of the hot water used to deliver heat and is intended to motivate the low return temperature. The LDC covers the DH companies' cost to maintain a certain level of capacity for the peak load, the initial investment of new facilities, depreciation, etc. It is charged based on the peak load of the end-users. The EDC covers the fuel cost and is charged based on the total heat use of end-users.

Based on the review article of [22], the existence and the average share of each component for the Swedish DH systems are illustrated in Fig. 2. About half of the heating price models include the FXC (60%) and the FDC (50%), however, they only account for 1–2% of the total heating cost. In contrast, the LDC and the EDC are the most commonly used components. About 87% of the current

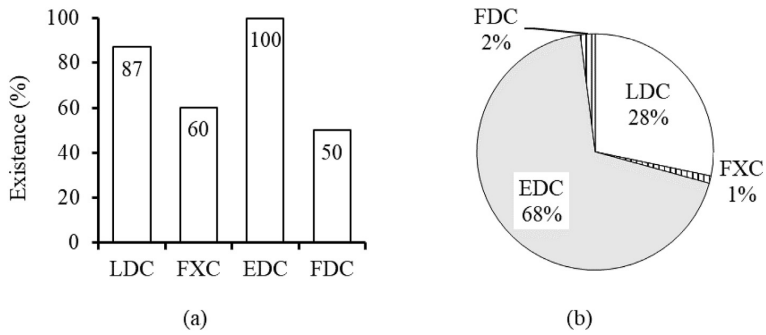

Fig. 2. The existence (a) and average share (b) of each component in investigated heating price models [22].

heating price models have the LDC, and all the current heating price models have the EDC. They together account for 96% of the total heating cost. There are technical-economic reasons for the configuration of a heating price model. All the DH companies want to cover their production cost and therefore the EDC is always included. For newer DH companies that may be oversized than the current heat demand, the most important component to charge the customers is the EDC. In addition, for existing DH companies that may have issues in further capacity increase, more effective utilization of the existing capacities is crucial and therefore the LDC is becoming very important and valuable. According to the above discussion, a generalized heating price model was proposed considering only the LDC and EDC as shown in Equation (1). The introduced generalized heating price model is just a theoretical suggestion and DH companies may organize their models based on their needs.

$$C_{tot} = C_{ldc} + C_{edc} \tag{1}$$

where C_{tot} is the total heating cost, C_{ldc} is the LDC, and C_{edc} is the EDC.

The LDC, C_{ldc}, was calculated as Equation (2):

$$C_{ldc} = LP \cdot \dot{Q}_{pea} \tag{2}$$

where LP is the LDC heating price, and $\dot{Q}_{pea}$ is the yearly peak load according to Refs. [35,36].

The EDC, C_{edc}, was calculated as Equation (3):

$$C_{edc} = \int_{t_0}^{t_f} EP(t) \cdot \dot{Q}(t) dt \tag{3}$$

where $\dot{Q}(t)$ is the heat flow rate supplied to the heat user and $EP(t)$ is the EDC heating price.

2.2. System design for a heat prosumer with WTTES

As introduced in Section 1, WTTES may be integrated into a heat prosumer to improve the economic performance of the heat prosumer under the current heating price models. Fig. 3 illustrates the proposed system design for a prosumer with WTTES, which may increase the self-utilization rate of the heat supply from the prosumer's DHSs and shave the prosumer's peak load. In the system, the DHS may be low-temperature heat sources from renewables or waste heat. There are mainly three configurations to integrate the DHSs into DH grids: 1) extraction from the return line and feed into the supply line (R2S), 2) extraction from the return line and feed into the return line (R2R), and 3) extraction from the supply line and feed into the supply line (S2S). In this study, the R2R mode was chosen, because it is preferable for low-temperature heat sources [4].

In addition, the MS connects the prosumer with the central DH system. The heat exchanger 1 (HE1) in the MS is connected to the TES and used for the heat charging of the WTTES. During the warm period with lower heat demand, the HE1 may supplement the heat supply from the prosumer's DHS. During the cold period with higher heat demand, the HE1 contributes to the peak load shaving, because it may charge the TES at non-peak hours and thus the stored heat can be used at peak hours. Heat exchanger 2 (HE2) is connected to the prosumer's distribution system directly and acts as a high-temperature heat source. It boosts the supply temperature of the prosumer to the required level after the preheating by low-temperature DHSs.

Moreover, the WTTES in the system is a short-term TES. As described in Section 1, it has two key functions. Firstly, it relives the mismatch problem between the DHS's heat supply and the buildings' heat demand during the warm period. When the DHS's heat supply is higher than the buildings' heat demand, the surplus heat supply from the DHS is stored in the WTTES instead of being fed into the central DH system. When the DHS's heat supply is lower than the buildings' heat demand, the stored heat in the WTTES together with the heat from DHS is supplied to the buildings. Secondly, the WTTES shaves the prosumer's peak load during the cold period. The WTTES is charged at non-peak hours and discharged at peak hours, therefore part of the central DH system's heat supply is shifted to non-peak hours and the peak load is shaved.

Finally, the heat-users in the system are buildings. As illustrated in Fig. 1, the heat-user may be one building when the prosumer is an individual prosumer or a cluster of buildings when the prosumer is a community prosumer.

2.3. Optimal operation for a prosumer with WTTES

To optimize prosumers' economic performance, the optimal operation strategy should minimize prosumers' heat use from the central DH system by increasing the self-utilization rate of the heat supply from prosumer's DHSs, minimize the prosumers' peak load. In addition, the operation should track the reference indoor temperature by minimizing the deviation between the simulated indoor temperature and its reference value. To achieve the above

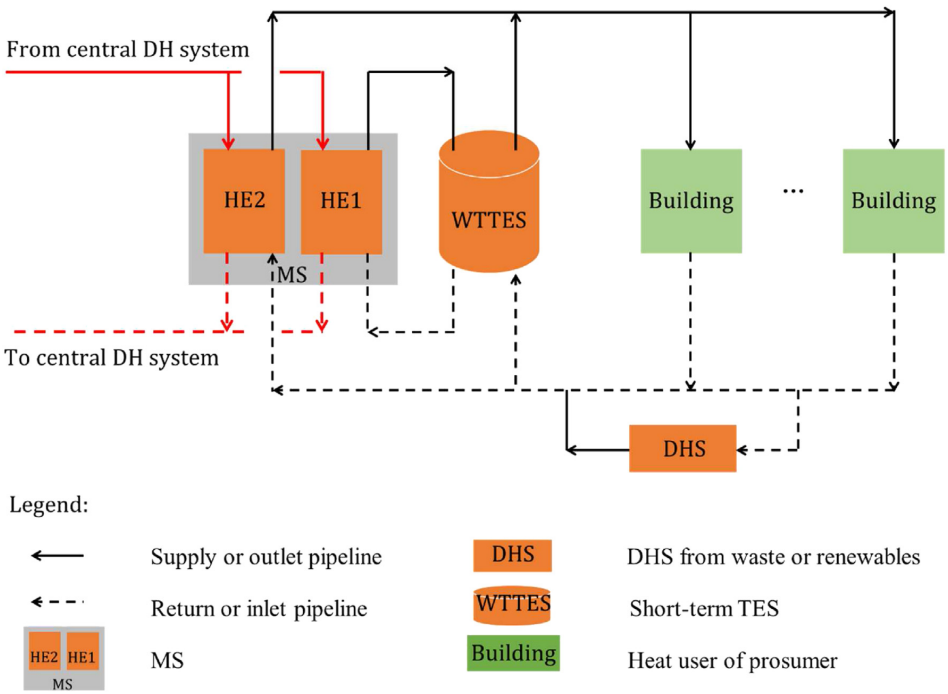

Fig. 3. Schematic illustrates the system design for a prosumer with WTTES.

goals, a multi-objective dynamic optimization problem was formulated as Equations (4), (5), (6), (7), and (8):

Minimize:

$$\int_{t_0}^{t_f} EP(t)\cdot\dot{Q}(t)dt + LP\cdot\dot{Q}_{pea} + W\cdot\int_{t_0}^{t_f}\left(T_{ia}(t) - T_{ia}^{ref}(t)\right)^2\cdot dt \tag{4}$$

subject to:

$$\dot{Q}(t) \le \dot{Q}_{pea} \tag{5}$$

$$F(t, \boldsymbol{z}(t)) = 0 \tag{6}$$

$$F_0(t_0, \boldsymbol{z}(t_0)) = 0 \tag{7}$$

$$z_L \le \boldsymbol{z}(t) \le z_U \tag{8}$$

where $\dot{Q}(t)$ is the heat flow rate supplied from the central DH to the prosumer. $\dot{Q}_{pea}$ and LP are the peak load and the LDC heating price, respectively. $EP(t)$ is the heating price for the EDC. $T_{ia}(t)$ and $T_{ia}^{ref}(t)$ are the simulated indoor temperature and its reference value at time t. $\boldsymbol{z}\in\mathbb{R}^{n_z}$ represents the time-dependent variables, which includes the manipulated variable $\boldsymbol{u}\in\mathbb{R}^{n_u}$ to be optimized, the differential variable $\boldsymbol{x}\in\mathbb{R}^{n_x}$, and the algebraic variable $\boldsymbol{y}\in\ \mathbb{R}^{n_y}$. Equation (6) defines the system dynamics and Equation (7) is the initial conditions of the system. $z_L\in[-\infty,\infty]^{n_z}$ and $z_U\in\ [-\infty,\infty]^{n_z}$ are the lower and upper bounds, respectively.

The system dynamics defined in Equation (6) included the dynamics of the MS, TES, DHS, buildings, and pipelines, as illustrated in Fig. 3. The energy and mass flow exchanged between these components were described by Equations (9), (10), (11), (12), and (13).

$$\dot{Q}(t) = \dot{Q}_{HE1} + \dot{Q}_{HE2} \tag{9}$$

$$\dot{Q}_{HE1} + \dot{Q}_{HE2} + \dot{Q}_{DHS} = \dot{Q}_{Bui} + \dot{Q}_{TES} + \dot{Q}_{loss,\ TES} + \dot{Q}_{loss,\ pip} \tag{10}$$

$$\dot{Q}_{HE1} = c\cdot\dot{m}_{HE1}\cdot(T_{HE1,sup} - T_{HE1,ret}) \tag{11}$$

$$\dot{Q}_{HE2} = c\cdot\dot{m}_{HE2}\cdot(T_{HE2,sup} - T_{HE2,ret}) \tag{12}$$

$$\dot{Q}_{DHS} = c\cdot\dot{m}_{DHS}\cdot(T_{DHS,sup} - T_{DHS,ret}) \tag{13}$$

where $\dot{m}_{HE1}$, $\dot{m}_{HE2}$, and $\dot{m}_{DHS}$ are the mass flow rate of HE1, HE2, and DHS, respectively. $\dot{Q}_{HE1}$, $\dot{Q}_{HE2}$, and $\dot{Q}_{DHS}$ are the heat flow rate of HE1, HE2, and DHS, respectively. $\dot{Q}_{TES}$ is the charging (positive values) and discharging (negative values) heat flow rate of WTTES. $\dot{Q}_{Bui}$ is the heat demand of buildings. $\dot{Q}_{loss,\ TES}$ and $\dot{Q}_{loss,\ pip}$ are the heat loss from WTTES and pipelines, respectively. $T_{HE1,sup}$, $T_{HE2,sup}$, and $T_{DHS,sup}$ are the supply water temperature of HE1, HE2, and DHS, respectively. $T_{HE1,ret}$, $T_{HE2,ret}$, and $T_{DHS,ret}$ are the return water temperature of HE1, HE2, and DHS, respectively. c is the specific heat capacity of water.

In this study, the manipulated variables, $\boldsymbol{u}$ in Equations (6), are the supply water temperature of HEs in the MS ($T_{HE1,sup}$ and $T_{HE2,sup}$), the mass flow rate of HEs and buildings ($\dot{m}_{HE1}$, $\dot{m}_{HE2}$, and $\dot{m}_{Bui}$), and the heat supply flow rate from the radiator to the

building ($\dot{Q}_{rad}$). The heat flow rate of a prosumer, $\dot{Q}(t)$ in Equation (4), means the total heat flow rate of the two HEs in MS ($\dot{Q}_{HE1}$ and $\dot{Q}_{HE2}$) as shown in Equation (9). In addition, the variables $\dot{Q}_{TES}$, $\dot{Q}_{loss,\ TES}$, $\dot{Q}_{Bui}$, and $\dot{Q}_{loss,\ pip}$ are described in the models of WTTES, buildings, and pipelines, which are explained in Sections 2.3.1-2.3.3.

2.3.1. Model for short-term WTTES

WTTES was chosen as the TES in this research because it is easily applied [37,38] and economically reasonable [39] for DH systems. A one-dimensional WTTES model was used to describe the dynamics of the thermocline tank. The model can be represented as a single partial differential equation as Equation (14) [40]:

$$c \cdot \rho \cdot A_{XS} \cdot \frac{\partial T}{\partial t} = c \cdot (\dot{m}_{sou} - \dot{m}_{use}) \cdot \frac{\partial T}{\partial x} - U \cdot P \cdot (T(t,x) - T_{amb}) + \varepsilon \cdot A_{XS} \cdot \frac{\partial^2 T}{\partial x^2} \tag{14}$$

where T is the water temperature in the tank. x is the height of the tank. t is the time. ρ is the density of water. A_{XS} and P are the cross-sectional area and the perimeter of the tank, respectively. $\dot{m}_{sou}$ and $\dot{m}_{use}$ are the water mass flow rate from the heat source side and the user side, respectively. T_{amb} is the ambient temperature. U is the U-value of the tank wall. ε is a parameter representing the combined heat transfer effect of water through diffusion, conduction, and mixing due to turbulent flow.

To solve Equation (14) by using numerical methods, spatial derivatives were approximated by discretizing the tank into n nodes. Using the discretization scheme shown in Fig. 4 and computing energy balances on each node, Equation (14) was converted into a set of ordinary differential equations. The ordinary differential equation for the *ith* node is shown in Equation (15) [40]. Therefore, the heat loss and the heat flow rate of the *ith* node are obtained by Equations (16) and (17), and the total heat loss and heat flow rate of WTTES was calculated as Equations (18) and (19). In addition, the parameter ε has two different types of values representing the situations without and with buoyant mixing effect. When the temperature of a node is lower than the node above it, ε has lower values. Otherwise, the values become several orders of magnitude higher due to the buoyant mixing effect [40].

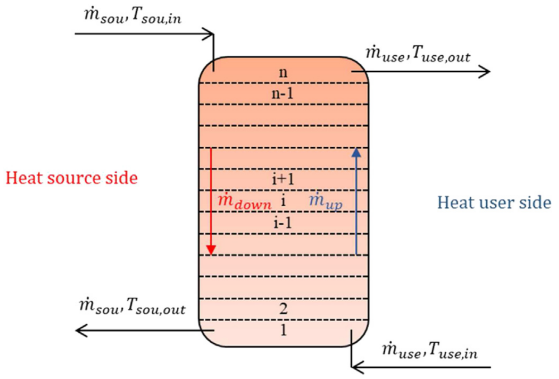

Fig. 4. Diagram illustrates the spatial discretization for a thermocline tank.

$$c \cdot \rho \cdot A_{XS} \cdot \Delta x \cdot \frac{dT_i}{dt} = c \cdot \dot{m}_{use} \cdot (T_{i-1} - T_i) + c \cdot \dot{m}_{sou} \cdot (T_{i+1} - T_i) - U \cdot P \cdot \Delta x \cdot (T_i - T_{amb}) + \frac{\varepsilon \cdot A_{XS}}{\Delta x} \cdot (T_{i+1} - 2 \cdot T_i + T_{i-1}) \tag{15}$$

$$\dot{q}_{loss,\ TES,\ i} = U \cdot P \cdot \Delta x \cdot (T_i - T_{amb}) \tag{16}$$

$$\dot{q}_{TES,i} = c \cdot \dot{m}_{sou} \cdot (T_{i+1} - T_i) \tag{17}$$

$$\dot{Q}_{loss,\ TES} = \sum_{i=1}^{n-1} \dot{q}_{loss,\ TES,\ i} \tag{18}$$

$$\dot{Q}_{TES} = \sum_{i=1}^{n-1} \dot{q}_{TES,i} \tag{19}$$

where Δx is the length of the node, and T_i is the water temperature of the *ith* node. $\dot{q}_{loss,\ TES,\ i}$ and $\dot{q}_{TES,i}$ are the heat loss and heat flow rate of the *ith* node, respectively.

2.3.2. Model for buildings

To improve computational efficiency, a single-equivalent building model was used to represent the overall performance of all the buildings in this study. This simplification has been proved feasibility by previous research [39,41]. After these simplifications, Equation (20) is used to describe the thermal behaviours of all the buildings connected to the prosumer' heating system, and Equations (21)–(23) are the inequality constraints for the variables ΔT_{Bui}, T_{sup}, and $\dot{m}_{Bui}$.

$$\dot{Q}_{Bui} = c \cdot \dot{m}_{Bui} \cdot (T_{sup} - T_{ret}) \tag{20}$$

$$\Delta T_{Bui,\ L} \le \Delta T_{Bui} = T_{sup} - T_{ret} \le \Delta T_{Bui,U} \tag{21}$$

$$T_{sup,L} \le T_{sup} \le T_{sup,U} \tag{22}$$

$$\dot{m}_{Bui,\ L} \le \dot{m}_{Bui} \le \dot{m}_{Bui,\ U} \tag{23}$$

where $\dot{Q}_{Bui}$ is the buildings' heat demand including demand for the SH and the DHW system. $\dot{m}_{Bui}$ and ΔT_{Bui} are the mass flow rate and temperature difference of water at the primary side of the building's substation, respectively. T_{sup} and T_{ret} are the supply and return temperature of water at the primary side of the building's substation, respectively. $\Delta T_{Bui,\ L}$, $T_{sup,L}$, and $\dot{m}_{Bui,\ L}$ are the lower bounds for ΔT_{Bui}, T_{sup}, and $\dot{m}_{Bui}$, respectively. $\Delta T_{Bui,U}$, $T_{sup,U}$, and $\dot{m}_{Bui,\ U}$ are the upper bounds for ΔT_{Bui}, T_{sup}, and $\dot{m}_{Bui}$, respectively.

The lower bound of the supply temperature, $T_{sup,L}$, should be high enough for the SH system and the DHW system to keep a comfortable indoor temperature and avoid hygiene issues, as defined in Equation (24). The lower bound of the supply temperature was defined by Equation (25) for the SH system [42], and the lower bound of the supply temperature for the DHW system was 60 °C as defined in Equation (26), which is required by European standard CEN/TR16355 [43]. In addition, the upper bound for the supply temperature was determined by the supply temperature of

the central DH system, which can be deduced through measured data.

$$T_{sup,L} = max(T_{sup,SH,L}, T_{sup,\ DHW,L}) \tag{24}$$

$$T_{sup,SH,L} = T_{ia} + 0.5 \cdot \left(T_{sup,SH,des} + T_{ret,SH,des} - 2 \cdot T_{ia,des}\right) \cdot \left(\frac{T_{ia,des} - T_{oa}}{T_{ia,des} - T_{oa,des}}\right)^{1/b} + 0.5 \cdot \left(T_{sup,SH,des} - T_{ret,SH,des}\right) \cdot \left(\frac{T_{ia,des} - T_{oa}}{T_{ia,des} - T_{oa,des}}\right) \tag{25}$$

$$T_{sup,\ DHW,L} = 60 \tag{26}$$

where $T_{sup,SH,L}$ and $T_{sup,\ DHW,L}$ are the lower bound of the supply temperature for the SH and the DHW system, respectively. T_{ia} and T_{oa} are the indoor and the outdoor temperature, respectively. $T_{sup,SH}$ and $T_{ret,SH}$ are the supply and the return temperature of the SH system, respectively. b is a parameter depending on the characteristic of the radiator. The subscript *des* refers to the design conditions.

The lower bound of the water mass flow rate $\dot{m}_{Bui,L}$ is zero, and the upper bound of the water mass flow rate $\dot{m}_{Bui,U}$ is constrained by the capacity of the distribution system. In this study, the upper bound of the water mass flow rate $\dot{m}_{Bui,U}$ was obtained by the measurement data. In addition, the characteristics of the system and equipment determine the feasible region of the water temperature difference as described in Equation (21). In this study, the lower bound of the water temperature difference $\Delta T_{Bui,\ L}$ was zero, and the upper bound of the water temperature difference $\Delta T_{Bui,U}$ was obtained by the linear regression using measured data as Equation (27).

$$\Delta T_{Bui,U} = a_0 + a_1 \cdot T_{sup} \tag{27}$$

where a_0 and a_1 are parameters.

The buildings' heat demand, $\dot{Q}_{Bui}$, includes the heat demand for the SH and the DHW system, as in Equation (28).

$$\dot{Q}_{Bui} = \dot{Q}_{SH} + \dot{Q}_{DHW} \tag{28}$$

where $\dot{Q}_{SH}$ and $\dot{Q}_{DHW}$ are the heat demand of the SH and the DHW systems, respectively. $\dot{Q}_{SH}$ can be further divided into the demand for the radiator heating system $\dot{Q}_{rad}$ and the demand for the ventilation system $\dot{Q}_{ven}$, as described in Equation (29).

$$\dot{Q}_{SH} = \dot{Q}_{rad} + \dot{Q}_{ven} \tag{29}$$

Considering the thermal inertia of buildings, a simplified-lumped-capacity model derived from resistance-capacitance networks analogue to electric circuits was used to describe the building dynamics, as defined in Equations (30)–(32).

$$C_{env} \cdot \frac{dT_{env}}{dt} = \frac{T_{ia} - T_{env}}{R_{i,e}} + \frac{T_{oa} - T_{env}}{R_{o,e}} \tag{30}$$

$$C_{ia} \cdot \frac{dT_{ia}}{dt} = \frac{T_{ma} - T_{ia}}{R_{i,m}} + \frac{T_{env} - T_{ia}}{R_{i,e}} + \frac{T_{oa} - T_{ia}}{R_{win}} + \frac{T_{oa} - T_{ia}}{R_{ven}} + \dot{Q}_{rad} + \dot{Q}_{ven} + \dot{Q}_{in} \tag{31}$$

$$C_{ma} \cdot \frac{dT_{ma}}{dt} = \frac{T_{ia} - T_{ma}}{R_{i,m}} \tag{32}$$

where C and R represent the heat capacitance and resistance, T is the temperature. Subscripts *env*, *ia*, *oa*, *ma*, *win*, and *ven* denote building envelopes (including exterior walls and roofs), indoor air, outdoor air, internal thermal mass, window, and ventilation (including infiltration and mechanical ventilation), respectively. In addition, $R_{i,e}$ is the heat resistance between the indoor air and the building envelopes, $R_{o,e}$ is the heat resistance between the outdoor air and the building envelopes, and $R_{i,m}$ is the heat resistance between indoor air and interior thermal mass. $\dot{Q}_{in}$ is the internal heat gains. All the introduced heat capacitances, thermal resistances, temperatures, and heat flow rates in Equations (30)–(32) are marked in Fig. 5.

2.3.3. Model for pipelines

The pipeline model representing the heat loss from the pipelines was described as the following Equations (33)–(35) [44]:

$$\dot{Q}_{loss,\ pip} = \dot{Q}_{loss,\ pip,sup} + \dot{Q}_{loss,\ pip,ret} \tag{33}$$

$$\dot{Q}_{loss,\ pip,sup} = L \cdot \pi \cdot d \cdot \frac{(R_g + R_i) \cdot \Delta T_{pip,sup} - R_c \cdot \Delta T_{pip,ret}}{(R_g + R_i)^2 - R_c^2} \tag{34}$$

$$\dot{Q}_{loss,\ pip,ret} = L \cdot \pi \cdot d \cdot \frac{(R_g + R_i) \cdot \Delta T_{pip,ret} - R_c \cdot \Delta T_{pip,sup}}{(R_g + R_i)^2 - R_c^2} \tag{35}$$

where $\dot{Q}_{loss,\ pip}$, $\dot{Q}_{loss,\ pip,sup}$, and $\dot{Q}_{loss,\ pip,ret}$ are the total heat loss from pipes, the heat loss from supply pipes, and the heat loss from return pipes, respectively. L is the route length for the pair of pipes. d is the outer pipe diameter. R_i, R_g, and R_c are the resistances for insulation, ground, and coinciding, respectively, and they can be obtained by Equations (36)–(38). In addition, $\Delta T_{pip,sup}$ and $\Delta T_{pip,ret}$ are the temperature difference for the supply pipe and the return pipe, and can be obtained by Equations (39) and (40):

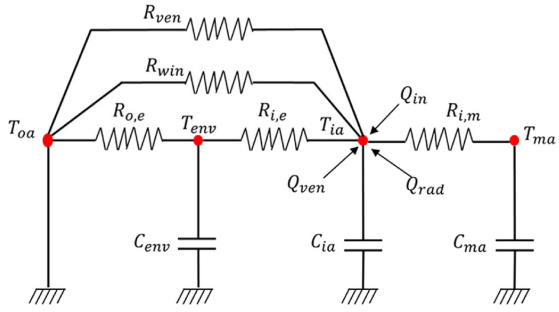

Fig. 5. Schematic of the simplified-lumped-capacity building model.

$$R_i = \frac{d}{2 \cdot \lambda_i} \cdot ln \frac{D}{d} \tag{36}$$

$$R_g = \frac{d}{2 \cdot \lambda} \cdot ln \frac{4 \cdot h}{D} \tag{37}$$

$$R_c = \frac{d}{2 \cdot \lambda} \cdot ln \left(\frac{2 \cdot h}{s} \right) \left(\frac{2 \cdot h}{s} \right) \left(\left(\frac{2 \cdot h}{s} \right)^2 + 1 \right)^{0.5} \tag{38}$$

$$\Delta T_{pip,sup} = T_{pip,sup} - T_{grou} \tag{39}$$

$$\Delta T_{pip,ret} = T_{pip,ret} - T_{grou} \tag{40}$$

where D is the outer insulation diameter, h is the distance between the pipe centres and the ground surface, s is the distance between pipe centres, and λ and λ_i are the heat conductivity for the ground and insulation. In addition, T_{grou} is the ground temperature, which was obtained from Equations (41)–(43). $T_{pip,sup}$ and $T_{pip,ret}$ are the water temperature in the supply pipe and the return pipe, respectively.

2.3.4. Model for the ground

In this study, the WTTES model and pipelines model used the ground temperature to calculate the heat losses. Equations (41)–(43) were applied to estimate the ground temperature as follows [45]:

$$T_{grou}(z,t) = T_{oa,aver} - T_{peak} \cdot e^{-z \cdot \sqrt{\frac{\omega}{2 \cdot \alpha}}} \cdot cos\left(\omega \cdot t - \phi - z \cdot \sqrt{\frac{\omega}{2 \cdot \alpha}} \right) \tag{41}$$

$$\omega = \frac{2 \cdot \pi}{T_{peri}} \tag{42}$$

$$\alpha = \frac{k}{\rho \cdot C} \tag{43}$$

where $T_{grou}(z,t)$ is the ground temperature in the depth z and at time t. $T_{oa,aver}$ is the annual average temperature of the outdoor air. T_{peak} is the peak deviation of the function from zero. ω is the angular frequency, T_{peri} is the period of the temperature cycle, and ϕ is the phase. α, k, ρ, and C are the thermal diffusivity, thermal conductivity, density, and heat capacity of the ground, respectively.

2.4. Indicators to evaluate the economic performance

In this section, the economic indicators including the initial investment cost and the payback period are introduced to evaluate the economic performance of the heat prosumers with TESs. The initial investment cost required for the WTTES depends strongly on the storage size. Fig. 6 illustrates the relationship between the initial investment cost and the size of WTTESs that with storage volumes larger than 200 m^3. The black dots in Fig. 6 present previous projects [52]. Fig. 6 shows that a power function approximates the relationship very well, with a coefficient of determination (R^2) of 0.99 and without obvious overfitting. In this study, the power function in Equation (44) was used to estimate the initial investment cost for large scale WTTESs in DH systems.

$$Invt = 0.0047 \cdot V^{0.6218} \tag{44}$$

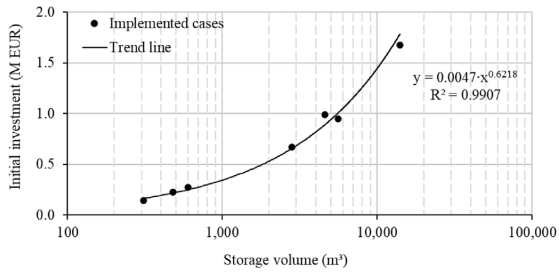

Fig. 6. The initial investment cost for WTTES.

where $Invt$ is the initial investment cost and V is the storage volume of WTTES.

The payback period is the time taken to fully recover the initial investment cost. It is one of the most commonly used methods for evaluating the economic performance of a system [47]. The payback period, PB, was calculated by using Equation (45):

$$B_{sav} \cdot \frac{(1+i)^{PB} - 1}{i \cdot (1+i)^{PB}} - Invt = 0 \tag{45}$$

where B_{sav} is the annual energy bill saving and i is the prevailing interest rate.

3. Case study

The proposed method in Section 2 was tested on a campus DH system in Norway. The background of the case study, research scenarios, and simulation settings are introduced below.

3.1. Background for the case study

A campus DH system in Trondheim, Norway, was chosen as the case study. As illustrated in Fig. 7, the campus DH system is a prosumer with DHS and heat users. The DHS is the university DC, which recovers the condensing waste heat from its cooling system. The heat users are buildings at the campus with a total building area of 300,000 m^2. The campus DH system is connected to the central DH system via the MS. Detailed information on the campus DH system can be found in Refs. [48,49]. According to the measurements from June 2017 to May 2018, the total heat supply for the campus DH system was 32.8 GWh. About 80% of the heat supply comes from the central DH system through the MS. The other 20% comes from the waste heat recovery from the DC.

Fig. 8 plots the heat demand for buildings and waste heat from the DC for the year 2017–2018. As shown with the green line in Fig. 8, the waste heat supply from the DC was around 1.0 MW throughout the year. However, as shown with the black line in Fig. 8, the building heat demand fluctuated from 0.2 MW to 13.8 MW. The mismatch between the waste heat supply and the building heat demand resulted in the surplus waste heat supply, especially for the period between June to October, as shown with the red line of Fig. 8. This surplus waste heat supply was fed into the central DH system via the MS. However, the university got no economic benefit from this surplus waste heat fed in, because as introduced in Section 1, the current heating price models do not support the reverse heat supply from the end-users to the central DH system.

In addition, the building heat demand was not equally distributed and there were high peak loads during the period from

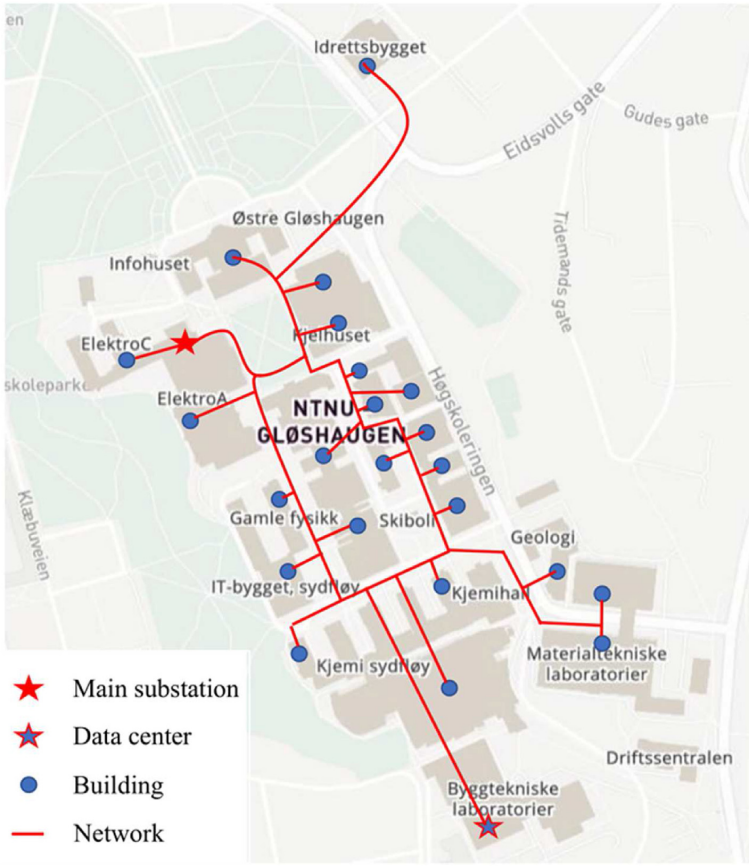

Fig. 7. Campus district heating system.

November to March, as shown with the black line of Fig. 8. The local DH company charged the heating bill also considering the peak load and the university paid about 5.3 million NOK[1] for the peak load each year, which accounted for 26% of the total heating bill.

3.2. Scenarios and simulation settings

To explore the economic feasibility after introducing a WTTES to the prosumer, different research scenarios were proposed based on the storage capacity of WTTES. The storage capacity meant the maximum discharging time for a WTTES under the discharging heat flow rate equals buildings' annual average heat demand. Eight scenarios including the reference scenario were proposed as listed in Table 1. The reference scenario, *Ref*, represented the current campus DH system without any TES. The other scenarios represented the WTTES solutions with storage capacities ranging from three hours to one week. The WTTESs were cylinder-shaped. All the tanks had the same height of 15 m, while the diameters were modified to provide certain storage capacities.

This research was conducted through three steps. Firstly, WTTESs with different storage capacities were integrated into the prosumer's campus DH system, respectively, as introduced in Section 2.2. Secondly, the optimal operation trajectories for the prosumer's campus DH system with the different storage capacities were obtained through the method provided in Section 2.3. Finally, these operation trajectories were evaluated in terms of economic indicators explained in Section 2.4. This study was based on the conditions of the year 2017–2018, and the detailed settings for the simulations are explained as follows. The used buildings' heat demand and the DC's waste heat came from the measured data as shown in Fig. 8. The key parameter settings are presented in Table A 1 in Appendix A. Among them, the parameters for the WTTES model were set according to the research [50], and the parameters of the pipeline model were set based on the book [44]. In addition, the heating prices were obtained from the website of the local DH company [51]. The local DH company used the monthly EDC heating price as shown in Fig. A 1 in Appendix A. Meanwhile, the used LDC heating price was 33 NOK/kW/month. Measured air temperature and estimated ground temperature of the simulation year are presented in Fig. A 2 in Appendix A.

4. Results

This section firstly presents the model validation results and

[1] The currency rate between NOK and EUR can be found from https://www.xe.com/, in this study 1 EUR = 10 NOK.

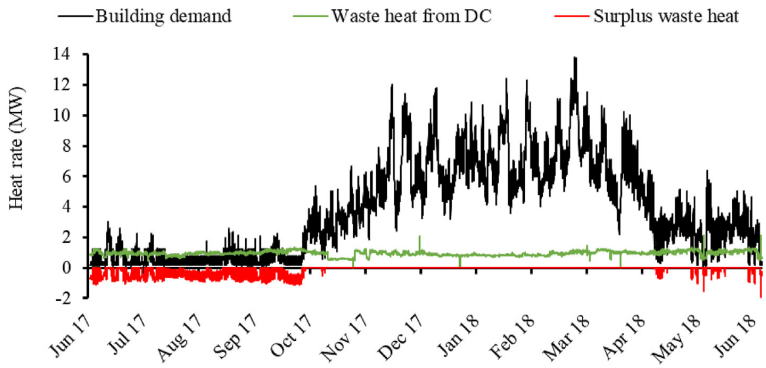

Fig. 8. Heat demand and waste heat supply.

Table 1
Information for the scenarios.

Scenario abbreviation	Storage capacity (hour)	Storage volume (m^3)	Tank diameter (m)
Ref	N/A	N/A	N/A
3 h	3	200	4.1
6 h	6	400	5.8
12 h	12	900	8.7
1 d	24	1700	12.0
3 d	72	5200	21.0
5 d	120	8600	27.0
7 d	168	12,000	31.9

then evaluates the proposed scenarios in terms of energy and economic analyses.

4.1. Model validation

As introduced in Section 2.3, the system model includes the following components: the WTTES, the building, and pipelines. In this study, the current campus DH system does not have any WTTES, and there is no measured data for the heat loss from the pipelines as well. Therefore, the WTTES and the pipeline model were validated according to the reference values from technical reports and textbooks instead of measured data. In a report from the International Energy Agency on large scale TESs [52], the reference storage efficiency for a WTTES is 50–90%. In this study, the corresponding value was about 90%, which was within the reference range. In practice, the low storage efficiency is caused by moistened insulation, because these WTTESs' envelopes are often deficient to protect against moisture penetration. However, it was assumed that the WTTES's envelope had a good quality to protect moisture penetration. Therefore, the WTTES used in this research had high storage efficiency.

According to the textbook *District Heating and Cooling* [44], for the DH systems in high heat density areas, the reference values for pipeline heat loss is 5–8% of the total heat supply. In this study, the corresponding value was close to 5%. This low pipeline heat loss was caused by two reasons. Firstly, compared to the typical DH systems with linear heat densities lower than 20 MWh/(m·a), the studied campus DH system had a higher linear heat density of 22 MWh/(m·a). The higher linear heat density made it more efficient during the distribution process and hence led to less pipeline heat loss. Secondly, the studied campus DH system had an annual average supply temperature of 65 °C that was lower than the typical DH system with 70–80 °C. Therefore, the low-temperature difference between the pipelines and the ground led to low pipeline heat loss.

The building model proposed in Section 2.3.2 was validated against the measured data. To quantify the deviation of the simulated data from the measured data, two indicators, i.e. coefficient of variation of the root mean square error (CV(RMSE)) and normalized mean bias error (NMBE), were used to evaluate the prediction performance of building model according to ASHRAE Guideline 14–2014 [53]. The validation criteria required in ASHRAE Guideline 14–2014 is within ±30% for CV(RMSE) and within ±10% for NMBE when using hourly data [53]. Fig. 9 shows the hourly simulated and measured building heat demand. As shown in Fig. 9, the values of the two indicators satisfied the requirements. In addition, Fig. 9 shows that the simulated building heat demand captured the trend in the measured data very well, with coefficients of determination (R^2) higher than 0.9 and no obvious overfitting.

4.2. Peak load shaving and heat use saving

The heat load duration diagram for the proposed scenarios is illustrated in Fig. 10, and the corresponding peak load is presented in Fig. 11. As shown in Fig. 10, compared to the reference scenario, *Ref*, part of the heat load for the scenarios with WTTES was shifted from the peak hours (the area highlighted with red colour) to the non-peak hours (the area highlighted with green colour). This load shifting contributed to the peak load shaving effect. As shown in Fig. 11, all the scenarios with WTTES had a lower peak load compared to the reference scenario. Furthermore, the load shifting effect was more significant for the scenarios with the larger WTTES. The maximal peak load shaving effect was achieved by scenario *7 d*, which had the largest WTTES. The peak load was shaved from 10.8 MW to 6.6 MW, a reduction of 39%. In contrast, the scenario with the smallest WTTES, *3 h*, had minimal peak load shaving, a reduction of only 4%.

Fig. 12 presents the annual heat use for the proposed scenarios. As introduced in Section 2.3, the prosumer's heat use means the heat supply from the central DH system via the MS. As shown in Fig. 12, the scenarios with the medium size WTTES (*3h*, *6 h*, *12 h*, and *1 d*) had minimal heat use, about 26.1 GWh, a heat use saving of 0.4 GWh compared to the reference scenario, *Ref*. However, the scenarios with the larger WTTES (*3 d*, *5 d* and *7 d*) had more heat use and hence less heat use saving. These results may be explained by Fig. 13. As shown by the columns filled with the orange colour in Fig. 13, the larger WTTES showed better performance on the

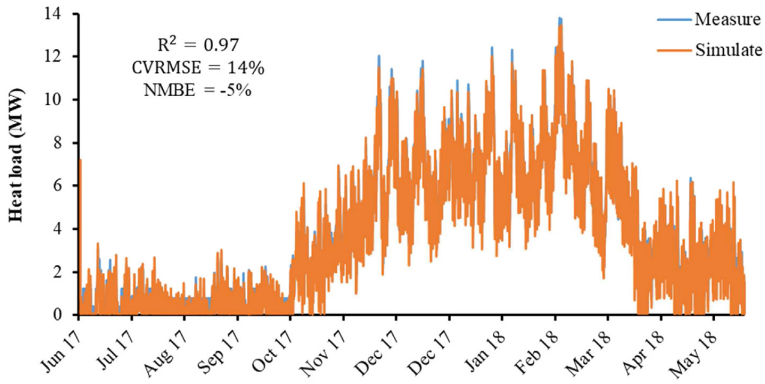

Fig. 9. Comparison between the simulated and measured building heat demand.

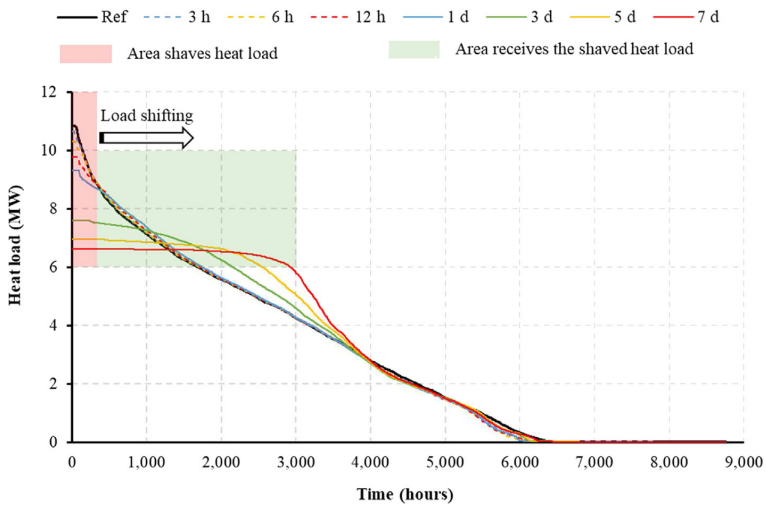

Fig. 10. Heat load duration diagram for the proposed scenarios.

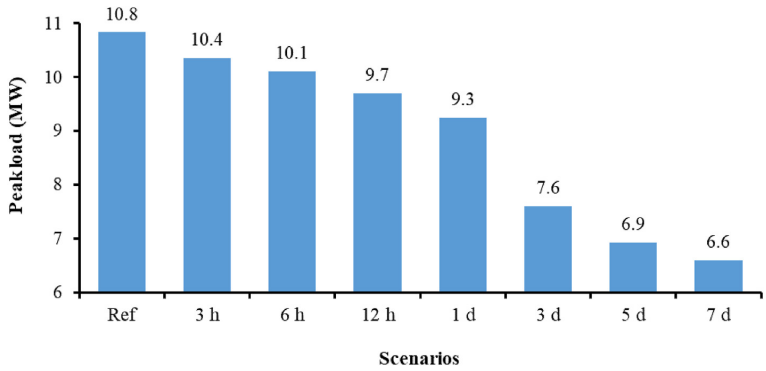

Fig. 11. Peak load for the proposed scenarios.

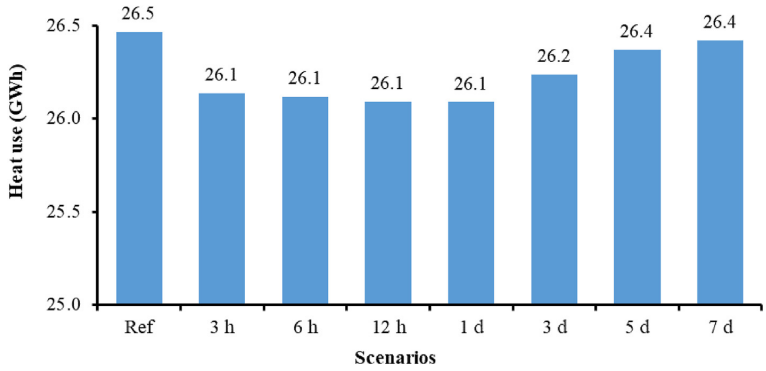

Fig. 12. Annual heat use for the proposed scenarios.

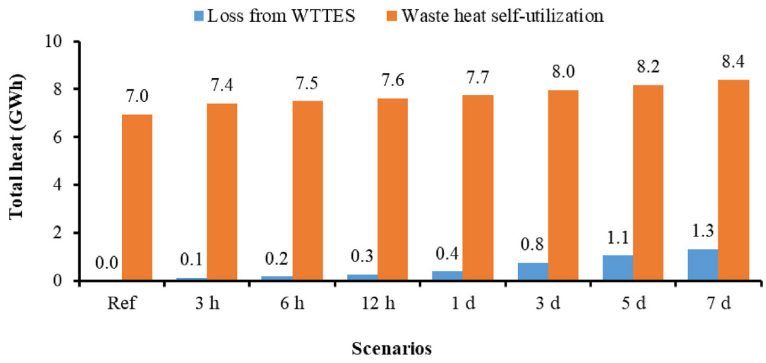

Fig. 13. Annual WTTES's heat loss and DC's waste heat self-utilization for the proposed scenarios.

mismatch relieving, and the waste heat self-utilization rate was increased from 79% to 96% (7.0 GWh to 8.4 GWh). However, the larger WTTES had higher heat loss to the environment as the columns filled with the blue colour in Fig. 13, because of its larger heat transfer area. The overall heat use saving performance of the WTTES depended on the sum of the above two effects. For the smaller WTTES, the mismatch relieving effect dominated the overall heat use performance. In contrast, for the larger WTTES, the heat loss effect dominated the overall heat use performance. Consequently, in this study, the WTTESs with three hours' to one day's storage capacity were the optimized storage size in terms of heat use saving.

4.3. Heating cost saving and payback period

The annual heating cost for the proposed scenarios is presented in Fig. 14 and the corresponding heating cost saving is shown in Fig. 15. Please note that all the currency in this section is presented in NOK. Two phenomena could be observed through Figs. 14 and 15: 1) the heating cost saving mainly came from the LDC, and 2) the larger WTTES brought more significant heating cost saving. As shown in Fig. 14, the annual EDC heating cost for the proposed scenarios was 15.4±0.1 million NOK, and the difference among these scenarios was less than 1%. In contrast, the annual LDC heating cost ranged from 4.7 million NOK to 2.8 million NOK with the increasing storage capacity of the WTTES, meaning a maximum difference of 39%. This significant reduction in the LDC contributed to the total heating cost saving. As shown in Fig. 15, as increasing the storage capacity of the WTTES, the annual heating cost saving increased from 0.4 million NOK to 1.9 million NOK, meaning a saving of 2%–9%. In this study, despite the waste heat self-utilization rate was increased up to 96%, as explained in Section 4.2, the relieving mismatch problem played a limited role in heating cost saving due to the original high waste heat self-utilization rate of 79%. However, for other cases with lower waste heat self-utilization rates, the relieving mismatch problem may contribute more to heating cost savings.

Fig. 16 presents the payback periods for the scenarios with the WTTES. It can be seen that the payback periods ranged from four years to ten years with the increasing WTTES storage size. Although the scenario with the largest WTTES needed the longest payback period, it achieved the highest heating cost saving. In contrast, the scenario with the smallest WTTES saved the lowest heating cost, while its payback period was the shortest. Therefore, the prosumer should make a trade-off between the payback period and the heating cost saving based on its own economic situation.

5. Discussion

This section first discusses the impacts of peak load definition on prosumers' economic performance. Afterwards, the thermoclines of the WTTESs during the charging and discharging processes are investigated.

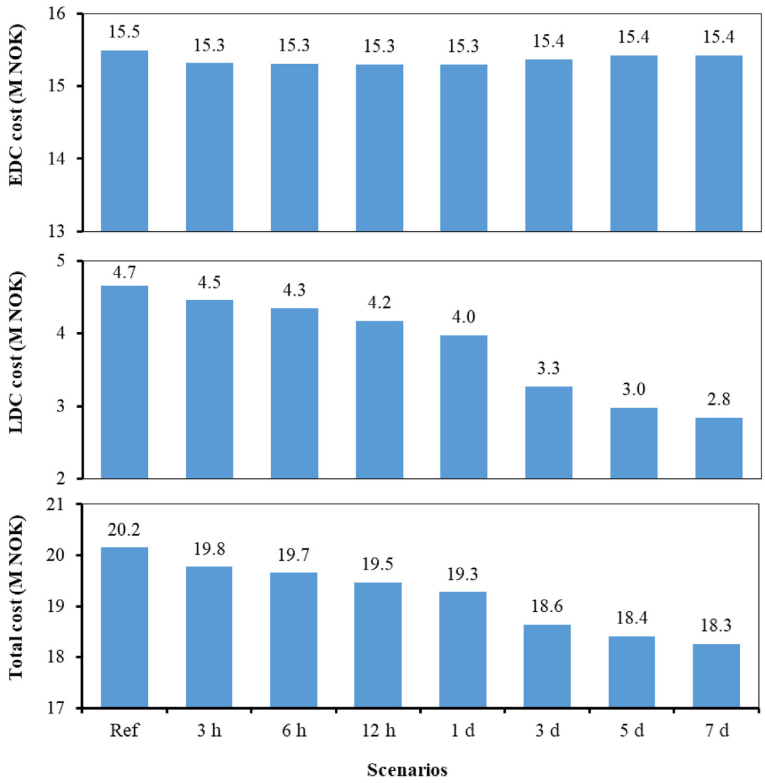

Fig. 14. Annual heating cost for the proposed scenarios.

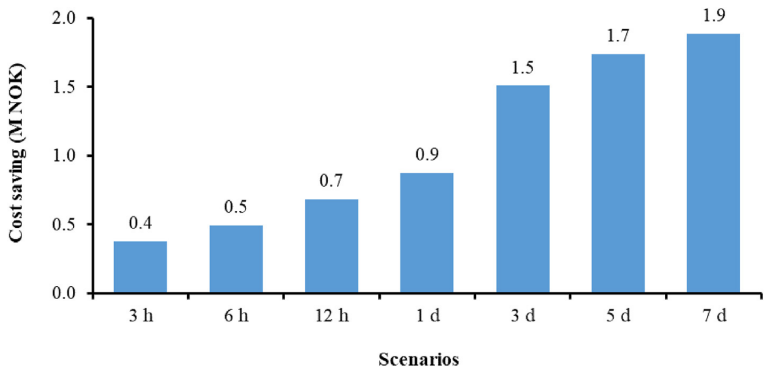

Fig. 15. Annual heating cost saving for the proposed scenarios.

5.1. Impacts of peak load definition

Based on a survey of heating contracts, methods of defining the peak load may be divided into two categories: hourly method and daily method [54]. For the hourly method, the peak load was the maximum hourly heat use, while the daily method was the maximum daily heat use. For this case study, the total heating cost saving was mainly determined by the reduction in LDC as observed in Section 4.3, which was linked to the peak load. Therefore, the way of defining the peak load may have a significant impact on the economic performance of prosumers with WTTESs. The results presented in Section 4 are based on the hourly method and this section presents further results based on the daily method.

The peak load under the daily method for the proposed scenarios is illustrated in Fig. 17, and the corresponding heating cost saving and the payback period are presented in Fig. 18 and Fig. 19,

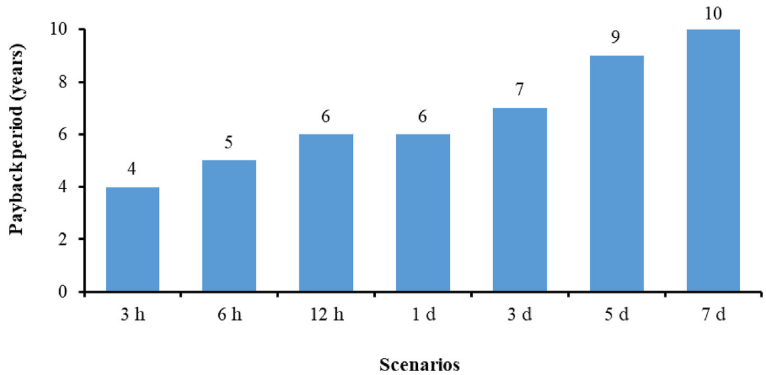

Fig. 16. The payback period for the scenarios with WTTES.

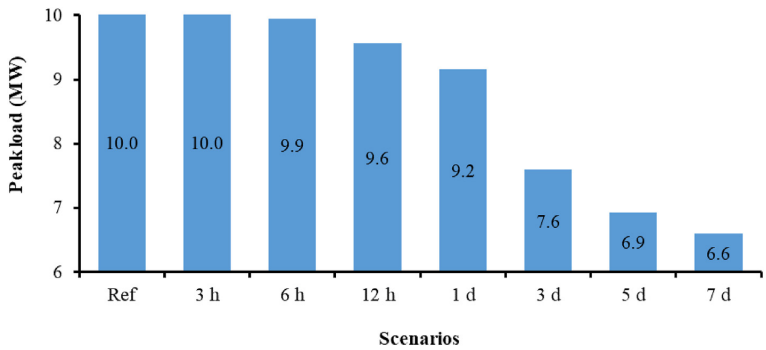

Fig. 17. Peak load for the proposed scenarios under the daily method.

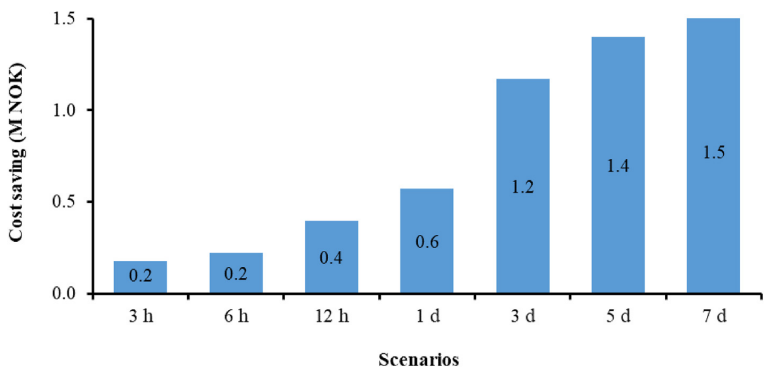

Fig. 18. Heating cost saving for the proposed scenarios under the daily method.

respectively. Similar to the hourly method, the larger WTTES brought a higher peak load shaving effect under the daily method as presented in Fig. 17. The peak load shaving increased from 0.1 MW to 3.4 MW as the increasing storage capacity of the WTTES from six hours to one week. However, compared to the hourly method, the peak load shaving effect under the daily method was different in two aspects: 1) it was less significant, and 2) it was not observed for the scenarios with the small WTTES. As shown in Fig. 17, the maximal peak load shaving effect was 3.4 MW, which was 19% less compared to the hourly method. Moreover, no peak load shaving effect was observed for the scenarios with the storage capacity smaller than six hours, their peak loads equalled that of the reference scenario, *Ref*, with the same value of 10.0 MW. The smaller WTTESs had a limited peak load shifting effect and was only capable to shift the heat load at the hourly level instead of the daily level. Therefore, the daily heat load kept almost the same.

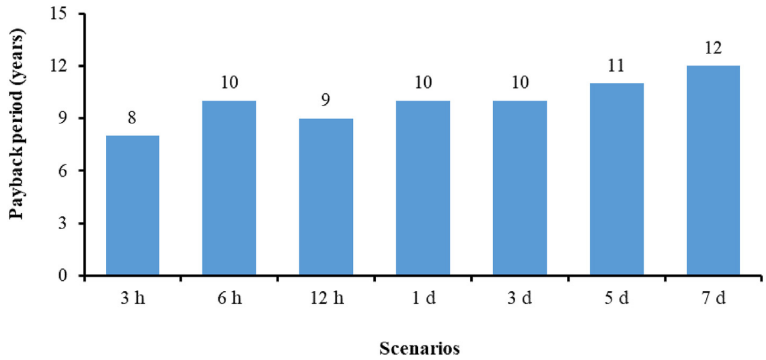

Fig. 19. The payback period for the proposed scenarios under the daily method.

The above impacts on the peak load shaving led to further impacts on the prosumer's economic performance. The prosumer obtained less heating cost saving under the daily method. As shown in Fig. 18, the heating cost saving ranged from 0.2 million NOK to 1.5 million NOK under the daily method, which was 18%–54% less compared to the hourly method. Furthermore, the payback period under the daily method ranged from 8 years to 12 years, and it was longer than the hourly method, especially for the WTTESs with smaller storage volumes.

Some recommendations from the discussion on the peak load definition are given as follows. Firstly, for the heat prosumers, special attention should be paid to the effect of the peak load definition. It may bring economic risk due to the changing of the heating contract. For example, DH companies may change their methods of defining the peak load from the hourly method to the daily method, and hence the economic benefit on heating cost saving may be drastically reduced and the payback period for TESs may be significantly prolonged. Secondly, for DH companies, it is better to use the hourly method to define the peak load, because the heat prosumers would be more motivated to introduce TESs and participate in user-side heat load management. One vital advantage brought by the user-side heat load management is peak load shaving, which may bring significant economic and technical benefits for DH companies.

5.2. Thermocline of the WTTES

In a WTTES, a thermocline is a layer where the water temperature changes more dramatically with depth than in the layers above and below it. It separates the lower density hot water at the top of the tank from the higher density cold water at the bottom of the tank. Generally, the thermocline should be as thin as possible to obtain a better thermal stratification and a less mixing effect between the hot and cold water [55]. Moreover, the position of the thermocline should be adjusted as the result of the optimized charging and discharging processes. Research showed that an optimal thermocline condition guaranteed high performance of the WTTES. For example, according to a study, the storage efficiency may be improved by 6% by optimizing the charging and discharging processes that led to an optimal thermocline condition [56]. Similar results were obtained in this study, which highlighted the importance of the thermocline of the WTTES. To assist the analysis of thermocline, the variable dimensionless temperature was used. As calculated by Equation (46), the water temperature of an individual layer in the WTTES was scaled into a real number ranging from 0 to 1. The two extreme values, 0 and 1, indicated the lowest and highest water temperature among all the layers in the WTTES. In a figure that illustrates the distribution of dimensionless temperature of layers in a WTTES, the thermocline can be identified as the layer that has significantly higher dimensionless temperature gaps between the layers above and below it.

$$T_{i,nonD} = \frac{T_i - T_{i,min}}{T_{i,max} - T_{i,min}} \tag{46}$$

where $T_{i,nonD}$ is the dimensionless water temperature of the Layer i. T_i is the water temperature of the Layer i. $T_{i,max}$ and $T_{i,min}$ are the highest and lowest water temperatures among all the layers in the WTTES.

Fig. 20 gives an example that illustrates an optimal thermocline condition of the WTTES, in which the plotted data were collected from Scenario *5 d* from February 06 to March 02 of 2018. As shown in Fig. 20 (c), the original heat load ranged from 4 MW to 14 MW during the presented period. However, after the load shifting by the WTTES, the heat load was almost constant at around 7 MW. To achieve this flattened heat load, the WTTES adjusted its operation strategies based on the heat load conditions and the whole period was divided into four subperiods. From February 06 to February 18, the WTTES might work for peak load shaving or valley filling depending on the heat load condition. However, as shown in Fig. 20 (a), the charging process dominated the period, which featured a rising water temperature in the tank. In addition, as illustrated in Fig. 20 (b), a thermocline was gradually formulated and enhanced around Layer 2, which was indicated by increasing dimensionless temperature gaps between the layers above and below it. Moreover, the position of the thermocline was at the lower side of the tank, therefore, more space was available to store the hot water above it. From February 18 to February 21, the WTTES serviced for peak load shaving, as shown in Fig. 20 (c). This period demanded a continually discharging process, and thus the water temperature in the tank was decreased as observed in Fig. 20 (a). Moreover, opposite to the charging dominated process in the previous period, the thermocline attenuated with reducing dimensionless temperature gaps, as observed in Fig. 20 (b). The following two periods, from February 21 to February 25 and from February 25 to March 02, repeated the above two periods with a charging dominated process and a discharging dominated process, which was characterised by an enhanced and attenuated thermocline, respectively.

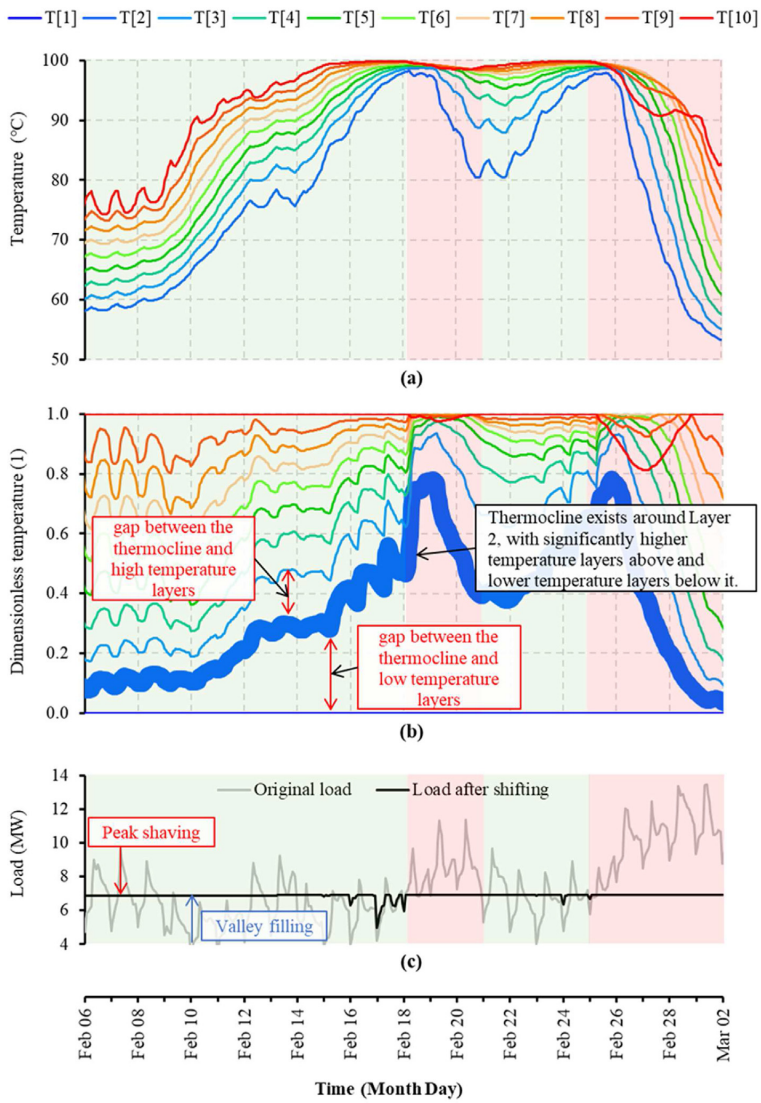

Fig. 20. An example of the charging and discharging processes of the WTTES, T [10] to T [1] refers to the water temperature from the top layer to the bottom layer, (a) temperature, (b) dimensionless temperature, and (c) heat load.

Some recommendations from the investigation of the thermocline of the WTTES are summarized as follows. Firstly, thermocline can be used as an effective indicator to understand the conditions and forecast the performance of WTTESs. Secondly, both the thickness and position are important to evaluate the conditions of the thermocline.

6. Conclusions

This study aimed to optimize prosumers' economic performance under the current unidirectional heating price models by using short-term TESs. A WTTES was chosen as the short-term TES and integrated into the prosumer. A dynamic optimization problem was formulated to explore the economic potential of the prosumer with TES. The size parameters of the TESs were swept to obtain the optimal storage size considering the trade-off between the payback period and the heating cost saving. The proposed method was tested on a campus DH system in Trondheim, Norway.

Results showed that by introducing the WTTES into the heat prosumer, the peak load was shaved by up to 39%, and the waste heat self-utilization rate was increased from 79% to 96%. These significantly improved the economic performance of the heat prosumer during the transformation period of the DH system. The annual heating cost was saved up to 1.9 million NOK, a saving of 9%, meanwhile, the initial investment of the WTTES was able to be fully recovered in less than ten years.

In addition, the effects of the peak load definition on the economic performance of the heat prosumers were discussed. It was found that the prosumers' economic performance was much better when using the hourly method to define the peak load instead of the daily method. Therefore, it was recommended that prosumers should consider the potential economic risk of introducing WTTES when the daily method is used in the heating contract. Moreover, research results highlighted the importance of the thermocline and showed that an optimal thermocline condition can lead to the high performance of the WTTES.

This study may provide guidelines on improving the heat prosumers' economic performance during the transformation period of the DH system, and hence promote the development of prosumers in DH systems.

Declaration of competing interest

The authors declare that they have no known competing financial interests or personal relationships that could have appeared to influence the work reported in this paper.

Acknowledgement

The authors gratefully acknowledge the support from the Research Council of Norway through the research project understanding behaviour of district heating systems integrating distributed sources under the FRIPRO/FRINATEK program (project number 262707) and the innovation project low-temperature thermal grids with surplus heat utilization under the EnergiX program (project number 280994).

Appendix A. Setting for the case study

Table A 1
Parameter setting for the simulation.

Category	Parameter	Value
WTTES and ground	U	1.2 W/(m^2·K)
	$T_{oa,aver}$	5.0 °C
	T_{peak}	4.5 °C
	T_{peri}	31,536,000 s
	k	2.7 W/(m·K)
	ρ	2800 kg/(m^3)
	C	840 J/(K·kg)
	ϕ	4.25 rad
Pipeline	L	1500 m
	d	0.273 m
	D	0.4 m
	h	1.2 m
	s	1.2 m
	λ	1.5 W/(m·K)
	λ_i	0.03 W/(m·K)
Buildings	C_{env}	45,000,000,000 J/K
	C_{ia}	1,300,000,000 J/K
	C_{ma}	2,900,000,000 J/K
	$R_{i,e}$	1.18 (m^2·K)/W
	$R_{o,e}$	1.03 (m^2·K)/W
	$R_{i,m}$	0.35 (m^2·K)/W
	R_{win}	0.48 (m^2·K)/W
	$\dot{Q}_{sen}$	0-8,000,000 W
	$\dot{Q}_{in}$	0-4,500,000 W
	$\dot{Q}_{DHW}$	0-1,200,000 W

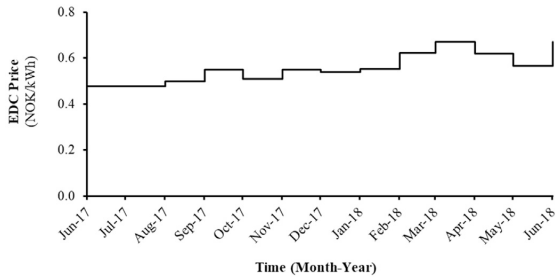

Fig. A 1. The EDC heating price [51]

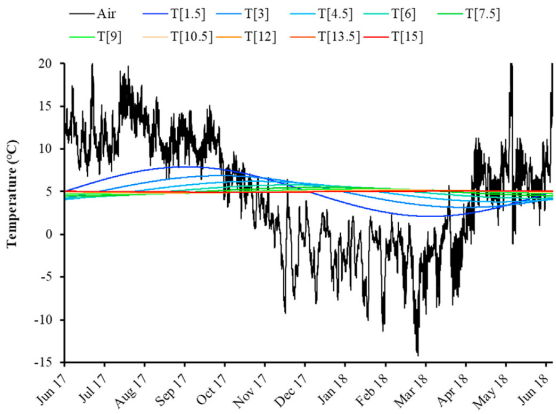

Fig. A 2. Measured air temperature and estimated ground temperature of the simulation year, T [15] to T[1.5] refers to the ground temperature from the 15 m depth to 1.5 m depth

Author statement

Haoran Li: Conceptualization, Methodology, Software, Validation, Writing – original draft Juan Hou: Conceptualization, Methodology, Writing – original draft Zhiyong Tian: Writing – review & editing Tianzhen Hong: Conceptualization, Writing – review & editing Natasa Nord: Conceptualization, Writing – review & editing, Supervision Daniel Rohde: Software, Writing – review & editing

References

[1] In focus: Energy efficiency in buildings, https://ec.europa.eu/info/news/focus-energy-efficiency-buildings-2020-feb-17en#:∼:text=Collectively%2C%20buildings%20in%20the%20EU,%2C%20usage%2C%20renovation%20and%20demolition, accessed September 2020.
[2] Heating and cooling, https://ec.europa.eu/energy/topics/energy-efficiency/heating-and-cooling_en?redir=1, accessed September 2020.
[3] Mapping and analyses of the current and future (2020-2030) heating/cooling fuel deployment (fossil/renewables), https://ec.europa.eu/energy/studies/mapping-and-analyses-current-and-future-2020-2030-heatingcooling-fuel-deployment_en, accessed September 2020.
[4] Li H, Nord N. Transition to the 4th generation district heating - possibilities,

bottlenecks, and challenges. Energy Procedia 2018;149:483–98.
[5] Sayegh MA, Danielewicz J, Nannou T, Miniewicz M, Jadwiszczak P, Piekarska K, et al. Trends of European research and development in district heating technologies. Renew Sustain Energy Rev 2017;68:1183–92.
[6] Åberg M, Fälting L, Lingfors D, Nilsson AM, Forssell A. Do ground source heat pumps challenge the dominant position of district heating in the Swedish heating market? J Clean Prod 2020;254:120070.
[7] Connolly D, Lund H, Mathiesen BV, Werner S, Möller B, Persson U, et al. Heat Roadmap Europe: combining district heating with heat savings to decarbonise the EU energy system. Energy Pol 2014;65:475–89.
[8] Werner S. International review of district heating and cooling. Energy 2017;137:617–31.
[9] Buffa S, Cozzini M, D'Antoni M, Baratieri M, Fedrizzi R. 5th generation district heating and cooling systems: a review of existing cases in Europe. Renew Sustain Energy Rev 2019;104:504–22.
[10] Christian Holmstedt Hansen OG, Hanne Kortegaard Støchkel, Detlefsen Nina. The competitiveness of district heating compared to individual heating. 2018.
[11] Dalla Rosa A, Li H, Svendsen S, Werner S, Persson U, Ruehling K, et al. IEA DHC Annex X report:Toward 4th generation district heating. Experience and Potential of Low-Temperature District Heating; 2014.
[12] Persson U, Werner S. Heat distribution and the future competitiveness of district heating. Appl Energy 2011;88(3):568–76.
[13] Nord N, Shakerin M, Tereshchenko T, Verda V, Borchiellini R. Data informed physical models for district heating grids with distributed heat sources to understand thermal and hydraulic aspects. Energy 2021;222:119965.
[14] Lickleder T, Hamacher T, Kramer M, Perić VS. Thermohydraulic model of Smart Thermal Grids with bidirectional power flow between prosumers. Energy 2021;230:120825.
[15] Marguerite C, Schmidt R-R, Pardo Garcia N. Concept development of an industrial waste heat based micro DH network. Conference Concept development of an industrial waste heat based micro DH network. LESO-PB, EPFL, p. 597-602.
[16] Pipiciello M, Caldera M, Cozzini M, Ancona MA, Melino F, Di Pietra B. Experimental characterization of a prototype of bidirectional substation for district heating with thermal prosumers. Energy 2021;223:120036.
[17] Nielsen S, Möller B. Excess heat production of future net zero energy buildings within district heating areas in Denmark. Energy 2012;48(1):23–31.
[18] Brand L, Calvén A, Englund J, Landersjö H, Lauenburg P. Smart district heating networks – a simulation study of prosumers' impact on technical parameters in distribution networks. Appl Energy 2014;129:39–48.
[19] Gross M, Karbasi B, Reiners T, Altieri L, Wagner H-J, Bertsch V. Implementing prosumers into heating networks. Energy 2021;230:120844.
[20] Huang P, Copertaro B, Zhang X, Shen J, Löfgren I, Rönnelid M, et al. A review of data centers as prosumers in district energy systems: renewable energy integration and waste heat reuse for district heating. Appl Energy 2020;258:114109.
[21] Kauko H, Kvalsvik KH, Rohde D, Nord N, Utne Å. Dynamic modeling of local district heating grids with prosumers: a case study for Norway. Energy 2018;151:261–71.
[22] Song J, Wallin F, Li H. District heating cost fluctuation caused by price model shift. Appl Energy 2017;194:715–24.
[23] Tian Z, Perers B, Furbo S, Fan J. Thermo-economic optimization of a hybrid solar district heating plant with flat plate collectors and parabolic trough collectors in series. Energy Convers Manag 2018;165:92–101.
[24] Shah SK, Aye L, Rismanchi B. Seasonal thermal energy storage system for cold climate zones: a review of recent developments. Renew Sustain Energy Rev 2018;97:38–49.
[25] Köfinger M, Schmidt RR, Basciotti D, Terreros O, Baldvinsson I, Mayrhofer J, et al. Simulation based evaluation of large scale waste heat utilization in urban district heating networks: optimized integration and operation of a seasonal storage. Energy 2018;159:1161–74.
[26] Rohde D, Andresen T, Nord N. Analysis of an integrated heating and cooling system for a building complex with focus on long–term thermal storage. Appl Therm Eng 2018;145:791–803.
[27] Rohde D, Knudsen BR, Andresen T, Nord N. Dynamic optimization of control setpoints for an integrated heating and cooling system with thermal energy storages. Energy 2020;193:116771.
[28] Verrilli F, Srinivasan S, Gambino G, Canelli M, Himanka M, Del Vecchio C, et al. Model predictive control-based optimal operations of district heating system with thermal energy storage and flexible loads. IEEE Trans Autom Sci Eng 2017;14(2):547–57.
[29] Verda V, Colella F. Primary energy savings through thermal storage in district heating networks. Energy 2011;36(7):4278–86.
[30] Harris M. Thermal energy storage in Sweden and Denmark: potentials for technology transfer. IIIEE Master thesis; 2011.
[31] The Modelica Association, https://www.modelica.org/, accessed Jan 2021.
[32] Åkesson J, Gäfvert M, Tummescheit H. Jmodelica—an open source platform for optimization of modelica models. Conference Jmodelica—an open source platform for optimization of modelica models.
[33] Amrit R, Rawlings JB, Biegler LT. Optimizing process economics online using model predictive control. Comput Chem Eng 2013;58:334–43.
[34] Nocedal J, Wright S. Numerical optimization. Springer Science & Business Media; 2006.
[35] Sernhed K, Gåverud H, Sandgren A. Customer perspectives on district heating price models. International Journal of Sustainable Energy Planning and Management 2017;13:47–60.
[36] Song J, Wallin F, Li H, Karlsson B. Price models of district heating in Sweden. Energy Procedia 2016;88:100–5.
[37] Bott C, Dressel I, Bayer P. State-of-technology review of water-based closed seasonal thermal energy storage systems. Renew Sustain Energy Rev 2019;113:109241.
[38] Pinel P, Cruickshank CA, Beausoleil-Morrison I, Wills A. A review of available methods for seasonal storage of solar thermal energy in residential applications. Renew Sustain Energy Rev 2011;15(7):3341–59.
[39] Li H, Hou J, Hong T, Ding Y, Nord N. Energy, economic, and environmental analysis of integration of thermal energy storage into district heating systems using waste heat from data centres. Energy 2021;219:119582.
[40] Powell KM, Edgar TF. An adaptive-grid model for dynamic simulation of thermocline thermal energy storage systems. Energy Convers Manag 2013;76:865–73.
[41] Li H, Hou J, Nord N. Using thermal storages to solve the mismatch between waste heat feed-in and heat demand: a case study of a district heating system of a university campus. 2019.
[42] He P, Sun G, Wang F, Wu H, Wu X. Heating engineering (in Chinese). China Architecture & Building Press; 2009.
[43] CEN. CEN/TR16355 Recommendations for prevention of Legionella growth in installations inside buildings conveying water for human consumption. 2012.
[44] Frederiksen S, Werner S. District heating and cooling. Studentlitteratur Lund; 2013.
[45] Andújar Márquez JM, Martínez Bohórquez MÁ, Gómez Melgar S. Ground thermal diffusivity calculation by direct soil temperature measurement. Application to very low enthalpy geothermal energy systems. Sensors 2016;16(3):306.
[47] Jaluria Y. Design and optimization of thermal systems. CRC press; 2007.
[48] Nord N, Sandberg NH, Ngo H, Nesgård E, Woszczek A, Tereshchenko T, et al. Future energy pathways for a university campus considering possibilities for energy efficiency improvements. Conference Future energy pathways for a university campus considering possibilities for energy efficiency improvements, vol. vol. 352. IOP Publishing, p. 012037.
[49] Guan J, Nord N, Chen S. Energy planning of university campus building complex: energy usage and coincidental analysis of individual buildings with a case study. Energy Build 2016;124:99–111.
[50] Cruickshank CA. Evaluation of a stratified multi-tank thermal storage for solar heating applications. Doctoral thesis; 2009.
[51] Charging method for heating bill in Trondheim, https://www.statkraftvarme.no/globalassets/2-statkraft-varme/statkraft-varme-norge/om-statkraft-varme/prisark/20190901/fjernvarmetariff-trondheim-bt1.pdf, accessed September 2020.
[52] Mangold D, Deschaintre L. Task 45 Large Systems Seasonal thermal energy storage Report on state of the art and necessary further R+ D. International Energy Agency Solar Heating and Cooling Programme; 2015.
[53] ASHRAE. ASHRAE guideline 14–2014, measurement of energy, demand, and water savings. ASHRAE Atlanta; 2014.
[54] Larsson O. Pricing models in district heating. Master thesis; 2011.
[55] Li G. Sensible heat thermal storage energy and exergy performance evaluations. Renew Sustain Energy Rev 2016;53:897–923.
[56] Ghaddar NK. Stratified storage tank influence on performance of solar water heating system tested in Beirut. Renew Energy 1994;4(8):911–25.

PAPER 4

Li H, Hou J, Hong T, Nord N. Distinguish between the economic optimal and lowest distribution temperatures for heat-prosumer-based district heating systems with short-term thermal energy storage. Submitted to Journal of Energy (Status: Under review).

This paper is awaiting publication and is not included in NTNU Open

APPENDIX- PUBLICATIONS

PAPER 5

Li H, Nord N. Operation strategies to achieve low supply and return temperature in district heating system. E3S Web Conf. 2019;111:05022. The 13th REHVA World Congress CLIMA 2019.

APPENDIX- PUBLICATIONS

Operation strategies to achieve low supply and return temperature in district heating system

Haoran Li[1,*], and *Natasa* Nord[1]

[1]Department of Energy and Process Technology, Norwegian University of Science and Technology (NTNU), Kolbjørn Hejes vei 1 B, Trondheim 7491, Norway

Abstract: Low temperature is the most significant feature of the future district heating (DH) - the 4th generation district heating (4GDH). The revolutionary temperature level (50–55/25°C) will improve the efficiency of heat sources, thermal storages, and distribution systems, meanwhile, bring huge potentials to renewable energies. One challenge of transition to the future DH is the compatibility of current customer installations and the future temperature level. The aim of this study was to find the temperature potential of Norwegian residential buildings for the future DH system. A reference apartment was created, and typical space heating (SH) system was designed. A detailed building and SH system model were built in Modelica® language, and simulation was conducted via Dymola environment. Different operation strategies: PI control of the supply temperature, weather compensated control of the supply temperature, and PI control of the return temperature were tested. The results of the study showed the average supply temperature could be as low as 56~58°C, and only limited time the temperature was above 60 °C, when the controlled supply temperature strategies were applied. For the case with controlled return temperature strategies, the average return temperature were 30 and 37°C, while the average required supply temperature could be 72 and 94°C. The conclusion was that the low supply temperature could be achieved through optimized operation strategies. Whereas, the low return temperature was not able to be achieved only by improving the operation strategy.

1 Introduction

District heating (DH) is an energy service, which moves the heat from available heat sources to customers. The fundamental idea of DH is to use local fuel or heat resources, which would otherwise be wasted, to satisfy local customer heat demands, by using heat distribution networks [1].

In historical development of DH, the three generations of DH have been developed successively. The 1st generation DH system uses steam as heat carrier. Almost all DH systems established until 1930 use this technology. The 2nd generation DH system uses pressurized hot water as the heat carrier, with supply temperature mostly higher than 100°C. These systems emerge in the 1930s and dominate all new systems until the 1970s. The 3rd generation DH system still uses pressurized water as the heat carrier, but the supply temperatures are often below 100°C. The system is introduced in the 1970s and take a major share of all extensions in the 1980s and beyond [2].

The direction of DH development has been in favour of lower distribution temperatures [1]. In addition, low temperature is the most significant feature of the future DH - the 4th generation district heating (4GDH). The revolutionary temperature level (50-55/25°C) will improve the efficiency of heat source, thermal storage, and distribution system, meanwhile, bring huge potential to renewable energies [3].

One challenge of transition to the future DH is the compatibility between current customer installation and future temperature level. Older buildings will continue to make up large share of building stock for many years (for Denmark and Norway, the share will be about 85-90% [4] and 50% [5] in 2030, respectively). Those buildings are usually equipped with space heating (SH) systems designed with supply temperature around 70°C or higher, thereby reduction of supply temperature would be expected to cause discomfort for the occupants [6]. However, studies show houses from the 70s or 80s without any renovation are possible to be heated with supply temperature of 50°C most of the year, and only limited time the supply temperature has to be above 60°C. If original windows of the houses are replaced, it is possible to decrease the supply temperature to less than 60°C for almost the entire year [4, 7, 8].

The aim of this study was to find the temperature potential of residential apartment buildings for the future DH systems in Norway. Reference apartment was created, and typical space heating (SH) in the apartment was designed. Different operation strategies to achieve low supply and return temperature were tested. The results were used to analyse the possibilities and limitations of different control strategies.

* Corresponding author: haoranli@ntnu.no

2 Methodology

2.1 Reference apartment and weather data

2.1.1 Reference apartment

Statistical data for Norwegian apartments constructed in different periods is presented in Table 1. Requirement development for the U-values for building envelop based on the Norwegian building code (TEK) are displayed in Fig. 1.

Table 1. Statistical data for Norwegian apartments [9].

Construction period	Number of buildings	Share of percentage (%)
Before 1956	161554	27
1956~1970	106324	18
1971~1980	90441	15
1981~1990	56379	9
1991~2000	63820	11
2001~2010	115080	19

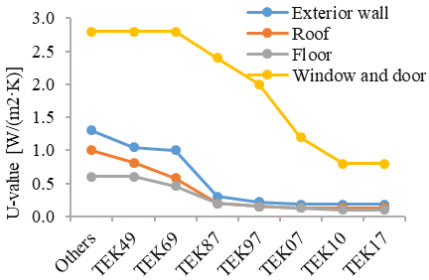

Fig. 1. Limit U-value of envelopes in developed Norwegian standards [9-11].

As Table 1 and Fig. 1 show, apartments built before 1990 account for about 70% of the total apartments, and the thermal requirement of envelopes during the years before 1990 show minor changes. Therefore, the apartment built around the years 1970s or 1980s can represent the thermal conditions of the majority of Norwegian apartments. In addition, the Norwegian building code TEK69 can be chosen as representative standard of the period.

The reference apartment was chosen from the middle floor of one building, there were five rooms: a living room, a children room, a bedroom, a bathroom, and a kitchen. The total floor area was about 70 m^2. The condition of the reference apartment was selected based on the statistics of Norway, about 46% of the dwellings have 4-6 rooms, and about 17% of the dwellings have the size of 60-79 m^2 [12]. Detailed information of the apartment is listed in Table 2, and the sketch of the apartment is shown in Fig. 2.

Only natural ventilation was considered, and the air exchange rate was 0.5 1/h, which is recommended 0.2~0.5 1/h in [9] and 0.5 1/h in the standard SN-CEN/TR 12831 [13]. The set indoor air temperature in the living room, the children room, the bedroom, and the kitchen was 20°C, which is the recommended value for category II in the standard EN 15251 [14]. For the bathroom, the set indoor air temperature value was 24°C, considering the higher thermal comfort requirement.

Table 2. Thermal conditions of the reference apartment.

Component	Value
Proportion of window and door area of heated use area (%)	15
U-value of exterior wall [W/(m^2/K)]	0.67
U-value of exterior window [W/(m^2/K)]	2.50
U-value of ceiling [W/(m^2/K)]	2.16
U-value of floor [W/(m^2/K)]	2.46
U-value of interior wall within apartment [W/(m^2/K)]	7.13
U-value of interior wall between apartment [W/(m^2/K)]	2.93
Thermal bridges [W/(m^2/K)]	Included in U-values

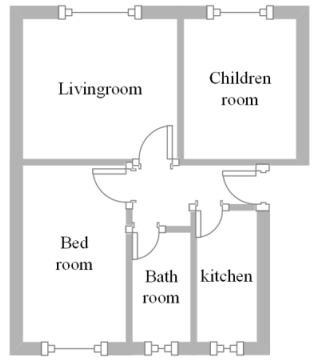

Fig. 2. Sketch map of the reference apartment.

The simulation result for the heat demand of the reference apartment was 121 kW·h/(m^2·year), which was close to 156 kW·h/(m^2·year) from a similar research [15].

2.1.2 Weather data

Test reference year (TRY) provides weather data for one year that characterize the local climatic conditions over a reasonably long period of time. TRY is widely adopted to get reliable simulation results [16]. The method to determine TRY is presented in ISO 15927-4 [17]. TRY for Trondheim, Norway was used in this study. The detail parameters for the air temperature, solar irradiance, and wind speed are shown in Fig. 3.

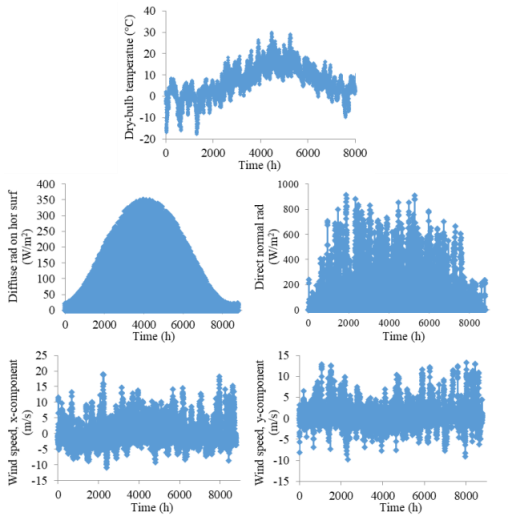

Fig. 3. TRY parameters of Trondheim, Norway.

2.2 Building and heating system model

2.2.1 Language and simulation environment

The model was built in Modelica® language [18], and the simulation was conducted via Dymola [19] environment. The components of the model were mainly from Modelica standard library [18], AixLib library [20], and Buildings library [21].

2.2.2 Apartment model

The apartment model was a high order model, which included all individual elements of envelopes and their spatial context. It could be used for in-depth analyses of building thermal behaviours. The overview of the apartment model is shown in Fig. 4.

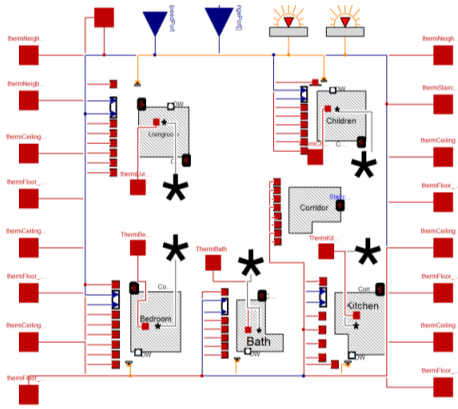

Fig. 4. Simplified overview of the building model.

For the submodule of each room, the following physical processes were considered: transient heat conduction through walls, steady-state heat conduction through glazing systems, radiation exchange between room facing elements. The detail information and evaluation work are presented in [22].

2.2.3 Radiator model

The radiator model is presented in Fig. 5. The calculation methods of convective and radiative heat transfer were described in [23, 24]. The calculation of water pressure loss was illustrated in [25].

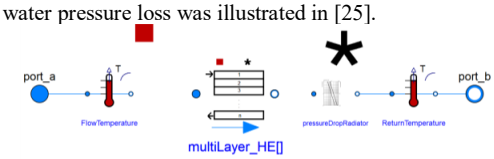

Fig. 5. Simplified overview of the radiator model.

The validation was conducted according to the standard EN 442-2 [26], and the simulation result was compared with the measured data from [27]. The results are presented in Fig. 6.

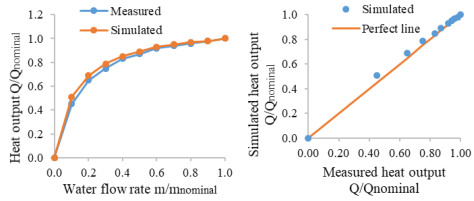

Fig. 6. Radiator heat output at different water flow rate at the operation condition 75/65/20°C.

2.2.4 Thermostatic valve model

The behaviour of thermostatic valve (TV) depends on the characteristic of TV as well as the overall system. Both of them should be taken into account to build the TV model [28]. According to the standard EN215 [29] and researches in [28, 30], the water flow rate through the TV depends on the difference between measured indoor air temperature and the closing temperature or opening temperature of TV. To simplify the control process, proportional integral (PI) controller is applied to approximate the performance of the TV in [31, 32]. The PI controller in the TV model is shown in Fig. 7.

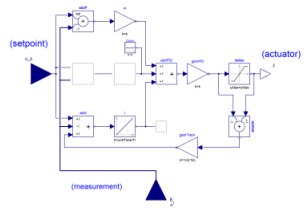

Fig. 7. Overview of the PI controller in TV model.

2.2.5 Space heating system model

The overview of the SH system is presented in Fig. 8. For each room one radiator was designed to satisfy the heat demand. Heat demand of each room during heating season and heat output of corresponding radiator at nominal condition are shown in Fig. 9. According to the standard SN-CEN/TR 12831 [13], the outdoor design temperature for heat load calculation is -12 °C, and the sizing of system is based on the calculated heat load. The room heat loads, nominal heat output of radiators, and system oversizing values are listed in Table 3. The oversizing values in this study agree with the median oversizing values from one investigation research, which is range from 15% to 25% [33] .

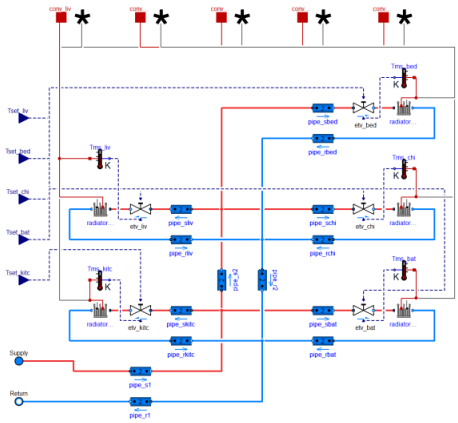

Fig. 8. Overview of the space heating system.

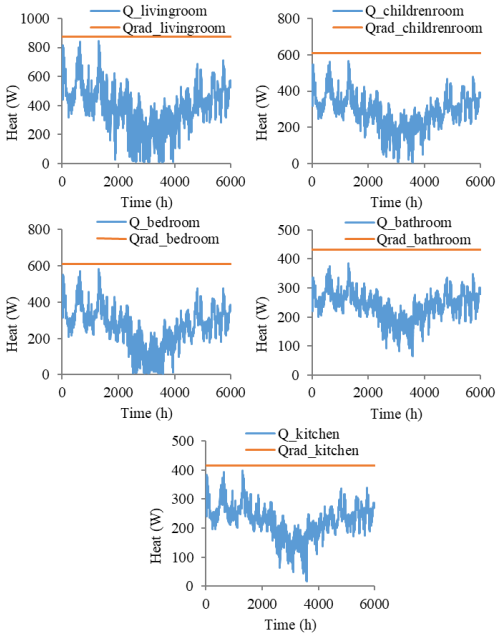

Fig. 9. Room heat demand during heating season and radiator heat output at nominal condition.

Table 3. Room heat load and Radiator design.

Room	Room heat load (W)	Radiator heat output (W)	Oversizing (%)
Living room	770	874	14
Children room	520	608	17
Bedroom	520	608	17
Bathroom	352	431	22
Kitchen	360	415	15

2.3 Scenarios

The considerations of different scenarios are listed as follows:

- The scenarios with low return temperature: Low supply and return temperature reduce the costs of heat generation and distribution. Some DH companies incentivize their customers through motivation tariffs to reduce their temperatures in exchange of discount in their energy bills. Researches show that low return temperature has higher economic benefits, and DH companies care more about low return temperature than low supply temperature [34].
- The scenarios with low supply temperature: In the future, more renewables will be integrated into DH system. Low supply temperature will increase output of solar energy, raise coefficient of performance for heat pumps, and increase the power to heat ratio of combined heat and power plans [3].
- The scenarios with minimum supply temperature: The favourable conditions for legionella proliferation ranging from 25 to 45°C [35]. In the European standard CEN/TR16355 [36], drinking water installation without hot water circulation, should be capable of reaching the minimum of 55°C. For a drinking water installation with circulation, should be the minimum of 55 °C, and within 30 s after fully opening a draw off fitting the temperature should not be less than 60°C. Meanwhile, to decrease the required temperature, some researches recommend to use supplementary heating devices, and the supply temperature can be decreased to 40°C [35].

In this study, six scenarios were proposed, see Table 4. For those scenarios, the controlled supply or return temperature were adjusted once in an hour, based on outdoor temperature, or the difference between the set and the measured indoor air temperature. Meanwhile, the maximum supply temperature for all the scenarios was 130°C.

For the theoretical calculation marked with TC in Table 4, the supply temperature was calculated based on equation (11-14) in [25], which is widely applied when the weather compensation (WC) control is used:

$$T_s = 20+10\cdot(20- T_{out})^{0.45}+0.14\cdot(20-T_{out}) \quad (1)$$

where T_s is the supply water temperature (°C), T_{out} is the outdoor air temperature (°C).

Table 4. Information of the six scenarios.

Scenario	Description
TS_PI_NL	Supply temperature control via PI controller with no minimum temperature limit
TS_PI_WL	Supply temperature control via PI controller with minimum temperature limit of 50°C
TS_TC_NL	Supply temperature control via theoretical calculation with no minimum temperature limit
TS_TC_WL	Supply temperature control via theoretical calculation with minimum temperature limit of 50°C
TR_PI_TC	Return temperature control via PI controller with constant target temperature of 30°C
TR_PI_TV	Return temperature control via PI controller with variable target temperature ranges from 30 to 50°C

3 Results

The system supply and return temperature during heating season are presented in Fig. 10. The relation between the average supply temperature, the average return temperature, and the average temperature difference during heating season is shown in Fig. 11. The indoor air temperatures for different scenarios are shown in Fig. 12. The total heat rates of the flat for different scenarios are displayed in Fig. 13. A summary of all the results is given in Table 5.

As Fig. 10 and Table 5 show, the low supply temperature was achieved via the PI control in the scenarios TS_PI_NL and TS_PI_WL, and with the WC control in the scenarios TS_TC_NL and TS_TC_WL. The average supply temperature in those scenarios could be as low as 56~58°C, and only limited time the required supply temperature was above 60°C. In addition, compared with the WC control, the PI control shown an advantage lowering the supply temperature. The percentage of required supply temperature above 60°C was 17% when the PI controllers were applied, while, the corresponding value was 36% in the case of the WC controls. The reason was that the WC control is an open loop control strategy and the supply temperature is only decided by the outdoor air temperature, ignoring any other impact factors, such as heat gain from solar radiation, occupant, and other devices. Whereas, the PI controller is a feedback control strategy and any overheating caused by extra heat gain will be compensated by the change in the supply temperature. In that way, unnecessary high supply temperatures are avoided. In this study, heat gains from occupants and devices were not taken into account, even though they might show more advantages for the PI controller. This model extension will be a topic for the future work.

As Fig. 10 and Table 5 show, the low return temperature was achieved through the PI controller in the scenarios TR_PI_TC and TR_PI_TV. The average return temperature in those scenarios were 30 and 37°C respectively, and the temperature below 40°C covers most of the heating season, with share of 99% and 83%, respectively. However, one obvious disadvantage for those operation strategies was the high supply temperature. The average supply temperature in the scenario TR_PI_TC was 94°C, and sometimes in order to achieve the low target return temperature, the required supply temperature was even up to 130°C. One way to solve this issue is to use flexible target return temperature. Compared with the scenario TR_PI_TC with constant target return temperature, TR_PI_TV uses flexible target return temperature. The average supply temperature of the scenario TR_PI_TV decreased to 72°C, meanwhile the maximum supply temperature decreases to 111°C.

As Fig. 10, Fig. 11, and Table 5 show, there is a clear relation between the supply temperature, the return temperature, and the temperature difference.

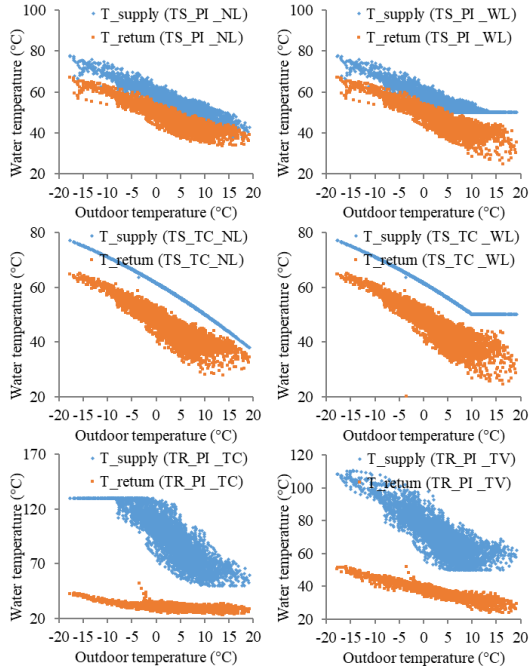

Fig. 10. Supply and return temperature during heating season.

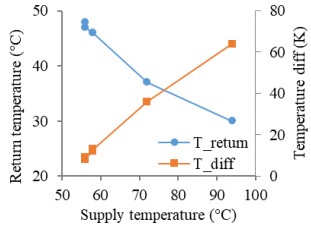

Fig. 11. The relation between average supply temperature, return temperature, and temperature difference.

As shown in Fig. 12 and Table 5, different operation strategies show small differences in the indoor air temperature. During most of the heating season, 98~99% of the entire season, the range of the indoor air temperature is within ±0.5°C around the set value. In addition, the results reveal the importance of indoor temperature control device, specifically TVs. Well-functioning TVs guarantee the indoor air temperature fluctuating within a certain range around the set values, no matter what operation strategy was applied. On the contrary, the indoor air temperature and the system return temperature would be with fault when the TVs have malfunctions [37, 38].

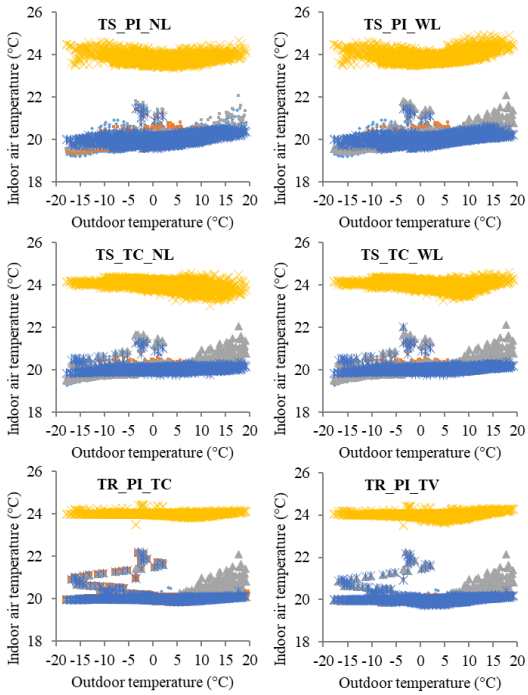

Fig. 12. Indoor temperature during heating season. The yellow dots present temperature of bathroom with setting temperature of 24°C, other color dots present temperature of living room, children room, bedroom, and kitchen with setting temperature of 20°C.

As shown in Fig. 13 and Table 5, different operation strategies show little difference on apartment heat use. As mentioned before, heat gains from occupants and devices were not taken into account in this study, otherwise energy savings from the PI controls would become bigger. More advanced control strategy, such as model predictive control (MPC) can bring even more energy savings and make the control process more smooth [39].

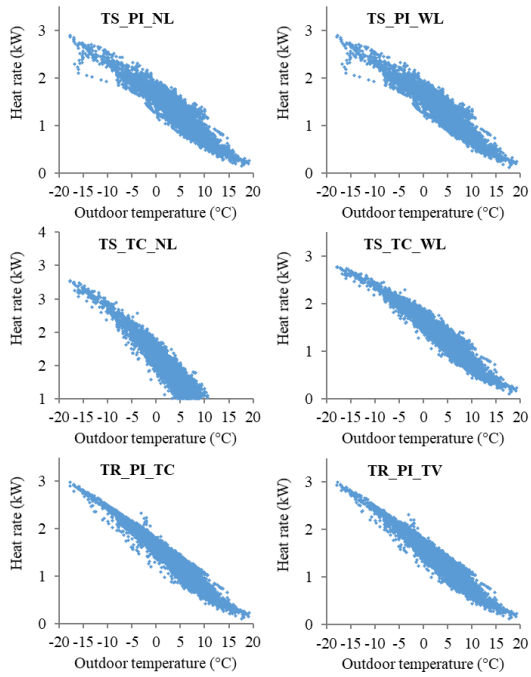

Fig. 13. Heat use during heating season.

Table 5. Summarized outcomes of different scenarios.

Scenario	TS_PI_NL	TS_PI_WL	TS_PI_WL	TS_TC_NL	TR_PI_TC	TR_PI_TV
Supply temperature						
Max (°C)	78	78	77	77	130	111
Min (°C)	38	50	38	50	50	50
Average (°C)	56	56	58	58	94	72
> 60 (%)	17	17	36	36	96	87
Return temperature						
Max (°C)	67	67	65	65	52	52
Min (°C)	34	25	28	20	23	24
Average (°C)	48	47	46	46	30	37
< 40 (%)	6	7	15	16	99	83
Temperature difference						
Average (°C)	8	9	12	13	64	36
Indoor temperature (%)						
< set-0.5	1	0	0	0	0	0
Within set ±0.5	98	98	99	99	99	99
> set+0.5	1	1	1	1	1	1

Scenario	TS_PI_NL	TS_PI_WL	TS_PI_WL	TS_TC_NL	TR_PI_TC	TR_PI_TV
Heat use per year						
Total (kWh)	8427	8435	8470	8477	8478	8478
Index (kWh/m^2)	120	121	121	121	121	121

4 Conclusion and discussion

This study aimed to optimize the operation strategy, and achieve the low supply and return temperature of the DH system. A building and a SH model were built using Modelica® language, and simulation was conducted in Dymola environment. Six scenarios, with controlled supply temperature or return temperature, were analysed based on the model.

The low supply temperature was achieved through the controlled supply temperature operation strategies: the PI control and the WC control. The average supply temperature could be as low as 56~58°C, and only limited time the required supply temperature was above 60°C, with 17% and 36% of the heating season, respectively. Meanwhile, the low return temperature was achieved through controlled return temperature operation strategy, the PI control. The average return temperature could be 30 or 37°C, while the temperature below 40°C covered the most time of heating season, with share of 99% and 83%, respectively.

One question come from this study, whether it is possible to achieve the low return temperature through optimizing operation strategy, without inappropriate high supply temperature. The results showed a clear coupling among the supply temperature, the return temperature, and the temperature difference between them. When the strategy with the constant target return temperature of 30°C was applied, the average supply temperature was 94°C, and during the coldest days, it was even up to 130°C, which is too high for the secondary side of DH system. One way to mitigate this issue was using flexible target return temperature. After the flexible target return temperature from 30 to 50°C was applied, the average supply temperature decreased to 72°C, and the maximum supply temperature decreased to 111°C. The results were still some distance from the temperature requirement of 4GDH, which is 50–55°C for the supply temperature, and 25°C for the return temperature. However, please note that the results are valid for the existing apartment building, built before 1980s and not for new buildings.

Another conclusion was the importance of TVs. Different operation strategies in this study showed small differences in the indoor air temperature and heat use. During the heating season, about 98~99% of the time, the fluctuation of the indoor air temperature was within ±0.5 °C around the set value. The results revealed the importance of TVs, which was the critical device to prevent overheating.

There were some limitations in this study. Renovations of buildings is a critical influencing factor in building energy analyses. Buildings have gone through reasonable renovations, such as changing the windows, use less heat and require a lower supply temperature. Building renovation was not taken into account in this study. In addition, the average heat gains from occupants and equipment can be assumed as 0.81 and 1.55 W/m^2 respectively [34]. If those heat gains were added, the oversizing of radiators would increase 5~10 %, the final value of oversizing will range from 21 to 27%. Under such condition, the required supply temperature could be further lower. Meanwhile, simplified occupant behavior mode was applied in this study, with constant set indoor temperature and fixed air exchange rate. Studies show occupant behaviour influence building energy use [40-42]. The simplification of the model may cause some inconsistent between simulation and reality. Finally, the research was conducted based on the simulation of two pipe SH system in an apartment with five rooms. To obtain more general and proper conclusions, further researches and experimentation studies are needed.

The authors gratefully acknowledge the support from the Research Council of Norway through the research project Understanding behaviour of district heating systems integrating distributed sources under FRIPRO/FRINATEK program (the project number 262707).

References

[1] Frederiksen S, Werner S. District Heating and Cooling: Studentlitteratur, 2013.
[2] Lund H, Werner S, Wiltshire R, Svendsen S, Thorsen JE, Hvelplund F, et al. 4th Generation District Heating (4GDH) Integrating smart thermal grids into future sustainable energy systems. Energy. 2014;68:1-11.
[3] Li H, Nord N. Transition to the 4th generation district heating-possibilities, bottlenecks, and challenges. Energy Procedia. 2018;149:483-98.
[4] Lund H, Möller B, Mathiesen BV, Dyrelund A. The role of district heating in future renewable energy systems. Energy. 2010;35(3):1381-90.
[5] IEA. Future low temperature district heating design guidebook. In: Schmidt D, Kallert A, editors. AGFW-Project Company Stresemannallee, Germany: International Energy Agency Technology Collaboration Programme on District Heating and Cooling including Combined Heat and Power; 2017.
[6] Brand M, Svendsen S. Renewable-based low-temperature district heating for existing buildings in various stages of refurbishment. Energy. 2013;62:311-9.
[7] Nord N, Ingebretsen M, Tryggestad I. Possibilities for Transition of Existing Residential Buildings to Low Temperature District Heating System in Norway. Conference Possibilities for Transition of Existing Residential Buildings to Low Temperature District Heating System in Norway. p. 22-5.
[8] Østergaard DS, Svendsen S. Theoretical overview of heating power and necessary heating supply temperatures in typical Danish single-family houses from the 1900s. Energy and Buildings. 2016;126:375-83.
[9] AS P, AS E. Potential and barrier study- Energy efficiency of Norwegian buildings (in Norwegian). 2012.

[10] Administration TNOoBTa. Guidance on technical requirements for construction work- Building Technology Regulations (TEK17) with guidance (in Norwegian) 2017.
[11] Administration TNOoBTa. Guidance on technical requirements for construction work- Building Technology Regulations (TEK10) with guidance (in Norwegian) 2010.
[12] Housing conditions, survey on living conditions, https://www.ssb.no/en/bygg-bolig-og-eiendom/statistikker/bo. 2019.
[13] CEN. SN-CEN / TR 12831-2: Energy Performance of Buildings - Method of Calculating Dimensional Power Requirements for Heat - Part 2: Explanation and Explanation of NS-EN 12831-1, Module M3-3. 2017.
[14] CEN. NS-EN 15251: Indoor environmental input parameters for design and assessment of energy performance of buildings addressing indoor air quality, thermal environment, lighting and acoustics. 2014.
[15] Ingebretsen ME. Possibilities for transition of existing buildings to low temperature district heating (in Norwegian): Norwegian University of Science and Technology, 2014.
[16] Kim S, Zirkelbach D, Künzel HM, Lee J-H, Choi J. Development of test reference year using ISO 15927-4 and the influence of climatic parameters on building energy performance. Building and Environment. 2017;114:374-86.
[17] Standardization ECf. EN ISO 15927-42005: Hygrothermal Performance of Buildings–Calculation and Presentation of Climatic Data–Part 4 Hourly Data for Assessing the Annual Energy Use for Heating and Cooling. 2005.
[18] Modelica and the Modelica Association, https://www.modelica.org/. 2019.
[19] CATIA SYSTEMS ENGINEERING - DYMOLA, https://www.3ds.com/products-services/catia/products/dymola/key-advantages/. 2019.
[20] Müller D, Lauster M, Constantin A, Fuchs M, Remmen P. AixLib-An Open-Source Modelica Library within the IEA-EBC Annex 60 Framework. BauSIM 20162016. p. 3-9.
[21] Open source library for building energy and control systems, https://simulationresearch.lbl.gov/modelica/. 2019.
[22] Constantin A, Streblow R, Müller D. The modelica housemodels library: Presentation and evaluation of a room model with the ASHRAE Standard 140. Conference The modelica housemodels library: Presentation and evaluation of a room model with the ASHRAE Standard 140. Linköping University Electronic Press, p. 293-9.
[23] Tritschler M. Assessment of the accuracy of heat cost allocators (in German): University of Stuttgart, 1999.
[24] Gluck B. Heat transfer: Heat dissipation of space heating surfaces and pipes (in German): Verlag für Bauwesen Berlin, 1990.
[25] He P, Sun G, Wang F, Wu H, WU X. Heating engineering (in Chinese): China Architecture & Building Press, 2009.
[26] CEN. EN 442-2: Radiators and Convectors–Part 2: Test Methods and Rating. 2003.
[27] Prek M, Krese G. Experimental analysis of an improved regulation concept for multi-panel heating radiators: Proof-of-concept. Energy. 2018;161:52-9.
[28] Seifert J, Knorr M, Meinzenbach A, Bitter F, Gregersen N, Krogh T. "Review of thermostatic control valves in the European standardization system of the EN 15316-2/EN 215". Energy and Buildings. 2016;125:55-65.
[29] CEN. EN215: Thermostatic Radiator Valves-Requirements and Test Methods. 2004.
[30] Xu B, Fu L, Di H. Dynamic simulation of space heating systems with radiators controlled by TRVs in buildings. Energy and Buildings. 2008;40(9):1755-64.
[31] Wang Y, You S, Zheng X, Zhang H. Accurate model reduction and control of radiator for performance enhancement of room heating system. Energy and Buildings. 2017;138:415-31.
[32] Tahersima F, Stoustrup J, Rasmussen H. An analytical solution for stability-performance dilemma of hydronic radiators. Energy and Buildings. 2013;64:439-46.
[33] Østergaard DS, Svendsen S. Are typical radiators over-dimensioned? An analysis of radiator dimensions in 1645 Danish houses. Energy and Buildings. 2018;178:206-15.
[34] Tunzi M, Østergaard DS, Svendsen S, Boukhanouf R, Cooper E. Method to investigate and plan the application of low temperature district heating to existing hydraulic radiator systems in existing buildings. Energy. 2016;113:413-21.
[35] Yang X, Li H, Svendsen S. Evaluations of different domestic hot water preparing methods with ultra-low-temperature district heating. Energy. 2016;109:248-59.
[36] CEN. CEN/TR16355: Recommendations for prevention of Legionella growth in installations inside buildings conveying water for human consumption. 2012.
[37] Østergaard DS, Svendsen S. Experience from a practical test of low-temperature district heating for space heating in five Danish single-family houses from the 1930s. Energy. 2018;159:569-78.
[38] Peffer T, Pritoni M, Meier A, Aragon C, Perry D. How people use thermostats in homes: A review. Building and Environment. 2011;46(12):2529-41.
[39] Prívara S, Široký J, Ferkl L, Cigler J. Model predictive control of a building heating system: The first experience. Energy and Buildings. 2011;43(2):564-72.
[40] Nord N, Tereshchenko T, Qvistgaard LH, Tryggestad IS. Influence of occupant behavior and operation on performance of a residential Zero Emission Building in Norway. Energy and Buildings. 2018;159:75-88.
[41] D'Oca S, Hong T, Langevin JJR, Reviews SE. The human dimensions of energy use in buildings: A review. 2018;81:731-42.
[42] Sun K, Hong T. A framework for quantifying the impact of occupant behavior on energy savings of energy conservation measures. Energy and Buildings. 2017;146:383-96.

PAPER 6

Li H, Hou J, Nord N. Using thermal storages to solve the mismatch between waste heat feed-in and heat demand: a case study of a district heating system of a university campus. Energy Proceedings. 2019;04. The 11th International Conference on Applied Energy.

APPENDIX- PUBLICATIONS

International Conference on Applied Energy 2019
Aug 12-15, 2019, Västerås, Sweden
Paper ID: #469

USING THERMAL STORAGES TO SOLVE THE MISMATCH BETWEEN WASTE HEAT FEED-IN AND HEAT DEMAND: A CASE STUDY OF A DISTRICT HEATING SYSTEM OF A UNIVERSITY CAMPUS

Haoran Li[1], Juan Hou[1], Natasa Nord[1*]

1 Department of Energy and Process Technology, Norwegian University of Science and Technology (NTNU), Kolbjørn Hejes vei 1 B, Trondheim 7491, Norway

ABSTRACT

Nowadays, the fundamental idea of district heating (DH) is to utilize local heat resources to satisfy local heat demands, otherwise those resources would be wasted. However, the mismatch between the achievable resources and fluctuating demand is challenging. This study analyzed the possibilities to solve this problem by introducing a short-term thermal storage and a seasonal thermal storage. A water tank (WT) and a borehole thermal storage (BTS) were chosen as the thermal storages. The DH system of a Norwegian university campus was selected as the case study. A high order system model was built in Modelica language. The results showed that the mismatch might be solved. The BTS brought about 3 GWh annual heat saving, and the WT brought about 110 kW average peak load shaving. However, around 0.8 GWh/year electricity was used by heat pump to recover the stored heat in the ground.

Keywords: 4th generation district heating, waste heat, ground source heat pump, seasonal thermal storage, water tank

1. INTRODUCTION

Nowadays, the fundamental idea of district heating (DH) is to utilize local heat resources to satisfy local heat demands, otherwise, those resources would be wasted. The suitable heat resources can be waste incineration, combustible renewables, geothermal energy, large solar collector fields, and waste heat from industry and other processes [1]. In 2014, renewables share 27% of European Union's DH supply, and the share of recycled waste heat share is 72% [2]. In the future, the share of recycled heat from combine heat and power plants will decrease, due to the increasing use of renewable power. However, waste heats from other sources bring huge potentials. To realize this idea, the current second or third generation DH system should transform into the 4th generation DH system. Characterized by flexible heat sources, low temperature, and smart management, the 4th generation DH system will show its energy and environment advantages in the coming years [1, 3]. However, the undergoing transformation has been facing many technical challenges [4, 5].

This study analyzed the challenge of harvesting waste heat from a data center. To solve the mismatch between the waste heat feed-in and heat demands, systems with thermal storages (TS) were investigated. A water tank (WT) and a borehole thermal storage (BTS) were chosen as the short-term TS and seasonal TS, respectively. The results of this study can provide guides for the development of the further DH system.

2. BACKGROUND

The DH system of a Norwegian university campus in Trondheim, Norway, was chosen as the case study. The topology of the network, the location of heat sources and buildings are presented in Fig 1.

The total building area of the campus is about 300,000 m^2. The main building function types are education, office, laboratory, and sport. Detail information of those buildings can be found in [6]. In the current situation, heat is delivered by two means: the main substation (MS) and a data center (DC). The MS obtains heat from the city DH system, and the DC recovers condensation heat from its cooling system. According to the measurement from June 2017 to May

Selection and peer-review under responsibility of the scientific committee of the 11th Int. Conf. on Applied Energy (ICAE2019).

2018, the total heat supply was 32.8 GWh, among them 77% came from the MS, and 23% came from the DC.

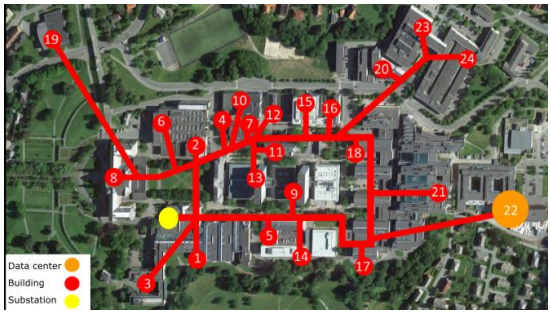

Fig 1 DH system of the university campus [7]

There was a mismatch between the waste heat feed-in and heat demands according to the measurement. As shown in Fig 2, the temperature difference between the supply and the return water of the secondary side of the MS showed negative values when the outdoor air temperature was above 7°C. This meant that the heat was transferred from the campus DH system to the city DH system. The reverse heat flow was caused by over waste heat feed-in.

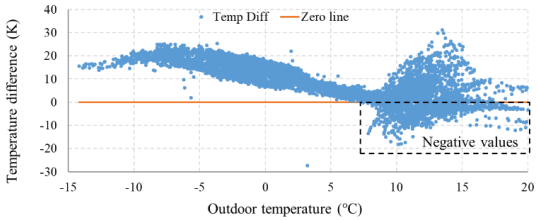

Fig 2 The measured water temperature difference of the secondary side of the MS

The short-term mismatch for a typical week is shown in Fig 3. During the periods with over waste heat feed-in, the reverse heat flow could be considered as heat loss for the campus DH system. In contrast, for the periods with insufficient waste heat feed-in, the deficit would be supplemented by the MS. Introducing a short-term TS can be one way to solve the short-term mismatch.

The net value of the over heat feed-in (over waste heat feed-in minus deficit in Fig 3) for a typical week was 0.02 GWh. In addition, the period with the over waste heat feed-in lasted for about half a year as shown in Fig 4. The long-term duration of the over heat feed-in makes it reasonable to introduce a seasonal TS.

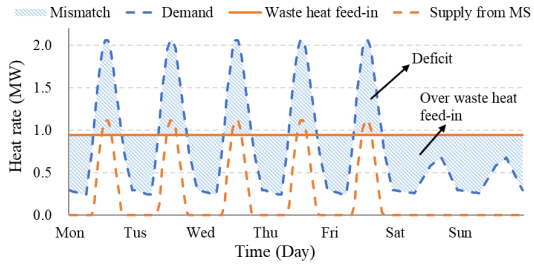

Fig 3 Heat balance for a typical week when the outdoor air temperature is above 7°C

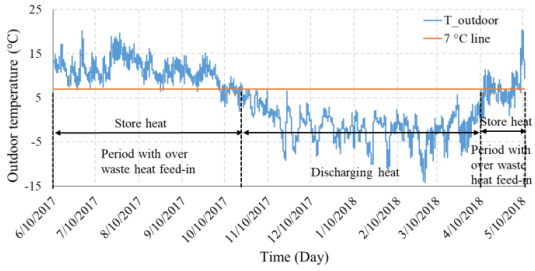

Fig 4 The measured outdoor air temperature and the period with over waste heat feed-in

3. METHODOLOGY

3.1 Simulation tool

The DH system model of the campus was built based on Modelica language [8]. Compared with other widely used tools such as Simulink, TRNSYS, and IDA ICE, Modelica presents the highest fidelity for DH system simulation [9]. Dymola [10] was used as the simulation environment. The libraries from IBPSA Project 1 [11] were selected to build the model.

3.2 Scenarios and model

Four scenarios with different system design were investigated. Detailed description about the scenarios is given in Table 1.

Table 1. System description of different scenarios

Scenarios	Short-term TS	Seasonal TS
NoShortNoSeasonal	-	-
WithShortNoSeasonal	WT	-
NoShortWithSeasonal	-	BTS
WithShortWithSeasonal	WT	BTS

Note. '-' refers to not exist.

The model structures of the scenarios in Table 1 are presented in Fig 5. The scenario 'NoShortNoSeasonal' was the reference scenario of this study, which was similar with the current situation of the DH system.

For all the scenarios, the way of waste heat feed-in was from return to return, which meant that the water from the return pipes of the DH system went through the condensation side of heat pumps (HP), and it went back to the return pipes after collecting the condensation heat. The return water would be further heated by the MS before it became the supply water of the system. The idea of the connection the return to return was to utilize the high supply temperature from the city DH system, while at the same time ensured a high coefficient of performance for HPs.

For the scenarios without the BTS, the cooling tower (CT) would exhaust the over heat of the DH system and decrease the cooling water temperature of the HP in the DC. In that way, the safety operation of the HP would be ensured. The function of the WT was peak load shaving. Heat would be stored during the low demand hours and used during the peak load hours.

For the scenarios with the BTS, when the outdoor air temperature was above 7°C, the high return water temperature would first go through the BTS and be cooled, while heat would be stored in the ground. The cooled water would go to the DC afterwards. In those scenarios, the BTS replaced the CT as the condensation heat cooling system. When the outdoor air temperature was below 7 ℃, the return water went through the DC directly. In addition, the stored heat in the ground would be extracted and boosted by a HP for heating use.

4. RESULTS

The daily peak load shaving induced by the WT is presented in Fig 6 and Fig 7. Significant effects of peak load shaving can be observed for the scenarios both with and without the BTS. In addition, the peak load shaving patterns were similar for the scenarios with and without the BTS. The maximum and the average shaving values were 1 519 kW and 110 kW for the scenarios without the BTS, and 2 168 kW and 103 kW for the scenarios with the BTS.

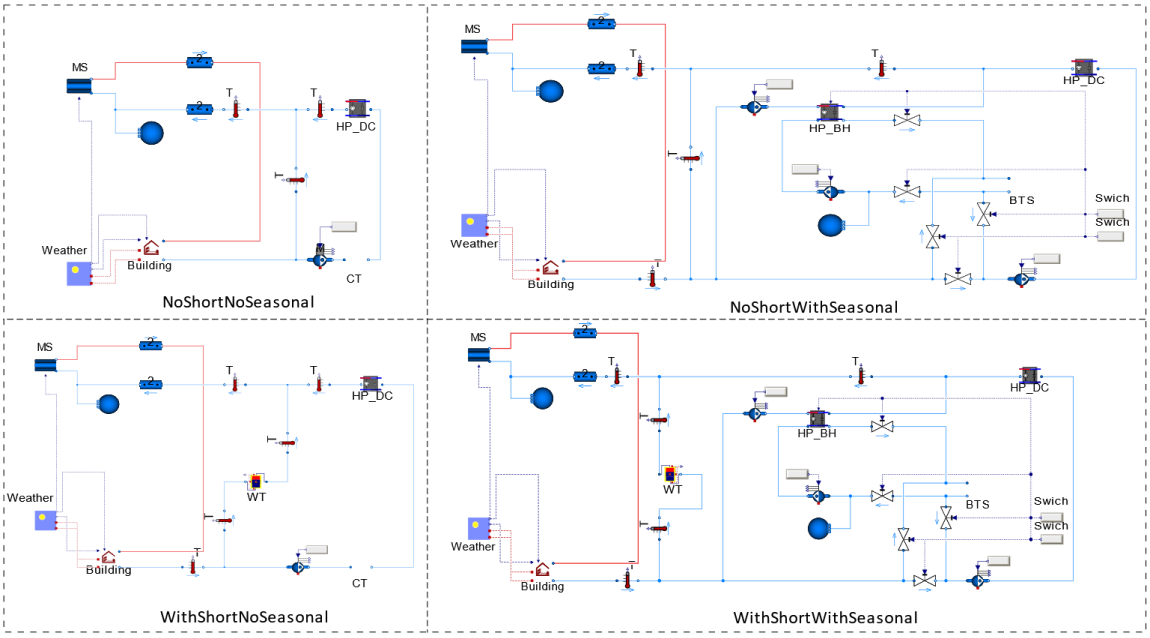

Fig 5 Model schematic of different scenarios

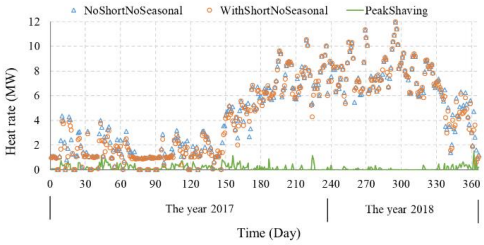

Fig 6 Daily peak load and peak load shaving due to the WT, for the scenarios without BTS

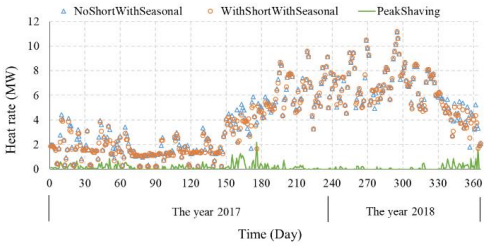

Fig 7 Daily peak load and peak load shaving due to the WT, for the scenarios with BTS

The seasonal mismatch was solved by introducing the BTS. As shown in Fig 8, about 0.8 GWh – 1.0 GWh heat was exhausted via the CT for the scenarios without the BTS. In contrast, no heat loss was found for the scenarios with the BTS.

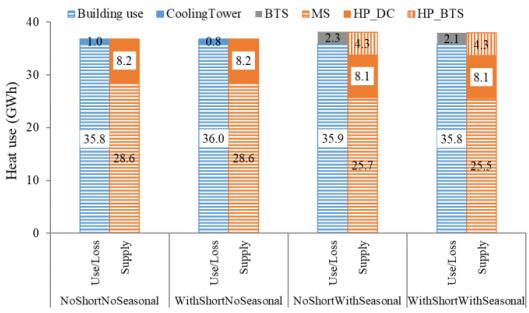

Fig 8 Annual heat use and heat supply for different scenarios

The heat supply from the MS could be reduced by introducing BTS. As shown in Fig 9, around 2.9 GWh – 3.0 GWh heat supply was saved. However, the electricity use increased around 0.8 GWh due to the HP of BTS.

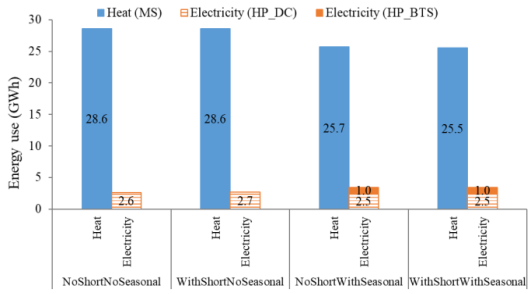

Fig 9 Annual heat and electricity use for different scenarios

5. CONCLUSIONS

The case study showed that the mismatch between waste heat feed-in and building heat demands could be solved by introducing TSs. The BTS brought about 3.0 GWh annual heat saving, and the WT brought about 110 kW average peak load shaving. However, about 0.8 GWh/year electricity was used for the HP of the BTS to recover the stored heat in the ground.

The research had some limitations. The sizing of the WT and BTS was conducted by the reference values from handbooks and engineering experience, optimal design analysis was not conducted. Meanwhile, the operation of the system was based on the rule of thumb, analyses of the optimal operation and control strategies were not conducted. More promising results might be achieved, if the optimal design, operation and control strategies were applied.

For the future work, more researches are needed for the optimal design, operation and control strategies. In addition, improving the heat storage efficiency is crucial for TSs.

ACKNOWLEDGEMENT

The authors gratefully acknowledge the support from the Research Council of Norway through the research project Understanding behaviour of district heating systems integrating distributed sources under FRIPRO/FRINATEK program (the project number 262707).

REFERENCE

[1] Frederiksen S, Werner S. District heating and cooling: Studentlitteratur Lund, 2013.

[2] Werner S. International review of district heating and cooling. Energy. 2017;137:617-31.

[3] Lund H, Østergaard PA, Chang M, Werner S, Svendsen S, Sorknæs P, et al. The status of 4th generation district heating: Research and results. Energy. 2018;164:147-59.
[4] Li H, Nord N. Transition to the 4th generation district heating - possibilities, bottlenecks, and challenges. Energy Procedia. 2018;149:483-98.
[5] Tian Z, Perers B, Furbo S, Fan J. Thermo-economic optimization of a hybrid solar district heating plant with flat plate collectors and parabolic trough collectors in series. Energy Conversion and Management. 2018;165:92-101.
[6] Guan J, Nord N, Chen S. Energy planning of university campus building complex: Energy usage and coincidental analysis of individual buildings with a case study. Energy and Buildings. 2016;124:99-111.
[7] Shakerin M. Analysis of district heating systems integrating distributed sources: NTNU, 2017.
[8] Modelica Association, https://www.modelica.org/ 2019.
[9] Schweiger G, Heimrath R, Falay B, O'Donovan K, Nageler P, Pertschy R, et al. District energy systems: Modelling paradigms and general-purpose tools. Energy. 2018;164:1326-40.
[10] DYMOLA Systems Engineering, https://www.3ds.com/products-services/catia/products/dymola/. 2019.
[11] IBPSA Project 1, https://ibpsa.github.io/project1/index.html. 2019.

APPENDIX- PUBLICATIONS

PAPER 7

Li H, Hou J, Ding Y, Nord N. Techno-economic analysis of implementing thermal storage for peak load shaving in a campus district heating system with waste heat from the data centre. E3S Web Conf; 2021;246: 09003. The 10th International SCANVAC Cold Climate Conference.

APPENDIX- PUBLICATIONS

Techno-economic analysis of implementing thermal storage for peak load shaving in a campus district heating system with waste heat from the data centre

Haoran Li[1*], *Juan* Hou[1], *Yuemin* Ding[1], and *Natasa* Nord[1]

[1] Department of Energy and Process Technology, Norwegian University of Science and Technology (NTNU), Kolbjørn Hejes vei 1 B, Trondheim 7491, Norway

Abstract. Peak load has significant impacts on the economic and environmental performance of district heating systems. Future sustainable district heating systems will integrate thermal storages and renewables to shave their peak heat demand from traditional heat sources. This article analysed the techno-economic potential of implementing thermal storage for peak load shaving, especially for the district heating systems with waste heat recovery. A campus district heating system in Norway was chosen as the case study. The system takes advantage of the waste heat from the campus data centre. Currently, about 20% of the heating bill is paid for the peak load, and a mismatch between the available waste heat and heat demand was detected. The results showed that introducing water tank thermal storage brought significant effects on peak load shaving and waste heat recovery. Those effects saved up to 112 000 EUR heating bills annually, and the heating bill paid for the peak load could be reduced by 15%. Meanwhile, with the optimal sizing and operation, the payback period of the water tank could be decreased to 13 years. Findings from this study might help the heat users to evaluate the economic feasibility of introducing thermal storage.

1 Introduction

Peak load has significant impacts on a district heating (DH) system. Firstly, a higher peak load means more investment, since larger capacity heat sources and distribution systems are demanded [1]. Secondly, peak load causes higher operation cost, since the energy price for the peak load heat sources is usually higher than the basic load heat sources. Finally, DH systems with higher peak loads tend to be less environmentally friendly, since the peak load is usually supplied by non-renewable energies, meaning an increase in the CO_2 emission per unit of heat. Therefore, DH companies try to encourage heat users to decrease their peak load by providing incentives on heating bills. When considering the peak load, the heating bill may be divided into two parts: fixed and variable. The fixed part is charged based on the seasonal peak load and may consist of a significant part of the total heating bill [2].

Introducing thermal storages (TSs) is a straightforward way for heat users to decrease their peak load and gain economic benefits. Previous studies show it is economically feasible to introduce TSs into DH systems [3-8]. However, these TSs are used for storing the free heat (e.g., solar thermal energy), not for shaving the peak load. Some researchers demonstrate the economic feasibility of using TSs for load shifting [9-11]. However, the load referred to electricity load, and these TSs were applied to the building's level instead of the district level. There is a limited study to analyse the economic feasibility of using TSs for peak load shaving in DH systems. This study aimed to investigate the economically feasible to use TS for peak load shaving in DH systems. A campus DH system in Norway was chosen as the case study. Water tank (WT) systems with storage capacities ranged from two hours to one week were proposed. The energy and economic performance of the proposed WT systems were investigated.

2 Method

This study was conducted through numerical experiments. Firstly, a campus DH system in Norway was introduced as the case study. The system suffered from the high proportion of heating bill paid for the peak load, meanwhile, part of heat supply was lost due to the mismatch between waste heat feed-in and building heat demand. WTs were applied as the short-term TS to solve the above problems and the WTs' storage capacities range from two hours to one week. Afterwards, the way to achieve the optimal operation with the minimized peak load and heat loss was illustrated. Finally, the method to calculate the heating bill was described. Detailed information about the method is introduced as follows.

* Corresponding author: haoranli@ntnu.no

2.1 Case study

A campus DH system in Trondheim, Norway, was chosen as the case study. The topology of the system is presented in Figure 1. The total campus building area is about 300 000 m^2, and the main building functions are education, office, laboratory, and sports. Currently, heat is delivered from the main substation (MS) and the data centre (DC). The MS obtains heat from the city DH system, and the DC recovers condensing heat from its cooling system. According to the measurements from June 2017 to May 2018, the total heat supply was 32.8 GWh. About 75% of the heat supply came from the MS and the other 25% came from DC. The measured heat use and heat supply from DC are presented in Figure 2.

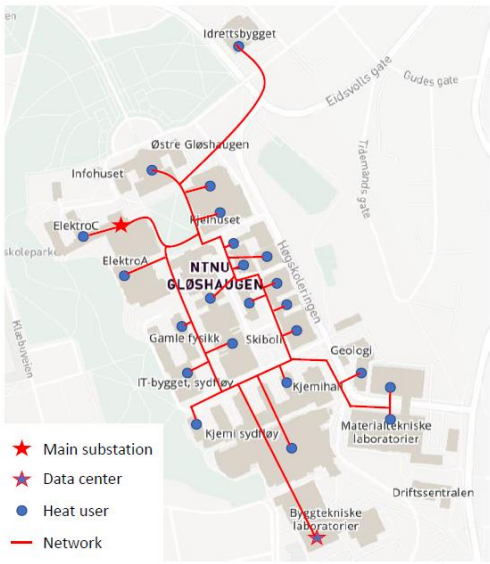

Figure 1. DH system of the university campus.

The main motivation for introducing a TS system was to reduce the heating bill. As mentioned in Section 1, a heating bill is divided into two parts: fixed and variable. The fixed part is related to the seasonal peak load (in kW). The variable part is charged based on the amount of heat use (in kWh). For the year 2017-2018, about 1.94 million EUR was paid for the heating bill, and 20% of it came from the fixed part, which was caused by the peak load. The heating bill paid for the peak load even dominated the total heating bill during the warm period from May to September. The average heating bill paid for the fixed part during this period was about eight times higher than the corresponding value for the variable part. Introducing a TS system is a straightforward way to shave the peak load and reduced the heating bill.

Another motivation for this work was to solve the mismatch between the waste heat feed-in and the building heat demand. According to the measurements, a mismatch between waste heat feed-in and building heat demand was observed during the warm period. The heat demand in warm periods came only from the domestic hot water system, and it showed an apparent daily fluctuation from 0.3 to 2.1 MW, while the amount of waste heat feed-in from the DC kept at a constant level, about 0.9 MW. Therefore, during the peak hours, the amount of waste heat feed-in was not enough to satisfy the heat demand, and the deficit would be supplemented by the MS. During the low demand hours, the amount of waste heat feed-in was higher than the demand, and the excess waste heat feed-in would become reverse heat flow to the city DH system. However, the university campus did not get any economic benefit from this reverse heat flow, because the local DH company has not yet adopted a method for charging the heating bill with bidirectional heat flow.

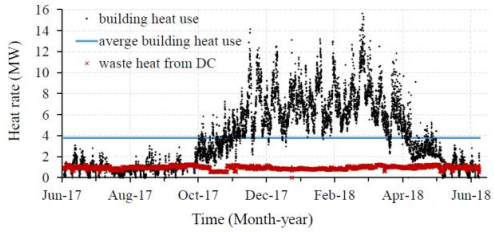

Figure 2. Building heat use and waste heat feed-in during the year 2017-2018.

2.2 Principles of WT sizing

In this study, the WT was chosen due to its easy application in different conditions. The simplified schematic of the campus DH system after integrating a WT system is illustrated in Figure 3. Before the economic study, the sizing of the WT was conducted and the operation strategy of the DH system was made.

The WT was sized based on the duration of the heat supply. The annual average building heat use was 3.79 MW. The storage capacity of the WT was quantified according to the heat supply at this heat flow rate. For example, if the WT was sized with two hours' capacity, it meant that the WT system could supply heat continuously for two hours with a discharging rate of 3.79 MW. In this study, the WT functioned as the short-term TS, and the investigated storage capacity ranged from two hours to one week. The detailed information on the WT sizing analysis is given in Table 1.

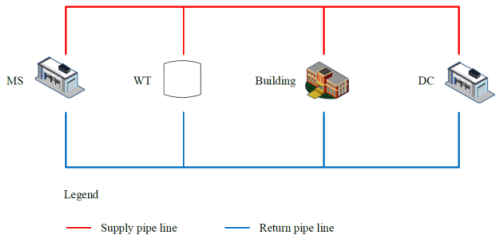

Figure 3. Schematic of the campus DH system after integrating a WT system.

Table 1. Information on the studied WTs.

Abbreviation	Sizing (m^3)
2h	163
4h	325
12h	975
1d	1 950
2d	3 900
3d	5 850
5d	9 750
1w	13 650

2.3 Operation strategy for the DH system with the WT

For the operation of the DH system, optimization was conducted to fully explore the potential of the WT system. An optimization problem was formulated to minimize the peak load and heat loss, the defined problem is presented as follows:

$$min \int \dot{Q}_{MS}{}^2 \, dt \quad (1)$$

subject to

$$\dot{Q}_{MS} + \dot{Q}_{DC} - \dot{Q}_{WT} - \dot{Q}_{buil} = 0 \quad (2)$$

$$\dot{Q}_{WT} - \dot{Q}_{loss} - c \cdot \rho \cdot V_{WT} \cdot \frac{dT_{WT}}{dt} = 0 \quad (3)$$

$$\dot{Q}_{loss} = U_{WT} \cdot A_{WT} \cdot (T_{WT} - T_{envi}) \quad (4)$$

$$\dot{Q}_{up} = c \cdot \dot{m}_{char} \cdot \nabla T_{char} \quad (5)$$

$$\dot{Q}_{low} = c \cdot \dot{m}_{disc} \cdot \nabla T_{disc} \quad (6)$$

$$T_{low} \leq T_{WT} \leq T_{up} \quad (7)$$

$$\dot{Q}_{low} \leq \dot{Q}_{WT} \leq \dot{Q}_{up} \quad (8)$$

where $\dot{Q}_{MS}$ is the heat supply rate (positive value) or heat loss rate (negative value) from the MS. $\dot{Q}_{DC}$ is the waste heat feed-in from DC. $\dot{Q}_{WT}$ is the charging (positive value) or discharging (negative value) heat flow rate of the WT. $\dot{Q}_{low}$ and $\dot{Q}_{up}$ are the lower and the upper limit of $\dot{Q}_{WT}$. $\dot{Q}_{buil}$ is the heat use of the buildings at the campus. $\dot{Q}_{loss}$ is the heat loss from the WT to the environment. T_{WT} is the water temperature in the WT. T_{low} and T_{up} are the lower and the upper limit of T_{WT}. For these limits, the values of 40℃ and 80℃ were chosen, respectively. ∇T_{disc} and ∇T_{char} are the maximum temperature difference during the discharging and charging processes. The values of -40K and 40K were chosen, respectively. U_{WT} is the U-value of the WT walls. T_{envi} is the temperature of the environment. c is the specific heat capacity of water, of 4 187 J/(K·kg). ρ is the water density, of 995.6 kg/m^3.

2.4 Method for the DH heating bill calculation

As mentioned in the introduction, the heating bill includes usually two parts: the fixed and the variable, defined as follows:

$$B_{tot} = B_{fix} + B_{var} \quad (9)$$

where B_{tot} is the total heating bill, B_{fix} is the fixed part, and B_{var} is the variable part.

The fixed part was calculated as:

$$B_{fix} = \dot{Q}_{peak} \cdot p_{fix} \quad (10)$$

where $\dot{Q}_{peak}$ is the peak load, which is obtained by averaging the top three highest daily average heat uses. p_{fix} is the unit fixed cost, which was given by the local DH company Statkraft Varme [12] in Trondheim.

The variable part was calculated as:

$$B_{var} = \int \dot{Q} \cdot p_{var} \, dt \quad (11)$$

where $\dot{Q}$ is the heat demand. p_{var} is the variable heat price, which was given by the local DH company Statkraft Varme [12] in Trondheim.

3 Results

In this section, the reference scenario (Ref) without any TS together with the scenarios with the WT are investigated. The heat use and heating bill of these scenarios are presented. The peak load shaving, heating bill saving, and payback periods of the scenarios with the WT are analyzed. Detailed information about the results is presented as follows.

3.1 Peak load shaving and heat use saving

The peak load shaving and heat loss reduction could be derived from the difference between the heat demand of the reference scenario and the heat demand of the scenarios with the WT. The heat demand referred to the heat supply from the MS. Please note that the negative value meant the reverse heat flow to the city DH system, meaning the heat loss of the campus DH system. The results showed that introducing a WT could bring significant peak load shaving and heat loss reduction. Figure 4 gives an example of the impacts after introducing a WT with one day's capacity. As illustrated in Figure 4, the *Ref* scenario had higher peak loads compared with scenario *1d*. The peak load shaving effect was up to 3.3 MW, and it accounted for 23% of the annual maximum heat load. In addition, heat loss existed for the scenario *Ref* during the warm period from May to September. In contrast, the heat loss was almost eliminated for scenario *1d*. The annual heat loss reduction was about 362 MWh, which meant 82% of the heat loss was avoided.

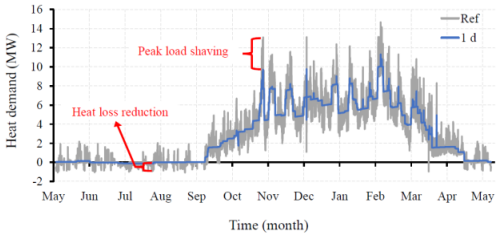

Figure 4. Example of peak load shaving and heat loss reduction after introducing WT.

The seasonal peak load shaving effect of the scenarios with the WT is presented in Figure 5. From Figure 5, it may be observed that the larger WT brought higher seasonal peak load shaving. For the scenario *2h* when the storage capacity was two hours, the seasonal peak load shaving was 10 kW in the winter season and 5 kW in the summer season, see Figure 5 the column filled with the black colour. For scenario *1w* when the storage capacity increased to one week, the corresponding reduction increased to 3.2 MW and 2.2 MW, respectively, see Figure 5 the column filled with the red colour.

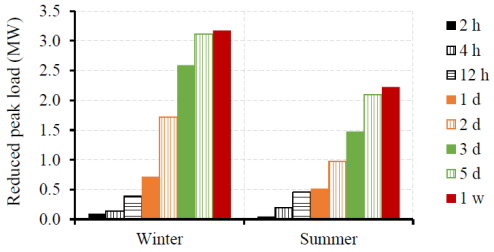

Figure 5. Seasonal peak load shaving for the scenarios with different storage capacity.

The heat demand saving effect of the scenarios with the WT is presented in Figure 6. From Figure 6, it can be observed that the scenario *1d* with one day's storage capacity showed the best performance regarding heat demand saving. The reason was that the total heat loss was minimized for scenario *1d*. The total heat loss included two parts: the heat loss through the MS (reverse heat flow to the central DH system), and the heat loss from the WT to the environment. The larger WT reduced the heat loss from the MS because the short-term mismatch between the waste heat feed-in and building heat demand could be relieved. However, the larger WT suffered from more heat loss to the environment, because of the larger heat transfer area. The size of the WT in scenario *1d* was at the optimal point considering these two parts of heat loss.

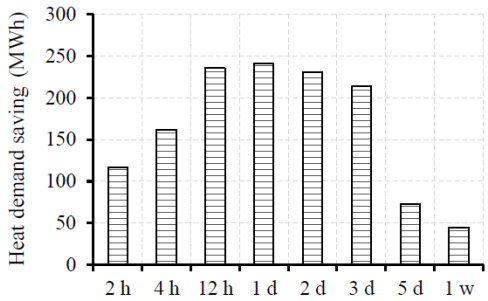

Figure 6. Heat demand saving for scenarios with different storage capacity.

3.2 Heating bill saving and payback period

The heating bill considering the share between the fixed and variable parts for the proposed scenarios is presented in Figure 7. The two impacts could be observed due to introducing the WT: 1) the total heating bill was decreased, 2) the share of the fixed part in the total heating bill was reduced. For the reference scenario *Ref*, the total bill was 1.94 million EUR, and 20% of it came from the fixed part. After introducing the WT system, the total bill could decrease to 1.83 million EUR, and only 15% of it came from the fixed part.

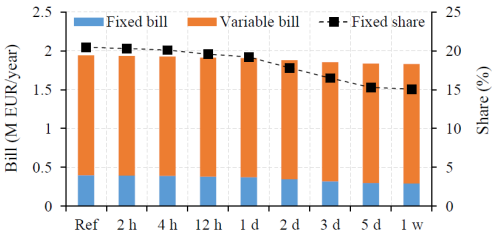

Figure 7. Annual heating billing for the scenarios before and after introducing a WT system.

The detailed information on heating bill saving is presented in Figure 8. The saving from the fixed part increased as the storage capacity increased, as shown in Figure 8. The reason was that larger WT brought higher seasonal peak load reduction. The variable part of the heating bill achieved a higher saving for the scenarios with medium storage capacities, as shown in Figure 8. This can be explained by the higher heat demand saving for those scenarios with medium storage capacities.

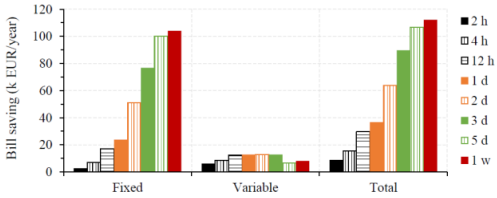

Figure 8. Annual heating billing saving for the scenarios after introducing a WT system.

The payback periods for the scenarios with different storage capacities are presented in Figure 9. As shown

in Figure 9, the payback periods ranged from 13 years to 19 years. Further, the two optimal WT sizes could be observed: the storage capacities with four hours and three days. The payback periods of the WT may be explained by the indicator *unit bill saving*, which was obtained by dividing the heating bill saving by the WT size. As shown in Figure 10, the value of *unit bill saving* ranged from 8 EUR/m^3 to 55 EUR/m^3, it decreased as the WT size increased. This meant the larger WT had less heating bill saving effect. A two order polynomial trend line could be drawn to show the relationship between the unit bill saving and the WT size. The WT capacity with the unit bill saving above the trend line tended to have shorter payback periods, see Figure 10 the dots filled with the red colour. In contrast, the WT capacity with the unit bill saving below the trend line tended to have longer payback periods, see Figure 10 the dots filled with the black colour.

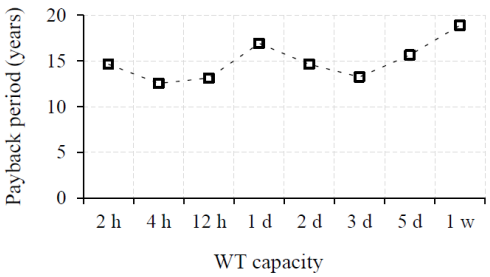

Figure 9. The payback period for the scenarios with different storage capacity.

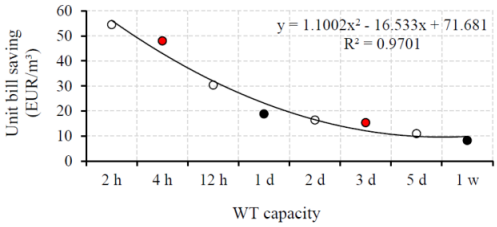

Figure 10. Unit heating bill saving for the scenarios with different storage capacity.

4 Conclusions

In this study, the economic analysis of using WT for peak load shaving in a DH system with waste heat feed-in was conducted. A campus DH system in Norway was chosen as the case study. WTs with storage capacities ranged from two hours to one week were tested. The peak load shaving, heat use saving, heating bill saving, and payback period for the WT system were investigated.

The results showed that WT had significant effects on peak load shaving and heat use saving. Those effects brought up to 112k EUR annual heating bill saving, which accounted for 6% of the total heating bill. Meanwhile, the payback periods of WT ranged from 13 years to 19 years.

Finding from this study may help heat users to evaluate the economic feasibility of introducing a WT system.

The authors gratefully acknowledge the support from the Research Council of Norway through the research project Understanding behaviour of district heating systems integrating distributed sources under FRIPRO/FRINATEK program (the project number 262707).

References

[1] Tereshchenko T, Nord N. Energy planning of district heating for future building stock based on renewable energies and increasing supply flexibility. Energy. 2016;112:1227-44.
[2] Song J, Wallin F, Li H. District heating cost fluctuation caused by price model shift. Applied Energy. 2017;194:715-24.
[3] Tian Z, Perers B, Furbo S, Fan J. Thermo-economic optimization of a hybrid solar district heating plant with flat plate collectors and parabolic trough collectors in series. Energy Conversion and Management. 2018;165:92-101.
[4] Tian Z, Zhang S, Deng J, Fan J, Huang J, Kong W, et al. Large-scale solar district heating plants in Danish smart thermal grid: Developments and recent trends. Energy Conversion and Management. 2019;189:67-80.
[5] Rohde D, Knudsen BR, Andresen T, Nord N. Dynamic optimization of control setpoints for an integrated heating and cooling system with thermal energy storages. Energy. 2020;193:116771.
[6] Rohde D, Andresen T, Nord N. Analysis of an integrated heating and cooling system for a building complex with focus on long–term thermal storage. Applied Thermal Engineering. 2018;145:791-803.
[7] Li H, Hou J, Hong T, Ding Y, Nord N. Energy, economic, and environmental analysis of integration of thermal energy storage into district heating systems using waste heat from data centres. Energy. 2021;219:119582.
[8] Li H, Hou J, Nord N. Using thermal storages to solve the mismatch between waste heat feed-in and heat demand: a case study of a district heating system of a university campus. 2019.
[9] DeForest N, Mendes G, Stadler M, Feng W, Lai J, Marnay C. Optimal deployment of thermal energy storage under diverse economic and climate conditions. Applied Energy. 2014;119:488-96.
[10] Rismanchi B, Saidur R, Masjuki HH, Mahlia TMI. Energetic, economic and environmental benefits of utilizing the ice thermal storage systems for office building applications. Energy and Buildings. 2012;50:347-54.
[11] Sanaye S, Shirazi A. Thermo-economic optimization of an ice thermal energy storage system for air-conditioning applications. Energy and Buildings. 2013;60:100-9.
[12] Statkraft Varme at Tronheim, https://www.statkraftvarme.no/om-statkraftvarme/vare-anlegg/norge/trondheim/. Last accessed 2020.

PAPER 8

Li H, Hou J, Nord N. Optimize prosumers' economic performance by using water tank as thermal energy storage. The 17th International Symposium on District Heating and Cooling.

APPENDIX- PUBLICATIONS

The International Symposium on District Heating and Cooling, Nottingham Trent University, 17th, 6–9 September 2021, Nottingham, UK

Optimize prosumers' economic performance by using water tank as thermal energy storage

Haoran Li[a, *], Juan Hou[a], Natasa Nord[a]

[a]*Department of Energy and Process Technology, Norwegian University of Science and Technology (NTNU), Kolbjørn Hejes vei 1 B, Trondheim 7491, Norway*

Abstract

Heat prosumers will become important participants for future district heating (DH) systems. However, the current unidirectional heating price models reduce interest in prosumers and hinder the promotion of prosumers in DH systems, because the prosumers gain no economic benefit from supplying heat to the central DH system. This study aimed to break this economic barrier by introducing water tank thermal energy storage (WTTES) and optimizing the operation of heat prosumers with WTTESs, considering the widely used heating price models in Norway. Firstly, a generalized heating price model was introduced, which could represent the current widely used heating price models in Norway. Secondly, the WTTES was integrated into the heat prosumer to improve the self-utilization rate of the prosumer's heat supply from its distributed heat sources, meanwhile, shave the prosumer's peak load. Afterwards, an optimization framework was formulated to optimize the operation of the prosumer with the WTTES under the generalized heating price model. Finally, a numerical method for solving the proposed nonlinear optimization problem was given. A case study showed that the proposed method could cut the prosumer's annual heating cost by 7%, and the investment of WTTES could be recovered in four years.

Keywords: nonlinear optimization, thermal energy storage, heating price, distributed heat sources

1. Introduction

The widely used heating price models in Norway charge a heat prosumer's heating bill mainly based on heat prosumer's heat use and peak load [1]. Accordingly, two potential ways to minimize a heat prosumer' heating cost in a district heating (DH) system are: 1) decreasing the heat supply from the central DH system by increasing the heat supply from prosumer's distributed heat sources (DHSs), which are free and may come from renewables and waste heat, and 2) shaving the peak load by shifting the heat supply from peak hours to non-peak hours.

Thermal energy storages (TESs) may be used to achieve the above two goals. Firstly, TESs can increase the self-utilization rate of the heat supply from DHSs, because for the periods when the heat supply from the DHSs is higher than the demand of the prosumer, the surplus heat can be stored into the TESs and used for later heat supply instead of being fed into the central DH system [2, 3]. Secondly, TESs can shave the prosumer's peak load, because the peak demand can be satisfied by the stored heat from the non-peak hours [4, 5]. However, TESs are investment intensive. The high investment costs and the long payback periods are hindering the implementation of TESs in DH systems.

This study proposed a comprehensive method for optimal design and operation of prosumer-based DH systems with short-term TESs. The method was based on the heating price models in Norway, but can also give references for DH systems outside Norway.

2. Method

This section explains the proposed method. Firstly, a generalized heating price model is introduced, which may represent the current widely used heating price models in Norway. Secondly, WTTES is integrated into the heat prosumer based DH system to improve the self-utilization of the heat supply from the DHSs and shave the peak load. Afterwards, an optimization framework is formulated to optimize the operation of the proposed DH system under the

generalized heating price model. Finally, a numerical method for solving the proposed nonlinear optimization problem is given.

2.1. The method to obtain a generalized heating price model

Although heating price models may vary in Norway, this study introduced a generalized heating price model, which could approximate and generalize the widely used heating price models. According to the review article [1], a heating price model may include four components: energy demand component (EDC), load demand component (LDC), fixed component (FXC), and flow demand component (FDC). The EDC is charged based on the heat use and it is used to cover the fuel cost. The LDC is charged according to the peak load and it aims to maintain a certain capacity of heat production. The FXC is the fee for connecting to the central heating grid. The FDC motivates the low return temperature and it is charged based on the volume of the circulating water.

Fig. 1 gives the existence and the average share of each component for investigated heating price models in Sweden. Firstly, it can be found from Fig. 1 that, the LDC and the EDC are the most important components, which together share 96% of the total heating cost. Moreover, 87% of the investigated heating price models have the LDC and all the heating price models have the EDC. In contrast, the FXC and FDC play limited roles in the investigated heating price models, which only share less than 2% of the total heating cost. Furthermore, only about half of the investigated heating price models have the FXC and FDC.

Based on the above situations, a generalized heating price model used to approximate a prosumer's heating cost was introduced as Equation (1), in which the total heating cost includes the LDC and the EDC.

$$C_{tot} = C_{ldc} + C_{edc} \tag{1}$$

where C_{tot} refers to the total heating cost, C_{ldc} and C_{edc} are the LDC and the EDC, respectively, which can be obtained by Equation (3) and Equation (4).

$$C_{ldc} = LP \cdot \dot{Q}_{pea} \tag{2}$$

$$C_{edc} = \int_{t_0}^{t_f} EP(t) \cdot \dot{Q}(t) dt \tag{3}$$

where LP and $EP(t)$ are the LDC heating price and EDC heating price, respectively. $\dot{Q}_{pea}$ refers to the yearly peak load [6, 7] and $\dot{Q}(t)$ is the heat supply flow rate.

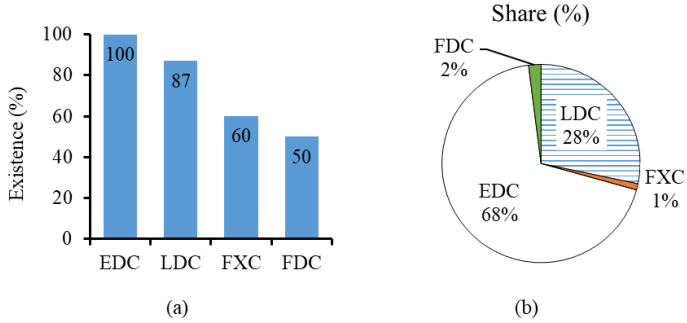

Fig. 1. The existence (a) and average share (b) of each component in investigated heating price models [1]

2.2. System design for heat prosumer-based DH system with TES

As introduced in Section 2.1, to minimize the heating cost of a heat user, it is required to decrease the LDC and the EDC heating cost, which are related to the peak load and the heat use, respectively. Moreover, as explained in Section 1, TESs may be used to achieve the above goals. Fig. 2 illustrates the proposed system for a heat prosumer based DH

system, which integrates a TES. In Fig. 2, DHS was a low-temperature heat source utilizing free heat from renewables or waste heat. DHS was integrated into the prosumer's local DH system using the R2R mode, in which DHS extracted water flow from the return line and fed it back into the return line after the heating process. The R2R mode was used because it is preferable for a low-temperature heat source [8].

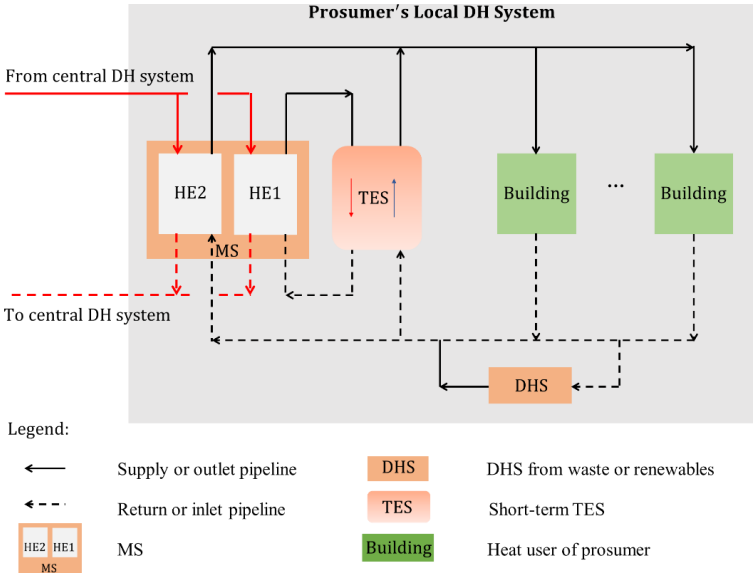

Fig. 2. System design for a heat prosumer's local DH system with TES

Moreover, MS in Fig. 2 referred to the main substation, which connected the central DH system with the prosumer's local DH system. Two types of heat exchanger (HE) were installed in the MS. HE1 was used for charging the TES. For the period with low heat demand, HE1 supplied heat to the local DH system through TES when the heat supply from the DHS was not enough. For the period with high heat demand, HE1 was used for peak load shaving by charging heat at non-peak hours. HE2 in the MS functioned as a high-temperature heat source, it boosted the supply temperature of the local DH system to the required level when the water temperature after the DHS was not high enough.

In addition, the TES was a short-term TES. As introduced in Section 1, the TES functioned in two ways to minimize the prosumer's heating cost. Firstly, it improved the self-utilization rate of heat supply from the DHS. For the period with low heat demand, the DHS from renewables and waste heat may have a higher heat supply than the demand, and the surplus heat supply would be stored in the TES and for later use instead of being supplied to the central DH system. Secondly, the TES may shave the prosumer's peak supply from the central DH system. For the periods around the peak periods, the central DH system may charge the TES at non-peak hours and the stored heat may shave the heat supply at the peak hours.

Fig. 2 gives an example of a community heat prosumer, which has a cluster of buildings as the heat users. However, for the cases of individual heat prosumers, the heat user is a single building.

2.3. Optimization framework for the operation of heat prosumer-based DH system

An optimization framework for the operation of a heat prosumer-based DH system is proposed in this section. The framework was based on the system design presented in Section 2.2, considering the generalized heating price model introduced in Section 2.1. The mathematical formulation of this framework is presented in Equations (4), (5), (6), (7), and (8). Equation (4) is the objective function, in which the first part is the EDC heating cost and the second part is the LDC heating cost. Equation (5) represents the effort to shave the peak load, Equation (6) describes the system dynamics and Equation (7) defines the initial states of the system. Equation (8) is the system constants.

Minimize:

$$\int_{t_0}^{t_f} EP(t) \cdot \dot{Q}(t)dt + LP \cdot \dot{Q}_{pea} \tag{4}$$

subject to:

$$\dot{Q}(t) \leq \dot{Q}_{pea} \tag{5}$$

$$F(t, \boldsymbol{z}(t)) = 0 \tag{6}$$

$$F_0(t_0, \boldsymbol{z}(t_0)) = 0 \tag{7}$$

$$z_L \leq \boldsymbol{z}(t) \leq z_U \tag{8}$$

where $\dot{Q}(t)$ is heat supply flow rate from the central DH system. $\dot{Q}_{pea}$ is the peak load, which is a parameter to be minimized. LP and $EP(t)$ are the heating price for the LDC and the EDC, respectively. $\boldsymbol{z} \in \mathbb{R}^{n_z}$ are the time-dependent variables, including the manipulated variable $\boldsymbol{u} \in \mathbb{R}^{n_u}$, the differential variable $\boldsymbol{x} \in \mathbb{R}^{n_x}$, and the algebraic variable $\boldsymbol{y} \in \mathbb{R}^{n_y}$. $z_L \in [-\infty, \infty]^{n_z}$ and $z_U \in [-\infty, \infty]^{n_z}$ are the lower bounds and upper bounds, respectively. The system dynamics described in Equation (6) contained the dynamics of the MS, DHS, TES, distribution network, and buildings. The interactions between these subsystems were defined in Equations (9), (10), (11), (12), and (13).

$$\dot{Q}(t) = \dot{Q}_{HE1} + \dot{Q}_{HE2} \tag{9}$$

$$\dot{Q}_{HE1} + \dot{Q}_{HE2} + \dot{Q}_{DHS} = \dot{Q}_{Bui} + \dot{Q}_{TES} + \dot{Q}_{loss,TES} + \dot{Q}_{loss,pip} \tag{10}$$

$$\dot{Q}_{HE1} = c \cdot \dot{m}_{HE1} \cdot (T_{HE1,sup} - T_{HE1,ret}) \tag{11}$$

$$\dot{Q}_{HE2} = c \cdot \dot{m}_{HE2} \cdot (T_{HE2,sup} - T_{HE2,ret}) \tag{12}$$

$$\dot{Q}_{DHS} = c \cdot \dot{m}_{DHS} \cdot (T_{DHS,sup} - T_{DHS,ret}) \tag{13}$$

where $\dot{m}_{DHS}$, $\dot{m}_{HE1}$, and $\dot{m}_{HE2}$ refer to the water mass flow rate of DHS, HE1, and HE2, respectively. $\dot{Q}_{DHS}$, $\dot{Q}_{HE1}$, and $\dot{Q}_{HE2}$ represent the heat supply flow rate of the DHS, HE1, and HE2, respectively. $\dot{Q}_{TES}$ is the heat flow rate of the TES for discharging (negative values) and charging (positive values). $\dot{Q}_{Bui}$ represents the building heat demand. $\dot{Q}_{loss,pip}$ and $\dot{Q}_{loss,TES}$ refer to the heat loss flow rate from the pipeline and the TES, respectively. $T_{DHS,sup}$, $T_{HE1,sup}$, and $T_{HE2,sup}$ represent the supply temperature of DHS, HE1, and HE2, respectively. $T_{DHS,ret}$, $T_{HE1,ret}$, and $T_{HE2,ret}$ refer to the return temperature of DHS, HE1, and HE2, respectively. c is the specific heat capacity of water.

The manipulated variables $\boldsymbol{u}$ in this study were $T_{HE1,sup}$, $T_{HE2,sup}$, $\dot{m}_{HE1}$, $\dot{m}_{HE2}$, and $\dot{m}_{Bui}$.

This article focuses on the introduction of the optimization framework, the detailed information on the sub-system models will be given in a journal article.

2.4. Algorithm to solve the optimization problem

Section 2.3 defines a dynamic optimization problem, which is challenging to solve because of the nonlinearity of the dynamic model. This study used the direct collocation method [9] to transform the original infinite-dimensional nonlinear programming (NLP) problem into a finite-dimensional NLP, which could be solved by NLP solvers.

Fig. 3 illustrates the direct collocation method. A time grid from t_0 to t_N was created over the optimization horizon by dividing the horizon into N internals with a constant interval. Afterwards, the state variables $x(t)$ were discretized on each time grid, and thus the state points from s_0 to s_N were obtained. The manipulated variables $u(t)$ were parameterized at each time grid, and thus on each interval $[t_k, t_{k+1}]$, a constant control signal q_k was yielded. Moreover, for each collocation interval $[t_k, t_{k+1}]$, a set of collocation points were generated from $t_{k,1}$ to $t_{k,d}$, and then a polynomial $p_k(t,\ v_k)$ was used to approximate the trajectory of the state within the interval. Therefore, Equation (6) was discretized into Equation (14) in the time interval $[t_k, t_{k+1}]$.

$$c_k(v_k, s_k, q_k) = \begin{bmatrix} v_{k,0} - s_k \\ F(\dot{p}_k(t_{k,1}, v_k), v_{k,1}, t_{k,1}, q_k) \\ \vdots \\ F(\dot{p}_k(t_{k,i}, v_k), v_{k,i}, t_{k,i}, q_k) \\ \vdots \\ F(\dot{p}_k(t_{k,d}, v_k), v_{k,d}, t_{k,d}, q_k) \end{bmatrix} = 0 \tag{14}$$

Besides, continuity conditions should be satisfied at the time grid points $k = 0,1,\cdots N-1$, i.e. the lengths of the red lines in Fig. 3 should be zero. Therefore, Equation (15) was added for these points.

$$p_k(t_{k+1}, v_k) - s_{k+1} = 0 \tag{15}$$

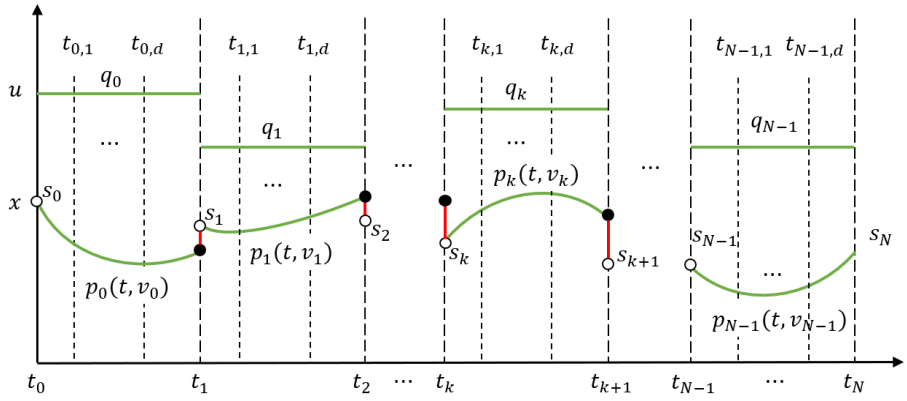

Fig. 3. Illustration of the direct collocation method

Finally, an NLP was yielded and it can be described in the following general form as Equations (16), (17), (18), (19), and (20).

Minimize:

$$\sum_{k=0}^{N-1} L_k(v_k, s_k, q_k) \cdot (t_{k+1} - t_k) + P \tag{16}$$

subject to:

$$x(0) = s_0 \tag{17}$$

$$c_k(v_k, s_k, q_k) = 0 \tag{18}$$

$$p_k(t_{k+1}, v_k) - s_{k+1} = 0 \tag{19}$$

$$h(s_k, v_k) \leq 0 \tag{20}$$

where $k = 0,1,\cdots N-1$. Equation (16) is the discretized form of Equation (4). In Equation (16), the first term approximates the integration term of Equation (4), and the second term represents the parameter to be minimized in Equation (4). Equation (17) represents the initial conditions described in Equation (6), Equations (18) and (19) discretize the system dynamics in Equation (6), and Equation (20) is the discretized constraints in Equation (8).

The NLP was solved by NLP solvers. Firstly, the inequality constraints were got rid of using the interior-point method, and then a local optimum was obtained via solving the first order Karush-Kuhn-Tucker condition using iterative techniques based on Newton's method. The optimization process was conducted using the open-source platform JModelica.org [10].

3. Case study

A DH system at a university campus in Norway was used as the case study, as presented in Fig. 4. The studied DH system was a prosumer, which got heat supply from the central DH system via the MS, meanwhile, recovered the waste heat from the university DC [2, 3].

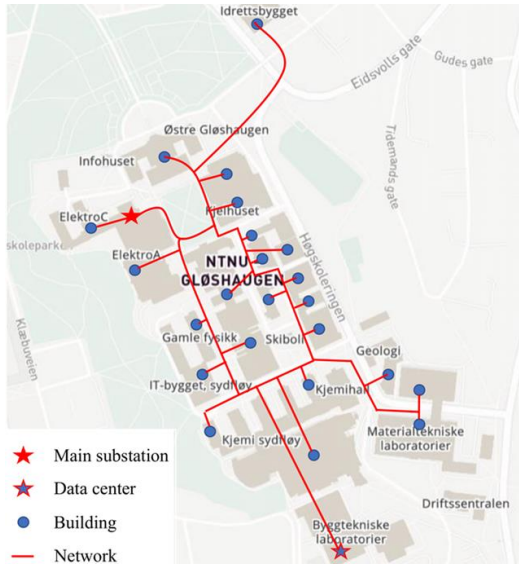

Fig. 4. DH system at the university campus [2, 3]

Fig. 5 presents the measured building heat demand and waste heat supply. The following problems can be observed 1) the mismatch between the waste heat supply from the DC and the building heat demand, which led to the surplus waste heat supply as shown with the red line in Fig. 5 and reduced the self-utilization rate of the heat supply from DHSs. 2) the high peak load during the wintertime as shown with the yellow line in Fig. 5.

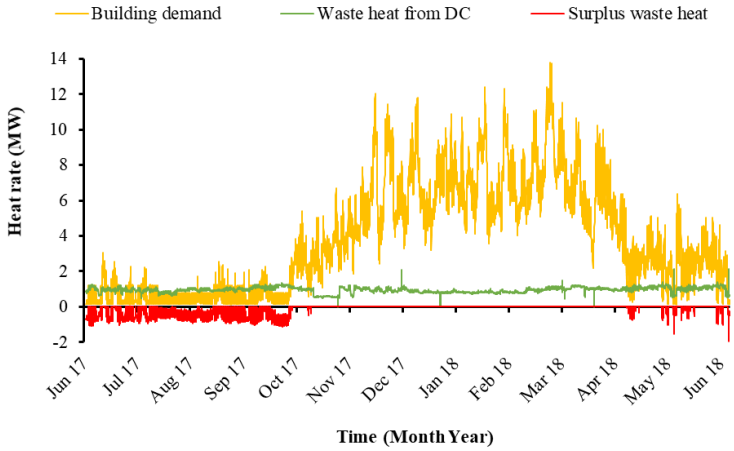

Fig. 5. Measured building heat demand, waste heat supply from the DC, and surplus waste heat

This study introduced a WTTES into the university DH system as proposed in the system design in Section 2.2 and used the optimal operation strategy proposed in Section 2.3 to optimize the economic performance of the studied DH system. The size of the WTTES was 1,700 m^3 and the heating price was obtained from the website of the local DH company [11].

4. Results

This section presents the simulation results, which demonstrate the improved economic performances of the heat prosumer by applying the proposed method. The scenario *Ref* and *WTTES* refer to the situation before and after introducing WTTES, respectively.

Fig. 6 and Fig. 7 present the annual heat use and the yearly peak load for the scenario before and after introducing WTTES, respectively. These two indicators quantified the heat supply from the central DH system to the heat prosumer through the MS. It can be observed from Fig. 6 that introducing WTTES reduced the annual heat use from 26.2 GWh to 25.9 GWh, meaning a heat use saving of 1%. Compared to this less significant heat use saving, a more obvious peak load shaving was obtained as shown in Fig. 7, the yearly peak load was shaved from 12.4 MW to 9.5 MW, a shaving of 24%.

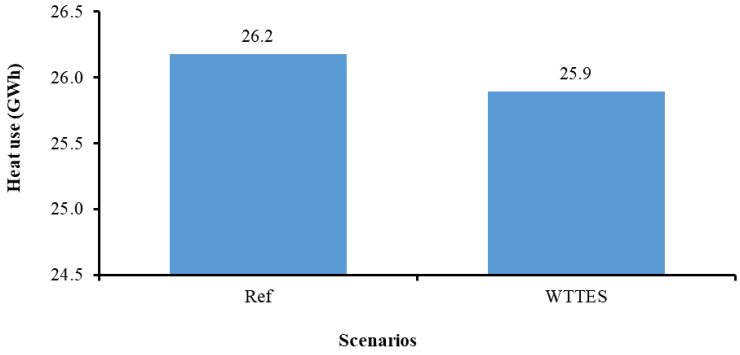

Fig. 6. Annual heat use for the scenario before and after introducing WTTES

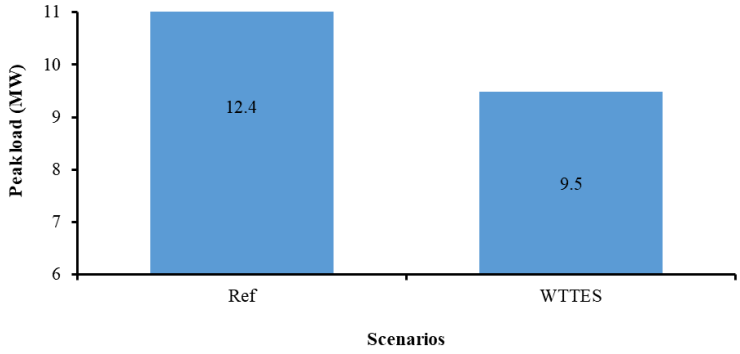

Fig. 7. Yearly peak load for the scenario before and after introducing WTTES

The resulting annual heating cost for the scenario before and after introducing WTTES is presented in Fig. 8. The proposed method cut the annual heating cost from 20.7 million NOK to 19.3 million NOK, which meant a cost saving of 7% was achieved. Moreover, this cost-saving could recover the investment of the WTTES in four years. These economic performances proved that the proposed system design and the operation strategy were economically feasible.

Fig. 8. Annual heating cost for the scenario before and after introducing WTTES

5. Conclusions

This study proposed a method to improve the economic performance of heat prosumers under the heating price models in Norway. The method included a type of system design, which integrated a WTTES into the heat prosumer based DH system, and an operational strategy to minimize the heating cost considering the widely used heating price models in Norway. A case study showed that the proposed method was economically feasible. The method could cut the prosumer's annual heating cost by 7% and recover the investment of WTTES in four years.

Acknowledgements

The authors gratefully acknowledge the support from the Research Council of Norway through the research project understanding behaviour of district heating systems integrating distributed sources under the FRIPRO/FRINATEK program (project number 262707) and the innovation project low-temperature thermal grids with surplus heat utilization under the EnergiX program (project number 280994).

References

[1] Song J, Wallin F, Li H. District heating cost fluctuation caused by price model shift. Applied Energy. 2017;194:715-24.
[2] Li H, Hou J, Nord N. Using thermal storages to solve the mismatch between waste heat feed-in and heat demand: a case study of a district heating system of a university campus. 2019.
[3] Li H, Hou J, Hong T, Ding Y, Nord N. Energy, economic, and environmental analysis of integration of thermal energy storage into district heating systems using waste heat from data centres. Energy. 2021;219:119582.
[4] Harris M. Thermal Energy Storage in Sweden and Denmark: Potentials for Technology Transfer. IIIEE Master thesis. 2011.
[5] Li H, Hou J, Ding Y, Nord N. Techno-economic analysis of implementing thermal storage for peak load shaving in a campus district heating system with waste heat from the data centre. Conference Techno-economic analysis of implementing thermal storage for peak load shaving in a campus district heating system with waste heat from the data centre, vol. 246. EDP Sciences, p. 09003.
[6] Sernhed K, Gåverud H, Sandgren A. Customer perspectives on district heating price models. International Journal of Sustainable Energy Planning and Management. 2017;13:47-60.
[7] Song J, Wallin F, Li H, Karlsson B. Price Models of District Heating in Sweden. Energy Procedia. 2016;88:100-5.
[8] Li H, Nord N. Transition to the 4th generation district heating - possibilities, bottlenecks, and challenges. Energy Procedia. 2018;149:483-98.
[9] Amrit R, Rawlings JB, Biegler LT. Optimizing process economics online using model predictive control. Computers & Chemical Engineering. 2013;58:334-43.
[10] Åkesson J, Gäfvert M, Tummescheit H. Jmodelica—an open source platform for optimization of modelica models. Conference Jmodelica—an open source platform for optimization of modelica models.
[11] Charging method for heating bill in Trondheim, https://www.statkraftvarme.no/globalassets/2-statkraft-varme/statkraft-varme-norge/om-statkraft-varme/prisark/20190901/fjernvarmetariff-trondheim-bt1.pdf, accessed September 2020.

ISBN 978-82-326-5828-2 (printed ver.)
ISBN 978-82-326-6402-3 (electronic ver.)
ISSN 1503-8181 (printed ver.)
ISSN 2703-8084 (online ver.)

NTNU

Norwegian University of
Science and Technology